BRUCE PEEL SPECIAL COLLECTIONS LIBRARY

UNIVERSITY OF ALBERTA LIBRARY

REQUEST FOR DUPLICATION

I wish a photocopy of the thesis by

Amajor, L.C. (author)

entitled Chronostratigraphy, depositional ...

The copy is for the sole purpose of private scholarly or scientific study and research. I will not reproduce, sell or distribute the copy I request, and I will not copy any substantial part of it in my own work without permission of the copyright owner. I understand that the Library performs the service of copying at my request, and I assume all copyright responsibility for the item requested.

Date	Name and address	Pages copied	Signature
6/13/91	ILL Card # 5000 000 464	All (1-691)	Thomas Madrid
JUL - 3 1991	Bow Valley Industries Calgary	All	ILL-ML

THE UNIVERSITY OF ALBERTA

CHRONOSTRATIGRAPHY, DEPOSITIONAL PATTERNS AND ENVIRONMENTAL ANALYSIS OF SUB-SURFACE LOWER CRETACEOUS (ALBIAN) VIKING RESERVOIR SANDSTONES IN CENTRAL ALBERTA AND PART OF SOUTHWESTERN SASKATCHEWAN

by

© LEVI CHUKWUEMEKA AMAJOR

A THESIS

SUBMITTED TO THE FACULTY OF GRADUATE STUDIES AND RESEARCH

IN PARTIAL FULFILMENT OF THE REQUIREMENTS FOR THE DEGREE

OF DOCTOR OF PHILOSOPHY

DEPARTMENT OF GEOLOGY

EDMONTON, ALBERTA

FALL, 1980

DEDICATION

To my parents, late Mr. and Mrs. Moses Ejikeme Amajor, brother Gilbert Nduka Amajor and wife Ogechi Ngozi Amajor who not only taught me to work painstakingly hard but are sources of inspiration and motivation in my life.

ABSTRACT

A regional subsurface study of the Lower Cretaceous oil and gas bearing Viking sandstones in central Alberta, as well as part of southwestern Saskatchewan, was undertaken to determine patterns and environments of deposition.

The chronologic and spatial development of the sandstone units were analysed by making use of four widely spread bentonite beds (E, C, A, A_O) which were used to subdivide the formation into three chronostratigraphic units designated informally as 'Basal', 'Lower', and 'Upper'. Sandbodies in these time units were mapped and diagnosed with the aid of more than 6,000 electric well logs, cores from 73 wells, and through the use of 62 stratigraphic cross-sections.

The Viking Formation in Alberta and Saskatchewan lies between two marine shale sequences. The formation consists of mineralogically and texturally mature sandstones interbedded with varying proportions of siltstone, mudstone, shale and chert pebble beds. Generally, the Formation thins from 200 feet (61 m) in the southwest to zero northeast of St. Paul.

The bentonite chronostratigraphy, sandstone geometry and vertical succession of lithology, sedimentary structures, textures and ichnofossils in cores reveal two main facies

ABSTRACT

A regional subsurface study of the lower Cretaceous oil and gas bearing Viking sandstones in central Alberta, as well as part of southwestern Saskatchewan, was undertaken to determine patterns and environments of deposition.

The chronologic and spatial development of the sandstone units were analyzed by making use of four widely spread bentonite beds (B, C, A, Ao) which were used to subdivide the formation into three chronostratigraphic units designated informally as 'Basal', 'Lower', and 'Upper'. Sandbodies in these time units were mapped and discussed with the aid of more than 6,000 electric well logs, cores from 73 wells, and through the use of 42 stratigraphic cross-sections.

The Viking Formation in Alberta and Saskatchewan lies between two marine shale sequences. The formation consists of mineralogically and texturally mature sandstones interbedded with varying proportions of siltstones, mudstones, shale and chert pebble beds. Generally, the Formation thins from 200 feet (61 m) in the southwest to zero north-east of St. Paul.

The bentonite chronostratigraphy, sandstone geometry and vertical succession of lithology, sedimentary structures, texture and ichnofossils in cores reveal two major facies

sequences (A and B) which are geographically restricted and distinct, and which migrated in opposite directions.

The shoreline-nearshore sandstones (Upper Western), located southwest of the study area, are predominantly wave-dominated regressive meso-tidal barrier island systems represented by facies sequence A and comprises 11 facies (ebb-tidal delta, transitional, middle shoreface, shelf clays, upper shoreface-beach, dune, back barrier mudflat, overwash and marshy lagoon, mixed tidal flat, tidal creek channel and overbank). The system trends northwest-southeast and prograded in a northeasterly direction approximately to a line which runs from Township 35, Range 28 through Township 30, Range 21 to Township 24, Range 18 W4M. Much of this sequence was deposited prior to the Upper chrono-interval.

The barrier island sequence differs slightly from the Recent classic regressive Galveston Island model in the presence of an ebb-tidal delta and marine shelf clays, respectively, beneath and above the middle shoreface facies. The South Carolina Recent barrier islands are considered closer modern analogs.

In contrast, offshore sand deposition was more localized and characterized by the development of chrono-taxial multiple sandbodies which migrated in a southwesterly direction (landward), in opposition to the shoreline-nearshore system. The locus of sand deposition also shifted intermittently in the same direction with time.

The earliest thin Viking sand units, some erosively based, were deposited during the Basal chrono-interval. They include the Beaverhill Lake, Hamilton Lake, Provost, and Dodsland-Hoosier reservoir sands. These were followed by the isochronous deposition of the Lower, Joffre, and Joarcam sandstone complexes slightly to the southwest of the Basal sandstones, but still during the Lower chrono-interval. These sandstone complexes are respectively characterized by 9, 4, and 12 chronotaxial elongate sandstone units arranged in linear and/or parallel rhythmic fashion and separated by swales characterized by poor sandstone development. A final southwesterly shift in the locus of deposition occurred during the Upper chrono-interval with the deposition of the thickest single Viking sandbody (Upper Central). During this period as well, deposition of much of the Upper Eastern sandstone complex continued in a southeasterly direction near the Alberta-Saskatchewan border from Townships 20 to 25. Generally, differential migration of these offshore sandbodies in the same average direction resulted in an imbricate pattern.

Facies sequence B (I to V) comprising 5 facies (bioturbated mudstone, heterolithic, cross-stratified sandstone, bioturbated sandstone and chert pebble conglomerate facies) characterizes the offshore sandbodies. Each facies consists of varying proportions of interbedded sandstone, siltstone, mudstone, shale and chert pebble beds. Bioturbation is ubiquitous but more pervasive in facies BI, BII and BIV.

Facies BIII comprises a variety of small to medium scale cross-stratified (some herringbone-like) and horizontal laminated sandstone beds with usually sharp (erosive?) cross-set contacts. Shale and glauconite drape foreset laminae. Facies BV consists of shaly, predominantly matrix-supported chert pebble conglomerate beds which have an erratic stratigraphic distribution largely controlled by seafloor topography. Coarsening upward textural gradient predominates, but lack of gradient is common. The facies are not stratigraphically dependent and each is the product of alternate bedload and suspension deposition from waning tidal, storm and perhaps semi-permanent currents.

Comparison with the poorly known responses to these agents in present-day environments, and with interpreted ancient examples indicates that the lateral facies variations, sedimentary structures in the cross-stratified facies, lithology, morphology and stratigraphic position and relationships of these sandbodies point to deposition in a subtidal, tide dominated shallow offshore marine environment below normal wave base.

Facies BI to BIII are believed to represent deposits of various parts of a tidal current sediment transport path such as exists in the Celtic Sea. Facies BIV is thought to represent either the bioturbated surface zone of stagnant ridges or the basal part of swale facies. The paleohydraulic regime is envisaged to be fairly analogous to the present-day North Sea tidal sand ridges where tidal currents

flow in mutually evasive ebb and flood channels. Facies BV was deposited during the highest energy level in the environment, perhaps when storms and/or semi-permanent currents (Boreal and/or Gulfian) boosted tidal currents.

On the basis of the stratigraphic position of the thin Viking sandstone members of the Dodsland-Hoosier area of southwest Saskatchewan, their lateral relations to the Upper Eastern sandstone, and their depositional pattern and trend, the writer suggests that they may represent a tide generated sandwave field.

In general, the shoreline-nearshore succession overlies the offshore tidal sand ridges around Township 34, Range 27W4M. Southeast of this locale, both are laterally separated by a thick mudstone interval. Although Viking sandbodies in the study area show varying degrees of diachronism parallel and perpendicular to the paleostrandline, the Upper Western and Upper Eastern units are the most diachronous and this is perpendicular to the shoreline. Parallel to the strandline, the Formation youngs to the southeast.

It is believed that deltas, probably located in the Jasper area and in the southern Alberta-northern Montana Foothills supplied much of the Viking sediment. This sediment was either funnelled directly into the offshore region during a still-stand shoreline condition, or is earlier low-sea-level deltaic deposits modified during a later sea-level rise. In either case, tidal currents augmented by

storm and/or semi-permanent currents redistributed and fashioned it into rythmic linear and parallel sandridges in water depths which were in excess of effective wave base much of the time.

All known economic accumulations of oil and much of the gas in the study area are hosted in the tide-generated sandstone units. In most of the reservoirs economic hydrocarbon accumulations are trapped updip along their northeastern margins. Although regional dip has obviously played a role, cleaner sandstone and coarser grain size along this margin in response to depositional pattern may be the more important.

ACKNOWLEDGEMENTS

The author is very highly indebted to Dr. J.F. Lerbekmo for suggesting the thesis topic and his intimate supervision of the study.

Thanks are due the Research Council of Alberta for providing electric well logs; and the Energy Resource Conservation Board of Alberta for making well cores available.

The following Canadian Oil and Gas Companies based in Calgary deserve special thanks for permitting us to slab their Viking cores and to move them to the Department of Geology, University of Alberta, Edmonton: Bow Valley Exploration, Ceja Corporation, Chevron Standard, Cominco, Dome Petroleum, Hudson Bay, Esso Resources, Mobil, Pan Canadian Petroleum, Petrofina Canada, Samedan, Shell Canada Resources, Texaco Canada, Texas Pacific, Union, Westcoast Petroleum, Westcoast Decalta, and 79902 Resources. In addition Esso Resources and Shell Canada slabbed their own cores, and the latter company provided copies of the core photographs. Most of the companies also paid the boxing and handling charges for their slabbed cores.

I am thankful to Mr. F. Dimitrov for part of the drafting and for help in the photographic work.

Grateful acknowledgement is also made to Drs. C.R. Stelck and J. Steiner for helpful discussion and suggestions.

Financial assistance for the project was provided by Imperial Oil Research Grant Number 55-09050, Petroleum Aid to Education Grant Number 55-16036, National Science and Engineering Research Council Operating Grant A2127, and a Department of Geology Graduate Appointment.

Finally, the author wishes to acknowledge the cooperation, understanding, advice and support given him throughout the preparation of the thesis by his wife Ogechi; children, Uzoma and Okwudiri; and his brothers, De-Nduka and Ihianyichukwu Amajor.

TABLE OF CONTENTS

Chapter Page

Chapter Page

APPENDICES (cont'd)

LIST OF TABLES

LIST OF FIGURES

Figure		Page

Figure		Page

Figure		Page

Figure		Page

Figure		Page

Figure		Page

LIST OF PHOTOGRAPHIC PLATES

CHAPTER I

INTRODUCTION

General Statement

In the subsurface of much of central, east-central, and southern Alberta, including the adjacent parts of western Saskatchewan, the Lower Cretaceous Viking Formation is enclosed between two well defined marine shale units, the underlying Joli Fou and the overlying Lloydminster Formations. The Viking Formation consists of several discrete sand bodies some of which are reservoirs for oil and gas. For maximum success, an exploration and exploitation program for these highly commercial reservoirs demands a thorough understanding of the genesis of the sands. This, in turn, aids in the reconstruction of a comprehensive paleogeographic picture of the region.

Although work has been directed towards these goals in the past, such studies were localized in different parts of the region. Hence, a variety of interpretations resulted from seeing only parts of the whole picture. A better understanding of the origins of these sand units in time and space can be gained only from a detailed regional subsurface study which integrates all available lines of evidence.

Objectives

The objectives of the present study are five-fold:

1. To establish a chronostratigraphic framework for the Viking Formation utilizing bentonite beds correlated in a previous study (Amajor, 1977).
2. To correlate and map the relatively thick and laterally persistent sand bodies within each time interval and to diagnose their geometries and depositional patterns using stratigraphic cross-sections and fence diagrams.
3. To determine the environments of deposition of the sands by integrating the above knowledge with that gained from a detailed core study.
4. To reconstruct the paleogeography of the study area during Viking deposition.
5. To examine in general terms the occurrence and distribution of hydrocarbons in the formation in relation to the interpreted depositional environments and paleogeography.

Study Area

Figure 1 shows the geographic setting of the area of study, located in south-central Alberta and part of south-western Saskatchewan. It roughly embraces Townships 16 to 53, Ranges 1 to 29W4M and Townships 23 to 32, Ranges 1 to 6W5M in Alberta; and Townships 20 to 32, Ranges 24 to 30W3M in Western Saskatchewan. This area is approximately bounded by latitudes 50°N and 55°N and by longitudes 106°W and 115°W. It covers an area of approximately 40,000 mi.^{2} (103,600 km^2).

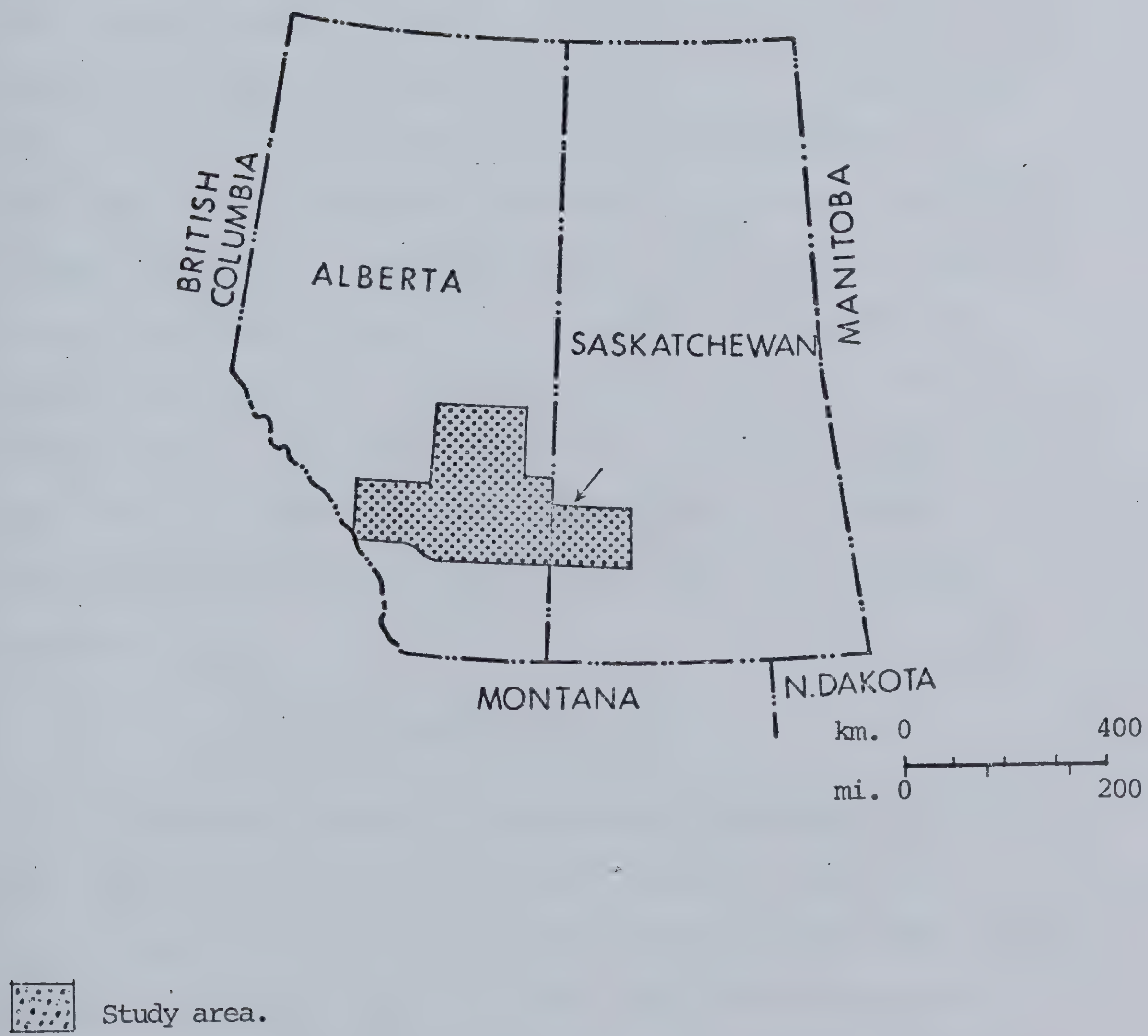

Figure 1. Location of study area.

Structurally, it is located in the Western Canada Sedimentary basin on the northern limb of the Sweetgrass Arch.

Most of the producing oil and gas pools in the Viking are located in the study area (Figure 2). These include the Hamilton Lake, Joarcam, Joffre, Smiley and Dodsland-Hoosier oil pools, and the Atlee-Buffalo Lake, Beaverhill Lake, Bindloss, Cessford, Huxley, Oyen, Provost, Red Willow, Sedalia, Sibbald, and Wayne Rosedale gas pools. Thus, the study area is considered the most suitable for this kind of regional subsurface analysis because it includes areas of maximum sandstone development and has the highest density of boreholes, which have yielded abundant subsurface data in the form of electric well logs and fairly good core control. In addition, non-productive Viking sands have been penetrated, logged and cored during the course of exploring for oil and gas in the deeper underlying formations, particularly the Devonian carbonates.

Previous Studies

Several aspects of the Viking Formation in Alberta and Saskatchewan have been investigated by past workers. The oil and gas prospects, reservoir and production history of the Formation in various areas have been treated by Slipper (1918), Badgley (1952), Jardine (1954), Reasoner and Hunt (1954), Ealph (1955), Gammell (1955), McPherson (1955), Larson (1960), Alhuo *et al.* (1977), Boethling (1977a), and Thomas (1977).

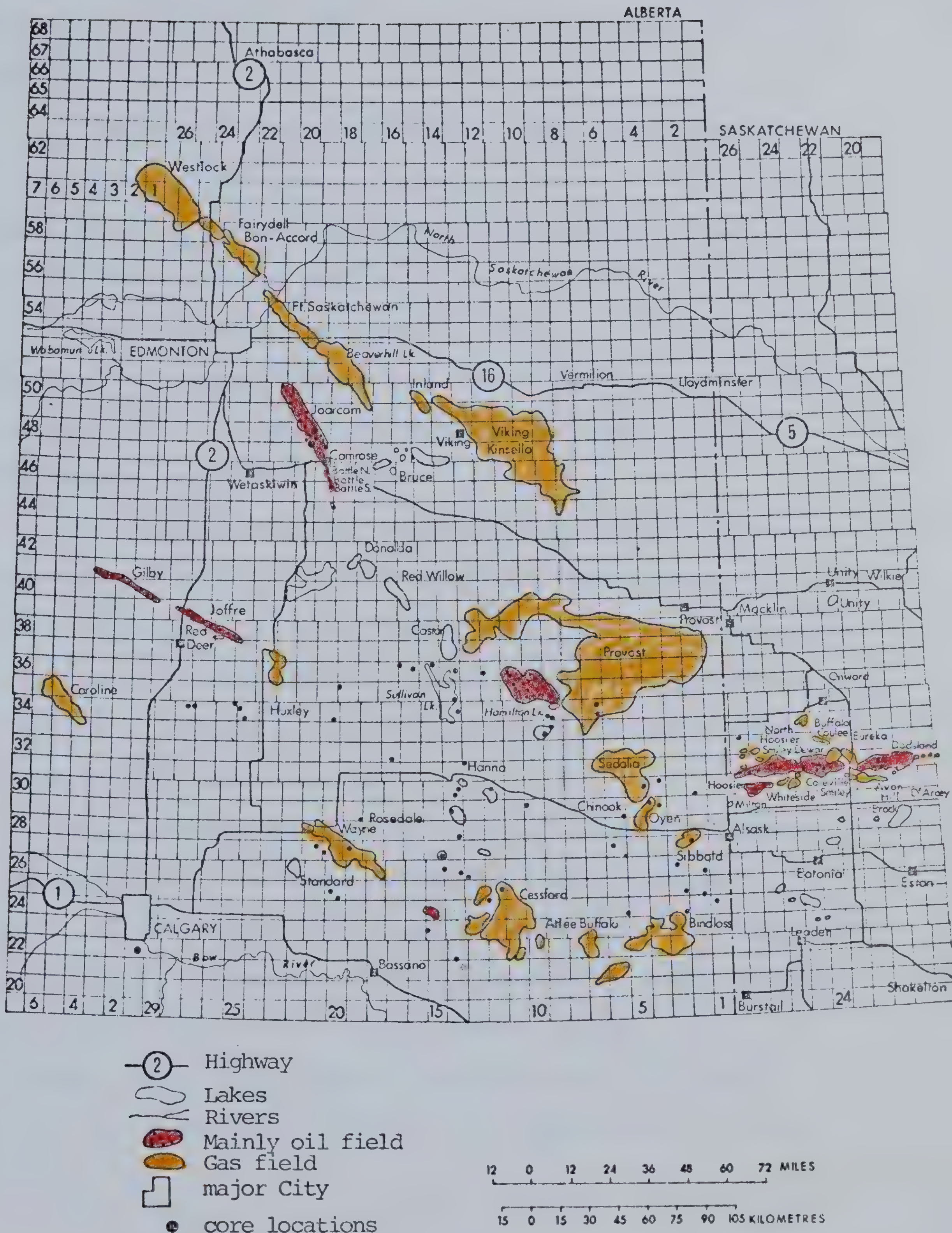

Figure 2. Location of some Viking oil and gas fields and cored wells studied.

The general subsurface lithostratigraphy has also bee examined by Hume (1933), Nauss (1945), Gammell (1955), Love (1955), Glaister (1958, 1959), Stelck (1958), Tizzard (1974) and Amajor (1977).

The foraminiferal biostratigraphy and paleocology of the Formation have been studied by Nauss (1947), Bullock (1950), Bahan (1951), Stansberry (1957), Stelck (1958, 1975) and North and Caldwell (1975).

The generalized geologic history of the Lower Cretaceous of Western Canada and of the North American continent have been reviewed respectively by Rudkin (1960), and Williams and Stelck (1975).

The more recent publications have focused attention on the depositional environments of the Viking sandbodies, and virtually all the common sedimentary processes operating in the nearshore and offshore regions have been invoked by one author or another. Hence, this aspect of the Formation has been highly controversial.

On the basis of the implied or interpreted depositional mechanism, six types of deposits have been envisioned: (a) Regressive and transgressive shoreline deposits; (b) Storm surge deposits; (c) Turbidites; (d) Beach-Barrier Island--offshore bars; (e) tidal current ridges; and (f) delta. These depositional concepts will be briefly reviewed in chronologic order of first appearance in the literature.

The Regressive-Transgressive Shoreline Concept

On the basis of lack of distinct or abrupt faunal changes before and during or after Viking deposition in the area of the Imperial Eldorena No. I well (4-27-57-20W4M), Bullock (1950) suggested the Viking to represent the sandy facies of the early Lloydminster flooding. However, Gammell (1955) stated that the Viking sands of central Alberta behave like regressive-type sand wedges in general, and vaguely suggested that currents moulded the sands into bars. More specifically, De Wiel (1956) attributed the sediment dispersal mechanism to longshore currents in front of a shifting strandline. Glaister (1959) interpreted the laterally equivalent Bow Island sandstones of southern Alberta to be deposited during repeated minor regressions within the major transgression. Thomas (1977) called the sandstone in the Provost 13-12-36-5W4M well a transgressive deposit.

Storm Surge Concept

The storm surge concept was first advanced by Hunt (1954) for the genesis of the Viking reservoir sands in the Joseph Lake-Armena-Camrose trend, located within Townships 46 to 50, Ranges 20 to 23W4M (Figure 2). This interpretation was based on the sedimentary structures and textures, and the uniform thickness of the sand unit. A similar view is shared by Koldijk (1976) and Thomas (1977) for the Gilby Viking 'B' reservoir sand located within Townships 41 and 42,

Ranges 3 to 5W5M. This sand unit is regarded as a northwesterly extension of the Joffre-Bentley trend. Based on the observations of Evans (1970), the Viking sands of Dodsland-Hoosier area of southwestern Saskatchewan were reinterpreted as storm deposits by Davies (1977).

The Turbidity Current Concept

The proponents of this concept were Beach (1955, 1956, 1962) and Roessingh (1959). The basis of the interpretation lies solely on the following:

1. A seemingly anamolous distribution of up to boulder size pebbles in the Formation.
2. The occurrence of bentonites.
3. Structures interpreted as due to slumping.
4. Interpreted non-diachroneity of the Formation.

The presence of bentonites is an evidence of volcanism probably related to tectonic activity during Viking deposition. They then reasoned that such a diastrophic process may have been accompanied by earthquakes, which are a likely cause of submarine slides and tsunamis. These in turn are possible sources of energy to trigger turbidity currents capable of transporting pebble size materials. This concept met with great opposition at that time from De Wiel (1956) and Jones (1961a, 1961b, 1962).

The Beach-Barrier Island--Offshore Bar Concept

Stelck (1958) interpreted the Viking sands as shoreline and offshore bars developed along the borders of the *Haplophragmoides gigas* (Joli Fou) sea. Jones (1961) suggested that the Upper Viking sandstone in the southwest of his study area, located within Townships 23 to 34, Ranges 20 to 30 W3M in western Saskatchewan, possibly represents beach deposits.

The first attempt to document evidence in favour of offshore bars for some Viking sandbodies was made by Shelton (1973). Based on the gradational lower and lateral contacts, a width-thickness ratio of 500:1, mixed bedding, and the presence of glauconite in the Formation at Joffre, he interpreted these reservoir sands as offshore barrier bars. He went on to postulate that the Joffre and Joarcam fields represent two lines of barrier bars 70 miles (113 km) apart deposited at different times (Joffre first), under regressive conditions as the sea retreated toward the northeast. A similar interpretation was arrived at by Tizzard (1974) and Tizzard and Lerbekmo (1975) from a more detailed study of the Viking sandstones in the Suffield area, located within Townships 19 to 26, Ranges 1 to 16W4M. Thomas (1977) also interpreted the Viking sands penetrated and cored in wells Kirkpatrick 2-11-33-10W4M and Westlock 10-9-59-26W4M as offshore bars.

Tidal Current Ridge Concept

A fairly detailed study of the Viking Formation in the Dodsland-Hoosier and Smiley areas of southwestern Saskatchewan, located within Townships 29 to 32, Ranges 19 to 28W3M was undertaken by Evans (1970). He showed that the relatively thin sand units characteristic of the area trend WSW-ENE at high angles to the NW-SE trend of most Viking sandbodies. He went on to demonstrate that these thin sand units, which he termed members, were stacked in imbricate fashion, with the younger units progressively displaced southward. He integrated these observations with the characteristic interlamination of thin shale and sandstone stringers, the presence of local chert pebble beds, and the general coarsening upward textural gradient, and concluded that the sand units were deposited by east flowing tidal currents relatively far from shore. He likened them to the present North Sea tidal ridges of Off (1963), and Stride (1963). However, he regarded the more normally NW-SE trending linear Viking sands to the southwest of his study area as shoreline and offshore bars. It is interesting to note, however, that his interpretation has become a textbook example of an ancient shelf tidal sand ridge system (Selley, 1976, p. 371; Klein, 1977, p. 91).

A compromise interpretation between barrier island, storm surge and tidal current ridges was made by Simpson (1975) in a regional study of the Colorado Group in west-central Saskatchewan (Townships 17 to 58, Ranges 9 to 23W3M)

and parts of southern Alberta. On the basis of the predominance of particular gross lithologies and sedimentary structures, and the distribution of significant heterostrate biofacies, he subdivided the Bow Island-Viking succession into three gradational environments, namely, nearshore, proximal and distal shelf. He then went on to hypothesize that:

1. The nearshore is characterized by shoreface and barrier island sands similar to the Recent Galveston Island of Texas.
2. The chief agents of sediment dispersal in the shelf region were storm surge, augmented by tidal currents. These were envisioned to produce tidal channel deposits and large scale sand ridges on a thin reworked relict sediment layer, similar and comparable to the tidal sand ridges of the North Sea investigated by Houbolt (1968). However, concerning the depositional history, Simpson had this to say:

> . . . .This gave rise to a net regression, through eastward and northeastward movement of successively younger, nearshore and shelf sands (. . . Bow Island sands, Viking Formation). . . ."

The Delta Concept

Amoco Canada Petroleum Company Limited (1976) mapped a Lower Viking delta in the area adjacent to and east of Jasper National Park, located approximately within Townships 40 to 56, Ranges 12 to 27W5M. Although this area was not

covered in the present study, Stelck (personal communications, 1979) supports this interpretation.

The great variation in interpretation of the depositional environments of the Viking Formation suggests that we are either dealing with a very complex depositional system in the Viking Sea, or that some interpretations are incorrect. Address to this problem constitutes the main thrust of this dissertation.

CHAPTER II

METHOD OF STUDY

Borehole and seismic logs, cores, sample cuttings and sidewall samples are basically the main sources of information on the subsurface geology of any area. The requirements for making a detailed reconstruction of the depositional environments of any sedimentary sequence from subsurface data can be summarized as:

1. Evenly spaced high density distribution of boreholes.
2. Precise electric, radioactivity or acoustic log correlation.
3. Mapping of genetically related time units, augmented by diagnostic stratigraphic cross-sections.
4. Sample analysis.

Density of Subsurface Control

The base map used in the study was one inch to four miles base showing Townships and Ranges. The subsurface well control consists of approximately 6,000 electric well logs. For a map area of approximately 40,000 mi^2 (103, 600 km^2), this amounts to about one well per seven square miles (18 km^2). However, the well density is not evenly distributed over the study area.

The dynamic exploration, production and development programs for the shallow Viking reservoir sands and the

underlying formations in the study area are responsible for the wealth of subsurface data available for this study.

Electric Well Log Correlation

A standardized procedure utilizing the spontaneous potential (SP) log as advocated by Hitchon (1964) was employed. However, where the resolution of this log was observed to be poor, the gamma ray log and/or the resistivity component of the electric log were used either as a cross-check or a substitute.

The correlation technique used is most similar to that described by Lowman (1949) called "correlation by stratal continuity." By this method all well logs in an area are studied in order to establish stratal continuity. It is akin to the surface correlation method often referred to as "walking the outcrop." In the present study, the method was first used to trace certain bentonite marker beds observed in the Formation in a previous study (Amajor, 1977). These chrono-horizons were used to subdivide the Viking Formation into three chronotaxial rock slices. The more laterally persistent, thicker and economically significant sand bodies within each slice were then correlated and mapped.

Isolith and Isopach Maps

Four isolith and two isopach maps were drawn to show by means of 10-foot contour intervals the variations in the apparent stratigraphic and lithologic thicknesses of the defined units.

The thicknesses of the Viking sand units in each time interval were taken from the spontaneous potential log. These measurements have been assumed to reflect the true thicknesses of units because it is impossible to adjust the log readings without a directional survey of the wells. Thickness readings were then contoured utilizing both the mechanical and the interpretative techniques of Krumbein and Sloss (1963, p. 437).

Isolith maps were constructed for reasonably discrete sand units whose lateral boundaries were easy to determine. In areas where discrete sandbodies are stacked vertically but separated by less than 30 feet (9.0 m) of shale, mudstone or siltstone, isopach maps include the whole interval. In such cases, separation of individual units was successfully achieved in stratigraphic cross-sections and fence diagrams. In areas where two sand units are interpreted to coalesce or overlap slightly, it is extremely difficult to partition the transitional area correctly. Some such zones may be mapped twice. However, these areas are few, and will be mentioned at the appropriate time in the discussion.

In a few areas with very poor well control isopach

lines were extrapolated to what was felt to be a reasonable interpretation. Areas of very little sand or no sand deposition, as interpreted mostly from electric and gamma ray logs, were not mapped. The resulting isopach and isolith maps were used as base maps for stratigraphic sections and core control, which in turn served as a check on the accuracy of the maps.

Stratigraphic Cross-Sections

Because stratigraphic sections are the most informative for this kind of study, (Porter, 1967), sixty two stratigraphic cross-sections utilizing 1,000 electric well logs were constructed either parallel or perpendicular to the depositional strike of the sand bodies. Generalized sketches were prepared of each cross-section and inserted in the text for easy reference (detailed sections are stored in the pocket and well identifications are listed in Appendix I).

The density of well locations allowed selected wells to be nearly in straight lines. In each stratigraphic cross-section a bentonite horizon was selected as a reference or datum line. Where the main datum is discontinuous, a subsidiary reference datum was also used. In areas where these bentonite marker beds can be correlated with considerable certainty, they were relied upon entirely. In areas where bentonite correlation is uncertain, distinct and laterally persistent electric log signatures were used as datum horizons. Electric well log spacing generally ranges

from 0.25 to 5 miles (0.4 to 8 km) in the cross-sections; however, in a few the spacing is somewhat greater.

Fence Diagrams

Six fence diagrams utilizing 600 electric well logs were prepared to demonstrate variations in the vertical and lateral stratigraphic relations of some sand bodies in the study area, since neither maps nor cross-sections alone portray the entire geologic story.

Basically, the fence diagrams were constructed from the spontaneous potential curve of well logs, with the tops of the logs placed approximately at the map locations. Identities of wells in the diagrams are listed in Appendix II.

Core Analysis

The isopach maps were useful as base maps for core control, as they restricted the search for cored wells to the mapped sand units, and facilitated the identification of the cored sand. The search for cored wells was conducted in the record files of the Geology Division of the Research Council of Alberta in Edmonton. This was supplemented with a computer print-out of the locations of cored wells in the Joarcam-Beaverhill Lake fields, supplied by Imperial Oil Company Limited of Calgary.

It was observed that many cores were cut from some sandstones,especially the producing sands, while only a few or none were cut from others. For most of the sand units enough different stratigraphic intervals were cored as to

represent almost the entire Formation, but in different areas. The entire sand body was completely cored in only a few wells.

A total of 4,173 feet (1,273 m) of unslabbed cores (plus a few cuttings and sidewall samples) recovered from 73 wells which penetrated the Formation were studied in the core storage laboratory of the Alberta Energy Resources Conservation Board at Calgary.

Description of the rock units included gross thickness, lithologic assemblage, grain size, sedimentary structures, nature of contacts, and trace and mega fossil content. Particular attention was paid to the vertical changes in single sand units. Descriptions of some cores studied by previous workers were also integrated into this study. When possible, cores from nearby wells were examined together so as to make qualitative comparisons of some of the above parameters.

Core diameter varied from 3 inches (7.5 cm) to one inch (2.5 cm), while core recovery ranged from excellent to very poor. Although some cores had been sampled previously, in most cases sufficient rock remained to allow the sequence of sedimentary structures and textures to be fairly well established. For some wells the cores were either lost or were so badly cut up that the sequence was difficult or impossible to establish.

Because the interval characteristics of well cores are easier to discern on sawed surfaces, it was decided to

slab the core from a select number of wells chosen on the basis of:

1. Degree of preservation of sedimentary structures and lithology.
2. Cored interval thickness, core diameter, core recovery and the condition of the core.
3. The stratigraphic position of the cored interval.
4. The number of independent sand units cored.
5. Location of the cored well on the sand unit.

Consideration of the above factors led to the selection of 1045 feet (318.5 m) of core from 24 wells. Photographs were taken of continuous slabbed core of some representative sandbodies, and of single core pieces containing diagnostic sedimentary features. Cored wells are described in Appendix III.

Thin Sections

Sixty-one samples of representative lithologies were taken from 13 wells and six different sandbodies. These were thin-sectioned and impregnated with blue epoxy to preserve the original texture and facilitate the recognition and identification of pores.

It was initially thought that the composition, texture and diagenesis of these sandbodies would be considered in some detail. However, the time factor restricted the number of thin sections examined to 44, and the analysis to quartz grain size distribution and textural maturity.

The technique of Berg and Davies (1968) was used to

determine the grain size distribution of the long axes of 200 monocrystalline quartz grains. Thus, grain size variation that may be caused by compositional differences are eliminated.

The mean grain size and standard deviation were determined by arithmetic methods. Iwuagwu (1979) did not observe any significant differences in the computation of these parameters by thin section graphic and arithmetic methods.

Although the sorting coefficient derived from the quartz grain size distribution shows the sand to be well sorted, it was noticed that most of the samples contain some matrix. It was then decided to characterize their overall textural maturity by the matrix-framework ratio method as this might provide some clues to the sediment dispersal mechanisms; matrix is defined according to Krynine (1948). Two hundred points were counted in each of 36 thin sections, and the matrix-framework ratio computed arithmetically. The data sheet for grain size is in Appendix IV.

CHAPTER III

REGIONAL GEOLOGIC HISTORY AND STRATIGRAPHY

Geologic History

The Lower Cretaceous geologic history of the Interior Plains of Western Canada summarized herein draws mainly from the works of Rudkin (1964), Stelck (1958, 1975), Douglas *et al.* (1970), Dickinson (1971, 1976), Wheeler *et al.* (1972), Williams and Stelck (1975), Simpson (1975) and Eisbacher (1977). It is intended to give the reader a broad paleogeographic picture of the tectono-sedimentary framework within which the Viking sandstone units were formed. However, such a discussion would not be complete without considering the adjacent older and younger strata.

The tectono-sedimentary framework which controlled and determined the course and patterns of Cretaceous sedimentation in the heart of the North American Continent was established in the Late Jurassic by the Columbian Orogeny (Nevadan and Coast Range Orogenies). This event was sporadic in time and space, with three major climaxes of intense activity punctuated with less intense pulses up to the early Late Cretaceous.

The early phase of the late Jurassic (Nevadan) orogeny was intense and mostly restricted to the Omineca

Geanticline.

The Aptian-Albian middle phase (Coast Range) orogeny was more widespread. During this period, rocks of the Cordilleran geosyncline were intensely deformed, metamorphosed, extensively intruded by granitic masses, and the whole area uplifted. The Sierra Nevada-Idaho-Nelson-Omineca batholithic mountains coalesced into a continuous highland. Volcanic eruptions accompanied this event, and several contemporaneous tectonic elements formed. The Rocky Mountain exogeosyncline, which represents the subsiding western cratonic margin, formed parallel to the eastern margin of the orogen and extended from the Arctic ocean to the Gulf of Mexico.

The early Late Cretaceous phase of the Coast Range Orogeny was characterized by widespread plutonic, tectonic, and volcanic activity. The earliest pulses of the Coast Range, Cassiar and Itsi batholiths, and later stages of the Nelson batholith were expressed at this time. This phase apparently coincides with the Lower-Upper Cretaceous geologic boundary. In the southern foothills of Alberta the Crowsnest volcanics coincides with this boundary approximately.

The less intense pulses of the Columbian orogeny may be partly reflected by volcanic rocks and ashes which punctuate the stratigraphic record. These Lower Cretaceous tectonic elements are generalized in Figure 3.

Consequent upon these events, episodic uplift and subsidence of the Rocky Mountain trough resulted in fluctuating marine incursions from both the Boreal and Gulfian Seas.

Legend:

- Granitic Batholiths
  - A- Southern Cassiar-Omenica
  - B- South Coast Range
  - C- Nelson
- Volcanic Islands
- Volcanic Deposits
  - ① Crowsnest Volcanics
  - ② Vaughn Bentonite
- Probable location of subduction zone
- Edge of the foothills disturbed belt.
- Sedimentary Basins
  - I Williston basin.
  - II Western Alberta basin.
  - III Northern Alberta basin.
- Lineaments
  - ⓐ Sweet Grass Arch
  - ⓑ Peace River High
  - ⓒ Aptian Ridge
  - ⓓ North Battleford Arch
- Probable outcrop edge of the PreCambrian Shield.
- Spreading Direction of the Pacific Plate

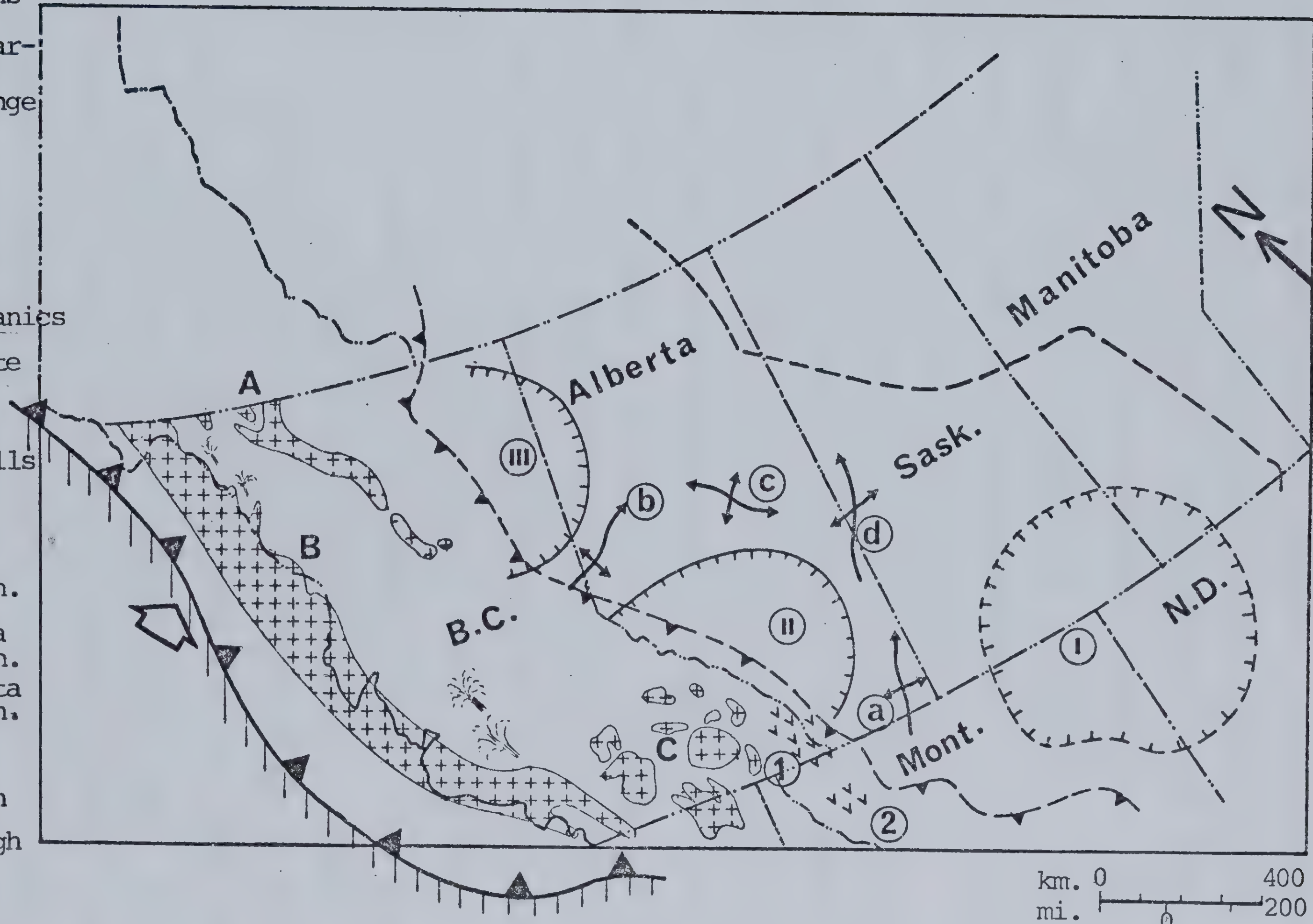

Figure 3. Major tectonic elements of the Lower Cretaceous of Western Canada. Modified from (Wheeler *et al.*, 1972; Douglas *et al.*, 1970; Dickinson, 1971, 1976; Rudkin, 1964; Williams and Stelck, 1975; Eisbacher, 1977; Simpson, 1975; Amoco, 1976).

The greatest subsidence occurred along the western margin of the trough; hence, the bulk of the detritus derived from the adjacent rising mountains was deposited along this margin. The Lower Cretaceous lithostratigraphic sequences in the Western Canadian basin thus record the transition from an early history of orogeny and nondeposition, to cycles of non-marine and marine paralic sedimentation.

The non-marine palludal, lacustrine and fluviatile sediments which overlie Late Jurassic beds unconformably are represented in Alberta by the Lower Manville map unit of Rudkin (1964), whilst the Upper Manville unit is essentially composed of continental to marine paralic interbeds. The Lower Colorado Group of Albian age is predominantly marine.

During the Late Albian, two major marine transgressions occurred in the Western Canadian basin. The basin was invaded by a southward advancing Boreal Sea and, to a lesser extent, by a Gulfian Sea which advanced toward the north. Evidence based on macro- and micro-faunal biostratigraphy in Western Canada and the United States demonstrate that the seas merged at least once in early Late Albian time. This was followed by a somewhat regressive phase at which time Viking sediments were laid down before the next flooding. The reconstructed extent of the Albian epicontinental seas in the North American Interior Plains is shown in Figure 4.

Sediments of these seas comprise the Lower Colorado Group, whose generalized isopachous map is shown in Figure 5. It shows that the greatest subsidence occurred within the

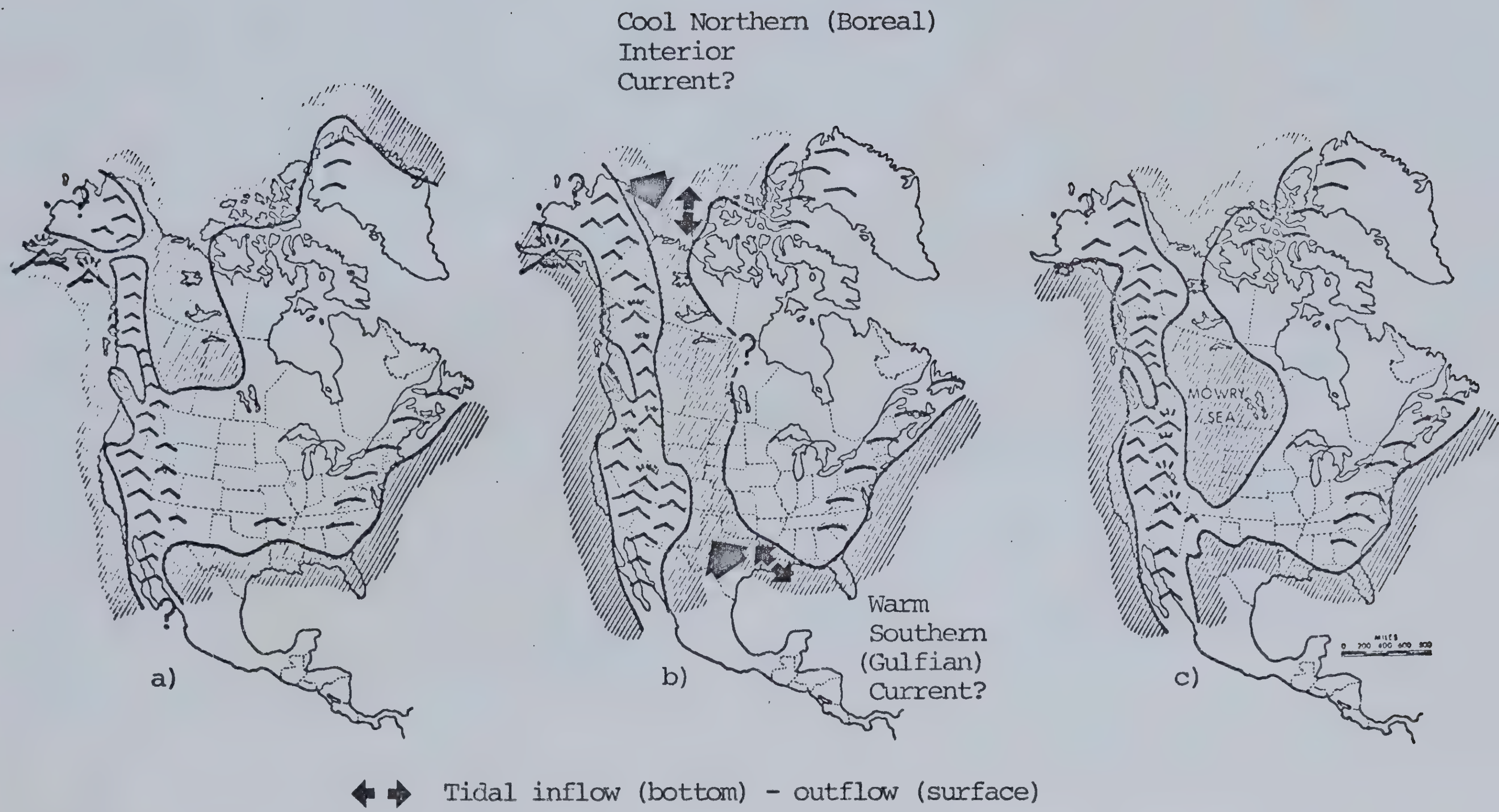

Figure 4. Maps showing the deduced extent of Albian Interior Seaway in North America.
a) Latest early Albian *Subarcthoplites* sea.
b) Early Late Albian *Inoceramus comancheanus* sea.
c) Late late Albian *Neogastroplites* sea. (Modified from Williams and Stelck, 1975; Kauffman, 1975.)

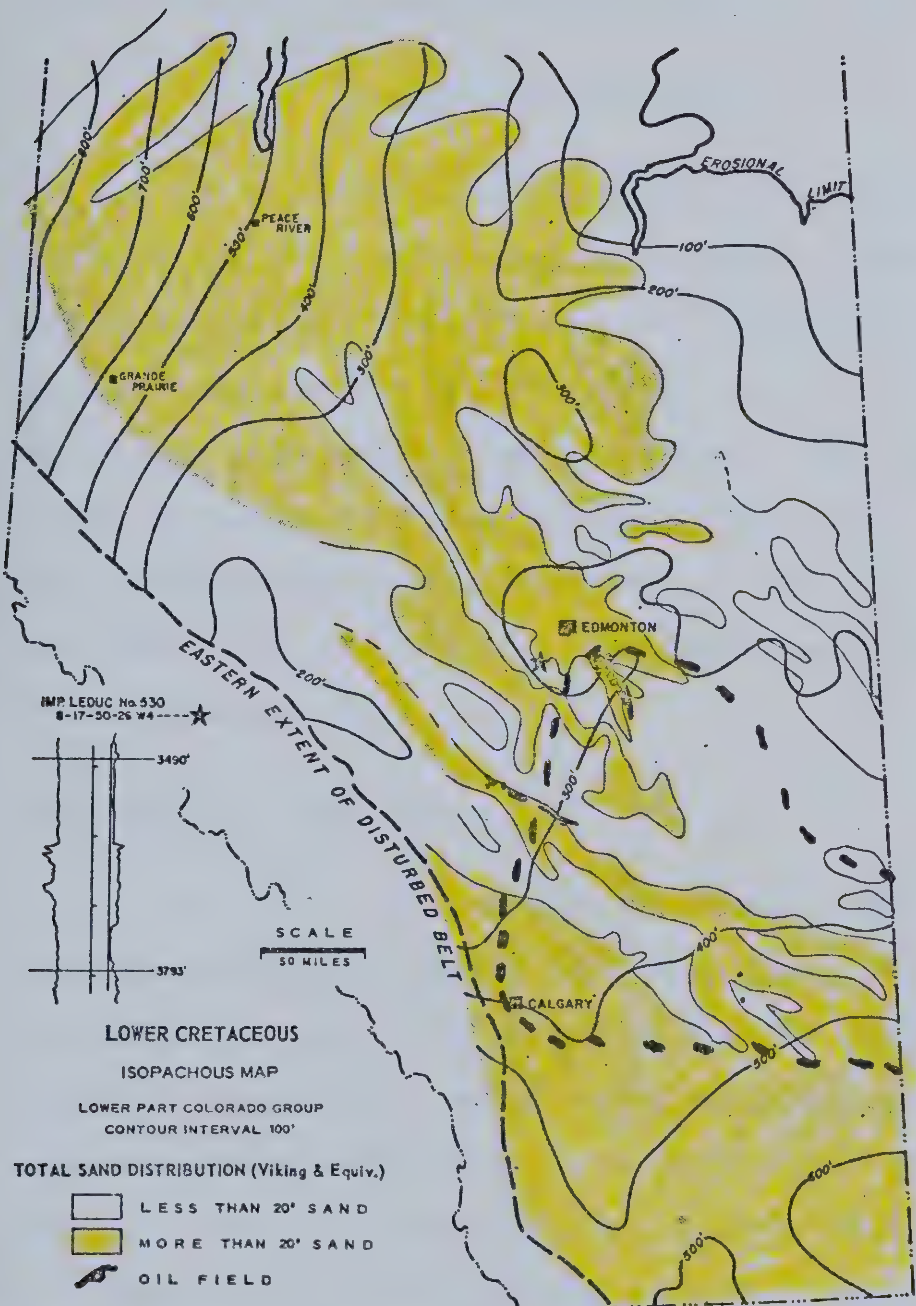

Approximate limit of study area.

Figure 5. Isopachous map of the Lower Colorado Group (Base of Fish Scales zone to top of Mannville Fm.) in Alberta. C.I. = 100'. (Adapted from Oil Fields of Alberta, A.S.P.G., 1960.)

Peace River area and in southern Alberta. These areas have been suggested to be characterized by deltas. Central Alberta appears to have been relatively stable.

Regional Stratigraphy

The stratigraphic sequence encompassed by the Lower Colorado Group of the study area consists predominantly of a marine sandstone (Viking Formation) intercalated between two marine shale units: the underlying Joli Fou Formation and overlying Lloydminster Shale. They are well defined and easily traced in electric well logs (Figure 6). The litho-bio-stratigraphic correlation between sections of the Lower Colorado Group in Alberta, Saskatchewan and Manitoba are shown in Figure 7.

The Joli Fou Formation

The Joli Fou Formation (Wickenden, 1949) is an extensive dark grey fissile marine bentonitic shale with occasional siltstone and sandstone lenses. These sediments represent the first true marine deposits of the Colorado sea whose early onlap phases are expressed as various paralic basal Colorado sandstones known as the Cessford, St. Edouard and Colony sands in Alberta, the Spinney Hill elastics of west-central Saskatchewan, the Swan River Group of Manitoba and the Dakota Silt of Wyoming (Stelck, 1958; Stapp, 1967; Simpson, 1975).

The Joli Fou Shale unconformably overlies the Grand

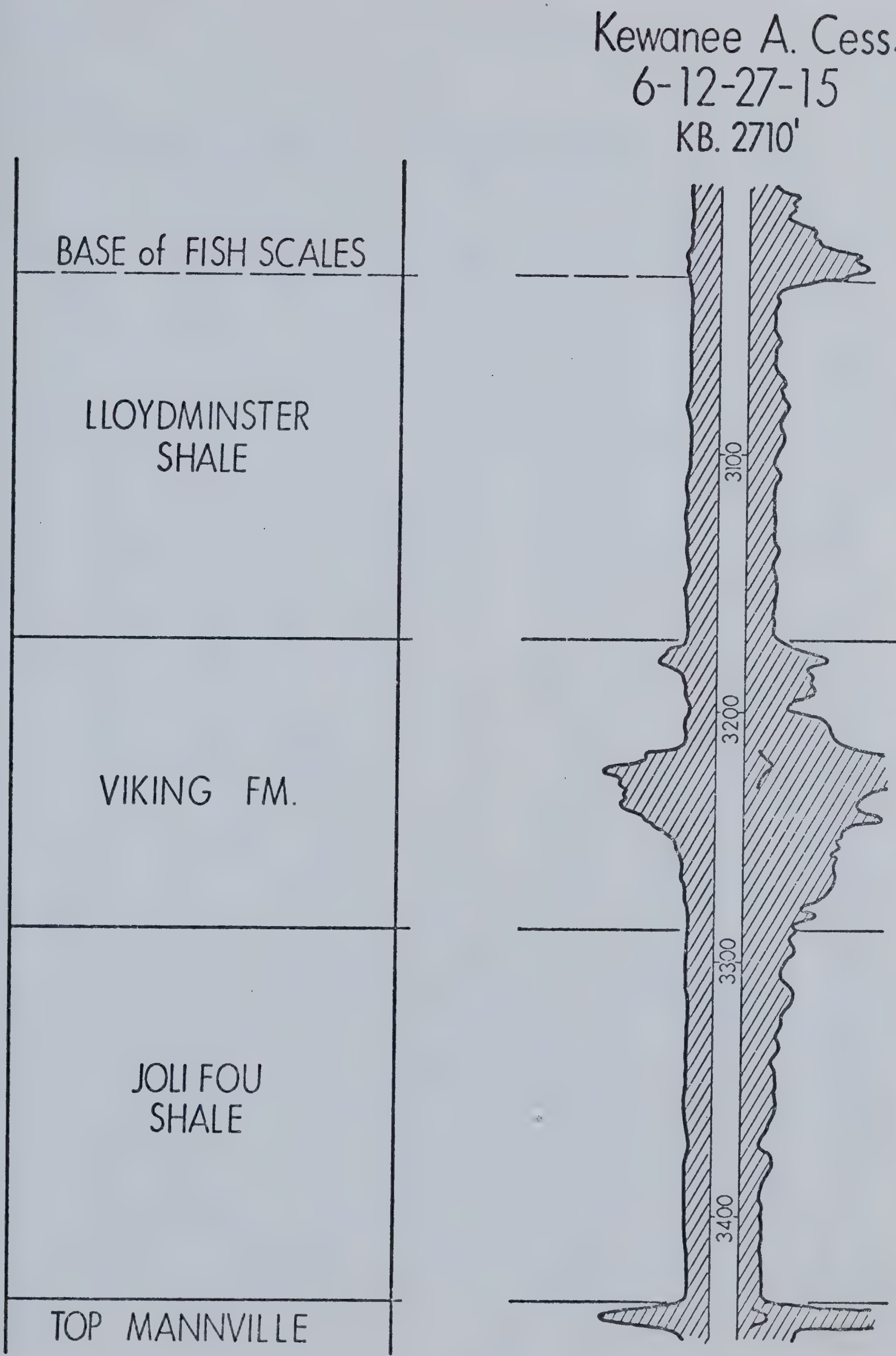

Figure 6. Electric log of the Lower Colorado Group showing the stratigraphic position of the Viking Formation.

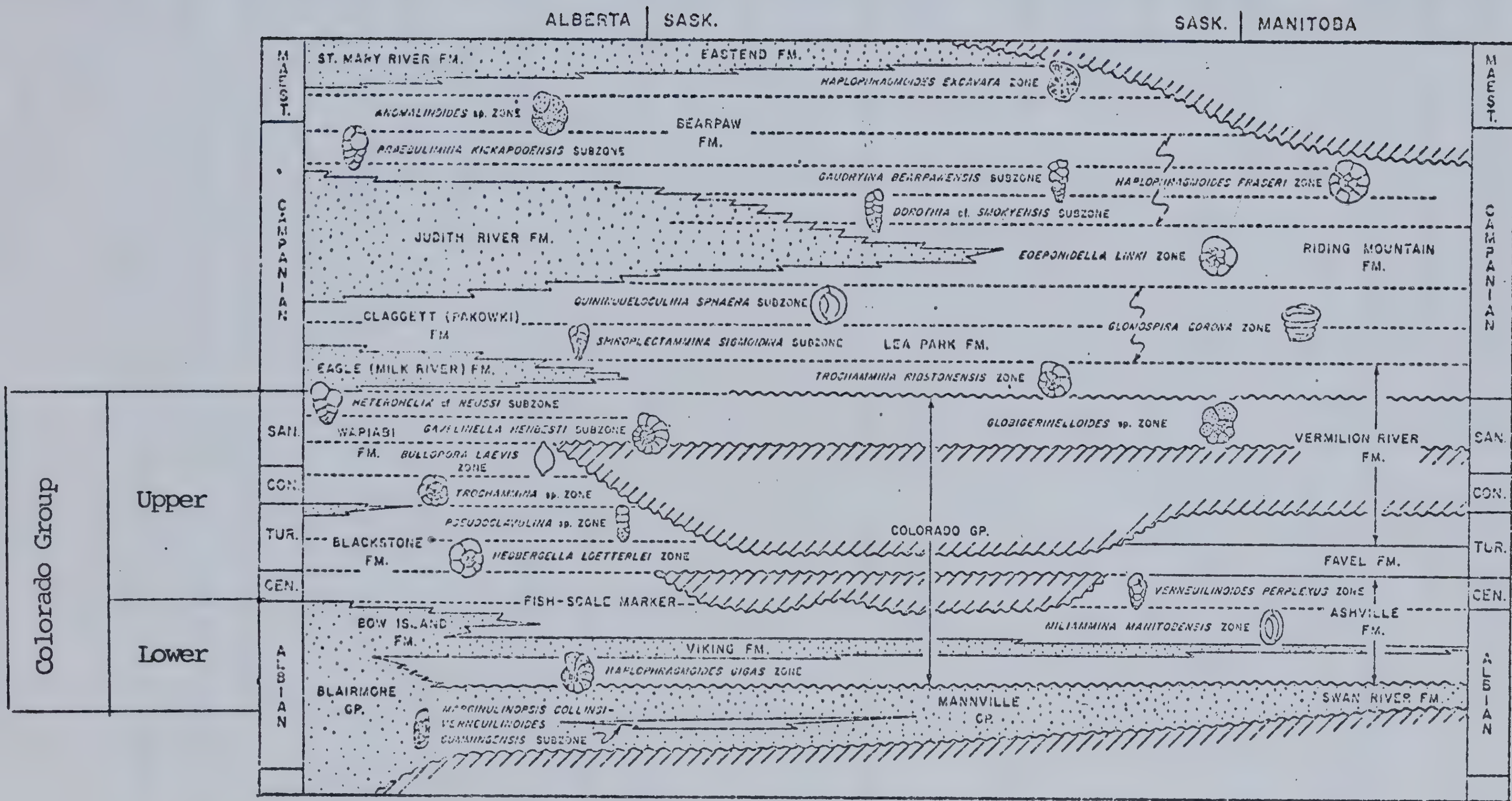

Figure 7. West-East biostratigraphic section of the Cretaceous of Western Canada showing the stratigraphic positions of the Lower Colorado Group (From Caldwell *et al.* (1978).

Rapids Formation and the Mannville Group in the northeastern and central to southeastern parts of the Province, respectively. It varies in thickness from 35 feet (11 m) in the Lesser Slave Lake area to about 135 feet (41 m) at the outcrop of the stratotype section on the Athabasca River near Pelican Rapids. It thins gradually toward the west and finally grades into the continental Blairmore Group of the foothills region. In southern Alberta, the Formation becomes silty and sandy south of Township 20 and finally loses its lithologic identity in the lower parts of the Bow Island Formation (Glaister, 1959).

In the subsurface as well as in outcrop sections the Formation carries the well known *Haplophragmoides gigas* foraminiferal assemblage near the base and the pelecypod *Inoceramus comancheanus* and *I. bellvuensis* a little higher in the section. Biostratigraphic correlatives in Montana and Wyoming include the Skull Creek and Thermopolis Formations and the Kiowa Shale of Colorado and Kansas. The common occurrence of the Boreal affiliated *H. gigas* with the Gulfian migrant *I. comancheanus* in some of these formations was used as evidence that both seas merged to form a continuous seaway in the Interior Plains of North America at this time (Figure 4b), (Stelck, 1958, 1975; Eicher, 1960; Williams and Stelck, 1975). The general region of western Kansas, southern Colorado, northern New Mexico and southeastern Utah has been suggested by Eicher (1960) and Kauffman (1973, 1977) as the transitional area of confluence of the two seas.

Joli Fou-Viking Contact

The contact between the Joli Fou and the overlying Viking is commonly placed at the base of the lowest prominent sand or sandy shale, although the lowest sand unit does not always occur at the same stratigraphic position.

Some workers in Saskatchewan (Jones, 1961; Evans, 1970; Simpson, 1975) have placed a break at the base of the Viking, or in the upper part of the Joli Fou Formation, based on physical evidence. However, foraminiferal biostratigraphic studies in Alberta by Bullock (1950) and in western Saskatchewan by North and Caldwell (1975) indicate that there is no significant faunal break before, during or after Viking deposition. Rather, the foraminiferal elements of the Viking are a combination of those of the underlying Joli Fou and overlying Lloydminster shale.

There is a consensus of opinion, however, that in parts of Montana, Wyoming, Colorado and the Dakotas, nonmarine conditions existed at the top of the Skull Creek-Thermopolis Shale, biostratigraphic equivalents of the Joli Fou Formation (Stapp, 1967; Scott, 1970; Reinert and Davies, 1975; Berg, 1976). However, Gopinath (1978) notes that in some other parts of these regions, the Thermopolis-Muddy (=Viking) transition is conformable.

Viking Formation

The name Viking was used by Dowling, Slipper and McLearn in 1919. It is thought that S.E. Slipper was the first to use the term to designate the gas-producing reservoir sands of the Viking-Kinsella field of east-central Alberta. Although no specific holostratotype was designated, it is generally considered to be a subsurface section in this field near the town of Viking (Norgaard, 1954). The formation is comparatively poorly developed in this area.

The Viking was initially classified as a Member of the Colorado Group (Hunt, 1954; Reasoner and Hunt, 1954; Gamell, 1955), but was later raised to the rank of Formation by Magditch (1955) and Stelck (1958).

The formation consists predominantly of a series of lenticular "salt and pepper" chert rich quartz sandstones with chert pebbles. Dark grey to grey siltstones, and bentonitic mudstones and shales are commonly interbedded in the sequence.

Regionally the Viking thins toward the east and northeast. Near Calgary it attains a maximum thickness of 200 feet (60 m), decreases to 100 feet (30 m) around Edmonton and to less than 40 feet (12 m) west of St. Paul. Beyond St. Paul (Township 58, Range 9W4M), it cannot be easily recognized in electric well logs as a sandy unit. This thickness distribution pattern has generally been taken to mean that the Viking or Joli Fou Sea regressed to the east and northeast, as the source area probably lay somewhere

to the west. This concept may have biased previous interpretations of the general depositional history.

A pertinent textural observation was made by Roessingh (1959) who correctly noted that there is no regional pattern of grain size variation; rather, thick sand bodies have coarser sand than the more frequent thin sand layers, regardless of location. Boethling (1977a) also correctly observed that while the Formation thickens toward the west, the sand content actually decreases. However, these authors did not offer any explanations for these phenomena. The thickness distribution pattern of the Formation will be shown later to be dependent on an interplay of basin configuration and depositional processes which shifted more or less systematically in time and space, probably in consonance with the tectonic activity going on in the west.

South of Township 20, the Viking is not recognizably distinct from the underlying Joli Fou Shale, as the latter changes into dominantly silty and sandy shales and both formations grade into interbedded sandstones and shales of the Bow Island Formation. To the west, the Bow Island merges with the Mannville Group to form the Blairmore of the foothills (Glaister, 1959; Rudkin , 1964).

In the northeastern and northwestern parts of Alberta, homotaxial sands are respectively known as the Pelican Formation and the Paddy Member of the Peace River Formation. In southeastern Saskatchewan and southwestern

Manitoba, the Viking is stratigraphically equivalent to the Silt Member of the Ashville Formation. South of the 49th parallel, the Newcastle Sandstone of Montana and the Dakotas, and the Muddy Sandstone of Montana and Wyoming are regarded as correlatives (Figure 8) (Berg and Davies, 1968; Rudkin, 1964; Simpson, 1975).

Stelck (1958) determined the age of the Viking Formation as the base of the Upper Albian Stage. An average radiometric age of 100 $\pm$2 Ma obtained by Tizzard and Lerbekmo (1975) supports the above age as it corresponds to the Upper Albian Stage of the Geologic Time Scale (Enysinga, 1975).

Most workers place the top of the Viking Formation at the top of a black chert pebble horizon or pebbly chert sandstone which has been said to occupy a fairly constant stratigraphic position (Stelck, 1958; Glaister, 1958). Because of the presence of numerous chert pebble beds within and near the top of the Formation, the difficulty of correlating them even in nearby wells, and their absence in some wells, Jones (1961) contended that the conglomerate beds are laterally restricted and do not present a consistent and reliable marker horizon in southwestern Saskatchewan. These observations and conclusions are consistent with those of the present writer. The stratigraphic distribution of the chert pebble beds appears to have been greatly influenced by the topography on the sea floor. Because these pebble beds cannot be reliably traced in electric well logs alone, in

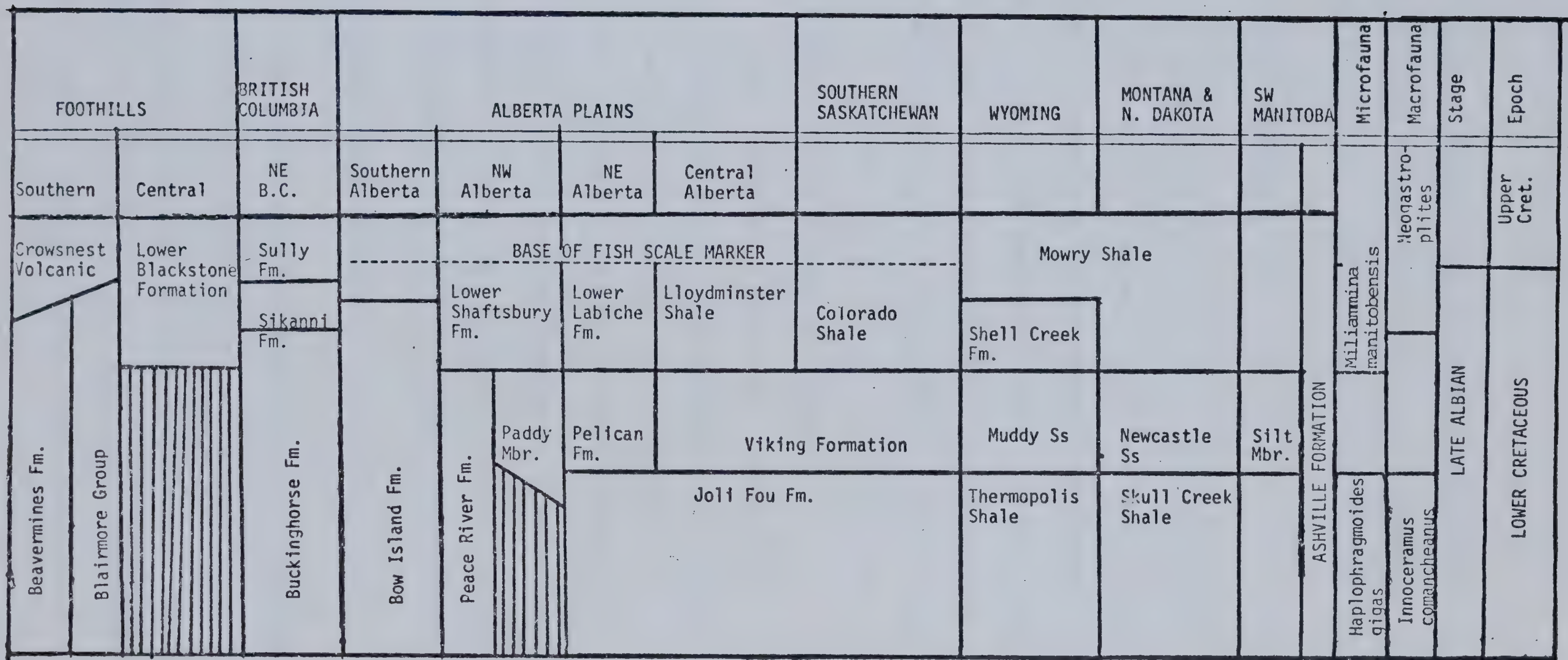

Figure 8. Stratigraphic Correlation of the Viking Formation in Central Alberta and Neighbouring Areas.

this study the top of the Viking Formation is placed at the highest inflection point of the spontaneous potential or resistivity log, indicating the top of the highest sand unit.

<u>Lloydminster Shale</u>

The Viking Formation is overlain by a dark marine shale variously referred to as the Upper Shale of the Lower Colorado Group (Norgaard, 1954), the Mowry Shale (Koldjick, 1976), or the Lloydminster Shale (Tizzard and Lerbekmo, 1975). The latter designation is preferred and used here as the unit is best developed around the town of Lloydminster. It is 200 feet (61 m) thick in this area and thins to 30 feet (9.0 m) west of Calgary.

The Formation bears the important *Miliammina manitobensis* foraminiferal assemblage indicative of the second major flooding of the Colorado sea, which covered the Viking shoreline and offshore sequences. The extent of this sea is inferred as Figure 4c. The biostratigraphic equivalents of the Lloydminster Shale include the Shell Creek and Mowry Shales of Montana and Wyoming.

<u>Base of the Fish Scales</u>

The Fish Scales Sandstone caps the above unit and terminates Lower Cretaceous sedimentation in a major portion of the Western Canadian Interior Plains. It is poorly sorted, light-colored, and has been described locally as subquartzose, cherty-quartz, and "salt and pepper" sandstone.

The upper part is shaly and contains light-colored chitinous remains of fish scales which are recognized as far north as Fort Nelson. The base of the Fish Scales marker is the base of this fossiliferous unit. It attains a maximum thickness of 30 feet (9.0 m) in central Alberta, and is widely recognized in the subsurface and in outcrops in much of Western Canada.

In northeastern British Columbia where this marker bed is absent, beds containing the Late Albian index ammonite *Neogastroplites* are used to delineate the Lower-Upper Cretaceous boundary.

CHAPTER IV

CHRONOSTRATIGRAPHY OF THE VIKING FORMATION

Published studies of the Viking Formation usually mention the occurrence of bentonites and/or bentonitic shales. However, only a few workers have attempted detailed local electric well log correlation of these beds, in spite of their time-stratigraphic significance. If their areal distributions are widespread and correlatable, time planes can be established which will facilitate interpretation of the depositional history of the Formation.

Roessingh (1959) noted the presence of a bentonite horizon in approximately the same stratigraphic position, relative to the top of the Viking, in well Parkland 4-12-15-27W4M and in a Grassy Island Lake well in Township 32, Range 7W4M in south-central Alberta. He used this relationship to interpret the Viking sands of central Alberta as non-diachronous.

Jones (1961) observed and correlated in some detail two bentonitic shales within the Viking Formation, and a 1 inch (2.5 cm) bentonite bed slightly above the Formation in southwestern Saskatchewan. The latter bed, designated bed 3, and located at the top of the Viking in Husky Phillips Prelate well 11-28-23-25W3M, was correlated to a ½ inch (1.3 cm) bentonite located in shale two feet (0.6 m) above

the Viking in well Imperial Marengo 11-21-29-27W3M. He used the two-foot difference in shale thickness between the two wells 38 miles (61 km) apart in a north-northwest direction to conclude that the Viking is slightly diachronous nearly parallel to the paleo-strandline, and that one would expect greater diachronism at right angles to the shifting strandline.

Evans (1970) correlated two bentonitic shales, designated "MN" and "K", located within Townships 32 and 30, Ranges 20 to 28 W3M in southwestern Saskatchewan. Using these bentontic shales, he interpreted an imbricate linear arrangement and southeastern diachronism of the Viking sandbodies in the Dodsland-Hoosier area of southwestern Saskatchewan.

Tizzard and Lerbekmo (1975) noted the presence of several bentonite horizons in the Suffield area (Townships 19 to 26, Ranges 1 to 16 W4M) of Alberta. They correlated one of them, a coarse biotite-rich bentonite 6 - 12 inch (15 -30 cm) thick and established a time datum for the Viking in this area. They used this chrono-horizon to deduce a slight northeasterly diachronism for the Viking sands of the area.

Although interpretation of the depositional history of the Formation, based on these bentonites, has varied, these studies indicated the occurrence of more than one bentonite bed in the Formation. Thus, the need for a regional study to identify and establish the geographic

distributions of the Viking bentonites was brought to light. An attack on this problem was made by Amajor (1977). A maximum of eight bentonite beds was observed in core from the Viking Formation in one well in central Alberta. A considerable areal extent for three was established by log and chemical correlation methods. They were informally designated "E", "C" and "A" in ascending order of occurrence. Another bentonite, designated Ao, was observed above the top of the Formation in the course of the present study. Figure 9 shows the approximate relative stratigraphic positions of these bentonite horizons. A brief account of them is included here because they constitute the time-framework of the Viking Formation utilized in the present study.

Bentonite E

This coarse grained biotite-rich bentonite is located at a depth of 2907 feet (886 m) and occurs at the base of the lowest prominent thin sandstone in the type well Ponderay *et al.* Youngstown 12-19-31-9W4M. Its thickness is greater than 60 cm. Log and chemical correlations indicate that it extends at least from Township 52 south to Township 23 and between Ranges 5 and 28 W4M. It was used to mark the beginning of Viking time in most parts of the study area.

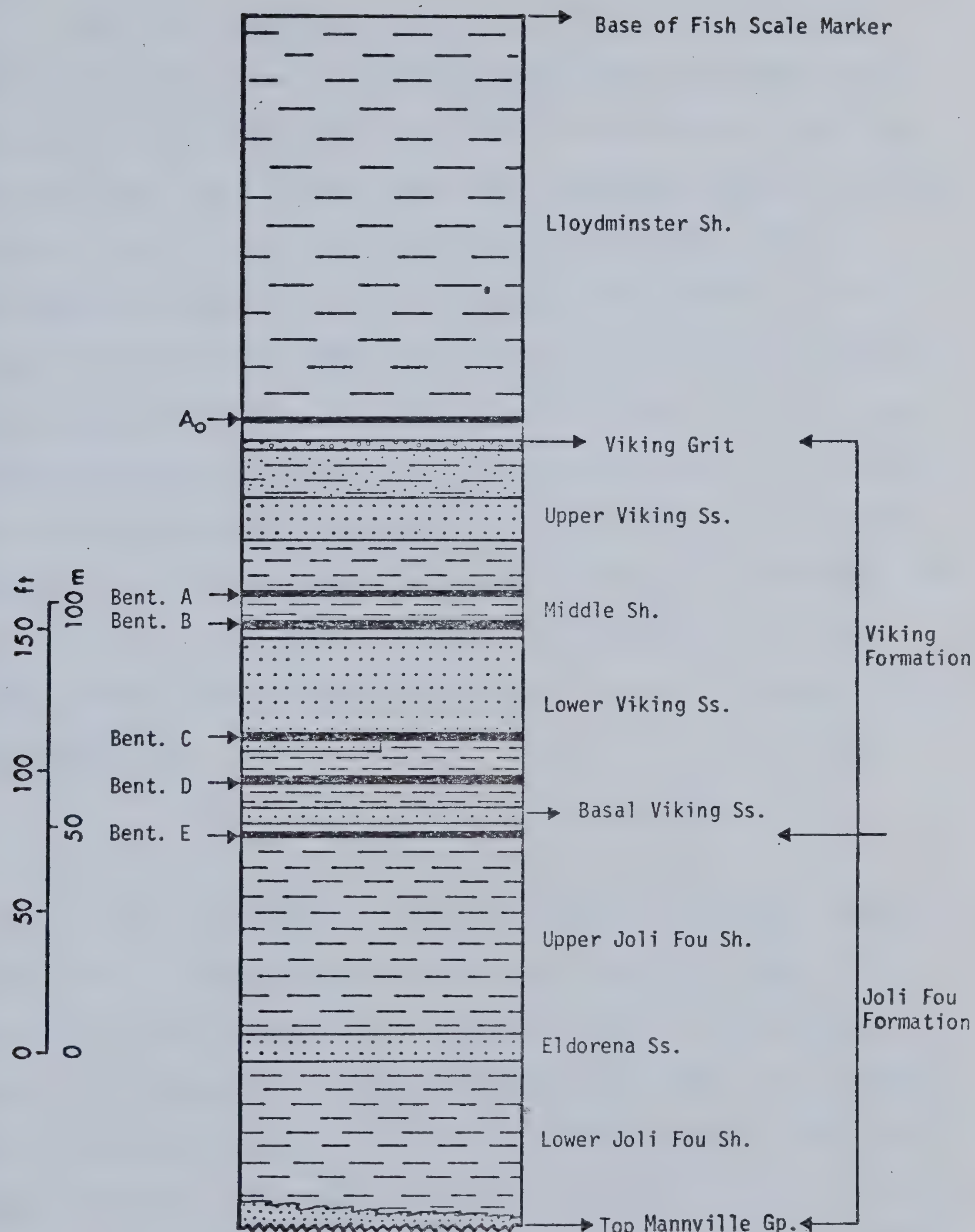

Figure 9. Schematic terminology diagram for the Viking Formation of East-Central Alberta.

Bentonite C

This is a medium grained biotite-rich bentonite which occurs at a depth of 3455 feet (1053 m) in the type well Ceja P.C.P. Leo 6-21-36-17W4M. It is 30 cm thick and lies in muddy sand at the base of a sand unit approximately 35 feet (10.7 m) above the E bentonite horizon. The C bentonite lies at the base of the Joarcam reservoir sand. Figure 10 shows that this bentonite is probably correlative with the K bentonitic shale of Evans (1970). A lower bentonite designated D (Amajor, 1977) may correlate with Evans' MN bentonitic shale. If the C to K correlation is correct, bentonite C covered the entire region bound by Townships 23 and 53, and Ranges 10 and 25 W4M, plus parts of western Saskatchewan. The identities of wells used in Figure 10 are in Appendix Ia.

Bentonite A

This is another coarse grained biotite-rich bentonite. It is 30 cm thick in the type well Mobil Matziwin 11-23-23-14W4M (Tizzard and Lerbekmo, 1975; and Amajor, 1977). It occurs at a depth of 2647 feet (806.7 m), where it is intercalated in a mudstone unit between a lower and an upper sandbody. In this well, it is 32 feet (9.7 m) above the top of the lower sand, and about 90 feet (27.4 m) above the E bentonite horizon. Generally it is identifiable in electric well logs and cores located within Townships 21 to 35, Ranges 6 to 24 W4M.

Bentonite Ao

This bentonite is greyish-white and very fine grained. In cores of the type well Banff *et al.* Matziwin 11-4-23-14W4M, it is 37 cm thick, and occurs at a depth of 2582 feet (787 m), which is 16 feet (4.9 m) above the top of the Viking. In cores from wells Mobil C.P.R. Hutton 3-19-24-15W4M and H.B. Cessford 14-26-25-12W4M, it has thinned to 30 cm. In the latter well, it is about 70 feet (21.3 m) above bentonite A; the stratigraphic position is shown in Figure 11. Based on its seemingly distinct electric well log signature, Ao appears restricted to within Townships 20 to 27, Ranges 10 to 22 W4M. The identities of wells in Figure 11 are in Appendix Ib.

In summary, bentonites Ao and A are geographically restricted to the southern part of the study area, while bentonite C is restricted in occurrence to the north. Bentonite E extends across the whole region, providing a link between the other two areas. Thus, a transitional area exists in which the three or four bentonite horizons overlap in space and can be reliably picked in cores and well logs. For instance, in well Westcoast Sulpetro Smore 10-13-30-11W4M, bentonites E, C, and A were all observed in core.

The regional distribution of these bentonites, coupled with their stratigraphic positions, permitted a general subdivision of the Viking Formation into three fairly distinctive chrono-intervals. These are informally

designated Basal, Lower and Upper. The Basal chrono-interval lies between bentonites E and C; the Lower, between C and A; while the Upper refers to that portion of the Formation above bentonite A, or between bentonites A and Ao if the latter is present. In the latter, however, the uppermost 10 to 15 feet (3.1 to 4.6 m) represents the basal section of the Lloydminster Shale. These isochronous intervals are shown in Figure 12. The well identities are in Appendix Ic.

This chronostratigraphic framework is the foundation of the present study, as representative sandbodies in each time interval were correlated and mapped, and the results integrated into a detailed sedimentological study of the probable sediment dispersal patterns and mechanisms during Viking and deposition.

General Sandstone Nomenclature and Terminology

The letters B, L, and U, denoting Basal, Lower and Upper, respectively, were used to assign sandbodies to their respective chronostratigraphic units. Discrete sandbodies within each time interval were further differentiated either by an attached numerical subscript (e.g., L_1, L_2), or were designated by the first letter of their geographic locations and subscripted with numerals, (e.g., BP_1 = Basal Provost number one; UE_2 = Upper Eastern number two). The latter scheme was used mostly for those time intervals in which sand development was localized in several geographic areas.

The assignment of numerical subscripts was either according to stratigraphic position, or was simply for convenience of discussion in cases where many sand units formed at the same time.

The terms sand-ridge, swale, and sand-ridge complex are used by some workers for storm and tide generated depositional topographic features (ridge-high, swale-low) on present-day continental shelves (Swift *et al*., 1974; Houbolt, 1968; Off, 1963).

Usage of these terms in this text follows the above because the Viking sandbodies studied are considered to be morphologically and possibly genetically similar to those of the Recent Epoch. However, the ridge and swale topography that may have existed during deposition was later highly subdued, partly as a result of sand-ridges coalescing, intergrading and overlapping, and partly due to post-depositional changes such as compaction.

Order of Discussion

The chronostratigraphic units and their sand members are discussed in stratigraphic order. Where sandbodies are chronotaxial they are treated in such a way as to best portray their lateral relationships and arrangement patterns.

Although a stratigraphic cross-section will often show all Viking sands in a given area, discussion is confined, as much as possible, to the specific sandbody developed within the specified time under discussion.

rather than including all the said units in the section. Although this means that a stratigraphic cross-section may be referred to several times, the writer believes that it makes for a more understandable treatment of the depositional behaviour of the many Viking sandbodies in time and space.

Legend for vertical facies models, cross-sections and fence diagrams is generalized and listed in Appendix VI.

CHAPTER V

SANDSTONES OF THE BASAL CHRONOSTRATIGRAPHIC UNIT

Sand units interpreted to be deposited during this time interval include the reservoir sands of the Hamilton Lake, Provost and Beaverhill Lake areas of Alberta, and the Dodsland-Hoosier areas of southwestern Saskatchewan.

A. Hamilton Lake Sand Units

Two laterally distinct thin sand units were partly mapped (Figure 13) and identified as B_1 and B_2.

The B_1 Sand Unit

The B_1 reservoir sandstone is locally referred to as the Hamilton Lake 'A' or the Provost Viking 'C' oil pool (Alho *et al.*, 1977). The sand unit is distributed within the general area roughly bound by Townships 29 and 36, Ranges 5 and 19 W4M. However, it extends further to the northwest to Township 45, Range 28W4M in linear chain-like fashion. It is therefore more than 130 miles (209 km) long and approximately 30 miles (48 km) wide. A maximum thickness of 22 feet (6.7 m) is attained around Township 31, Ranges 10 and 11 W4M. The unit is asymmetric in plan view with a steep southwest and a gentle northeast flank. The

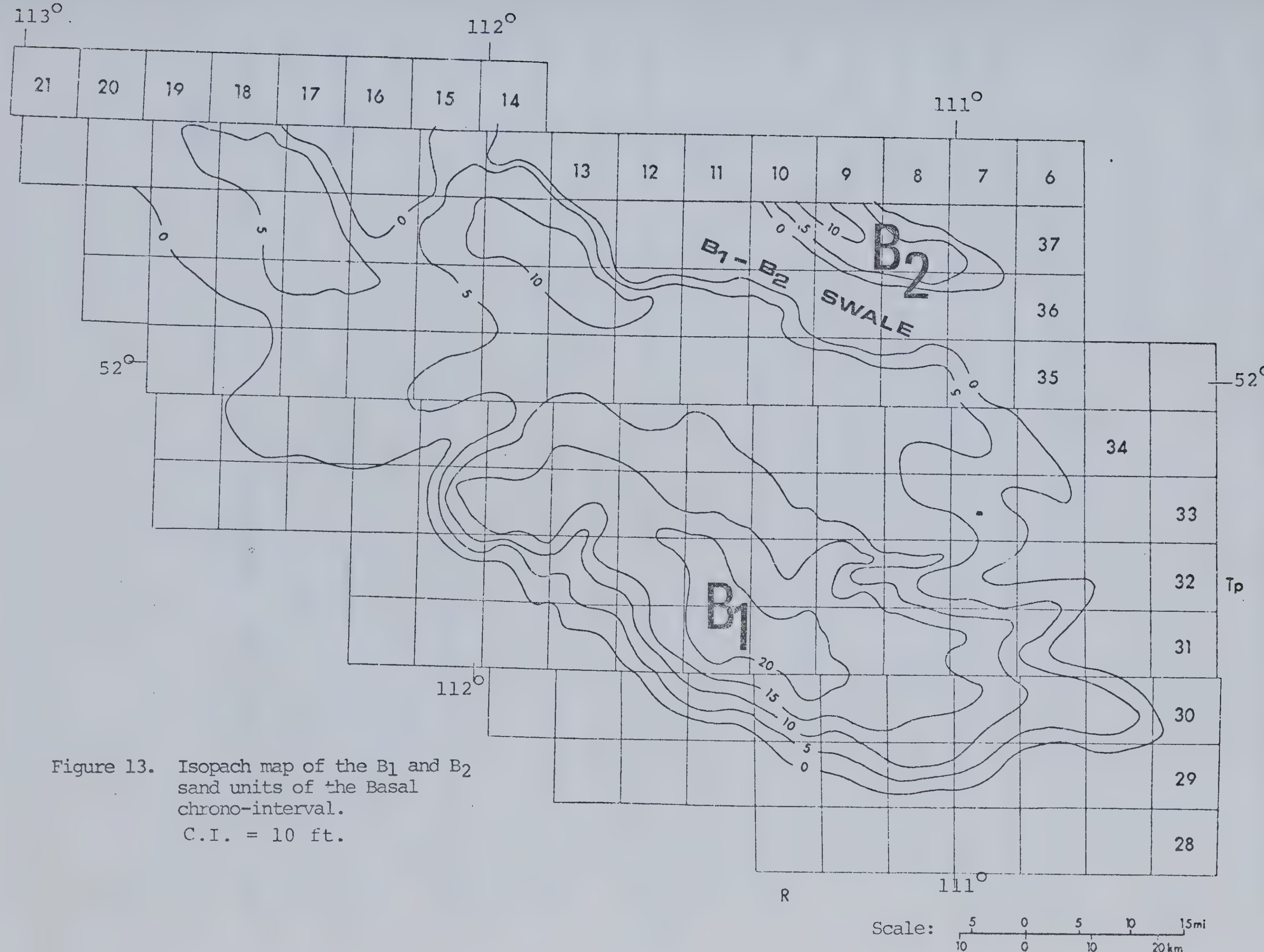

Figure 13. Isopach map of the B_1 and B_2 sand units of the Basal chrono-interval.
C.I. = 10 ft.

axis of maximum development trends approximately N45°W. Hitherto, only the net reservoir sandstone isopach map has been published.

The B_2 Muddy Sand Unit

This poorly developed very thin shaly sand unit is located northeast of the B_1 unit within Townships 36 and 37, Ranges 7 to 10 W4M. It appears to extend to Township 38, Range 11W4M in the northwest. It is more than 20 miles (32 km) long, strikes northwest-southeast, and is about six miles (9.7 km) wide. A maximum thickness of 12 feet (3.7 m) is attained in Township 37, Range 9W4M. This unit is presently uneconomic. It was not studied in detail but is included here to show its lateral relations to the B_1 and the Provost sand units, in order to generate a better picture of the prevalent paleoenvironmental conditions at that time.

The B_2 sand unit is laterally separated from the B_1 unit by an area of no sand deposition referred to as the B_1B_2 swale. It occurs between Townships 33 and 37, Ranges 6 to 13 W4M (Figure 13). B_2 is roughly 10 miles (16 km) wide and appears to continue northwest and southeast of the map area.

Cross-Sections

Three stratigraphic cross-sections were constructed perpendicular to the depositional strike of the B_1 unit with bentonite E as datum. Two of these transect the B_2 unit. The locations of the lines of section are shown in Figure 14, while well identities are given in Appendix Id.

Section D - D' (Figures 15, 18a) crosses the south-eastern part of the B_1 sand unit from Township 29, Range 9 to Township 35, Range 3W4M. Bentonites E and C are well correlated from wells 1 to 12, and 1 to 6, respectively. Northeast of these wells their respective positions are not as certain but are reasonably inferred. Most importantly, the relative position of the Basal chrono-interval is best defined by wells 1 to 6.

The B_1 unit is correlated between wells 3 and 11, and appears to lie conformably on the Joli Fou Shales. It grades into sandy mudstone in well 5 and shales out before reaching well 1 to the southwest. Its northeastern edge pinches out rather abruptly immediately beyond well 11. In the latter well the unit appears to be lower in the section suggesting, tentatively, that the unit may have shifted toward the southwest. The B_1B_2 swale appears in well 12. In general the unit is relatively poorly developed in this cross-section. Later, clean thick sand development occurs southwest of well 7.

Section E-E' (Figures 16, 18b) bisects the central

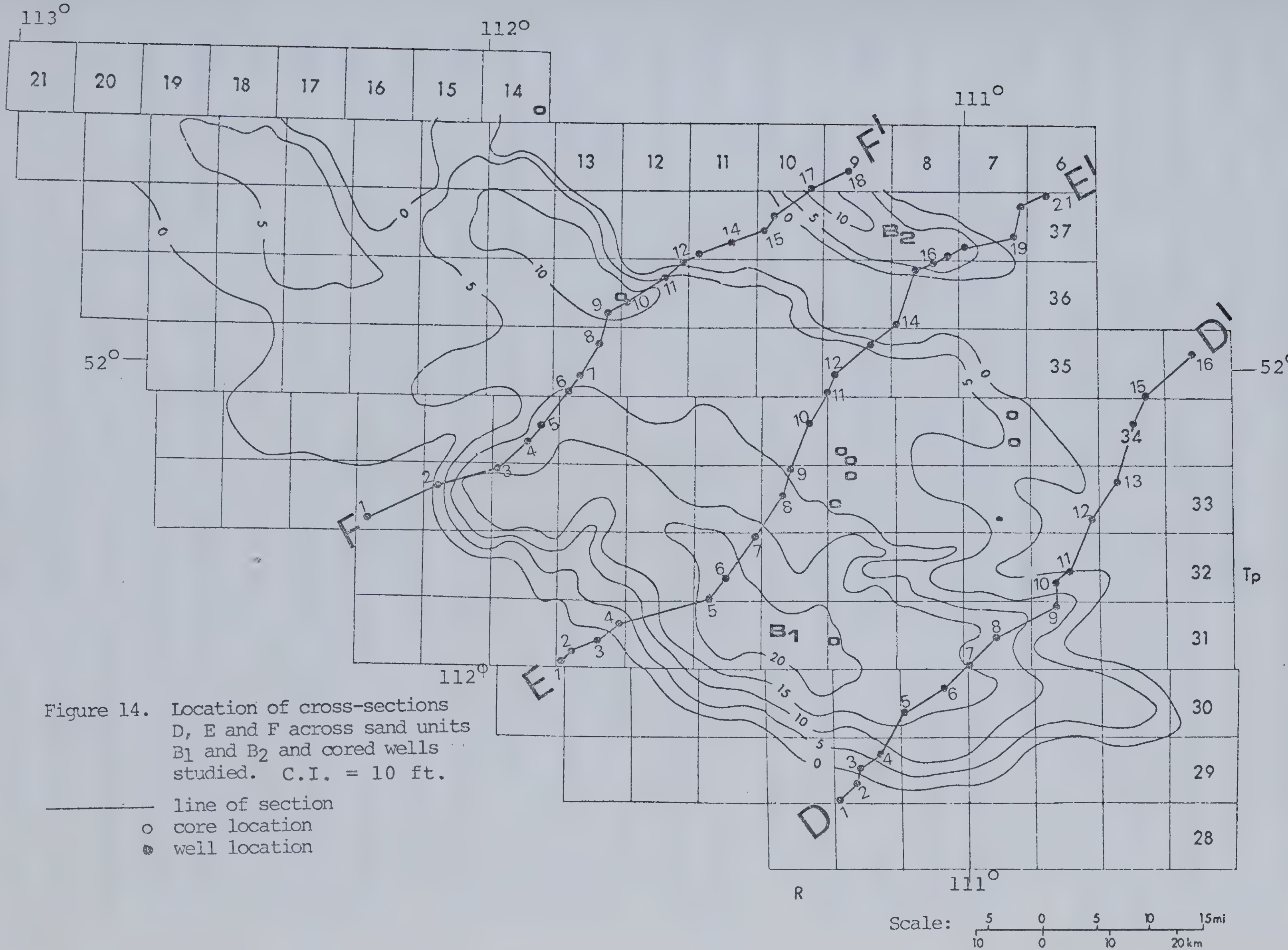

Figure 14. Location of cross-sections D, E and F across sand units B1 and B2 and cored wells studied. C.I. = 10 ft.

——— line of section
o core location
● well location

part of the B_1 sand unit and the southeastern portion of the B_2 unit. It trends southwest-northeast from Township 31, Range 13W4M to Township 37, Range 6W4M. Bentonite E is the datum and is fairly well correlated throughout the section except between wells 10 and 13, where it is interpreted to have fallen on a sandy bottom. On the other hand, the position of bentonite C is uncertain northeast of well 5.

The B_1 sand unit overlies the Joli Fou conformably between wells 3 and 14. The southwestern edge shales out southwest of well 3, whereas the northeastern margin thins and pinches out rather abruptly immediately beyond well 13. Although the resistivity curve of this unit indicates a maximum thickness of the unit near wells 4 and 8, the spontaneous potential curves indicate the sand content of the axis (wells 5 and 6) and the southwestern flank to be comparatively less than that of the northeastern part. When this observation is integrated with the interpreted relationship of bentonite E to this sand body, it indicates a southwesterly direction of B_1 migration. At the northeastern edge of the B_1 unit (wells 12 and 13), a probably discontinuous very thin sand unit occurs approximately two feet (0.6 m) and six feet (2.0 m) above the B_1 sand in wells 12 and 13, respectively, indicating a northeasterly shift of this unit. Well 14 is located on the B_1B_2 swale.

The southeastern end of the B_2 sand unit (wells 15 to 21) flanks the northeastern margin of the swale. Bentonite E is intercalated in this shaly and/or muddy sand.

Both sand units, B_1 and B_2, can be seen to be isochronous. Note the later development of thicker sand units southwest of well 5, and a thin sand northeast of well 13.

Section F-F' (Figures 17, 18c) trends southwest-northeast from Township 33, Range 16W4M through the north-western margins of B_1 and B_2 to Township 38, Range 9W4M; bentonite E is the datum. It is fairly well established between wells 1 and 6, and from 14 to 16. It must have fallen on an agitated bottom between wells 7 and 13. Bentonite C cannot be reliably correlated in this section.

The B_1 unit is recognized between wells 2 and 11. The gradational transition from sand to mudstone and finally to shale, typical of the southwestern flank, occurs between wells 5 and 1. This contrasts with the relatively cleaner sand of the northeastern edge, which pinches out rather abruptly beyond well 11 after a localized thickening around wells 9 and 10. Another local thin sand unit above the B_1 sand occurs between wells 6 and 11. In the former well it is approximately 4 feet (1.2 m) above the B_1 unit, whereas in well 10 it is about 8 feet (2.4 m), and in well 11 it is 6 feet (2.0 m) above. It also thickens and thins locally.

Wells 12 and 13 are located in the B_1B_2 swale. In these wells, particularly well 13, there appears to be a loss of about 2 to 5 feet (0.8 - 1.5 m) of upper Joli Fou section at the base of the Viking, as the Joli Fou interval is relatively thinner in these wells. The Viking interval is comparatively thinner as well, suggesting that there may

have been no deposition in the area of these wells during the early part of Viking time.

The B_2 unit at the base of the Formation in wells 14 to 18 is very muddy. Later sand development to the northeast of well 13 continued to be very sparse, whereas, to the southwest of well 12, sands became cleaner and relatively thicker. The stratigraphic relations of the Viking sandbodies in the above sections are sketched in Figure 18.

Fence Diagram

Figure 19(a,b) are fence diagrams of the Viking sandbodies within Townships 30 to 37, Ranges 1 to 19 W4M. They show the three dimensional picture of Viking deposition in the area. Figure 19a covers the area defined by Townships 30 to 37, Ranges 1 to 9 W4M. The northeastern pinchout edge of the B_1 unit occurs between the following wells 24 to 25, 34 to 35, 67 to 81, 68 to 69, 82 to 84, 83 to 84 and 88 to 110. Well 109 is located in the B_1B_2 swale, which also occurs between wells 88 and 111. The B_2 unit shows up in wells 111 and 112.

Figure 19b is a westerly continuation of the previous diagram from Ranges 9 to 19 W4M. It shows how the B_1 sand unit shales out to the southwest, pinches out to the northeast, and has a northwesterly extension beyond the limits of the diagram. Wells 108, 138 and 139 are located in the northwestern extension of the B_1B_2 swale.

To avoid crowding the diagram, the bentonites have

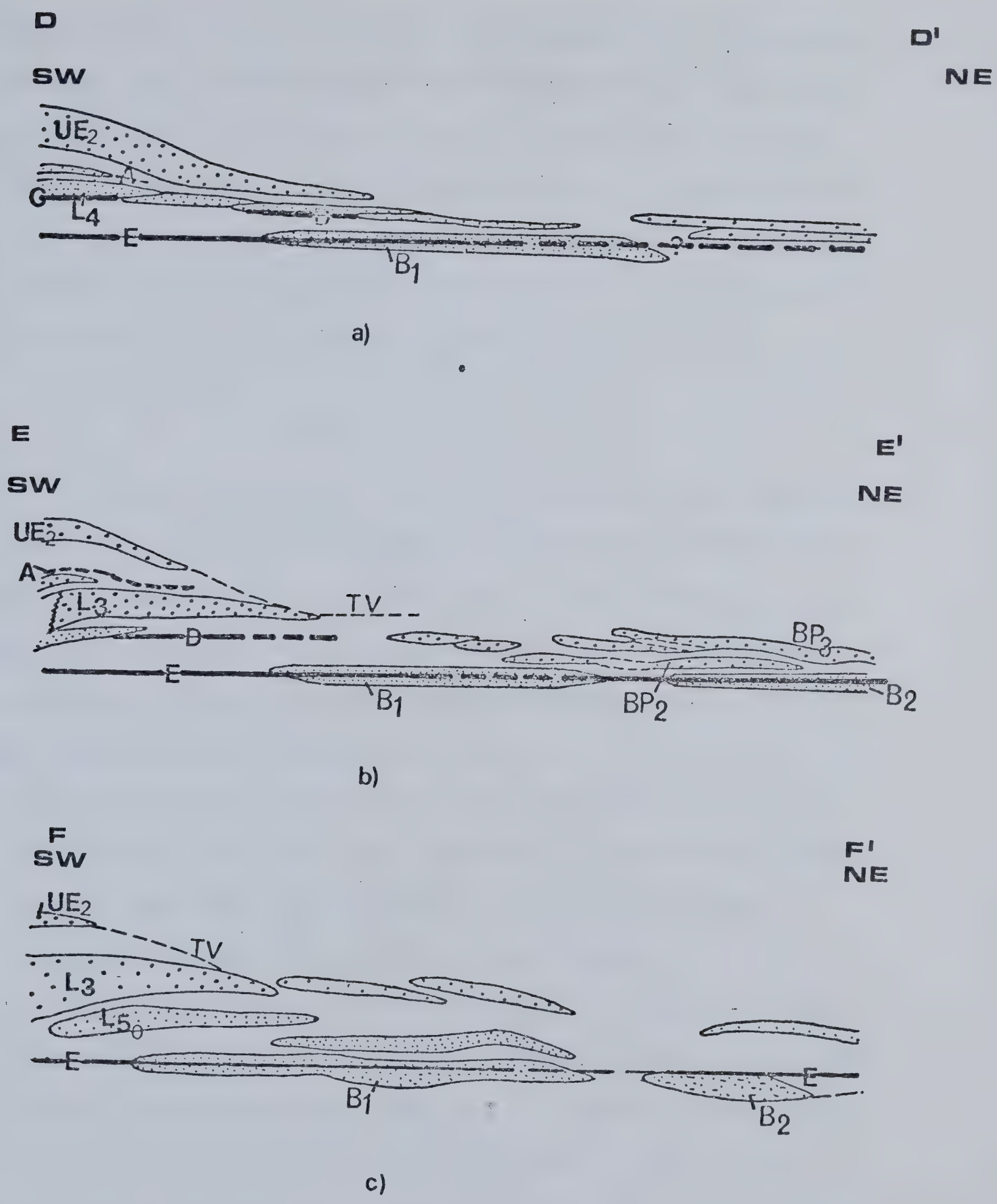

Figure 18 - Generalized sketch of gross sand distribution in cross-sections (See fig. 14 for location):

a) D - D[1]

b) E - E[1]

c) F - F[1]

– – – Top Viking

not been shown, but the trend of bentonite E in a southwest-northeast direction is most reliably followed in well succession 15 to 45 to 43 to 60, and 16 to 42 to 41 to 39 to 38 to 65. The bentonite may have fallen on a sandy bottom in the northeast, which supports a southwesterly direction of migration of the B_1 unit. The identities of wells used to construct the diagram are listed in Appendix IIa.

Core Analysis

Cores from the B_1 reservoir sandstone were studied in nine wells located in Figure 14; the detailed core descriptions are given in Appendix IIIa. The internal characteristics of this unit are treated in a generalized discussion of Viking lithofacies in Chapter VIII. However, some observations will be made here:

1. The northeast flank of this sand unit was observed to be thinner and relatively coarser and cleaner than the axial zone and the southwestern flank, which are thicker, finer, more shaly and more muddy.
2. A black fissile clay shale was found to cap this sand sharply in places. In wells 6-26-34-7 and 7-14-34-7W4M, it is respectively 4.5 feet (1.4 m) and 7.5 feet (2.3 m) thick. In the latter well the shale is silty.
3. A pebbly sand lens containing mainly black chert pebbles up to (1.2 cm) in longest dimension occurs within the above shale. The lens is located about 2.5 feet (0.8 m), and 5 feet (1.5 m), respectively, above the top of the B_1

unit in the same two wells. These wells are situated near the eastern margin of the B_1 sand unit. Although the dark fissile shale was observed in other wells it bears no pebbly sand lens where seen elsewhere.

4. In well 7-14-34-7W4M, a 3 inch (7.5 cm) coarse, biotite rich bentonite was observed very near the base of the overlying black shale. This bentonite is thought to be the E bentonite, although it is considerably thinner here.

B. The Provost Sand Units

Localized multiple sand development characterizes the Basal chronostratigraphic unit in the Provost area. Although bentonites E and C cannot be reliably picked in the electric well logs of the area, the stratigraphic positions and lateral relationships of these sandbodies to the B_1 and B_2 sandstones place them in this time interval. Some of these sand units act as reservoir for oil but they are mainly gas-bearing.

Isopach Map

A composite isopachous map of these sands is shown in Figure 20. The general poor sand development in the area, lateral restriction of the sandbodies, inadequate well control and poor electric log resolution in most places were some of the adverse factors which had to be contended with in preparation of the map. Thus, it gives only a general

indication of the thickness distribution of the Formation in the area, and the geometric configuration of individual sand bodies is not portrayed. However, as far as possible, they were differentiated and correlated in the cross-sections and fence diagrams.

The isopach map shows the Provost Viking sands to be slightly displaced to the east of the B_1 unit. They occupy the general area bound by Townships 34 and 39, and Ranges 1 and 12 W4M. This sand unit also extends into western Saskatchewan, but there it is very thin and poorly developed. A maximum thickness of about 32 feet (9.8 m) is developed around Township 35, Range 7W4M. The sandy area is slightly more than 66 miles (106 km) long and is about 30 miles (48 km) wide. Pronounced isopach noses are confined to the eastern and western margins of the map and may in part represent the margins of discrete sandbodies. The western nose is constricted within the B_1B_2 swale around Township 36, Ranges 9 to 12 W4M.

In cross-sections and fence diagrams, recognizable discrete sand units were designated BP_1, BP_2 and BP_3 according to stratigraphic position.

Cross-Sections

Six closely spaced stratigraphic cross-sections utilizing the top of the Formation as datum were used to diagnose this area in an attempt to unravel the rather complex depositional pattern of these sandbodies. The section

locations are shown in Figure 20(a,b). The identities of wells used in the cross-sections are given in Appendix Ie.

Section G-G' (Figs. 21,27a) is a southwest-northeast section from Township 34, Range 7W4M to Township 38, Range 3W4M.

The thin sand unit at the base of the Formation in wells 1 and 2, which pinches out before well 3, is the B_1 unit. It is overlapped by the BP_1 unit, best developed in wells 3 and 4. An intergradational area in wells 5 and 6 separates the latter sand unit laterally from the BP_2 sand unit to the northeast (wells 7 to 9). The basal contact of the BP_2 unit, as interpreted from the electric well logs, is sharp in wells 8 and 9, becoming gradational to the southwest (well 7). The BP_3 sand unit, which is slightly higher in the section, appears in well 10 and extends to the northeast up to and including well 16. The spontaneous potential curve displays characteristic sharp lower and gradational upper contacts. The lateral relationship with the BP_2 unit is not obvious in this line of section, probably due to the low borehole density in the area.

Section H-H' (Figs. 22,27a) trends southwest-northeast from Township 35, Range 7W4M to Township 36, Range 5W4M. It is about 3 miles (4.8 km) northwest of section G-G'. The lowest sands in the section are the B_1 (well 1) and another very thin unit in well 7 designated B_{2a}. The former pinches out before well 2. The poorly developed BP_1 unit in well 2 is stratigraphically lower but appears to override the B_1

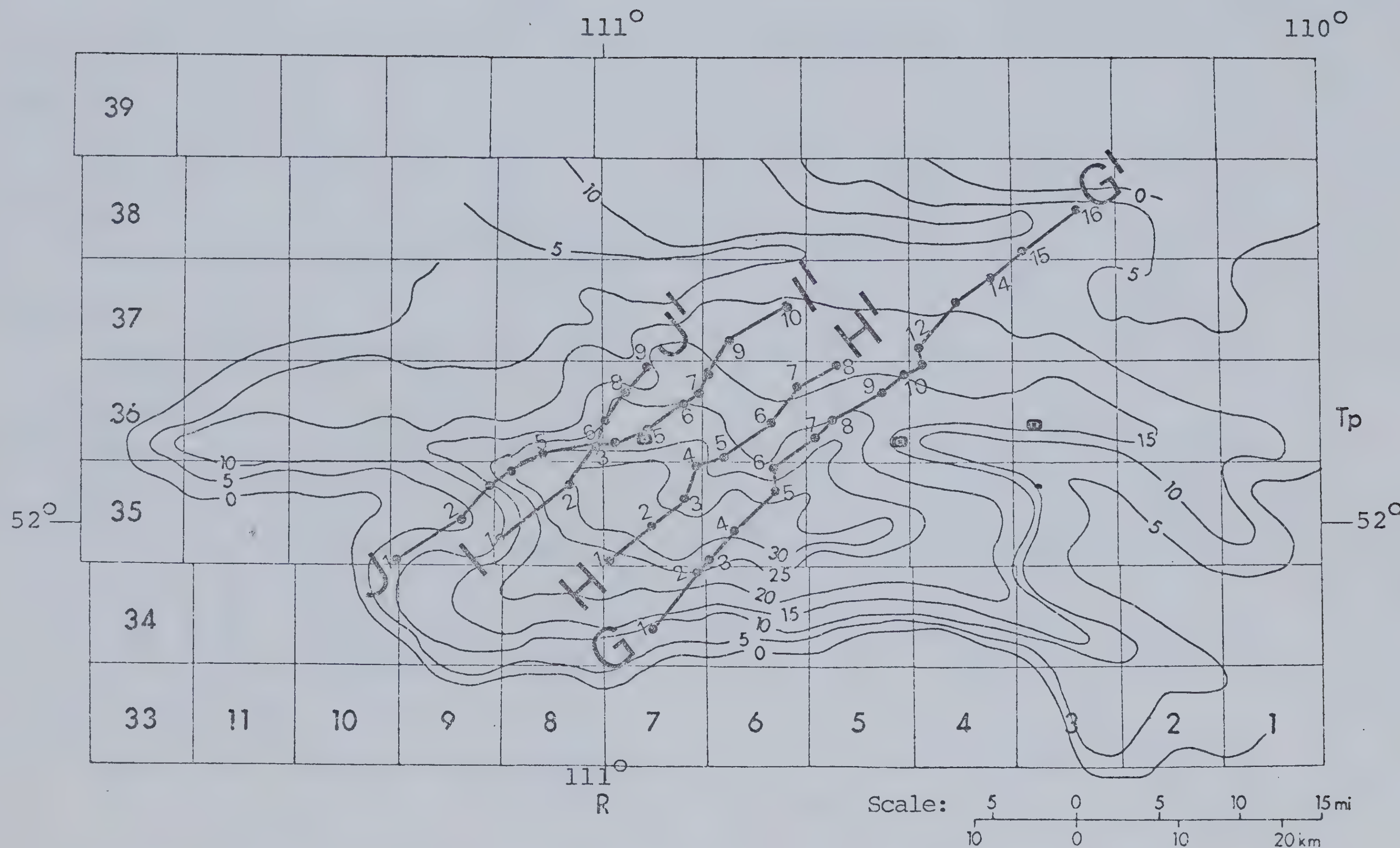

Figure 20a. Location of Provost cross-sections G to J and cored wells studied. C.I. = 10 ft.

——— line of section
⊙ core location
● well location

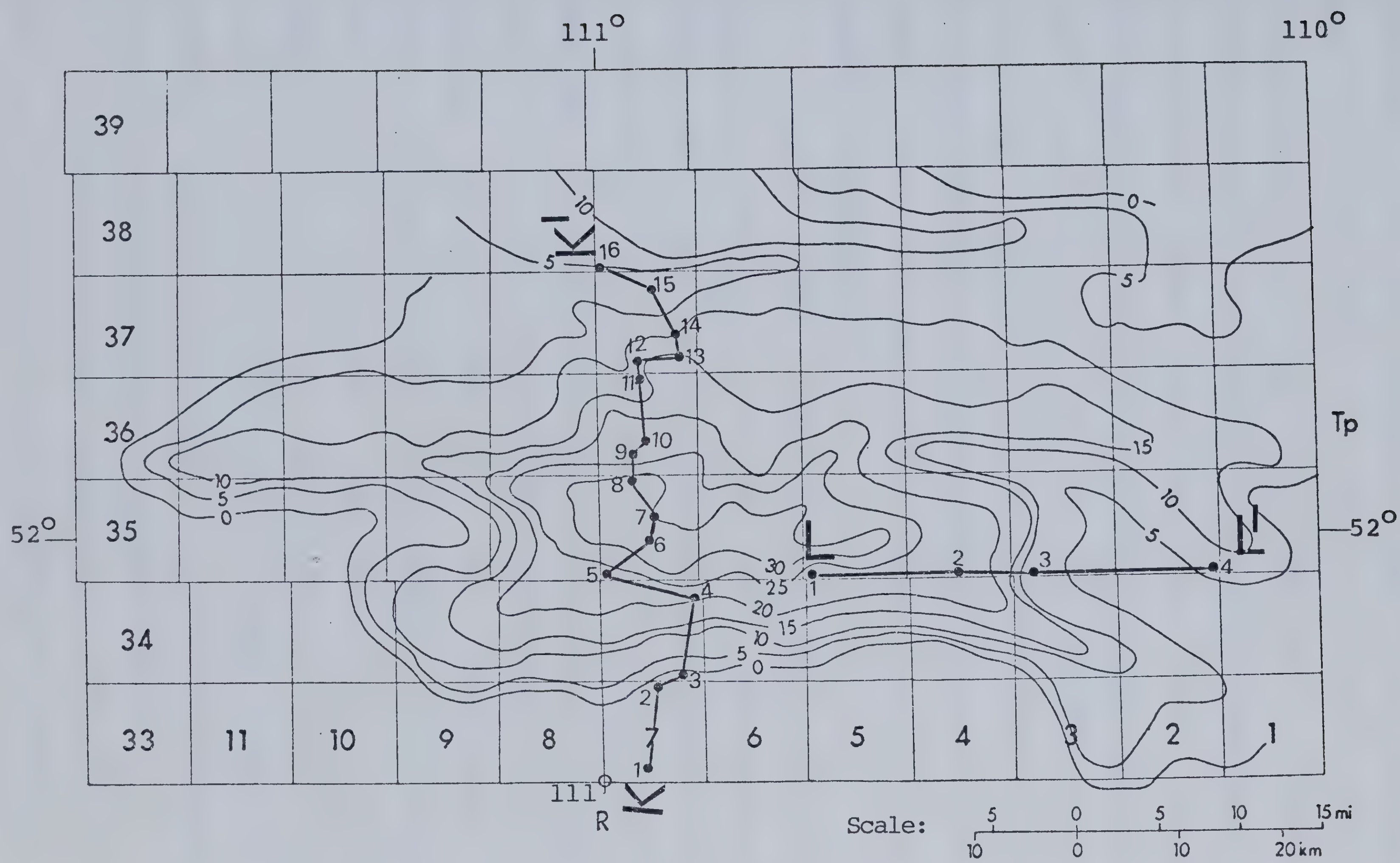

Figure 20b. Location of Provost cross-sections K and L.

——— line of section

● well location

unit to the southwest. Well 2 is located in the southeastern extension of the B_1B_2 swale very close to the northeast pinch-out edge of the B_1 unit (well 1). The very low stratigraphic position of BP_1 and its relation to B_1 may be evidence that the B_1B_2 swale was scoured in this area. The BP_2 sand unit is best traced from wells 4 to 6. Maximum thickness development is in well 5. It thins rapidly toward well 7, where it overlies the very thin B_{2a} unit, and pinches out before reaching well 8. The BP_3 unit in well 8 is well developed and higher in the section. It overrides the BP_2 and BP_1 units, in wells 7 and 2 respectively, in a southwesterly direction.

In this cross-section, the lateral relationship of BP_1 to BP_2 sandbodies is not very clear. It appears as if the BP_1 unit in well 2 is the mudstone-siltstone facies of the BP_2 unit to the northeast. However, the writer feels that well 2 probably represents the northwestern margin or edge of the BP_1 unit and that the two sand units may laterally coalesce in this area. This interpretation is based on the fact that the BP_1 unit and its lateral relations with the BP_2 are better defined in the previous cross-section (Figure 21). More well control is needed for better resolution of the lateral relations. This could be important because this sandbody (BP_1) is one of the few oil reservoirs in the Viking of the Provost area.

Section I-I' (Figs. 23,27a) is oriented southwest-northeast from Township 35, Range 8W4M to Township 37,

Range 6W4M, and is roughly 3 miles (4.8 km) to the northwest of section H-H'. The basal sand units in wells 1 and 2 and well 9 are, respectively, the B_1 and the very thin B_{2a} observed in section H-H'; B_{2a} was observed only in these 2 wells. It is interpreted as chronotaxial to the B_1 and B_2 sand units. However, it is slightly displaced to the southeast of the latter unit and may be laterally distinct from it.

The BP_1 is thought to pinch out southwest of this section. However, its thin northwestern edge is just recognizable at the base of wells 3 and 4. The BP_2 unit attains its thickest development in wells 5 and 6. It overlaps the B_1 to the southwest in wells 1 and 2, shaling out in that direction. It thins to the northeast (well 8) and pinches out before well 9. Careful examination of the logs of wells 5 and 6 shows the BP_2 unit to be lower in the section in well 6. It is felt that about 10 feet (3.0 m) of Upper Joli Fou section may be missing at the base of the Viking in this well, which is located in the B_1B_2 swale but near the southeastern edge of the B_2 unit. The missing section would be further evidence of scouring in the B_1B_2 swale. However, subdued and incomplete electric log response in the lower part of the Joli Fou section inhibits assessment of the true nature of the Viking-Joli Fou contact in the general Provost area. The BP_3 unit, best developed in wells 9 and 10, caps the BP_2 in this section. Erratic thickening and thinning of the BP_3 is probably related to the topography of the

underlying BP_2 sand. The BP_3 apparently thickens (wells 2 to 4 and 9 to 10) where the BP_2 is thin and thins (wells 5 to 8) where the BP_2 is thick.

Section J-J' (Figs. 24,27b) is also oriented southwest-northeast from Township 35, Range 9 to Township 36, Range 7W4M. This section best demonstrates the vertical stratigraphic relationship of the BP_2 to the BP_3 sand unit.

The B_1 and B_2 sandbodies are correlated at the base of the section in wells 1, 2 and 9. They are immediately overlain by the BP_2 unit, which attains maximum development in wells 6 and 7. This sand thins and shales out to the southwest before reaching well 1 and to the northeast beyond well 9. The best development of this unit is within the general area of the B_1B_2 swale. The BP_3 sandstone, in turn, overlies the BP_2. Maximum development is in the area of wells 4 and 5 on the southwestern flank of the underlying BP_2 unit. In general, this line of section demonstrates fairly well the independent existence of the BP_2 and BP_3 sands.

Section K-K' (Figs. 25,27b) runs south to north from Townships 33 to 38, Range 7W4M. The lowest Viking units are the B_1 and B_2, restricted respectively to the bottom of wells 1 to 5, and 11 to 15. The northern margin of the BP_1 unit is poorly developed in well 6. It is thought to override the B_1 sand in a southwesterly direction. An interridge area where the BP_1 and BP_2 coalesce may exist between wells 6 and 7. The latter unit attains maximum development

in wells 9 and 10 and thins toward the southwest to well 7. To the northeast, it thins very rapidly above the B_2 sandbody in well 10 and pinches out prior to reaching well 13. The BP_3 sandbody in wells 13 to 16 overrides the BP_2 sandstone in a southwesterly direction from well 12 up to well 6 and shales out beyond the latter well. It is seen to thin where the underlying BP_2 unit is thick and thickens where the BP_2 is thin.

Section L-L' (Figure 26) trends west-east along Township 35 from Ranges 2 to 5 W4M. It is included here to show the unequivocal loss of upper Joli Fou section at the base of the Viking. A comparative examination of the electric well log curves of wells 2, 3 and 4 indicates that about 14 feet (4.3 m) of upper Joli Fou section is missing at the base of the Viking in well 3. The similarity of the electric log curves of the Formation in these wells may indicate that the section has occurred prior to the deposition of Viking muddy sands in the area. The area lies on the southeastern extension of the B_1B_2 swale. The northeastern wells in section D-D' (Figure 15) also show the very poor Viking sand development east of the general Provost area.

The depositional relationships described in Figures 21 to 25 are sketched and shown in Figure 27(a,b).

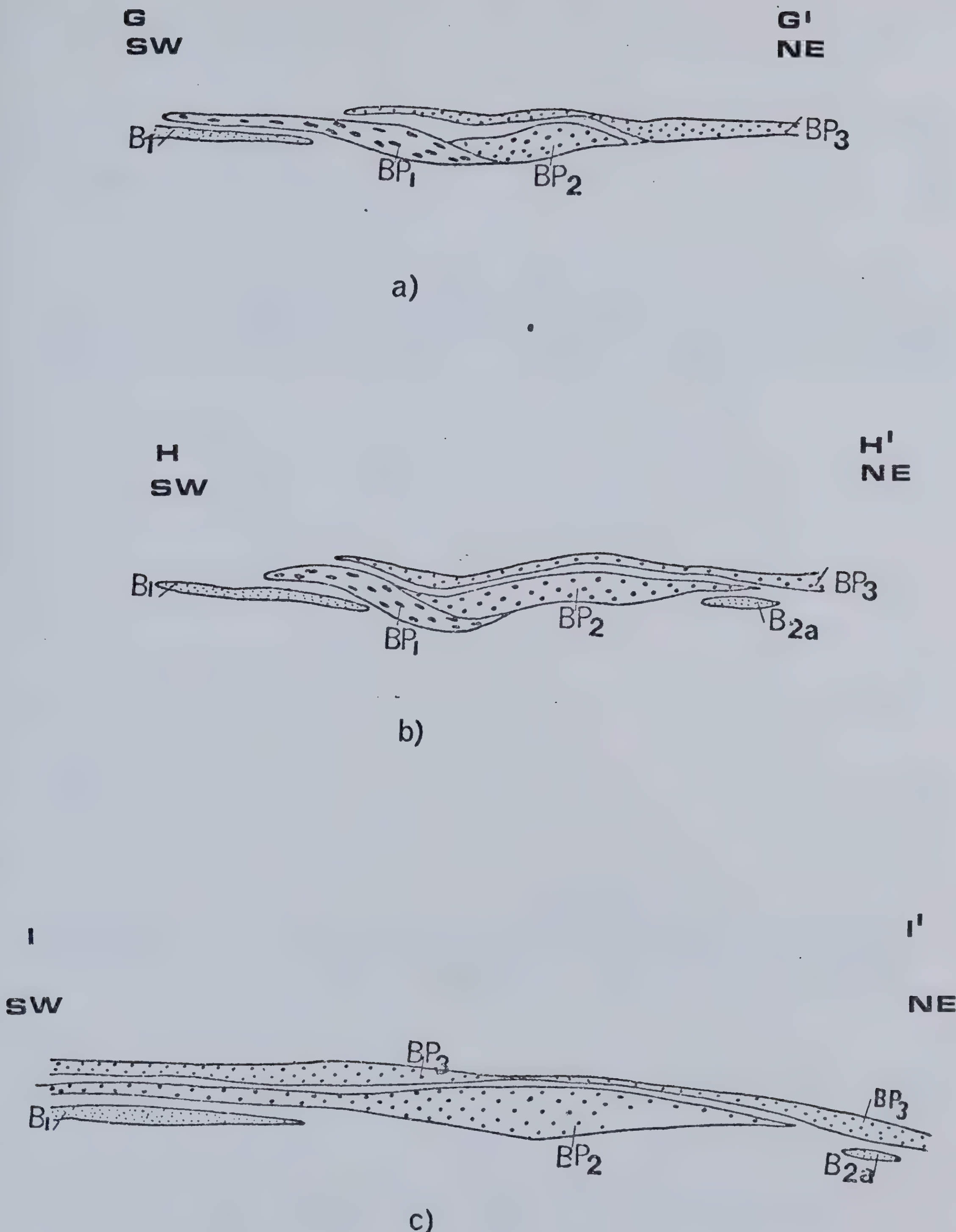

Figure 27a. Generalized sketch of gross sand distribution in cross-sections (see fig. 20a for location):
a) G-G'
b) H-H'
c) I-I'

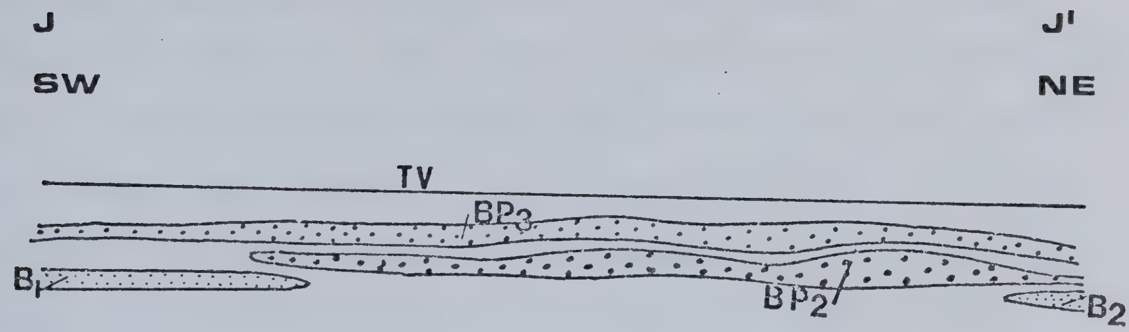

a)

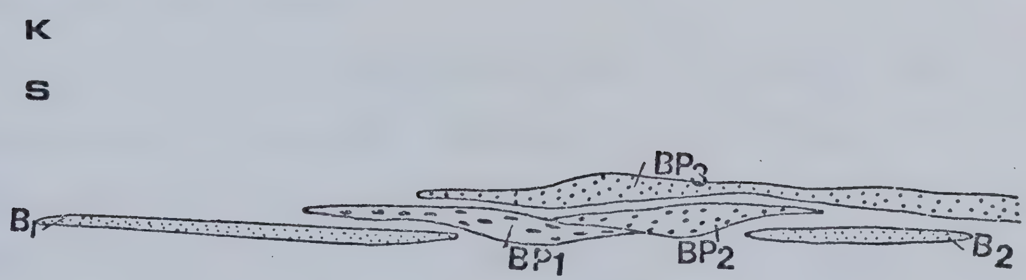

b)

Figure 27b. Generalized sketch of gross sand distribution in cross-sections (see figs. 20a & b for location):
a) J-J'
b) K-K'

Fence Diagram

The Viking thin sands in Figure 19a include the BP_1, BP_2, BP_3 and an extension of Evans' (1970) 'O' sand member into Alberta. The BP_1 unit can be seen to shale out to the northeast between wells 116 and 118, 120 and 121, and 120 and 122, while the BP_2 pinches out between wells 70 and 77, 81, 79 and 78 to the northeast and between wells 32 and 70, 34 and 69, 67 and 68, and 82 and 84, to the southwest. The BP_3 unit overlaps the latter and terminates Viking sand deposition in most parts of the area. The BP_1 and BP_2 units overlap the northeastern edge of the B_1 sandbody in turn in wells 68, 84, 87 and 88, while B_2 is overlapped by BP_2 in wells 111 and 112. In general, the diagram shows the localized nature and weakly defined NW/SE trend of these sands.

Poor sand development characterizes the eastern and southeasterly parts of the diagram (e.g., wells 2, 3, 4, 5, 26, 27) except for the Alberta extension of the 'O' sand member of the Dodsland-Hoosier area of southwestern Saskatchewan in well 28. The correlation shows the time of formation of this unit to be within the Basal chrono interval, probably the earliest part of the interval.

Core Analysis

Well Fina Provost 10-9-36-7W4M, which supposedly cored through the BP_2 and BP_3 units, was found to have only the upper 4 feet (1.2 m) of the BP_3 sandbody in core boxes; the rest of the cores were missing. The description of this short core is in Appendix IIIb. No other cores from this area were studied. However, Thomas (1977) noted that the Viking cores from wells 13-12-36-5W4M and 16-17-36-3W4M in the Provost area display a fining upward textural gradient with sharp basal contacts. Although he did not differentiate the sandbodies, it is now known that the cores were recovered from the BP_2 and BP_3 units, respectively. On the basis of the fining upward sequence, Thomas interpreted these sands as transgressive. To the present writer, the observed scours and/or channels, the sharp lower and gradational upper contacts inferred from most spontaneous potential curves, the fining upward textural gradient in cores, the lateral restriction of these sandbodies, and their northwest extension into the B_1B_2 swale, coupled with the apparent topographic control of BP_2 on the distribution of BP_3, favour an interpretation of channelized and channel fill deposits. These 'channels' may have overlapped in places producing a slightly imbricated arrangement. In a southwesterly direction, however, incomplete logging of the interval between the Base of the Fish Scales and the Base of the Joli Fou Shale in most wells in the area hinders absolute resolution of these channels. These scours and/or

channels occur at the southeastern extension of the B_1B_2 swale and may have formed prior to Provost Viking deposition by currents responsible for the later genesis of the B_1 sandbody.

Alternatively, the BP_1, BP_2 and BP_3 units may have been nucleated simultaneously within Township 35, Range 6; Township 36, Range 7 and Township 37, Range 7 W4M, respectively. Migration in a southwesterly direction coupled with pene-contemporaneous scouring of the seabed in places may explain the above observed characteristics.

The Beaverhill Lake sands of Alberta and the sand members of the Dodsland-Hoosier area of western Saskatchewan known to form during this time were not mapped but appear in cross-sections. They will be discussed later as they are closely related to sand units of other chronostratigraphic intervals in these areas.

After the deposition of the sands of the Basal chronostratipgrahic unit the locus of major Viking sand development shifted slightly to the southwest during the lower chrono-interval.

CHAPTER VI

SANDSTONES OF THE LOWER CHRONOSTRATIGRAPHIC UNIT

Bentonites C and A represent the lower and upper surfaces of this unit. In a few places, however, bentonite E marks the lower boundary. The unit is characterized by extensive deposition of relatively thick sand ridges. Multiple sand ridge developments, herein referred to as sand ridge complexes, were localized in three main areas. From south to north, they are: (a) the Lower sand ridge complex; (b) the Joffre sand ridge complex; and (c) the Joarcam sand ridge complex. The latter two contain units that are oil reservoirs.

A. The Lower Sand Ridge Complex

Figure 28 is an isolith map of this sandstone complex. The complex lies within the general area roughly enclosed by a line through Princess, Drumheller, Twinning, Innisfail, Clive, Ewing Lake, Sullivan, Youngstown, Oyen and Bindloss. The area lies to the southwest of the sands (Hamilton Lake - Provost) of the Basal chrono-unit. It trends northwest-southeast for a distance of more than 350 km. Maximum width and thickness are approximately 125 km and 38 m, respectively. Ten sandstone ridges

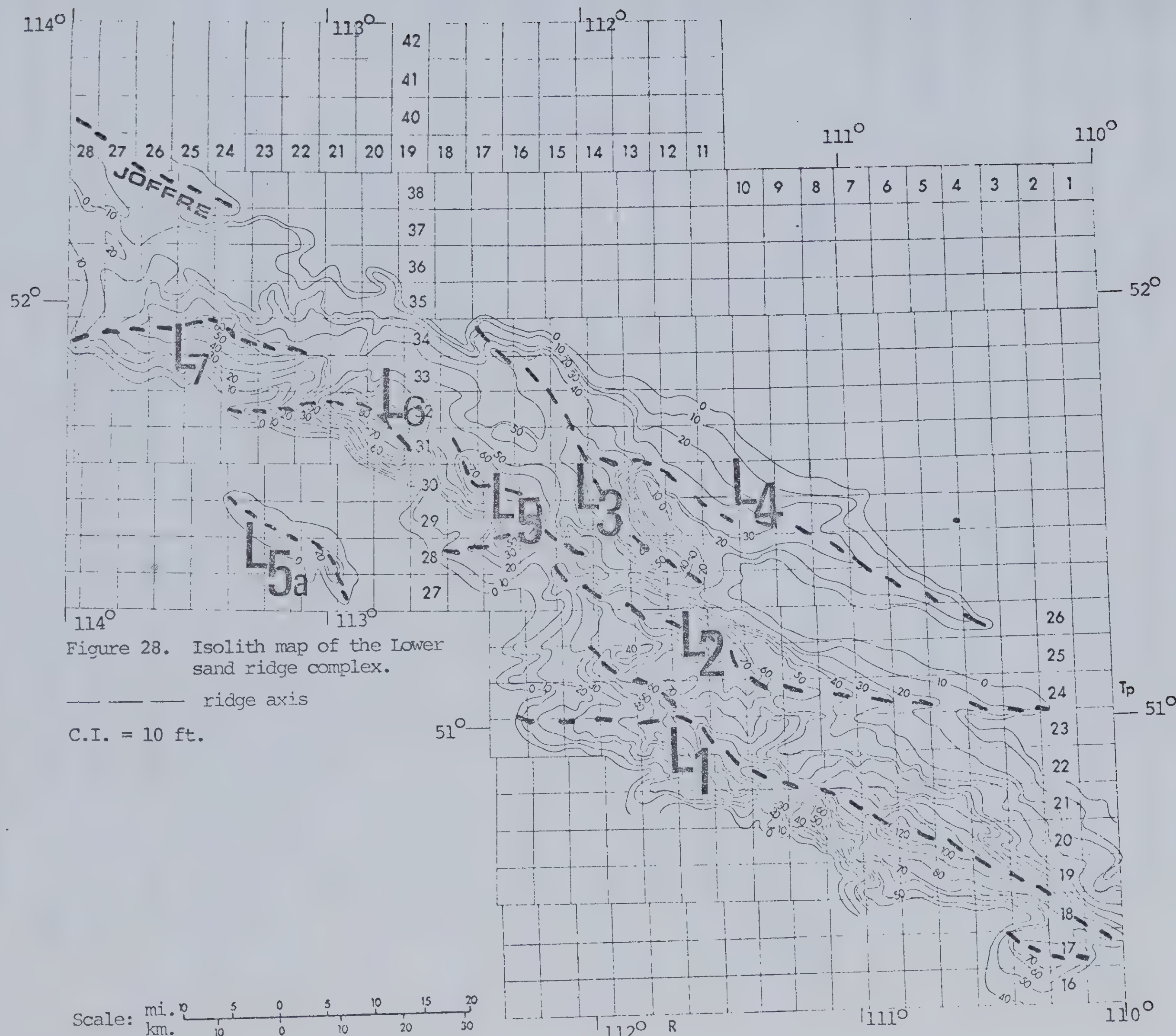

Figure 28. Isolith map of the Lower sand ridge complex.

—— —— —— ridge axis

C.I. = 10 ft.

designated L_0 to L_9, constitute the complex. Seven were mapped and three more are recognized in stratigraphic cross-sections. The ridges are linear in plan view and are arranged in a parallel to chain-like pattern in places. Poor to well defined interridge swales are characterized by relatively thin or no sand deposition. The northeastern margin of the complex is thin and remarkably straight. In contrast, the southwestern margin is thick, steep and indented.

In general, the Lower sand ridge complex was studied in most detail. Each unit was examined by means of several stratigraphic cross-sections plus cores, where available, in order to determine the depositional development. These ridges will be discussed from southeast to northwest for convenience.

The L_1 Sandstone Ridge

Isolith

This ridge occupies the northeastern half of the area bounded by Townships 16 and 23, Ranges 1 and 17 W4M. It is the most southwesterly ridge of the southwestern half of the Lower sandstone complex. The unit trends roughly N45°W for more than 90 miles (150 km). Maximum width is approximately 40 miles (65 km). Maximum thickness of 125 feet (38 m) is developed within Township 21, Range 6W4M. From there it thins to the northwest and southeast.

The ridge is linear and asymmetrical with a steep

southwest flank and indented margin resulting in localized thicker lobes and 'noses' such as those in Township 17, Ranges 2 and 3; Township 21, Ranges 7 and 8; and Township 23, Ranges 14 to 16. The southeast part of the northeast margin is fairly straight, whereas the northwestern part is irregular and indistinctly resolved from the L_1L_2 swale. The L_1 unit is the longest, widest and thickest member of the Lower sandstone ridge complex.

Cross-Sections

One northwest-southeast and four southwest-northeast oriented stratigraphic cross-sections were constructed parallel and perpendicular, respectively, to the depositional strike of this ridge. Distinct and laterally persistent electric log signatures were used as datum points because correlations of the C, D and E bentonite beds were thought not to be very certain. The locations of the lines of section are shown in Figure 29, while the identities of the wells are given in Appendix If.

Section M-M' (Figs. 30,35a) is oriented parallel to the depositional strike from Township 25, Range 14 to Township 17, Range 1W4M. Two distinct electric log kicks were used as datum points.

Nucleation of this ridge may have occurred with the development of a thin basal sand in wells 10 to 14. Maximum sandstone development occurs in these wells where the base of the sand is stratigraphically low. Well 10 occurs within the zone of multiple sand development, axial thinning and

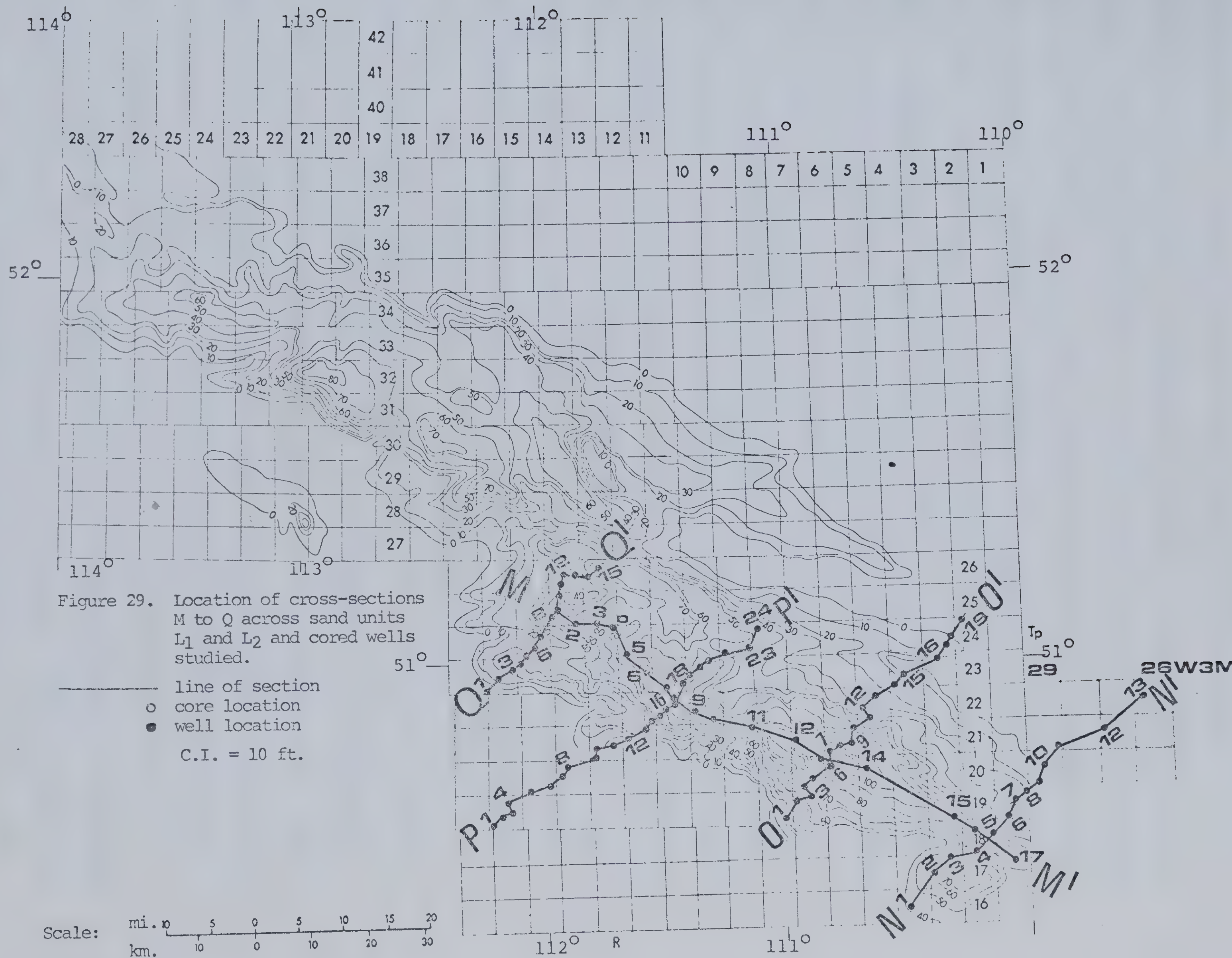

Figure 29. Location of cross-sections M to Q across sand units L_1 and L_2 and cored wells studied.

——— line of section
o core location
● well location

C.I. = 10 ft.

constriction. The L_1 sand shows varying thickness to the northwest of well 10. The writer is of the opinion that the phenomenon observed between wells 8 and 10 may indicate that the sand in wells 1 to 7 may in fact belong to another ridge. This question could not be resolved because of poor well control. Ridge growth parallel to the depositional strike is evident between wells 1 and 4 to the northwest and 14 to 17 to the southeast, as the base of the ridge rises in these directions relative to the datum.

Vertical ridge growth continued up to the time of the bentonite A ashfall as the latter lies immediately atop the ridge, except in wells 1 and 4 where it lies in mudstone about 12 feet (3.7 m) and 8 feet (2.4 m), respectively, above the ridge. This suggests that ridge growth in the northwest terminated earlier than in the southeast. Sandy mudstone deposition characterizes the post bentonite A (Upper Viking) interval. The Ao bentonite, reliably correlated between wells 1 and 9 to the northwest, maintains a fairly constant position of 15 feet (4.6 m) above the top of the Viking Formation. Relative to the top of the formation, the Base of Fish Scales horizon rises to the southeast as the Lloydminster Shale thickens in the same direction.

Section N-N' (Figs. 31,35a) is oriented in a southwest-northeast direction from Township 16, Range 4W4M to Township 22, Range 26W3M in southwestern Saskatchewan. A distinct electric log kick in the Joli Fou (probably a bentonite) is the datum. The section crosses the extreme southeastern

part of the L_1 ridge which extends from wells 1 to 8. The unit is thin near the northeastern margin (wells 6 to 8), thickening to the southwest as it rises relative to the datum, attaining maximum development in well 2. In well 1 it is shown to override the unmapped L_0 ridge. The spontaneous potential log curves show the lower contact to be fairly gradational and the upper to be sharp.

Bentonite A lies very close above the top of the ridge. An isochronous sand unit with an almost uniform thickness of 35 feet (10.7 m) overlies the L_1 ridge between wells 1 and 3. A swale area characterized by fine sand deposition in wells 4 and 5 separates this unit laterally from a series of southwesterly advancing sand units to the northeast in wells 6 to 13. These sand units are shown to override the northeastern thin margin of the L_1 ridge between wells 6 and 9.

The Lloydminster shale between the top of the Viking Formation and the Base of Fish Scales marker thins slightly to the southwest from 200 feet (61 m) in well 13 to 190 feet (58 m) in well 2.

Section O-O' (Figs. 32,35a) is also oriented southwest-northeast from Township 19, Range 8 to Township 24, Range 2W4M. A distinct and laterally persistent electric log kick in the Joli Fou Formation is used as datum. The cross-section transects the area of maximum sand development of the L_1 unit.

The characteristics of the L_1 ridge observed in the

previous section are repeated here (southwest diachronism; thin northeastern flank overlapped by a series of northeastern sands migrating to the southwest (wells 9-15); the L_o unit overlapped by the L_1 unit (wells 1 to 3); and the A bentonite atop the ridge). The principal difference is that in this section the unit is thickest between wells 5 and 8, and displays a stronger southwest asymmetry characterized by a thin northeast margin and a thick, steep southwest margin. It also shows the poorly developed southeastern tip of the chronotaxial L_2 sand ridge in wells 16 and 18, which is laterally separated from the L_1 by an interridge swale between wells 15 and 16.

Post A bentonite sand deposition is limited southwest of well 8. In this area the A_o bentonite is reliably correlated and the interval from the top of the Viking to the A_o bentonite thickens to the northeast, further indicating a probable southwest direction of early Lloydminster sea flooding. The deposits of this sea thicken to the northeast from 170 feet (52 m) in well 1 to 200 feet (61 m) in well 17.

Section P-P' (Figs. 33,35b) trends southwest-northeast from Township 19, Range 16 to Township 24, Range 8W4M. The D bentonite horizon is the datum. The section is constructed through the constricted axial zone of the L_1 ridge and the southwestern part of the adjacent L_2 unit.

Southwest of well 15 (Township 22, Range 11W4M) thin discrete sand units are developed within the Joli Fou

Formation. The distinct occurrence of the L_1 unit is restricted to the region between wells 12 and 20. Southwest of the latter well the L_1 rises stratigraphically as it migrates in that direction. Maximum thickness is attained in well 17, from where it thins to the southwest, finally grading into mudstone in well 12. It is clearly seen to override tne L_o unit between wells 13 and 17, as both units migrate landward. The L_o unit grades into mudstone in well 10. Northeast of well 20, an interridge swale (wells 21 and 22), characterized by multiple thin muddy sand deposition, separates the L_1 unit laterally from the L_2 unit in wells 23 and 24.

The vertical development of the ridges in this section continued up to about the time of bentonite A, which is better marked in the electric log of wells 18 to 24.

Note that post-A bentonite sand deposition occurs in two distinct areas. To the extreme southwest (wells 1 to 6) an Upper Western sand is seen to prograde to the northeast in the opposite direction to that typical of the lower L_o and L_1 units. It is laterally separated from them by a swale (wells 9 and 10) characterized by sandy mudstone deposition. In the extreme northeast (wells 19 to 24) two Upper sand units migrating to the southwest are developed. The lower thin unit, UE_o, develops in the L_1-L_2 swale (wells 21 and 22). The stratigraphic position of the A_o bentonite is as shown between wells 7 and 17, but is only inferred between wells 1 and 7. Relative to the top of the Formation, the Base of the Fish Scales horizon rises

slightly to the southwest as the Lloydminster shale thins in that direction.

Section Q-Q' (Figs. 34,35b) is oriented southwest-northeast from Township 23, Range 16 to Township 26, Range 13W4M; the D bentonite is the datum. The section crosses the extreme northwestern margin of the L_1 and part of the L_2 ridge.

The L_2 ridge is shown in well 15. The L_1-L_2 swale lies between wells 11 and 14. The L_1 ridge rises as it migrates to the southwest of well 10 and thins in well 7 located within a swale along the northwestern margin. It thickens again in well 6 and finally thins to well 3 grading into mudstone in well 2. The two areas of L_1 thickening are 'noses' developed along the northwestern margin. Within the L_1-L_2 swale in wells 12 to 14, a thin sand unit about 8 feet (2.4 m) above the Lower sand appears to migrate up the southwestern slope of the L_2 ridge. This may be an indication of the manner of sand accretion onto the ridge.

In this section L_1 and L_2 sand deposition ceased before the bentonite A ashfall, as the latter lies in mudstone about 10 to 12 feet (3 to 3.7 m) above the top of these ridges. Note that wells 1 and 2, characterized by very poor sand development, separate the Upper sand further to the southwest (not shown) from the very thickly developed Upper Central (UC) sand in wells 3 to 6. On the other hand, post-A bentonite sandy mudstone deposition in wells 7 to 10 separates the Upper Central (UC) unit from the thin Upper

Eastern sand (UE_o) in wells 11 and 13 to 15.

The depositional development of the units described above are depicted in the sketches in Figure 35(a,b).

Core Analysis

Well 11-6-25-12W4M cored through the upper 16 feet (4.9 m) of the northeastern flank near the northern limit of the L_1 ridge. The upper 14 feet (4.3 m) constitutes a coarsening upward sequence. This is underlain by a 2 foot (0.6 m) interval of medium to coarse grained sand which probably belongs to the upper part of an underlying coarsening upward unit. Detailed description of this core is found in Appendix IIIc.

The L_2 Sandstone Ridge

Isolith

The linear L_2 ridge member is located parallel to and northeast of the L_1 unit (Figure 36). A parallel swale separates the L_2 unit laterally from the L_3, L_4 and L_5 ridges. The less well developed L_1-L_2 swale separates the L_2 from the L_1 ridge to the southwest. The axis of maximum sand development of the L_2 is about 12 miles (19.0 km) away from that of the L_1 unit. The L_2 trends northwest-southeast for nearly 90 miles (145 km), attaining a maximum width of about 17 miles (27 km), and a maximum thickness of about 78 feet (24 m) in Township 26, Ranges 11 and 12W4M. On the isolith map, it appears asymmetric. A poorly defined southwestern flank and a steep north-northeastern flank, becoming

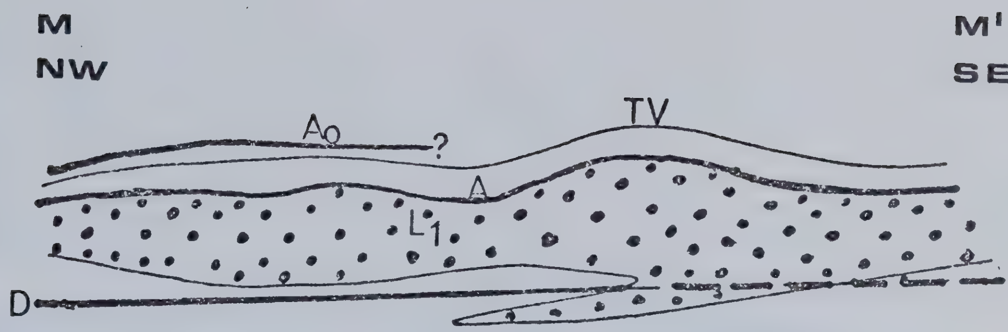

a)

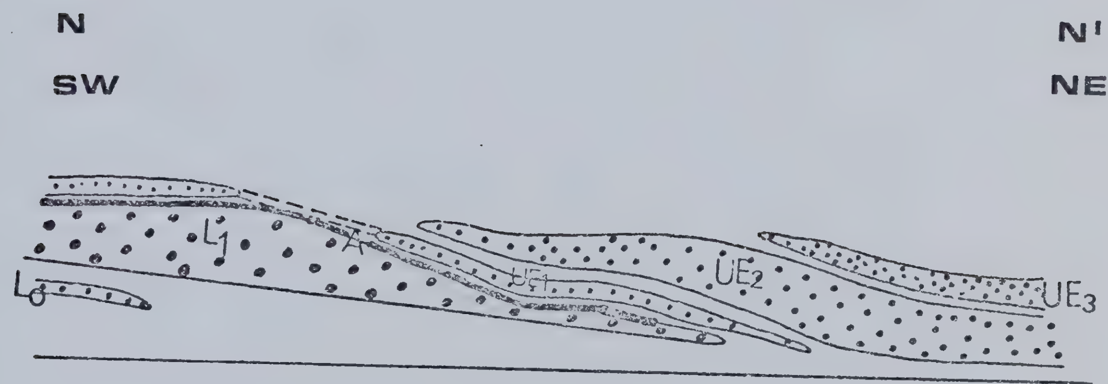

b)

c)

Figure 35a. Generalized sketch of sand distribution in cross-sections (see fig. 29 for location):
a) M-M'
b) N-N'
c) O-O'

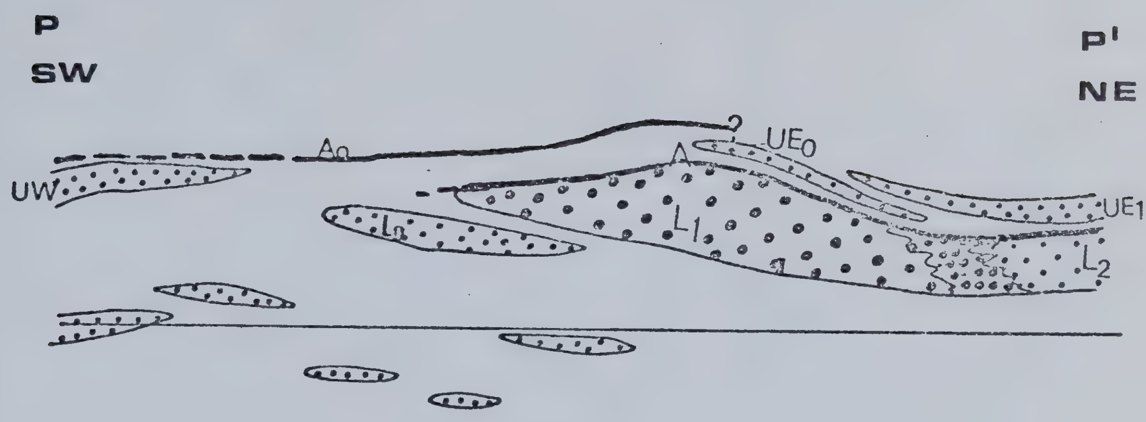

a)

b)

Figure 35b. Generalized sketch of gross sand distribution in cross-sections (see fig. 29 for location):
a) P-P'
b) Q-Q'

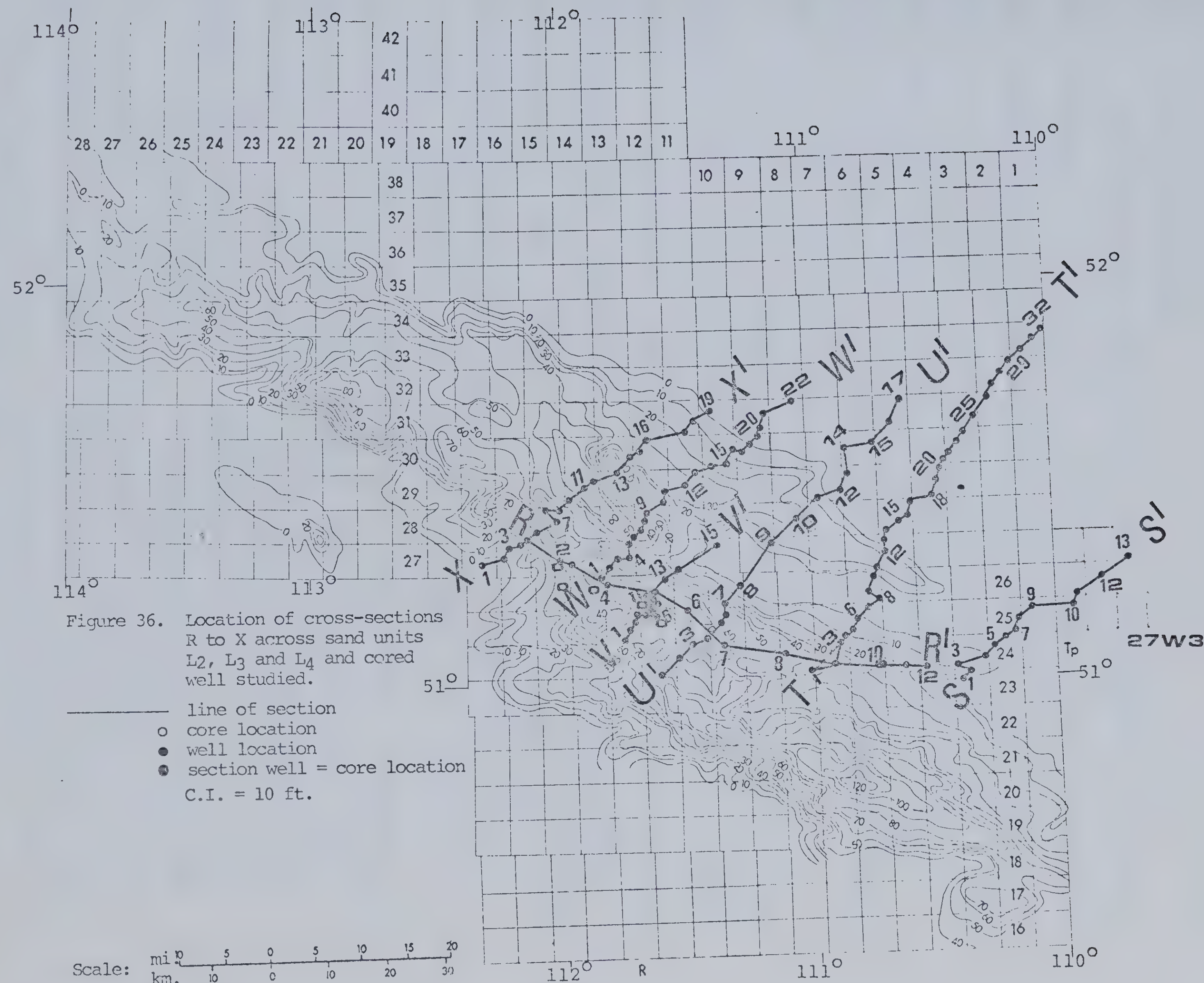

Figure 36. Location of cross-sections R to X across sand units L_2, L_3 and L_4 and cored well studied.

- line of section
- o core location
- ● well location
- ◉ section well = core location

C.I. = 10 ft.

Scale: mi. 10 5 0 5 10 15 20
km. 10 0 10 20 30

more gentle to the southeast, characterize the asymmetry; the northeastern margin is remarkably straight.

Cross-sections

One northwest-southeast, and six southwest-northeast stratigraphic cross-sections, respectively oriented parallel and perpendicular to the depositional strike, were drawn to diagnose this ridge. The horizons of bentonites E and D are the principal datum surfaces. The lines of section are shown in Figure 36; the identities of the wells used in the sections are listed in Appendix Ig.

Section R R' (Figs. 37,44a) is oriented parallel to the depositional strike of the L_2 ridge from Township 28, Range 16W4M to Township 24, Range 4W4M. The E bentonite is datum. As deduced from the SP curve, the unit is characterized by predominantly sharp lower and upper contacts, except for the extreme northwest and southeast margins where the base (wells 1 to 4 and 12) is gradational. The unit attains maximum development in wells 5 and 6 and thins gradually as the base rises from there toward both the northwest and southeast. Thus, the base is convex downward, indicating ridge growth parallel to the depositional strike.

The well defined A bentonite horizon in the section lies in mudstone between wells 1 and 5 and on top of the sandstone southeast of these wells. This indicates that the development of the L_2 unit terminated earlier in the northwest (similar to the L_1). This is supported by the later development of multiple Upper Eastern sand units which

overlap the southeastern margin of the L_2 unit (wells 6 to 13) after A bentonite deposition. Relative to the top of the Viking, the Lloydminster shale thickens to the southeast and thus the Base of Fish Scales horizon also appears to rise in this direction.

Section S-S' (Figs. 38,44a) is oriented southwest-northeast from Township 23, Range 3W4M, through the Alberta-Saskatchewan border to Township 27, Range 27W3M in south-western Saskatchewan. A distinct and persistent electric log kick near the top of the Joli Fou is the datum. This section shows how the southeastern margin of the L_2 unit pinches out, and its relations to other sand units to the northeast, which will be described later. The thin south-eastern margin of the L_2 unit, though not logged in wells 1 and 2, underlies the A bentonite horizon in wells 3 and 4, and pinches out before well 6. Note how the thickly developed northeastern ridge overrides the L_2 unit as the former migrates to the southwest.

Section T-T' (Figs. 39,44b) is oriented in a southwest-northeast direction from Township 24, Range 8 to Township 33, Range 1W4M; bentonite E is the datum. The L_2 ridge is correlated from wells 1 to 6, beyond which it pinches out. Wells 7 and 8 are located in the L_2-L_4 swale. The poorly developed southeastern end of L_4 lies at the base of the Formation in wells 9 to 12. Relative to the datum, the L_2 unit migrated to the southwest, and thickens in the same direction. The A bentonite horizon rests on top of the

sandbody in wells 1 to 6. Both the L_2 and L_4 units are imbricately overlain by the southwesterly advancing Upper Eastern ridges.

Section U-U' (Figs. 40,44b) is oriented perpendicular to the depositional strike of the L_2 ridge from Township 24, Range 12 to Township 31, Range 6W4M. The E bentonite is datum. The section crosses the L_1, L_2, L_4, Upper Eastern and B_1 units. The L_1-L_2 swale (well 2), characterized by relatively thin sand development, separates the L_1 unit (well 1) laterally from the L_2 member (wells 3 to 7). Relative to the datum, the L_2 ridge migrated to the southwest, thickening simultaneously. Maximum thickness is attained in wells 3 and 4. The lower and upper contact are fairly sharp.

To the northeast, the L_2 unit pinches out rather abruptly before reaching well 8. This well is located in the L_2-L_4 swale which distinguishes the two ridges. A thin sand unit appears to migrate from well 10 through the swale and to accrete onto the northeast flank of the L_2 unit up to well 5. Bentonite A lies very close to the top of the L_1 and L_2 sandbodies except in the L_1-L_2 swale (well 2) where it occurs in mudstone about 15 feet (4.6 m) above the top of the swale sand.

The L_1, L_2 and L_4 units are overlain in imbricate fashion by the Upper Eastern sandbodies migrating and thinning toward the southwest. The overlying Lloydminster shale thins to the southwest.

Section V-V' (Figs. 41,44b) is oriented southwest-northeast from Township 25, Range 13 through the central part of the L_2 ridge to Township 27, Range 10W4M. Bentonite D is datum. The L_1-L_2 swale (wells 4 to 6), characterized by relatively thin sand development, distinguishes the L_1 unit (wells 1 to 3) from the L_2 sandbody in wells 7 to 15. Both units migrated to the southwest relative to the datum.

The lower and upper contacts of the L_2 unit appear fairly sharp in wells 8 to 13, whereas the lower contact is more gradational in wells 6 and 7, a probable consequence of the southwesterly direction of migration. Maximum thickness development of this sandbody occurs around wells 10 to 12. The unit thins rather abruptly to the northeast in wells 13 and 14, pinching out prior to well 15 located in the L_2-L_4 swale. The abrupt thinning to the northeast is suggested to be probably due to syn-depositional erosion of the north-eastern flank of this ridge concommitant with the south-westward migration. Between wells 12 and 15, two additional sand units also migrated in a southwesterly direction onto the northeastern flank of the L_2 sandbody.

The A bentonite horizon occurs in mudstone about 8 feet (2.4 m) above the top of the L_2 unit, 22 feet (6.7 m) above the top of the L_1-L_2 swale sand (well 4), and about 12 feet (4 m) above the top of the L_1. This relationship indicates that the vertical growth of the L_2 unit continued longer than L_1, until near the time of bentonite A deposition. The L_1 and L_2 ridges are overlain by the Upper

Eastern sands which thin to the southwest.

Section W-W' (Figs. 42,44c) is oriented southwest-northeast from Township 26, Range 14 to Township 31, Range 8W4M. It transects the L_2, L_3, L_4, Upper Eastern and B_1 sandbodies. Bentonite E is the datum. The L_2-L_3 swale (well 4), characterized by multiple thin sand development, separates the northeastern flank of L_2 (wells 1 and 2) from the southwestern edge of the L_3 ridge in wells 5 to 9. An expanded section of the swale is shown in Figure 42a. Although the L_2 and L_3 units have been shown to be connected, it is equally possible that the L_3 ridge pinches out to the southwest before well 4, and that the L_2 unit (wells 1 to 3) nearly overlaps it there. This interpretation is provoked by the thickness distribution of these units in wells 1 to 6, and the rise and fall of their lower contacts relative to the datum.

Section X-X' (Figs. 43,44c) is oriented southwest-northeast from Township 27, Range 17 to Township 31, Range 10W4M. Bentonite E is the datum. The section crosses the northwest tip of L_2, the southeast margin of L_5, and the central parts of L_3 and L_4, plus the Upper Eastern and B_1 sandbodies. The northwest end of L_2 is thickly developed in well 5, from where it thins to the southwest in the direction of migration. This unit also overlaps the L_5 ridge member to the northeast in well 6 and pinches out before well 7. Note how the mudstone interval between the L_2 sand and bentonite A thickens to the southwest, where the Upper

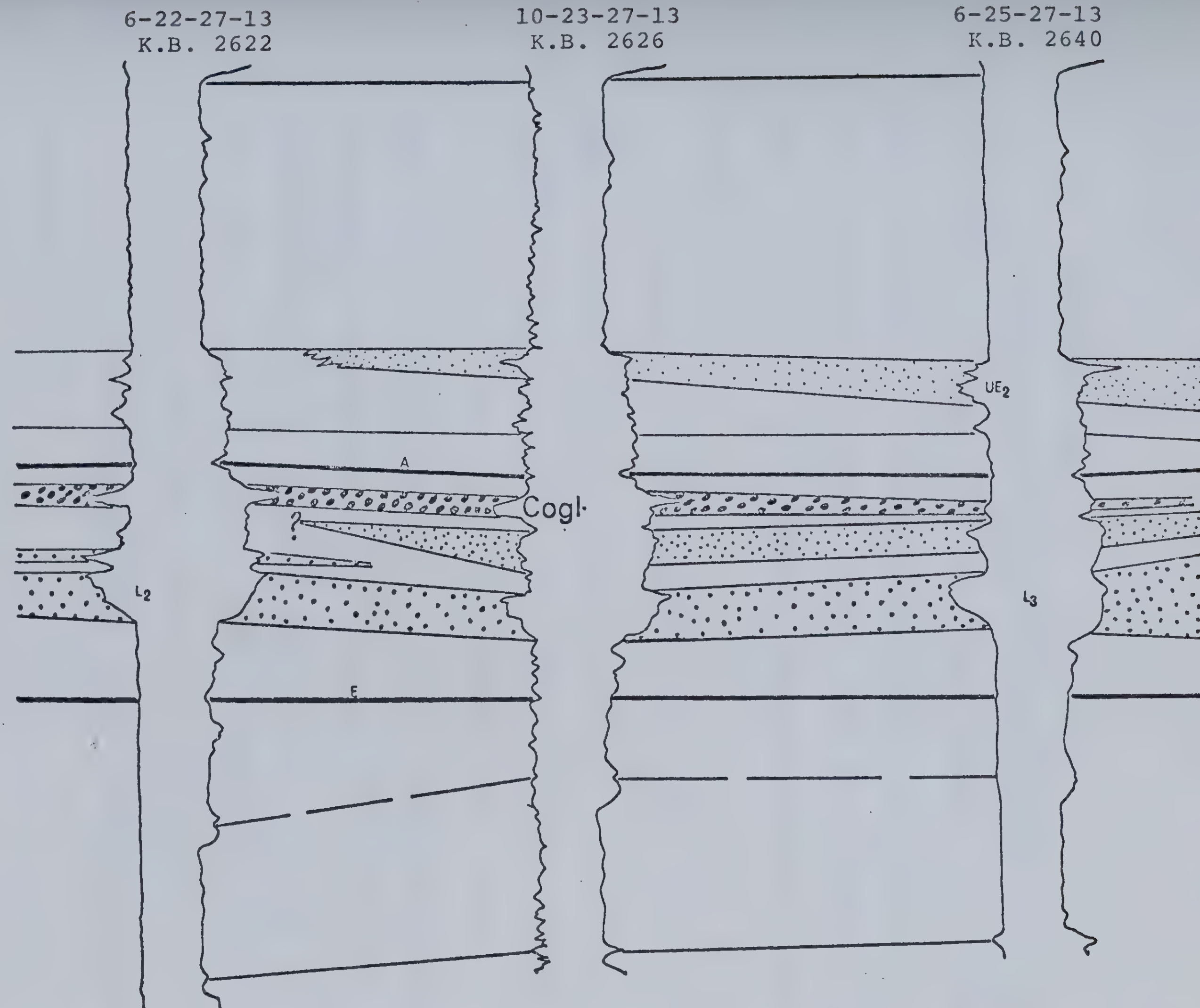

Figure 42a. The L_2-L_3 swale zone and the probable lateral relations between these sandstone ridges. Chert pebble conglomerate (cgl) beds thicken in the swale area and thins towards the axes of adjacent ridges.

Viking interval is thin and less well developed, especially between wells 1 and 5.

Cross-sections R to X are depicted in Figure 44(a,b,c).

Core Analysis

Cores from the L_2 ridge were studied in six wells located on the flank close to the L_1-L_2 swale (Figure 36). Five are from the northwestern area while only one is from the southeastern region. These are areas where ridge migration parallel to depositional strike exceeded that perpendicular to it.

In well 11-12-24-6W4M, the muddy and silty L_2 sandbody is observed to rest sharply on the bentonitic and fissile black shales of the underlying Joli Fou Formation.

Cores from the northwestern part of the L_2 showed from one to three coarsening upward textural gradients, commonly with mudstone at the base and black chert pebble conglomerate on top. The coarsest sand of this unit was observed in well 11-7-25-13W4M located in the L_1-L_2 swale. All the cores show very intense bioturbation.

Well details and core descriptions are given in Appendix IIId.

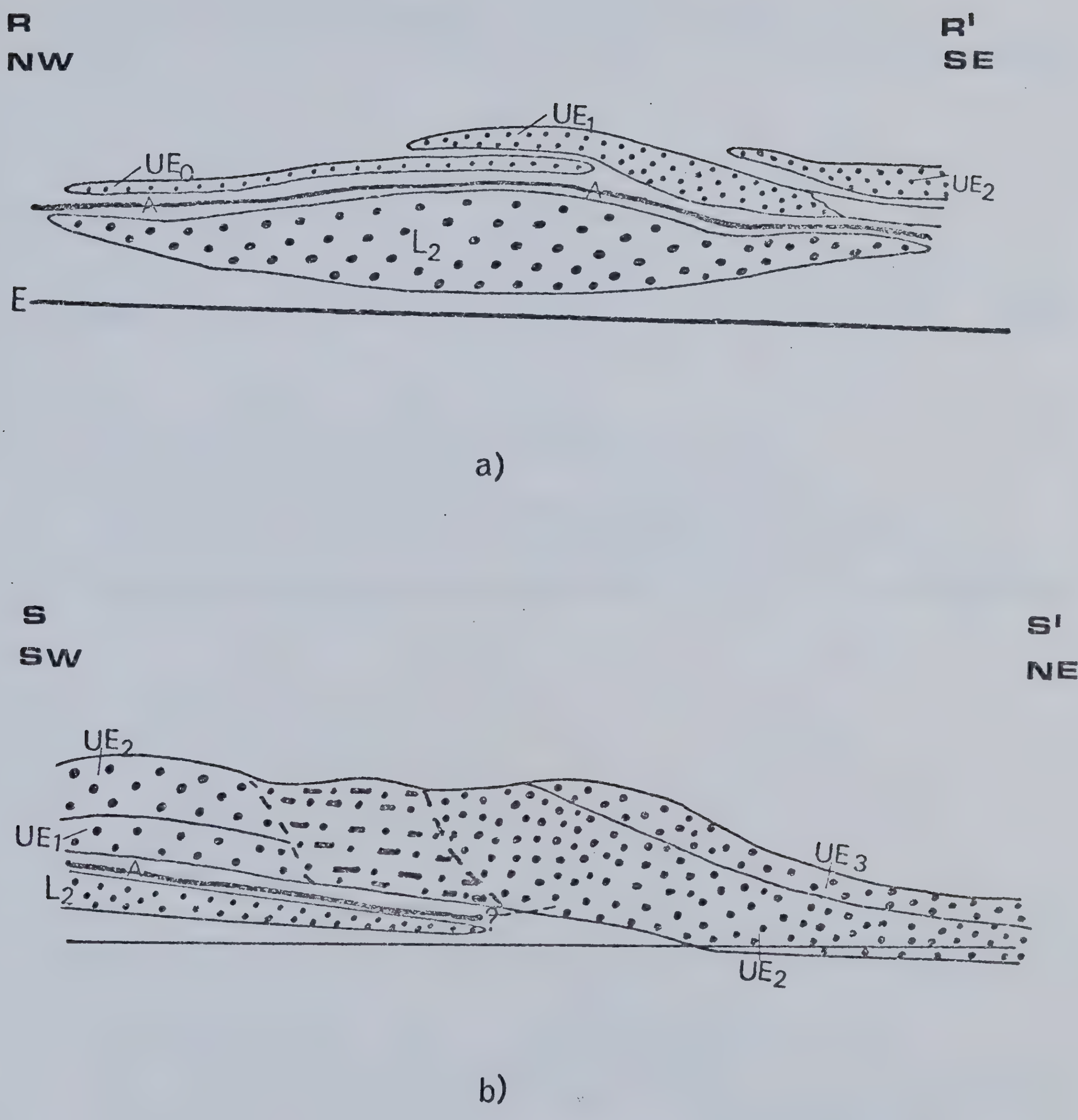

Figure 44a. Generalized sketch of gross sand distribution in cross-sections (see fig. 36 for location):
a) R-R'
b) S-S'

a)

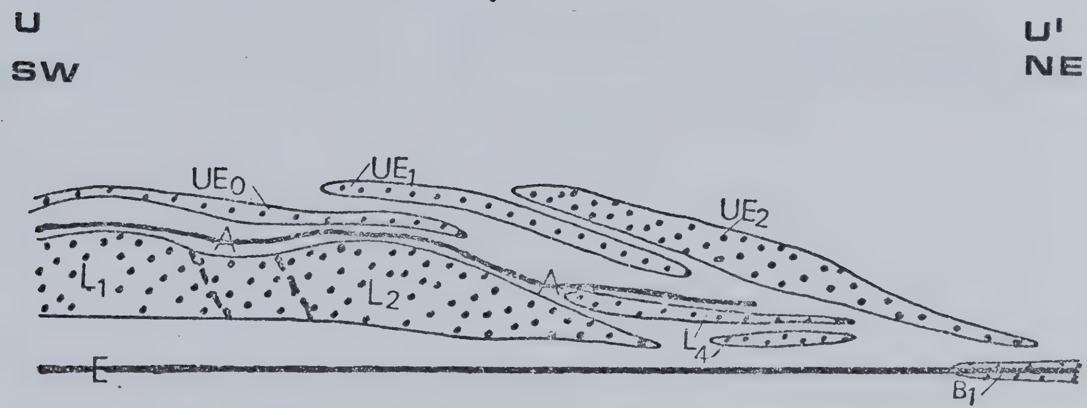

b)

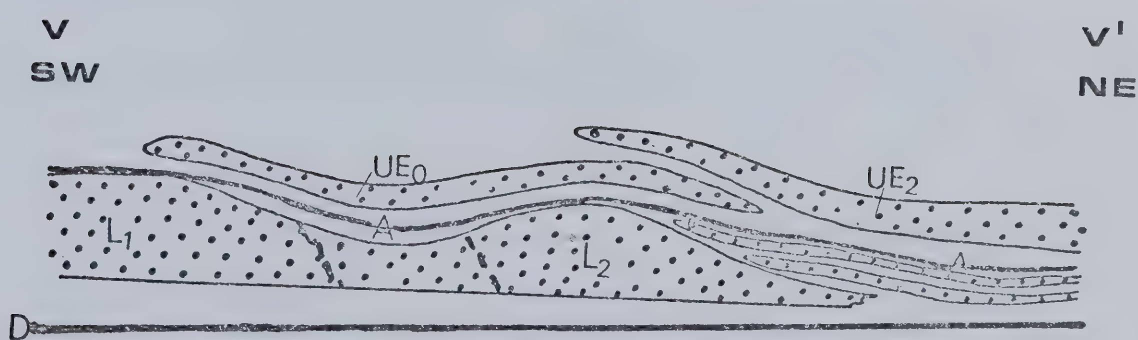

c)

Figure 44b. Generalized sketch of gross sand distribution in cross-sections (see fig. 36 for location):
a) T-T'
b) U-U'
c) V-V'

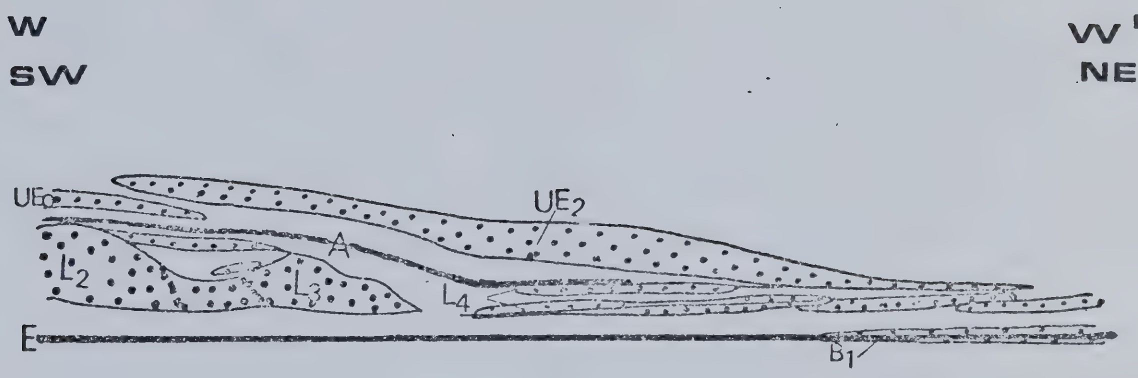

a)

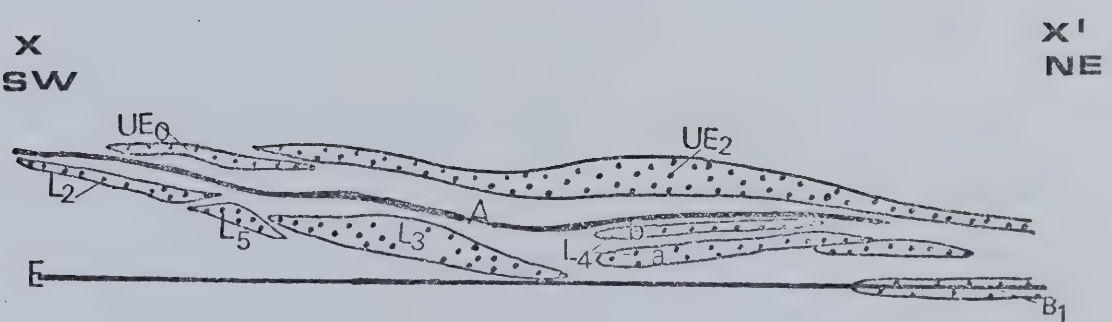

b)

Figure 44c. Generalized sketch of gross sand distribution in cross-sections (see fig. 36 for location):
a) W-W'
b) X-X'

The L_3 and L_4 Sandstone Ridges

Isolith

The L_3 and L_4 members of the Lower sand ridge complex (Figure 28) are located northeast of the L_2 sand unit, and within the area roughly bounded by Townships 27 and 34, Ranges 5 and 17W4M. The northwest extension of the L_2-L_4 swale up to Township 30, Range 13W4M differentiates the L_3 sandbody from the L_4.

Maximum thickness development of the L_3 and L_4 ridges occurs within Townships 29 and 30, where they are more than 60 feet (18 m) and 30 feet (9 m) thick, respectively. Taken together, the couplet is approximately 110 miles (177 km) long and has a maximum width of about 25 miles (40 km). It trends northwest-southeast parallel to the L_5 ridge to the west, but at a slight angle to the L_2 unit to the south.

The northeast margin is very straight. The southeastern and northwestern extremities of the southwest margin are occupied by swales, but the central part is indistinct due to the imbricate relationship of the L_3 and L_5 sand ridges (to be shown later).

Cross-sections

A total of eleven stratigraphic cross-sections utilizing bentonite E as datum were used to study these sand units. Section lines are shown in Figure 45. The identities of the wells used in the cross-sections are listed in

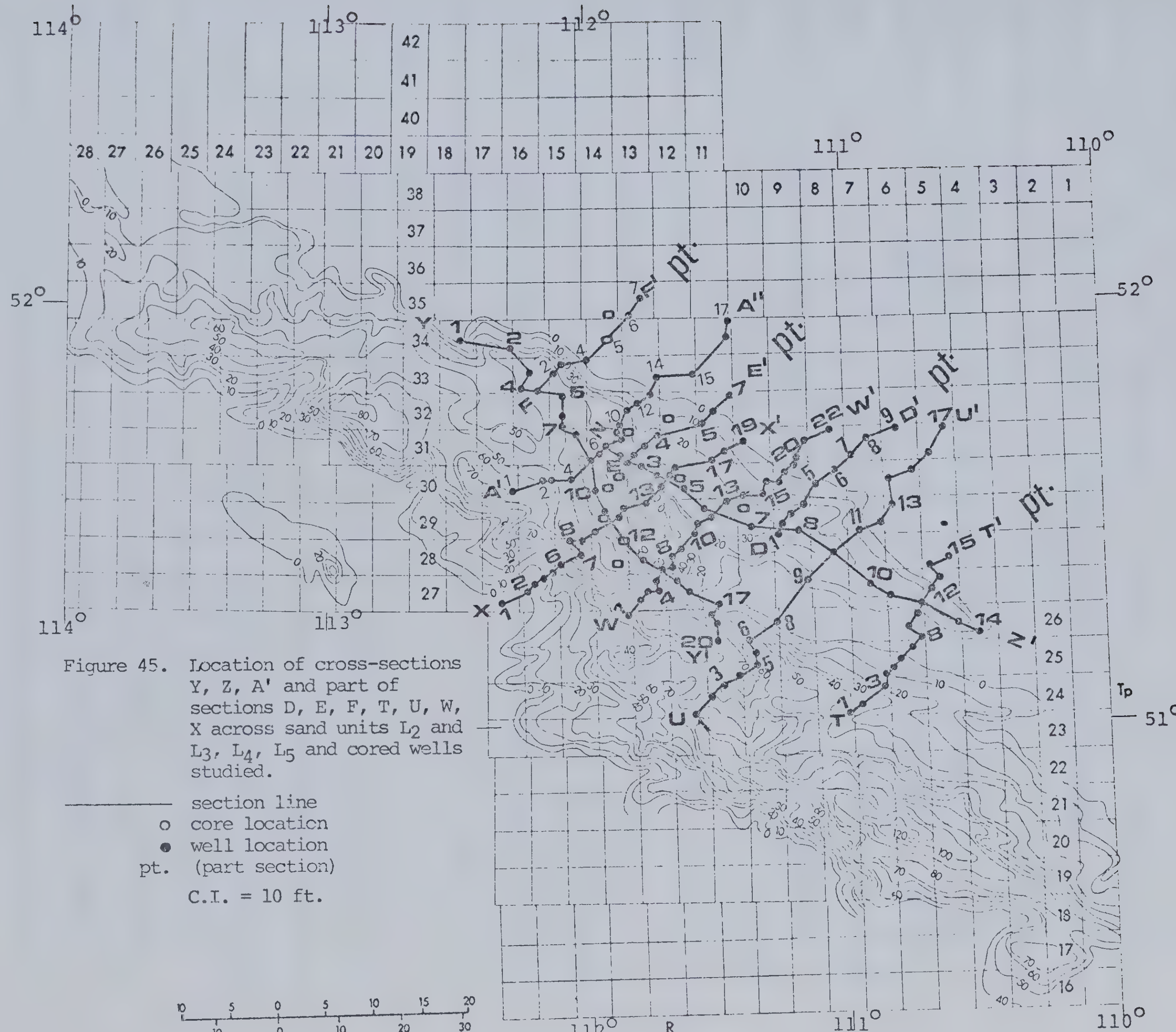

Figure 45. Location of cross-sections Y, Z, A' and part of sections D, E, F, T, U, W, X across sand units L_2 and L_3, L_4, L_5 and cored wells studied.

——— section line
o core location
● well location
pt. (part section)

C.I. = 10 ft.

Appendix Ih.

Section Y-Y' (Figs. 46, 49a) is oriented in a northwest-southeast direction parallel to the depositional strike of the L_3 sand unit from Township 34, Range 18 to Township 26, Range 11W4M. The L_3 sand attains maximum thickness development between wells 10 and 13. Southeast of the latter well, it thins toward well 16. The L_2-L_3 swale (wells 17 to 19) separates it laterally from the L_2 unit in well 20. Northwest of well 10, the L_3 sandbody overrides a basal thin sand unit, identified as $L5_o$ in this cross-section but mapped with L_3. The L_3 unit then thins as it rises to the northeast as far as well 5. It seems to thicken again in well 4, but thins again and shales out before reaching well 1. Relative to the E datum, the base of the $L5_o$ unit rises and falls slightly, suggesting the possibility of scour before or during deposition, especially in wells 3 and 5 where the lower contact is fairly sharp.

Bentonite A is intercalated in mudstone about 12 to 15 feet (3.7 - 4.6 m) above the top of the L_3 sandbody in wells 7 to 13. Between wells 14 and 19 to the southeast, however, the interval between the top of the L_3 sand unit and bentonite A thickens and becomes sandy and pebbly at the same time. A very thin, black chert pebble conglomerate bed appears to migrate towards the southeast, thickening simultaneously from well 15 to well 19 in the L_2-L_3 swale (see also Figure 42a). It appears then to have been accreted onto the L_2 unit in well 20 where bentonite A occurs very

near the top of this sandbody. Northwest of well 7, bentonite A cannot be correlated with much certainty, but is assumed to lie above the L_3 unit.

Section Z-Z' (Figs. 47,49b) is oriented parallel to the depositional strike of the L_4 unit from Township 31, Range 14 to Township 26, Range 4W4M. Well 1 of this cross-section and well 9 of the previous section (Figure 46) are both in Township 31, Range 14W4M, but in different sections. The L_3 sandbody occurs in both wells. The section shows that the L_4 sand ridge is essentially the southeastern extension of the L_3 ridge, herein designated L_{4a}, plus an overlying thin sand unit (L_{4b}). Both units thin to the southeast, and grade into mudstone between wells 12 and 14. Relative to the datum the base of the unit is lowest in well 9.

Bentonite A lies in mudstone about 10 feet (3 m) above the top of the L_3 unit in wells 1 and 2. It is believed to lie atop the L_{4b} unit between wells 3 and 12, and possibly at the base of the overlying thick Upper Eastern sandbody in wells 13 and 14. Note how this latter sandbody migrated rapidly to the northwest between wells 14 and 9, and then more slowly northwest of the latter well.

Section T-T' (Figure 39) bisects the muddy southeastern tip of the L_4 unit in wells 9 to 12. In these wells the unit is very poorly developed and not easily differentiated. The L_2-L_4 swale in wells 7 and 8 separates this unit from the L_2 ridge further to the southwest. The L_4 pinches out to the northeast around well 13 where it is

imbricately overlain by the Upper Eastern ridge advancing to the southwest. Bentonite A is inferred to lie just above the L_4 unit in these wells.

Section U-U' (Figure 40) shows the L_4 sands in wells 9 and 10. Whereas the underlying $L4_a$ unit pinches out to the southwest before well 8, located near the L_2-L_4 swale, the overlying thin $L4_b$ unit migrates to the southwest up the northeastern slope of the L_2 ridge (wells 6 and 7), thinning at the same time. To the northeast, however, both units pinch out before well 11 and are in turn imbricately overlain by the southwesterly advancing Upper Eastern sandbody. Bentonite A lies just above the $L4_b$ unit.

In Section D-D' (Figure 15), wells 1 to 5 penetrate the northeastern margin of the L_4 units. They are underlain by three imbricately arranged, very thin sands (wells 1 to 8) demarcated by bentonites D and C. These latter sands are laterally restricted, but migrated to the southwest. The L_4 units, in turn, appear to overlie them in an imbricate fashion as well. Bentonite A lies in mudstone about 5 feet (1.5 m) above the top of the $L4_b$ unit in wells 1 and 2. Northeast of these wells the bentonite cannot be traced with much certainty.

In Section W-W' (Figure 42), wells 5 to 9 and 9 to 18 penetrate the southeastern tip of the L_3 and the central portion of the L_4 units, respectively. The L_2-L_3 swale in wells 3 and 4 separates the L_2 ridge (wells 1 and 2) laterally from the L_3 sand , which attains its maximum

thickness in wells 6 and 7 and thereafter shales out rather abruptly grading into sandy shale or siltstone in well 9.

The northwest extension of the L_2-L_4 swale, there called the L_3-L_4 swale, occurs between wells 9 and 10, and distinguishes the L_3 from the L_4 sand ridges in this area. The L_4 units are traced between wells 10 and 18. Relative to the E datum, the base of the lower $L4_a$ unit is stratigraphically higher than that of the L_3 ridge to the southwest. Maximum development of the L_4 sands occur in well 12. Southwest of this well, both ($L4_a$, $L4_b$) thin, and while the $L4_a$ unit pinches out before well 9, the overlying $L4_b$ unit may overlap onto the L_3 ridge in well 9 and pinch out before well 8. To the northeast, the $L4_b$ thins and pinches out before well 15, while the underlying $L4_a$ also thins and pinches out prior to reaching well 19. Underlying the L_4 units in wells 10 to 22 are the three imbricating very thin sandbodies encountered in the previous section.

Bentonite A is intercalated in mudstone about 20 feet (6.0 m) above the top of the L_3 sand in wells 6 and 7, but lies near the top of the $L4_b$ unit in wells 11 and 12. This relationship indicates the later deposition of the L_4 sandbodies in this area. Northeast of well 15 bentonite A cannot be correlated with certainty. Overall, it appears as if wells 10 to 22 show 5 imbricately arranged thin sand units migrating to the southwest with the youngest unit ($L4_b$) overlapping onto the southeastern edge of the L_3 ridge.

In cross-section X-X' (Figure 43) wells 8 to 12, and 14 to 17, penetrate the central portions of the L_3 and L_4 sandbodies, respectively. Relative to the datum the L_3 ridge migrated to the southwest, thinning at the same time as it overlapped the muddy sand of the adjacent L_5 ridge in well 8. Northeast of well 12, it shales out rapidly before reaching well 13. This well is located in the L_3-L_4 swale. In this part of the swale, the base of the poorly developed Lower Viking is about 5 feet (1.5 m) above the horizon of bentonite E.

Northeast of the swale (wells 14 to 17) the stratigraphically higher L_4 units are very distinct from the L_3. The base of the $L4_a$ rises to the northeast as the unit thins and pinches out before well 18. The overlying $L4_b$ is laterally restricted between wells 13 and 17. Another thin sand underlies the L_4 units in wells 17 and 18. The three units appear to be successively stacked in imbricate fashion in a southwesterly direction. This pattern of arrangement continues into section E-E' (Figure 16) as shown between wells 1 and 8. However, as mentioned above, migration of the $L4_a$ unit at least appears to have been toward the northeast.

Section A'-A" (Figures 48, 49c) is oriented southwest-northeast from Township 30, Range 17 to Township 34, Range 11W4M. In this section, the base of L_3 is lowest in well 8. It thickens to the southwest to wells 5 as it begins to overlap the thin northeastern edge of the L_5 ridge, and then thins as it overrides the northeastern flank of the L_5 unit, finally pinching out before reaching well 1. Northeast of well 8, it overlies a laterally restricted thin sand unit, and both rise in that direction as they thin and pinch out before well 12. Thus, the base of the L_3 in the section is slightly trough-shaped due to a missing (eroded) 10 feet (3 m) of section at the base of the sand in well 8. This sea floor scouring or non-deposition preceeded deposition of the L_3 unit in this area and may be related to the deposition of the L_5, as it occurs at the extreme northeastern edge of that unit. Two relatively thin sand units, imbricately arranged, can be seen to migrate to the southwest onto the L_3 unit (well 11) from well 15. Two other thin units in wells 16 and 17 may have behaved in a similar fashion. A fairly similar relationship is shown in wells 1 to 11 in section F-F' (Figure 17).

Bentonite A occurs in mudstone about 20 feet (6.1 m) above the top of the L_5 unit in well 1 and approximately 15 feet (4.6 m) above the top of the L_3 in well 6. Relative to the

E datum, it falls toward the northeast, perhaps reflecting the regional depositional slope. Northeast of well 8, the A bentonite cannot be reliably traced in electric well logs.

The B_1 unit lies at the base of the Formation in wells 13 to 17. Figure 49 shows the exaggerated sketches of sections Y-Y', Z-Z' and A'-A".

Fence Diagram

Figures 50a and 50b are fence diagrams which give a pictorial view of the deposition of parts of the L_3 and L_4 sand units and show their lateral relations to adjacent sand-bodies. Bentonite E is the datum.

Figure 50a covers most of the area within Townships 26 to 29, Ranges 11 to 17 W4M. The L_2-L_3 swale, which distinguishes the L_2 from the L_3 ridge, can be followed in wells 3, 4, 6, 15, 20, 21, 24 to 30, 32, 33 46 and 50. The L_3-L_4 swale is located in wells 33, 34, 38, 41 and 60 to 62. The overlap relationship between the L_3 and L_5 units is shown between wells 47 and 48, and between 54 and 55. Well identity is given in Appendix IIb.

Figure 50b is a northern extension of the previous diagram from Townships 28 to 32, Ranges 9 to 18 W4M. The relative stratigraphic positions of the B_1 and L_4 units are shown in wells 35, 37, 62, 67 and 70. The thin imbricating sand units below the L_4 units occur between wells 31 and 33, and between wells 34 and 35. The L_3-L_4 swale occurs in wells 7 and 26 and between wells 25 and 27. The juncture between the L_3 and L_4 units can be followed from wells 39 to

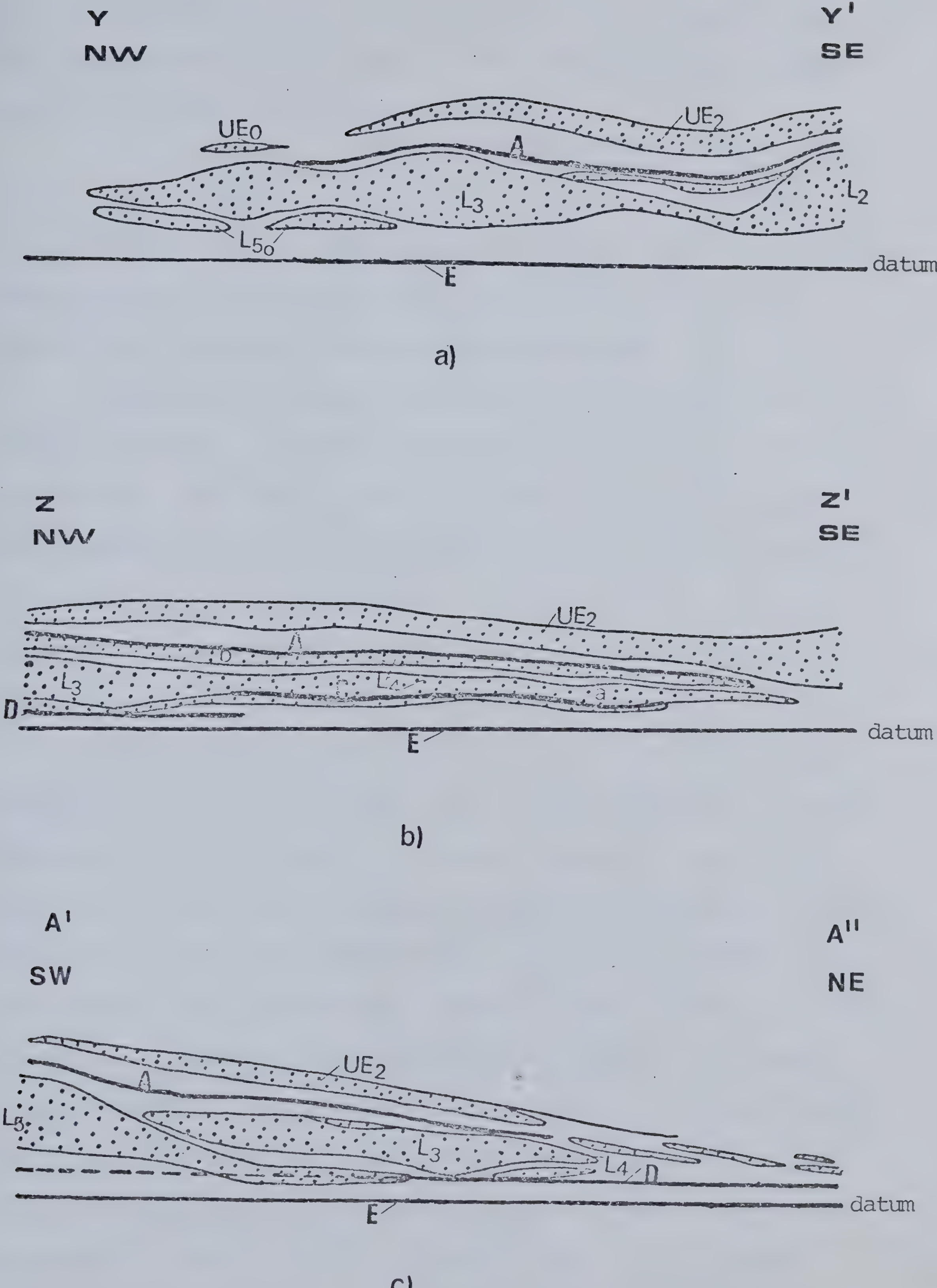

Figure 49. Generalized sketch of gross sand distribution in cross-sections (see fig. 45 for location):
a) Y-Y'
b) Z-Z'
c) A'-A"

45. The overlap relationship between the L_3 and L_5 units is best developed in wells 10, 19, 20, 49, 54 and 58. Well identity is given in Appendix IIc.

Core Study

Twelve wells recovered cores from different parts of the L_3 and L_4 ridges and nearby thin sands. These are located in Figure 46 and described in Appendix IIIe.

Coarsening upward sequences were observed in all the cores regardless of their positions with respect to the ridge axis. The axis of the L_3 ridge is characterized by a relatively thick single coarsening upward quartz gradient and fairly well preserved internal structures. Two such sequences ($L4_a$ and $L4_b$) typify the axial zone of the L4 ridge, but these are very strongly biotubated.

The flanks of the L_3 unit, especially those near swales, consist in places of two to three coarsening upward sequences of nearly equal thickness. Some of these are capped with black chert pebbles dispersed in an argillaceous sand matrix, generally moderately to strongly biotubated. Pebbly beds occur around the flanks of the L_3 ridge, not on the axis, at least not in the parts studied. No lateral textural gradient was apparent except for a thin sand unit which nearly overlapped the northeastern edge of the L_3, which showed a visual decrease in quartz grain size to the southwest in two wells (11-23-34-14 and 7-2-35-14 W4M) approximately three miles (4.8 km) apart. The lithofacies of these ridges will be treated in detail in a later chapter.

The L_5 Sandstone Ridge

Isolith

Figure 28 shows that the L_5 ridge is located immediately northwest of the L_2, within Townships 28 and 32, Ranges 15 to 19 W4M. It is roughly in line with the L_2 and L_6 ridges and parallels the L_3-L_4 units.

The ridge is shaped like an inverted S due to localized thickening in two areas (Twp. 30, Rge. 18 and Twp. 29, Rge. 16 W4M). The axis of maximum thickness trends northwest-southeast for approximately 40 miles ((64.0 km). Maximum width and thickness are, respectively, about 17 miles (27.0 km) and 75 feet (23.0 m). A fairly gentle northeastern and relatively steep and indented southwestern flank characterizes the ridge asymmetry. With the exception of the central part of the northeastern boundary, which has been shown to be overlapped by the L_3 ridge, the ridge is surrounded by swales that are fairly well defined.

To the southwest of the L_5 unit is a parallel, but laterally restricted elongate sand unit designated L_{5a}. It occurs within Townships 27 to 29, Ranges 21 to 24 W4M. It is about 45 miles (72.0 km) long, 8 miles (13.0 km) wide, and develops a maximum thickness of 70 feet (21.0 m) around Township 28, Range 22 W4M.

Cross-sections

Figure 51 shows the location of the cross-sections used to study this unit. Bentonite E was used as datum. The identities of wells in the sections are listed in Appendix Ii.

Section B'-B" (Figs. 52,55a) is oriented along the axis of maximum development parallel to the depositional strike of the ridge from Township 32, Range 19 to Township 28, Range 14W4M. The L_5 ridge attains maximum thickness between wells 6 and 10, and thins southeast of the latter well. In the L_5-L_6 swale, northwest of well 6, the L_5 ridge appears to override the southeast edge of the L_6 ridge (well 1) up to well 2. Relative to the datum, ridge migration parallel to depositional strike seems to have been toward the northwest.

Bentonite A lies in mudstone about 25 feet (7.6 m) above the top of this ridge. Except for the localized development of very thin sand units, the thin Upper Viking interval in this area is very poorly developed.

Section C'-C" (Figs. 53,55b) trends southwest-northeast from Township 29, Range 18 to Township 31, Range 15 W4M. A bentonitic sandy mudstone 'bank' at the base of the Viking in well 5 thickens as it rises in a southwesterly direction up to well 2. This unit is bounded at the base and top by bentonites D and C, respectively. The thickest development of the L_5 ridge occurs in wells 4 and 5; it thins rapidly and grades into mudstone near well 2, in the direction of

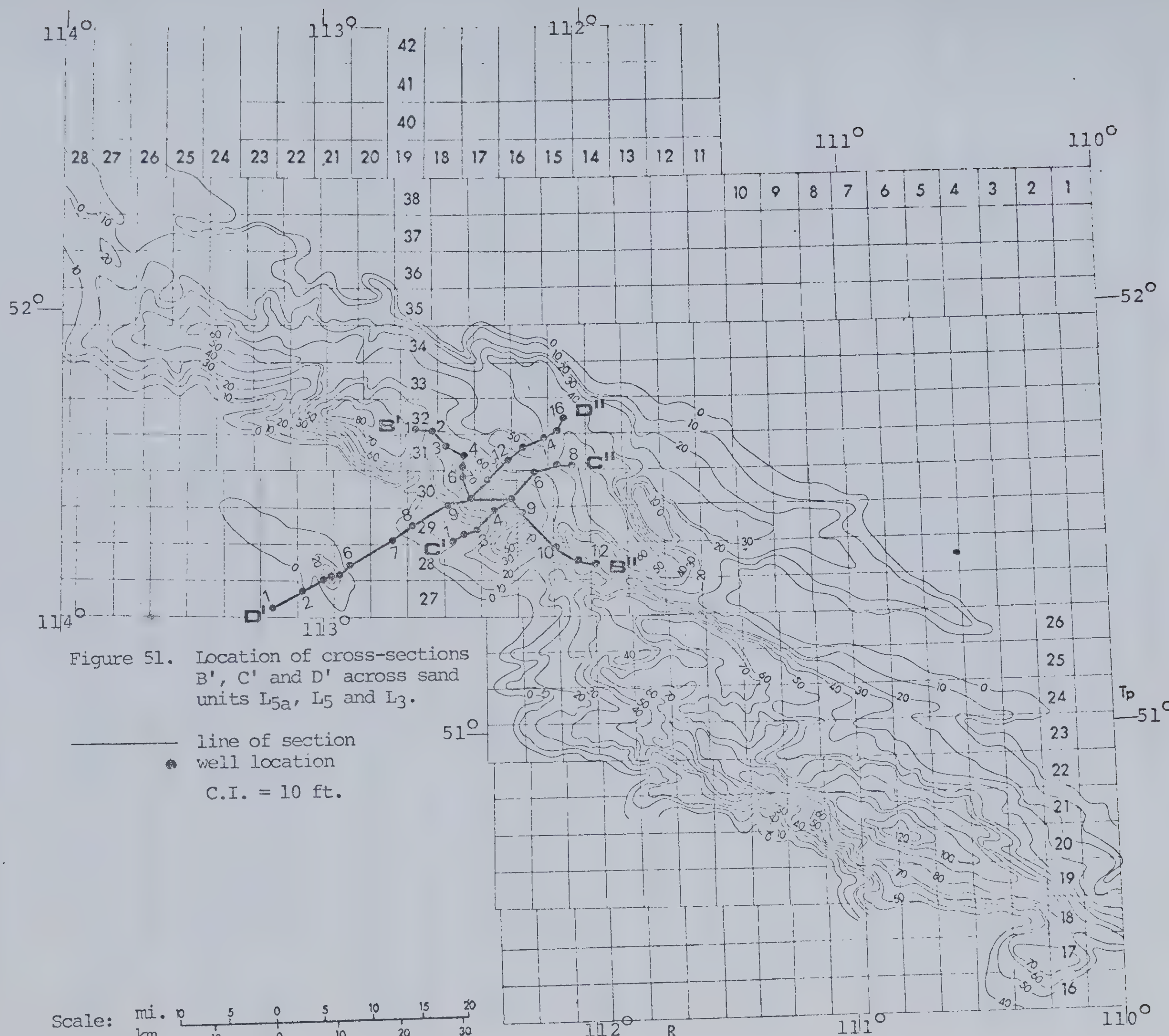

Figure 51. Location of cross-sections B', C' and D' across sand units L_{5a}, L_5 and L_3.

——— line of section
● well location

C.I. = 10 ft.

Scale: mi. 10 5 0 5 10 15 20
km. 10 0 10 20 30

migration to the southwest. An overlying thin sand unit maintains an offlap relationship with the L_5 between wells 1 and 6. Northeast of well 5, the L_5 unit thins and is overlapped by the southwesterly advancing L_3 ridge.

Bentonite A occurs in mudstone about 30 feet (9.0 m) above the top of L_5 in well 3, and 18 feet (5.5 m) above L_3 unit in wells 6 and 8. The Upper Viking interval is thicker and sandier to the northeast than to the southwest.

Section D'-D" (Figs. 54,55c) is another southwest-northeast oriented section from Township 27, Range 23 to Township 32, Range 15 W4M. This cross-section shows basically the same features noted in the previous one (Figure 53). The underlying bentonitic sandy mudstone of section C'-C" is shaly mudstone in this section (wells 8 to 10). The L_5 unit (wells 8-16) overrides this basal shaly mudstone in well 10 as it migrated to the southwest, and itself grades into mudstone in well 7. The northeastern flank of the L_5 sandbody is in turn overlain by the southwesterly advancing L_3 unit in wells 13 to 16.

The mudstone interval between the top of the L_5 unit and the A bentonite thickens to the southwest up to well 8, while the reverse is true for the Upper Viking interval, which is thicker and sandier to the northeast (wells 14 and 15).

Further to the southwest, the L_{5a} sand developed between wells 3 and 5. This lens-shaped unit has sharp lower and upper contacts and is laterally restricted.

According to the datum, it appears to have formed a little later than the L_5 unit, but at one stage they were synchronous.

The Upper Western sand (UW), which prograded rapidly to the northeast, is shown between wells 1 and 7. It overlies L_{5a} in wells 3 to 5 and shales out just before reaching well 8 where the underlying L_5 unit is also grading into mudstone. Bentonite A is interpreted to have fallen on this unit (UW) beyond well 8. These cross-sections are sketched in Figure 55.

The probable overlap relationship between the southwestern and northeastern flanks of the L_3 and L_5 ridges, respectively, discussed earlier, is shown in the fence diagram of Figure 50b. No cores were cut from the L_5 ridge.

The L_6 Sandstone Ridge

Isolith

Figure 28 shows that the L_6 ridge occurs within the area of Townships 31 to 33, Ranges 18 to 22 W4M, northwest of the L_5 ridge. It is one of the links of the roughly linear ridge chain comprising the L_2, L_5, and L_7 ridges. This ridge, with a pear-shaped outline, is characterized by an elongate western margin and a rather blunt eastern margin. A relatively steep southwest flank and a very gentle northeast flank characterize its thickness asymmetry.

The axis of maximum development is oriented approximately N80°W. It is about 45 miles (72.0 km) long, and

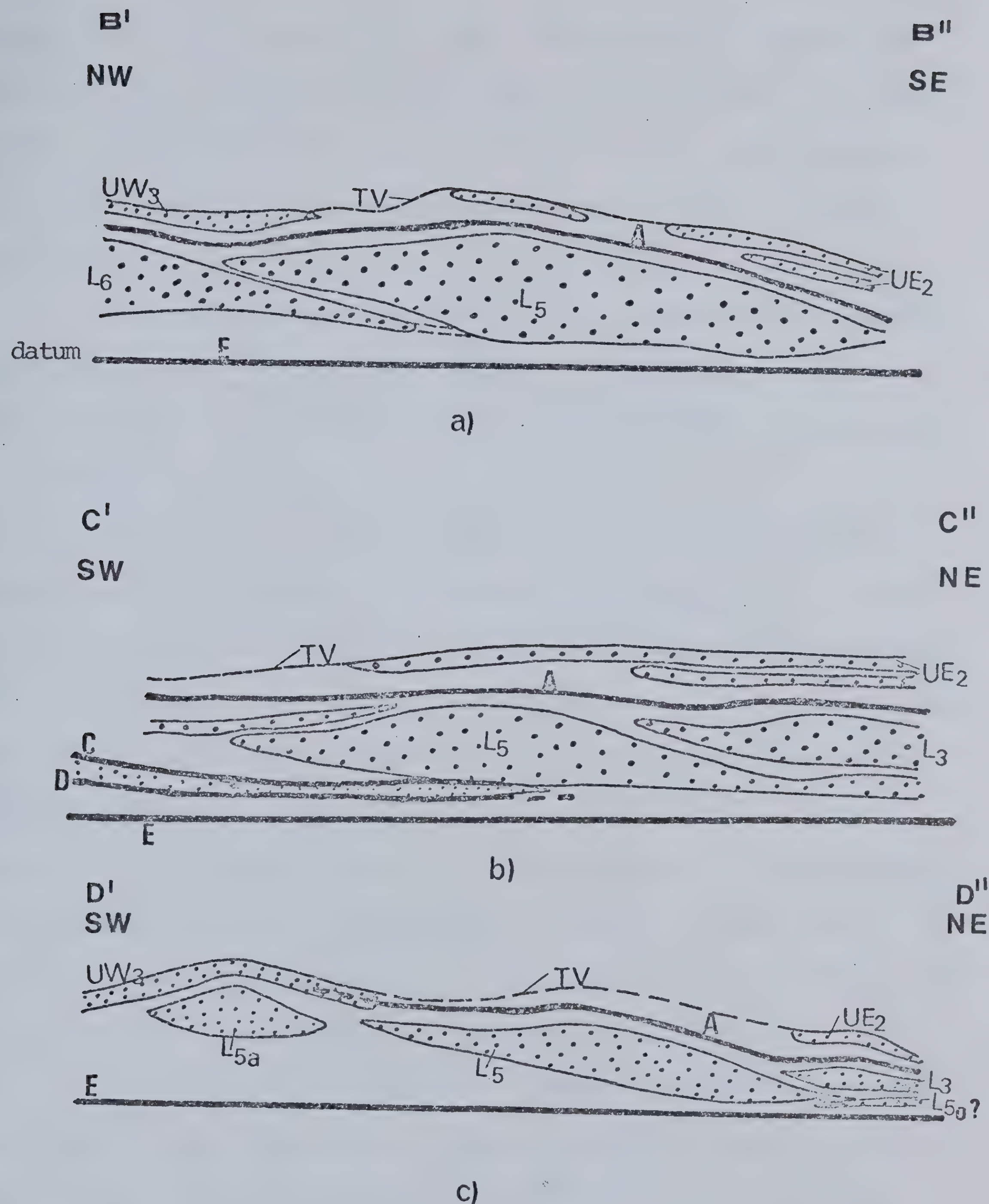

Figure 55. Generalized sketch of gross sand distributions in cross-sections (see fig. 51 for location):
a) B'-B"
b) C'-C"
c) D'-D"

roughly 30 miles (48.0 km) wide. A maximum thickness of about 85 feet (26.0 m) is attained in the extreme northwest corner of Township 32, Ranges 20 and 21 W4M. The ridge is entirely surrounded by swales characterized by poor sand development.

Figure 56 shows the location of cross-sections used to diagnose this ridge. Bentonites E and D were used as datum planes. The identities of wells used in the sections are listed in Appendix Ij.

Section E'-E" (Figs. 57,60a) is oriented northwest-southeast from Township 34, Range 22 to Township 31, Range 19 W4M. It closely follows the axis of maximum development of the L_6 ridge. The datum is bentonite D. The base of the unit is fairly flat relative to the datum except in the extreme southeast (well 13) and northwest (wells 1 to 3), where it is slightly higher as a consequence of ridge migration parallel to the depositional strike. In the latter area it seems to override or grade into the eastern edge of the L_7 unit in well 1 near the L_6-L_7 swale.

A saddle (wells 7 to 10), later occupied by a thin sand unit, gives the top of the L_6 ridge an undulatory appearance. This probably indicates that the ridge was breached in this area and later filled with the overlying thin sand unit. Another very thin sand unit is shown on the northwestern slope of L_6 in wells 3 to 5.

Bentonite A lies in the overlying mudstone unit. The profile of this chrono-horizon parallels the configuration

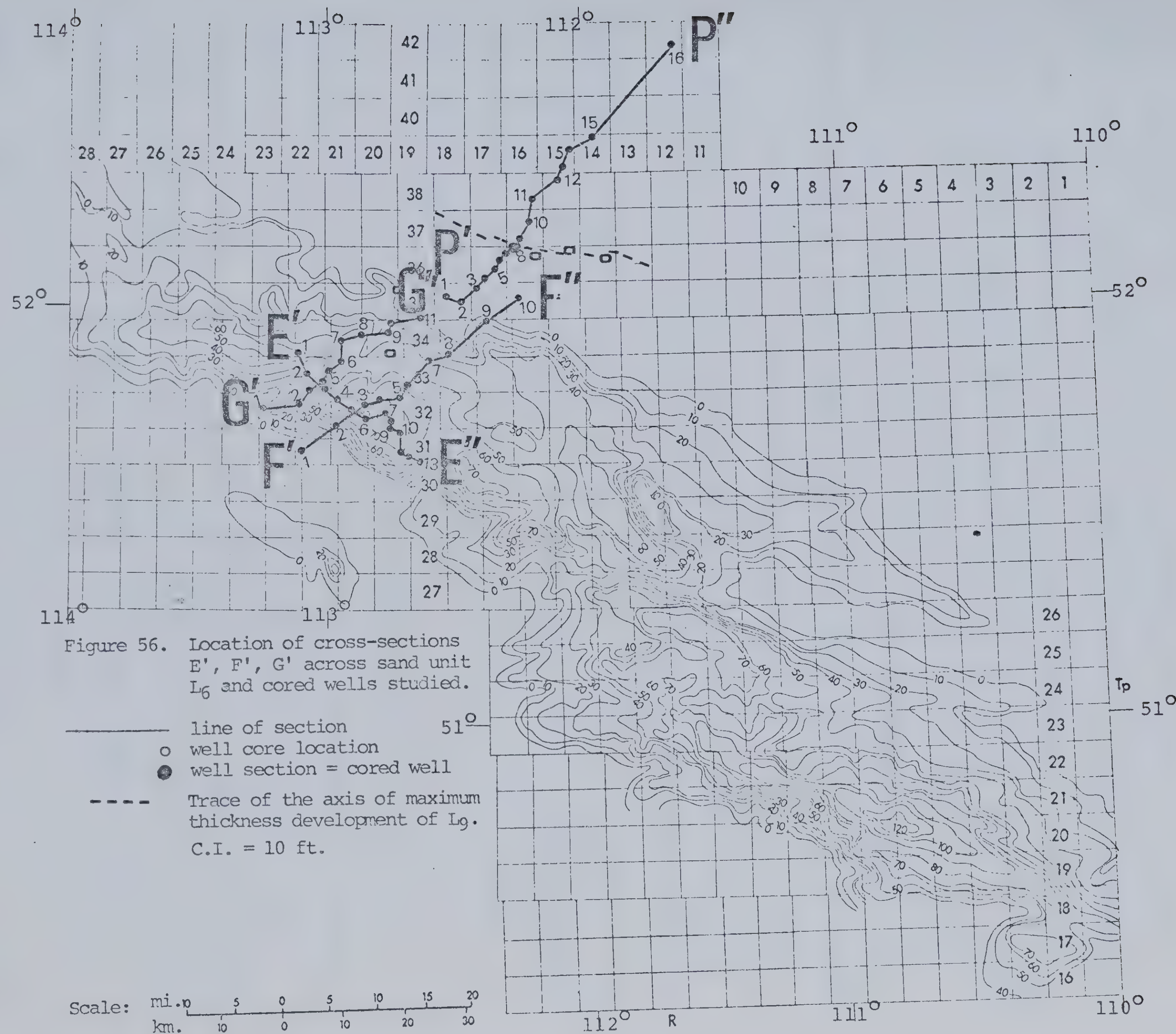

Figure 56. Location of cross-sections E', F', G' across sand unit L_6 and cored wells studied.

- line of section
- o well core location
- ● well section = cored well
- - - - Trace of the axis of maximum thickness development of L_9.

C.I. = 10 ft.

Scale: mi. 10 5 0 5 10 15 20
km. 10 0 10 20 30

of the top of this ridge. The thin Upper Viking interval is characterized by very poor sandstone development.

Section F'-F" (Figs. 58,60b) trends southwest-northeast from Township 31, Range 22 to Township 35, Range 16 W4M. The section shows that this ridge migrated to the southwest. A thin laterally restricted sand unit appears to migrate up the gentle northeast flank (wells 6 to 8). On the southwest flank (wells 1 to 4), another thin sand unit develops atop this slope of the L_6 ridge. The L_6 is bordered to the northeast by a swale (well 10) characterized by little sand.

Bentonite A occurs in the overlying mudstone unit. It defines a bottom surface which may have sloped slightly to the northeast. The northeasterly advancing Upper Western sandbody occurs in wells 1 and 2 and pinches out before well 3. Bentonite A may have fallen on this unit, although it is interpreted here to lie below it. The rest of the Upper Viking interval is exeedingly thin.

Section G'-G" (Figs. 59,60c) is oriented southwest-northeast from Township 32, Range 23 to Township 35, Range 19 W4M, along the northwest margin of the L_6 ridge. Bentonite E is the datum. Essentially the same features noted in the previous section are repeated here -- migration to the southwest, a thin gently sloping northeast flank with an overlying thin sand unit migrating upslope (wells 8 to 10). The northeast profile is defined by bentonite A, the top of the Viking, and the northeast swale (well 11). The Upper Western sandbody also occurs in wells 1 and 2.

The sketches of these sections are shown in Figure 60.

Core Study

The L_6 is not much cored, but unslabbed cores from the northeastern edge of this ridge were studied in two wells (2-30-35-19 and 11-2-34-20 W4M) located on a more or less southwest-northeast trend (see Figure 56 for location). They were examimed together allowing comparisons to be made regarding the textural attributes of this ridge. From the northeast to the southwest, the number of very thin coarsening upward sequences, average about 7 feet (2 m) thick, increased from 3 to 4; quartz also decreases in size toward the axis from medium or coarse to fine or very fine sand. The two youngest sequences are pebbly at the top. The average long axes of pebbles measured in these wells decreased from 1.25 cm to 0.625 cm in a southwesterly direction.

Detailed core descriptions are in Appendix IIIf; the facies are described and interpreted in Chapter VIII.

The L_7 Sandstone Ridge

Isolith

The L_7 ridge (Figure 28) is located within Townships 33 to 37, Ranges 22 to 28 W4M, northwest and south of the L_6 and Joffre sandbodies, respectively. It is almost entirely surrounded by swales characterized by very poor sand development. It trends northwest-southeast for more than 35 miles (56 km). This ridge is about 25 miles (40 km) wide and attains a maximum thickness of 60 feet (18 m) in

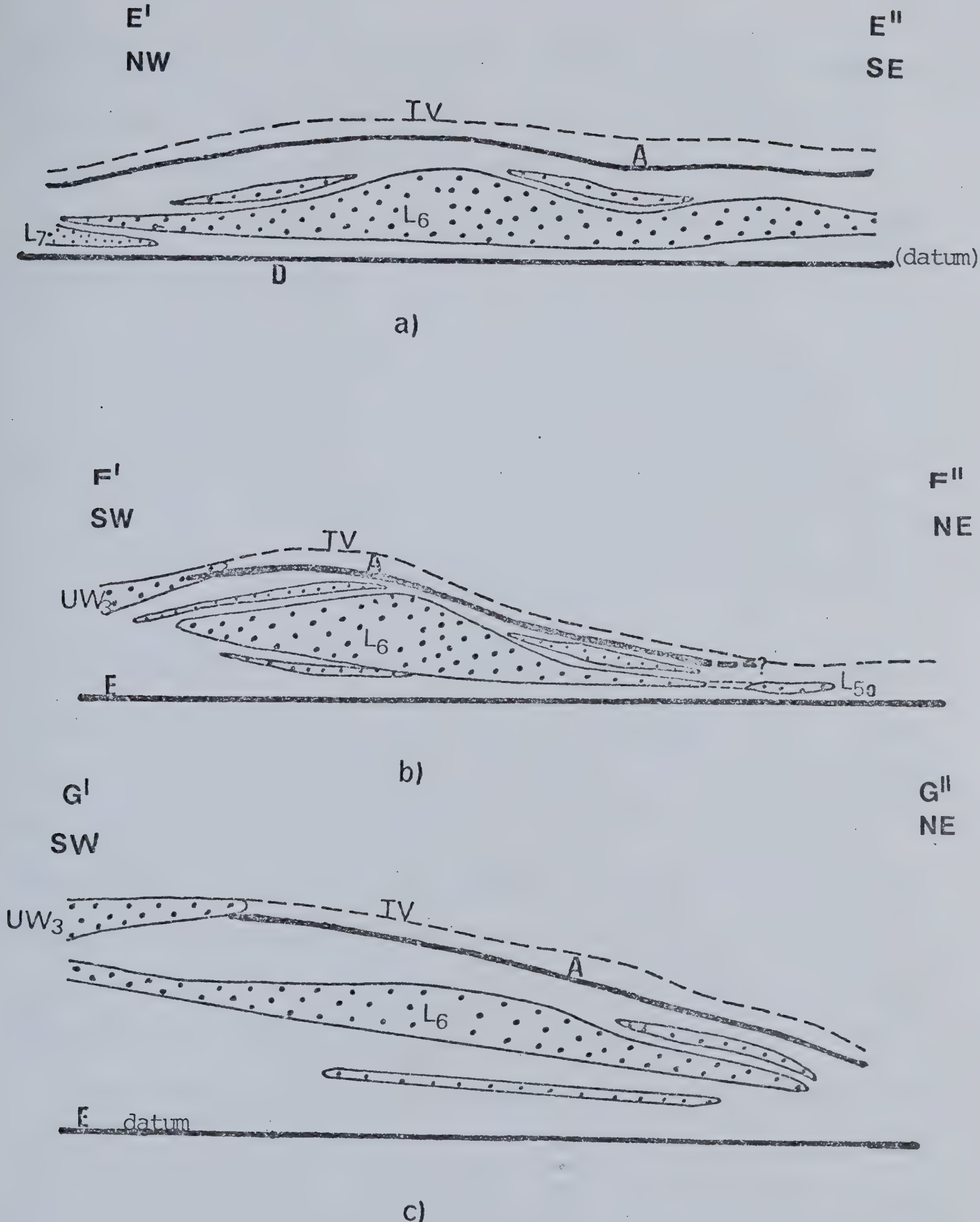

Figure 60. Generalized sketch of gross sand distribution in cross-sections (see fig. 56 for location):
a) E'-E"
b) F'-F"
c) G'-G"

the northern part of Township 34, Ranges 24 and 25 W4M. A steep southwestern flank and a wide gentle northeastern flank characterize the asymmetry of this ridge. In the study area, it is the 'terminal link' of the linear ridge chain to the southeast.

Cross-sections

Figure 61 shows the location of cross-section lines and cored wells used to study the depositional development of this unit. Bentonite E was used as datum. The identities of wells used in the sections are listed in Appendix Ik.

Section H'-H" (Figs. 62,65a) is oriented northwest-southeast from Township 34, Range 29 to Township 34, Range 21 W4M, roughly parallel to the trend of the axis of maximum sand thickness of the L_7 ridge. The section shows that ridge growth parallel to the depositional strike was more prolonged toward the northwest than the southeast, as it rises higher in that direction relative to the datum line. Maximum thickness occurs around wells 6 and 7. Northwest of these wells, the unit thins and grades into mudstone in wells 1 and 2. Wells 1 and 2 are believed to represent the northwestern part of the L_8 ridge located southwest of the L_7, as will be demonstrated later. To the southeast (wells 9 to 11) the L_7 ridge thins and pinches out before well 12. In this area, the L_6 ridge (well 13) appears to overlap the L_7 ridge as far as well 9.

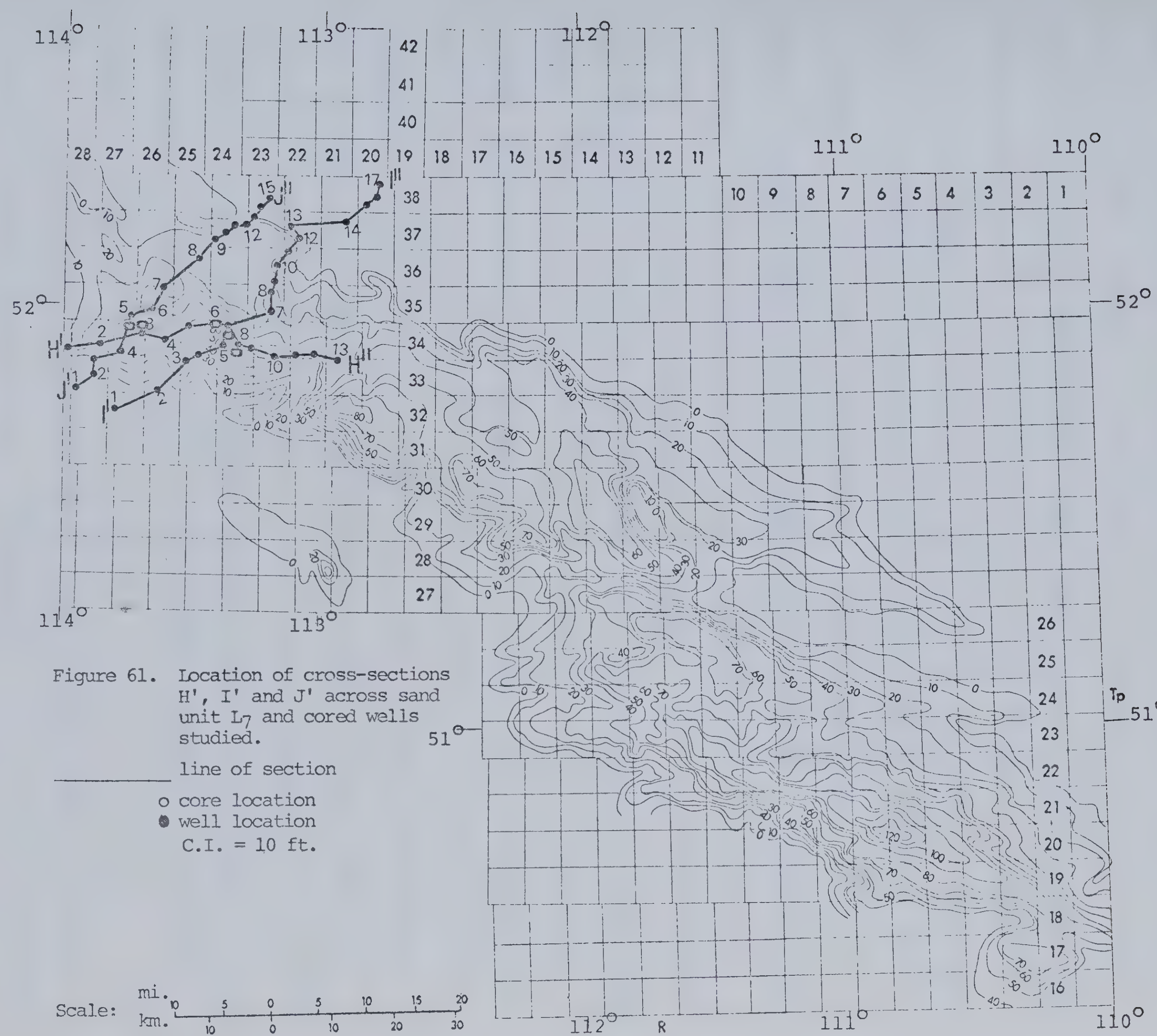

Figure 61. Location of cross-sections H', I' and J' across sand unit L_7 and cored wells studied.

——— line of section

o core location
● well location
C.I. = 10 ft.

Scale: mi. 10 5 0 5 10 15 20
km. 10 0 10 20 30

Bentonite A is well correlated between wells 11 and 13, and its position is reliably inferred northwest of these wells. In general, it approximates the end of Viking time in this area, except to the northwest (wells 1 to 4) where it is thought to have fallen on sand bottom. This sand unit is part of the northeast migrating Upper Western sandbody.

Section I'-I" (Figs. 63,65b) trends southwest-northeast from Township 32, Range 27 across the central part of the L_7 unit, to Township 38, Range 20 W4M. The datum line is bentonite E. Although its position northeast of well 12 is inferred, it is considered to be fairly reliable.

According to the datum, the L_7 ridge migrated in a southwesterly direction from well 12, thickening at the same time. Maximum thickness is developed in well 6. It then thins farther to the southwest and grades into mudstone in wells 3 and 4 as it overlaps the L_8 unit near well 2. In wells 10 to 12, the L_7 is underlain by a poorly developed thin basal sand which is chronotaxial to the B_3 sandbody further to the east. Wells 13 to 15 are located in a north-eastern swale about 10 miles (16 km) wide which separates the Lower sand ridge complex from the Joarcam Complex in wells 16 and 17.

Bentonite A is reliably correlated between wells 5 and 7. Beyond these wells it cannot be recognized with much certainty. It may have fallen on the Upper Western sand-body (wells 1 to 4) prograding to the northeast. Note that the Viking Formation thickens to the southwest. This

results mainly from the L_7 and Upper Western sandbodies migrating in opposite directions. The Lloydminster transgression also began earlier here. In the cross-section, the Base of Fish Scales marker also appears to rise to the southwest relative to the datum (probably because of increased sand in the section).

Section J'-J" (Figs. 64,65c) is another southwest-northeast oriented section from Township 33, Range 28, through the northwestern margin of L_7, to Township 38, Range 23 W4M. Bentonite E is again the datum. Basically, the section shows almost the same features as the previous section (Figure 63). However, the relationship between the L_7 and the L_8 sandy mudstone, on the one hand, and the southeastern part of the Joffre Complex on the other, are better protrayed. The L_7 clearly overlaps the L_8 unit in well 3. To the northeast, the L_7 unit appears to pinch out before well 12, and a muddy bank (well 12) separates the latter from the poorly developed southeastern part of the Joffre units in wells 14 and 15. This portion of the section is indicative of the chronotaxial relationship between the Joffre sands and the L_7 ridge. Bentonite A cannot be traced with certainty in this area, but may have fallen on the Upper Western sandbody between wells 1 and 6.

The described cross-sections of the L_7 sand ridges are sketched in Figure 65.

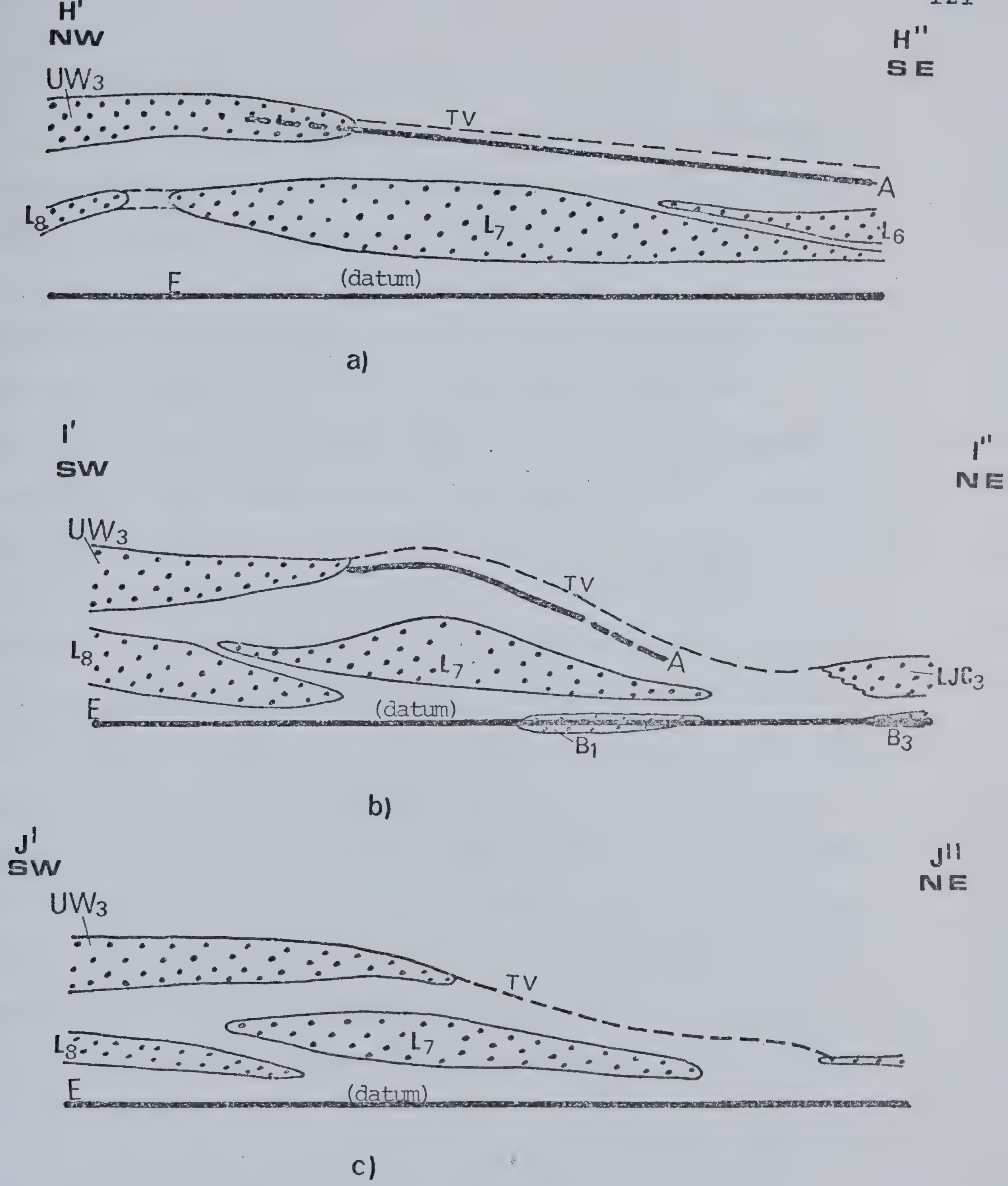

Figure 65. Generalized sketch of gross sand distribution in cross-sections (see fig. 61 for location):
a) H'-H"
b) I'-I"
c) J'-J"

Core Analysis

Five wells, which recovered cores from different parts of this unit, provided data on the anatomy of this ridge (see Figure 61 for the location of cored wells). A thick coarsening upward sequence characterizes the axis of maximum sand development and parts of the southwest and northeast flanks very close to the axis of the ridge. On the northeastern flank near the ridge axis, the sequence is capped by a thin conglomerate bed composed of subangular to subrounded black and brown chert pebbles. This bed was not found either on the ridge axis or the southwest flank. However, a few black chert pebbles were dispersed in the overlying nonbioturbated mudstone interval in the latter area. On the other hand, two east-west trending wells which cored through the northeastern portion of the northwest margin of this ridge show an upslope increase in the number and thickness of the coarsening upward sequences from two to three. The youngest sequence is capped by a thin conglomerate bed composed of nearly equidimensional black and brown chert pebbles. Detailed descriptions of these cores are in Appendix IIIg.

The Lower Sandridge Complex: A Summary

The complex comprises 9 ridges (L_0 to L_8) which formed southwest of the B_1 unit, but later in time. They are generally conformable on the Joli Fou Formation, except in parts of the northwestern margin of the L_3 member, the

L_3-L_4 swale and the southeastern margin of the L_2 member, where core evidence, thinner than normal sections, and shape of spontaneous potential curves indicate or suggest a disconformable contact. It is thought that pre- or syn-dispositional scouring of the sea floor was responsible for this phenomenon.

At certain times ridges were entirely surrounded by swales, generally characterized by very limited sandstone development. In places where ridges are known to overlap (e.g., L_1 on L_0, and L_3 on L_5), this is interpreted to be due to laterally separated isochronous ridges migrating in the same general direction, but usually at different rates. It is envisioned that the principal current flow pattern responsible for the genesis of these ridges paralleled that of the swales; hence, the predominant occurrence of pebbly beds in lows around the L_2, L_3 and L_7 ridges. This reflects the topographic control of the seafloor on the distribution of some of the conglomerate beds.

The orientations and nature of the swales, coupled with the indented margins of some of the ridges, probably indicate that currents at times flowed in more or less opposite directions. For instance, ridge growth parallel to depositional strike seems to be almost equal in both northwest and southeast directions for the L_1 and L_2 ridges; whereas, a northwesterly flow direction may have been predominant for the L_3, L_6 and L_7 units, and the opposite direction true for the L_4 unit.

A general thickness asymmetry characterized by a

steep southwest and a gentle northeast thickness gradient, interpreted as reflecting flank slope, is consistent with the deduced southwesterly (landward) direction of migration for these ridges. In general, however, the northwesterly ridges (L_6 and L_7) have a broader, northeastern flank. The very thin sand units often noted to have migrated up the gentle northeast and/or southwest flanks of pre-existing ridges may indicate the manner in which sand was accreted onto these ridges when they were developing.

The stratigraphic position of bentonite A relative to the top of these ridges indicates that:

1. Deposition of the northwestern ridges (L_5, L_6 and L_7) terminated earlier than the southeastern ridges (L_1, L_2, L_3-L_4). Thus, the mudstone interval which overlies the former ridges is thought to be mostly the offshore facies for the overlying Upper Western sand prograding to the northeast in the opposite direction to that of the underlying sand ridges. In contrast, the mudstone above the southeastern ridges is predominantly the shoreward facies of the southwest (landward) migrating Upper Eastern units.
2. Deposition of the L_1, L_2 and L_4 ridges up to the time of bentonite A, coupled with continued deposition of the Upper Eastern sand unit, may indicate sediment contribution by a source area different from that of the northwestern ridges. This may in part be reflected in the large dimensions (length, width, thickness) of the

southeastern (L_1 and L_2) ridges.

3. A general northeast sloping profile suggested by the slope of bentonite A may reflect the topographic gradient at that time.
4. Coarsening upward textural gradients, at times in cycles, characterize sandstone ridges. The occurrence and distribution of some pebble conglomerate beds appear to be topographically controlled.

B. The Lower Joffre Sandstone Ridge Complex

The Lower Joffre sand ridge complex is located within Townships 38 and 39, Ranges 25 to 28 W4M. This area lies approximately 10 miles (16 km) east to northeast of the town of Red Deer, Alberta. The complex is also north-northeast of the L7 ridge member of the Lower sand ridge complex (Figure 28). Further to the northwest the Joffre complex may be continuous with the Gilbey field reservoir sands.

The complex is elongate and trends northwest-southeast parallel to the structural and depositional strike, but at a fairly high angle to the L7 unit. The Joffre complex is more than 30 miles (48 km) long and only about 6 miles (10.0 km) wide on the average. The areal distribution of these sand units is outlined (Figure 28) but not mapped. They are oil-bearing and, as such, have been fairly well mapped by previous workers. In cross-sections, four relatively thin sand units are recognized and designated LJ_1 to LJ_4 for convenience of discussion.

Cross-Sections

Five stratigraphic cross-sections were used to diagnose these sandbodies. Laterally persistent and distinct electric log kicks were used as datum planes as the diagnostic bentonite horizons could not be correlated with certainty. The cross-section lines are located in Figure 66, while the identities of wells used in the sections are given in Appendix Il.

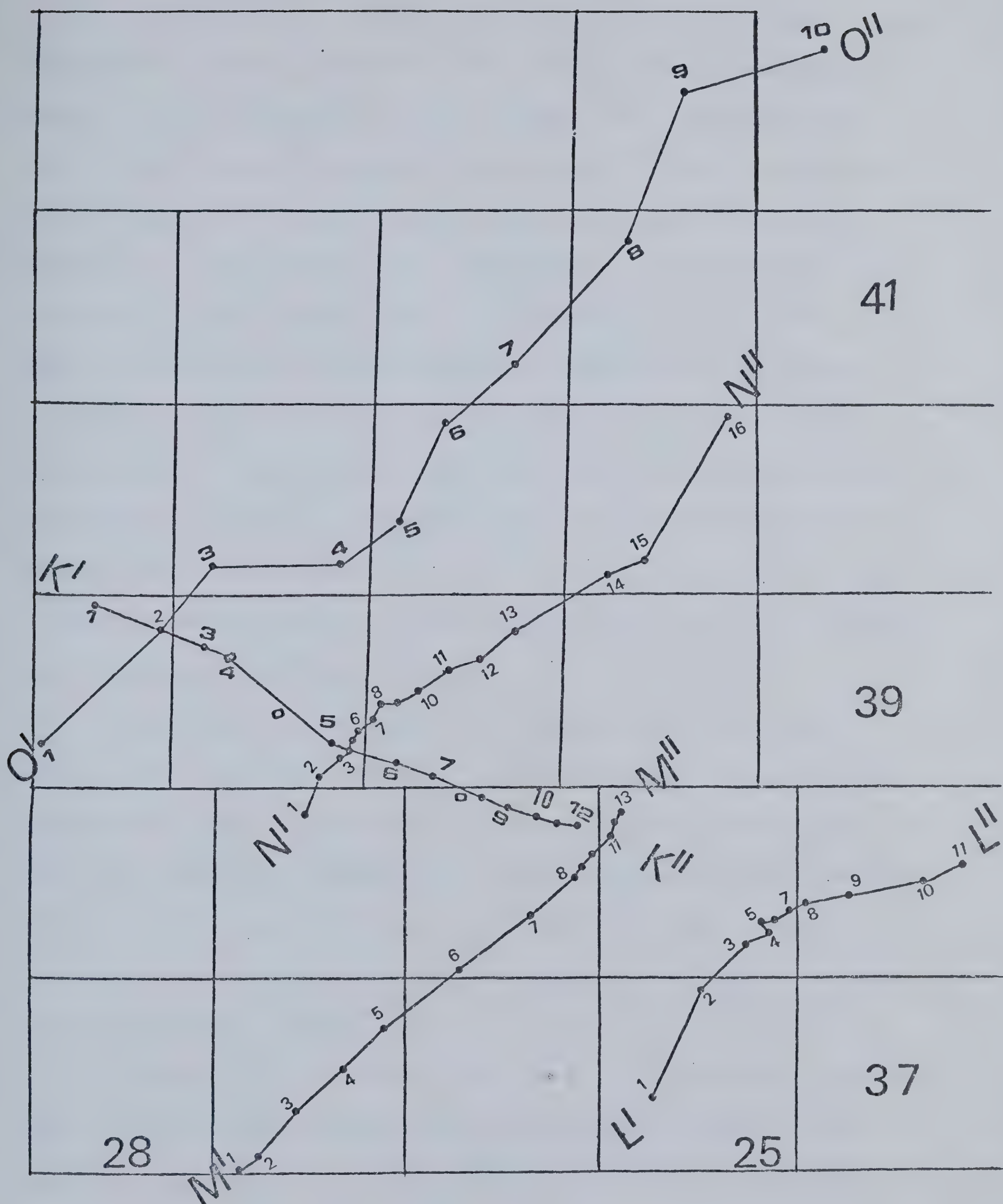

Figure 66. Location of cross-sections K' to O' across Lower Joffre sand units and cored wells studied.

——————— section lines
o core location

Section K'-K" (Figures 68, 72a) runs parallel to the depositional strike of the Joffre complex from Township 39, Range 28 to Township 38, Range 26 W4M. An electric well log kick is the datum; however, bentonite E horizon is shown in wells 4 and 8. The relatively thin LJ_1 unit in well 12 pinches out before well 11. The LJ_2 unit develops maximum thickness in the latter well, overlaps the LJ_1 in well 12, thins as it rises to the northwest relative to the datum, finally overlaps the LJ_3 unit in well 8 and pinches out before well 7. The latter sandbody (LJ_3) also rises to the northwest from well 8, attains maximum thickness in well 5, and overlaps the LJ_4 unit in well 3. The LJ_4 in turn rises to the northwest from well 3 to beyond the limits of the map area (Township 39, Range 28W4M).

Relative to the datum, it would appear that all these units began to evolve at about the same time, but the LJ_3 and LJ_4 bodies continued up to the end of Viking time in this area, whereas formation of the LJ_1 and LJ_2 units ceased earlier. The above relationships indicate that the axes of the LJ_2, LJ_3 and LJ_4 units may be displaced slightly to the northwest in that order.

Section L'-L" (Figures 68, 72a) is oriented southwest-northeast from Township 37, Range 25 to Township 38, Range 24 W4M. The thin bentonite bed near the top of the Formation (Love, 1955) is the datum. However, the inferred position of bentonite E is shown between wells 1 and 2, and wells 9 and 10. The L_7 ridge member of the Lower sand ridge

complex in well 1 is laterally separated from the Joffre units (wells 3 to 8) by well 2 located within a swale characterized by sandy mud development.

The LJ_1 unit at the base of the Viking in wells 6 to 8 consists of two very thin imbricating sandbodies to the southwest. These laterally restricted units pinch out around well 5. The LJ_1 is in turn overlain by the LJ_2 in imbricate fashion. This sandstone attains maximum thickness in well 5, thins as it rises to the southwest, and pinches out before well 2.

Northeast of these sandbodies, wells 9 and 10 are located in a swale characterized by mudstone. It is this swale which differentiates the Joffre sandbodies from the sandy mudstone facies of the Lower Joarcam sand ridge complex in well 11. This cross-section shows the L_7 ridge member, the Joffre units and the Joarcam ridges to be chronotaxial.

A poorly developed isochronous equivalent of the B_1 unit, herein referred to as B_3, lies at the base of the Viking in wells 10 and 11, near bentonite E.

Section M'-M" (Figures 69, 72a) is a southwest-northeast trending section from Township 37, Range 27 to Township 38, Range 25 W4M. The bentonite horizon near the top of the Formation is the datum. The position of bentonite E is shown in wells 1 to 4. The northeastern margin of the L_7 ridge member of the Lower sand ridge complex is correlated between wells 1 and 7. The unit maintains a

fairly level base, with only a slight diachronous tendency toward the southwest between wells 1 and 3. In wells 1 and 2 it is imbricately overlain by a thinner unit probably advancing to the southwest. The thinning in well 4, and the rather poor spontaneous potential log response in well 5 may indicate that this area represents a swale which separates the sand unit of wells 1 to 2 from that of wells 6 and 7. However, inadequate well coverage in the area hinders accurate interpretation.

The LJ_2 unit attains maximum development between wells 10 and 12, thins as it migrates to the southwest, and pinches out before well 7. Northeast of well 12, the LJ_2 pinches rather abruptly into the Joffre-Joarcam swale. The very thin sand which underlies the LJ_2 in well 10 may be the northwestern edge of the LJ_1.

The Viking Formation thins to the northeast between wells 1 and 7 and maintains a fairly constant thickness northeast of well 7. This thinning is shown by the profile of the top of the Sandstone, which slopes gradually to the northeast and flattens in the area of the LJ_2 unit. The relationship of the top of the Formation to the bentonite horizon near the top of L_7 in wells 1 to 7 indicates that whereas Viking sand deposition continued between wells 1 and 4, little or no sand deposition occurred northeast of the latter well. It is suggested that the overlying sandy mudstone interval between wells 1 and 4 represents the offshore facies of the northeast prograding Upper Western sand

encountered near the axial zone of the L7 member.

Section N'-N" (Figures 70, 72b) is oriented in a southwest-northeast direction from Township 37, Range 28 to Township 40, Range 25 W4M. An electric well log kick is the datum. Relative to the datum, the LJ3 unit migrates to the southwest from well 6, attains maximum thickness in well 5, thins and grades into mudstone beyond well 1. Northeast of well 6, this unit thins rather abruptly in well 7, and finally pinches out before well 8. Based on the shapes of the spontaneous potential curves, the lower contact is sharp around wells 5 and 6 and somewhat gradational southwest of these wells.

Whereas the southwestern edge of the LJ3 unit is overlain by mudstone (wells 1 to 3), the northeast margin is imbricately overlain by thin sand units in wells 6 to 10. The sands northeast of the latter well constitute the south-westernmost members of the Lower Joarcam ridge complex to be discussed later. The cross-section shows the isochroneity of the Joffre and Joarcam sand ridge complexes.

Section O'-O" (Figures 71,72b) trends southwest-northeast from Township 39, Range 28 to Township 40, Range 26 W4M. A distinct and laterally persistent electric log kick is the datum. The position of bentonite E in well 14-28-41-26W4M (Amajor, 1977) correlates with the base of the thin B3 sand unit in well 8. The LJ4 unit is best developed in well 2 from where it rises to the southwest relative to the datum, becoming muddy in well 1. A low area

of minor sand development (well 3) separates the LJ4 laterally from the LJC_1 member (wells 4 and 5) of the Lower Joarcam sandstone complex.

The B3 sand unit at the base of the Formation in wells 4 to 10 is a time equivalent of the B1 unit to the southeast. These cross-sections are sketched in Figure 72(a,b).

Core Analysis

Cores recovered from the LJ_3 unit were studied in two wells, while the LJ_2-LJ_3 overlap relationship was examined in another well. These cores are located in Figure 66 and described in detail in Appendix IIIh.

Although, on the average, the LJ_3 unit could be regarded as a coarsening upward sequence from mudstone to conglomerates, the change is not gradational. In the northwestern part of the LJ_3 unit, the coarsest chert pebble beds are concentrated near the middle of the sequence and the lower contact is sharp. In the central area a thick, generally coarsening upward sequence is internally constituted by three thinner coarsening upward sequences which overlie one another sharply. These are then capped by another thin but distinct coarsening upward sequence. In well 13-33-38-26W4M where the LJ_2 overlaps the LJ_3, two relatively thin coarsening upward sequences belonging to these units were recognized. The LJ2 unit has a sharp base followed by mudstone, and terminates with very coarse sand. Generally, the fairly well rounded black and brown chert

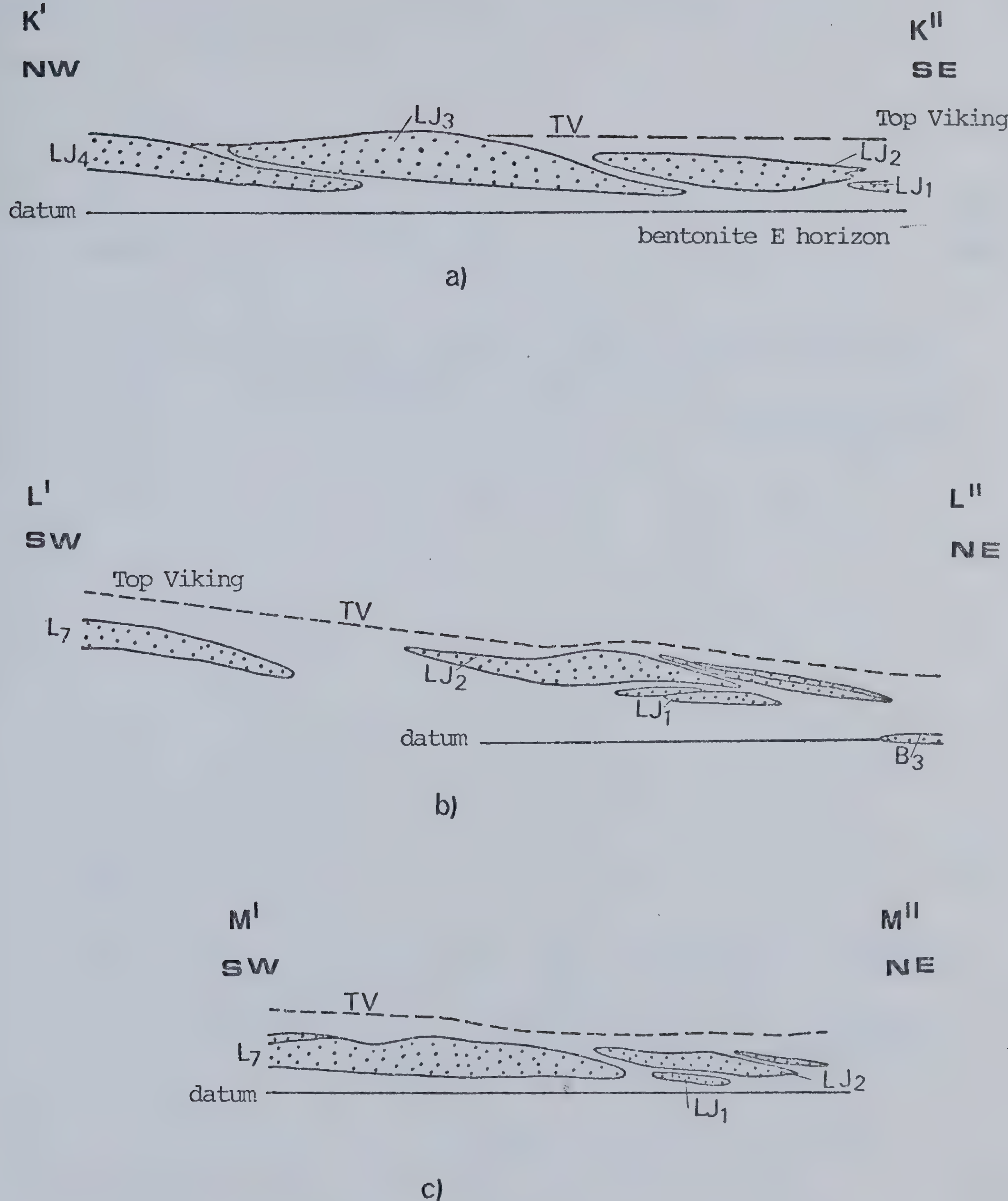

Figure 72a. Generalized sketch of gross sand distribution in cross-sections (see fig. 66 for location):
a) K'-K"
b) L'-L"
c) M'-M"

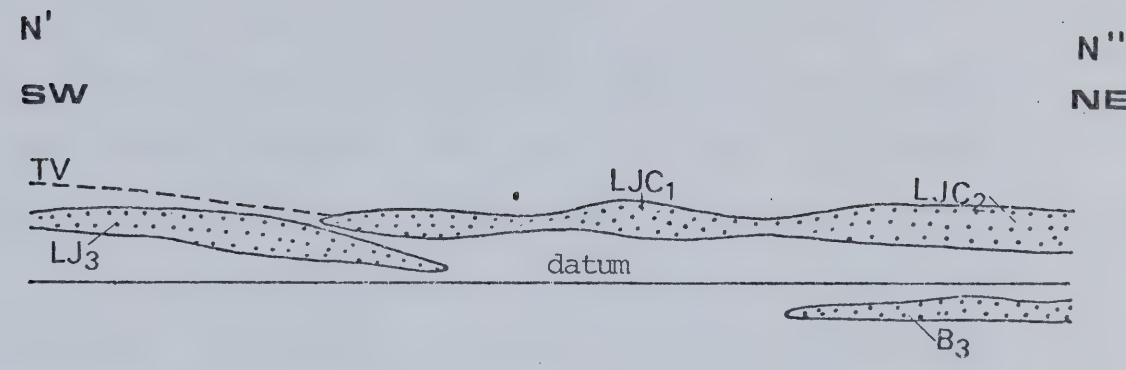

a)

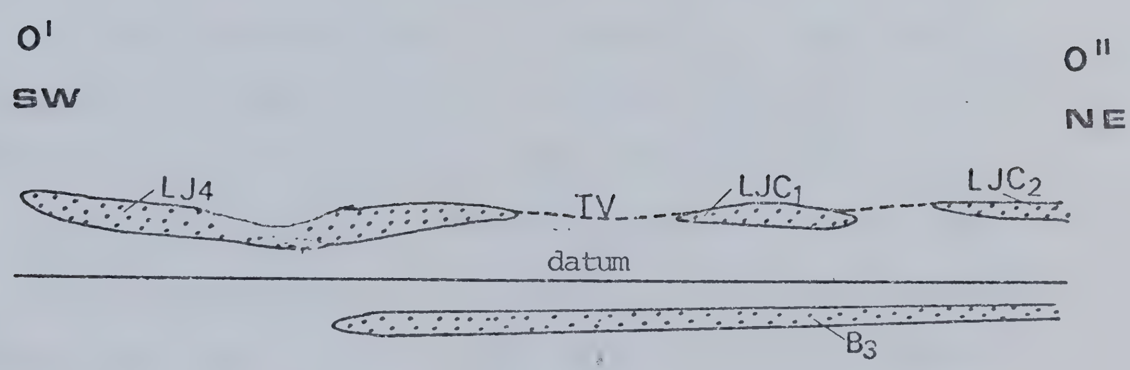

b)

Figure 72b. Generalized sketch of gross sand distribution in cross-sections (see fig. 66 for location):
a) N'-N"
b) O'-O"

pebbles are larger in size in the central part of the LJ_3 than to the northwest or southeast.

Summary

At least four laterally restricted, elongate, roughly linear northwest-southeast trending ridges constitute the Joffre reservoir sand ridge complex. Succeeding ridges are displaced laterally to the northwest of previous ones. The northeastern margins are relatively clean, better well developed, and pinch out rather sharply, whereas the southwestern margins are muddy and grade into mudstone. This is consistent with a deduced southwesterly direction of sand ridge migration. The sandbodies often begin with a rather sharp lower contact in the northeast which becomes gradational in the southwest. In places, migration produced an imbricate arrangement. The sharp lower contacts of these units at their northeast edges as observed in core and indicated by the shape of the spontaneous potential logs, coupled with the rather abrupt manner in which they terminate in this part, and the indication of missing section near the base of the LJ_4 unit (Figure 71) strongly suggest scouring along the northeast edge before or during deposition. A similar observation was made and interpreted for the northeast edge of the B_1 (Hamilton Lake) reservoir sandstone. The evidence does not favour ridge migration toward the northeast, as interpreted by Shelton (1973).

Sand-ridge growth terminated earlier in the

southeast than in the northwest, although they may have begun their sedimentary evolution at the same time. The LJ_2 and LJ_3 ridges exhibit coarsening upward textural gradients from mudstone at the base to brown and black chert pebble conglomerate beds at the top.

Two swales, characterized by little sand development and located to the southwest and northeast of these ridges, differentiate them laterally from the Lower and Joarcam sand ridge complexes to the southwest and northeast, respectively. Well log correlations indicate that the three complexes are chronotaxial. The coincidence of the top of the Joffre sands with the apparent top of the Viking Formation in this area is not indicative of the later genesis of these units. Rather, the writer believes that this phenomenon is partly a function of depth and the distance from the northeast prograding shoreline to nearshore Upper Western unit whose offshore mudstone facies overlies much of the L_7 ridge member of the Lower sand ridge complex to the southwest. This is consistent with the earlier interpretation that Viking deposition ceased earlier in the northwest of the study area than in the southeast.

C. The Lower Joarcam Sandstone Ridge Complex

Figure 73 is the isolith map of the Lower Joarcam sand ridge complex. It is approximately located within Townships 38 to 52, and Range 18W4M to the fifth Meridian within the map area, but extends farther to the northwest

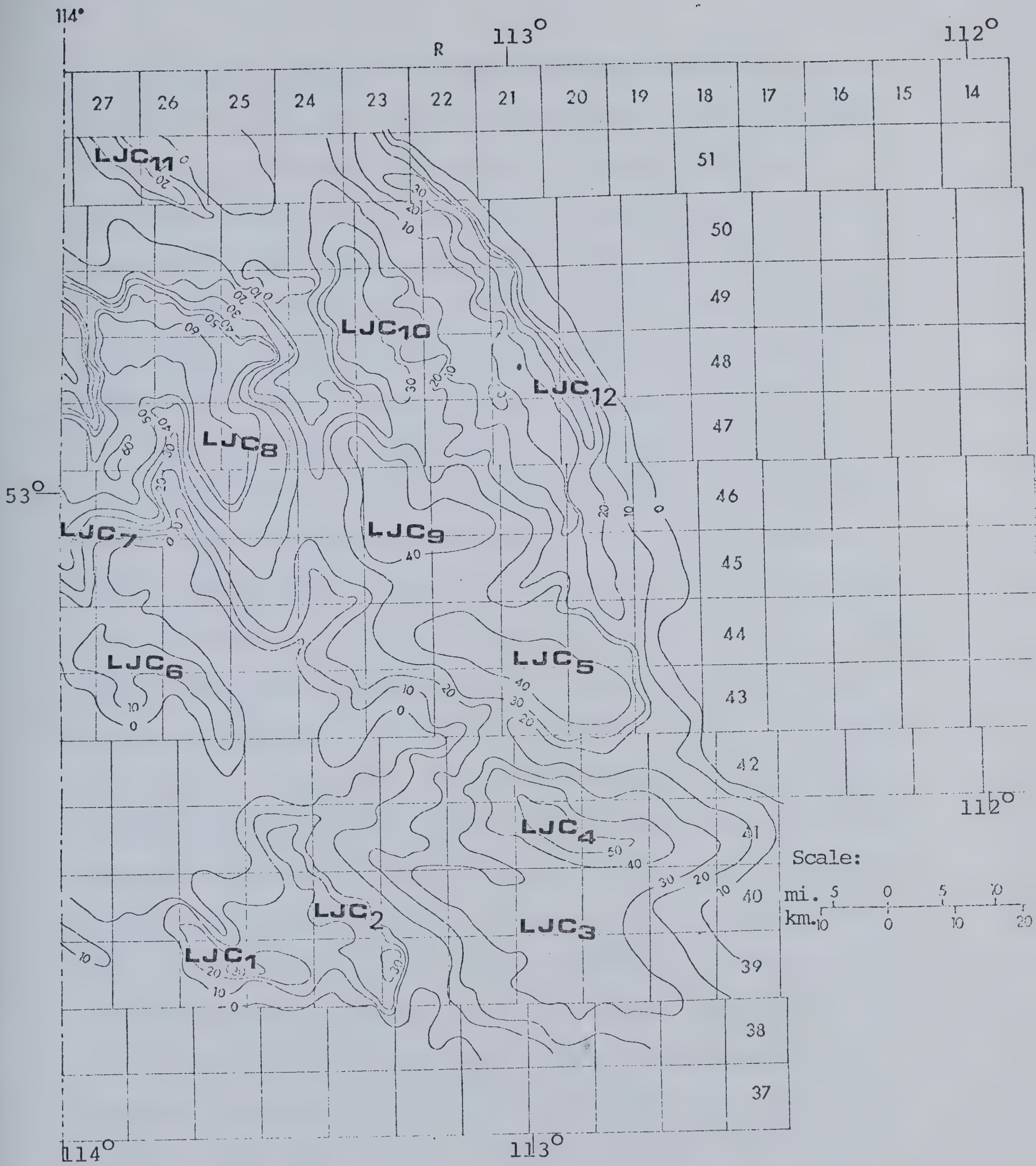

Figure 73. Isolith map of the Lower Joarcam sand ridge complex.

and southeast. Thus, it trends northwest-southeast like its southern correlatives, the Lower and Joffre complexes, but is laterally separated from them by a major northwest-southeast trending swale (see the northeast edge of the Lower sand ridge complex, Figure 28, for location.

Twelve fairly well developed sand ridges are recognized and designated LJC_1 to LJC_{12} from south to north. However, the LJC_5, LJC_9 and LJC_{10} represent localized thickening within the same ridge. Township 44 roughly divides the ridges into two groups: southern and northern.

The southern ridges (LJC_1 to LJC_6) are relatively smaller and generally more poorly developed. Length varies roughly between 15 miles (24 km) and 35 miles (56 km), while width ranges approximately from 5 miles (8 km) to 10 miles (16 km). A maximum thickness of 50 feet (15.1 m) is developed by the LJC_4 within Township 41, Ranges 20 and 24 W4M. On the other hand, the northern ridges are larger and better developed. The LJC_{12} ridge (Joarcam oil reservoir sandbody) is more than 50 miles (80 km) long, and the LJC_8 unit is more than 15 miles (24 km) wide in places, and attains a maximum thickness slightly greater than 60 feet (18 m).

Both sets of ridges are roughly parallel trending northwest-southeast. However, the northern ones trend more northerly than the southern. The ridges are elongate and fairly linear except for the LJC_7 and LJC_8 units which show rather complicated shapes. The ridges are more or less surrounded by well defined swales characterized by thin or poor sand development. Some swales bifurcate while others run

uninterruptedly northwest-southeast paralleling the trend of ridges.

<u>Cross-Sections</u>

Nine concatenated stratigraphic cross-sections were used to diagnose the complex. Distinct and laterally persistent electric well log kicks were used as datum horizons because the diagnostic bentonite horizons could not be reliably correlated in the well logs of the area. Even bentonite C, which underlies the LJC_{12} reservoir sandbody in places, does not seem to be laterally persistent.

Cross-section lines are located in Figures 56 and 74. The identities of wells used to construct these sections are given in Appendix Im.

Section P'-P" (Figures 75,85a) is an extension of section G'-G" (see Figures 56 and 59 for location) in a northeasterly direction from Township 35, Range 18 to Township 42, Range 12 W4M. Bentonite E is datum; its stratigraphic position is correlated with certainty between wells 1 and 4, and 14 and 15. In wells 9 and 10 it is reliably inferred. Wells 1 to 4 are located near the central part of the northwest-southeast trending swale which extends from beyond Township 39, Range 26 southeastward to at least Township 33, Range 15W4M. This swale seems to continue to the southeast almost paralleling the L_4 unit. In the latter area, however, it is obscure because sand units are thin and laterally very restricted. It is this swale that

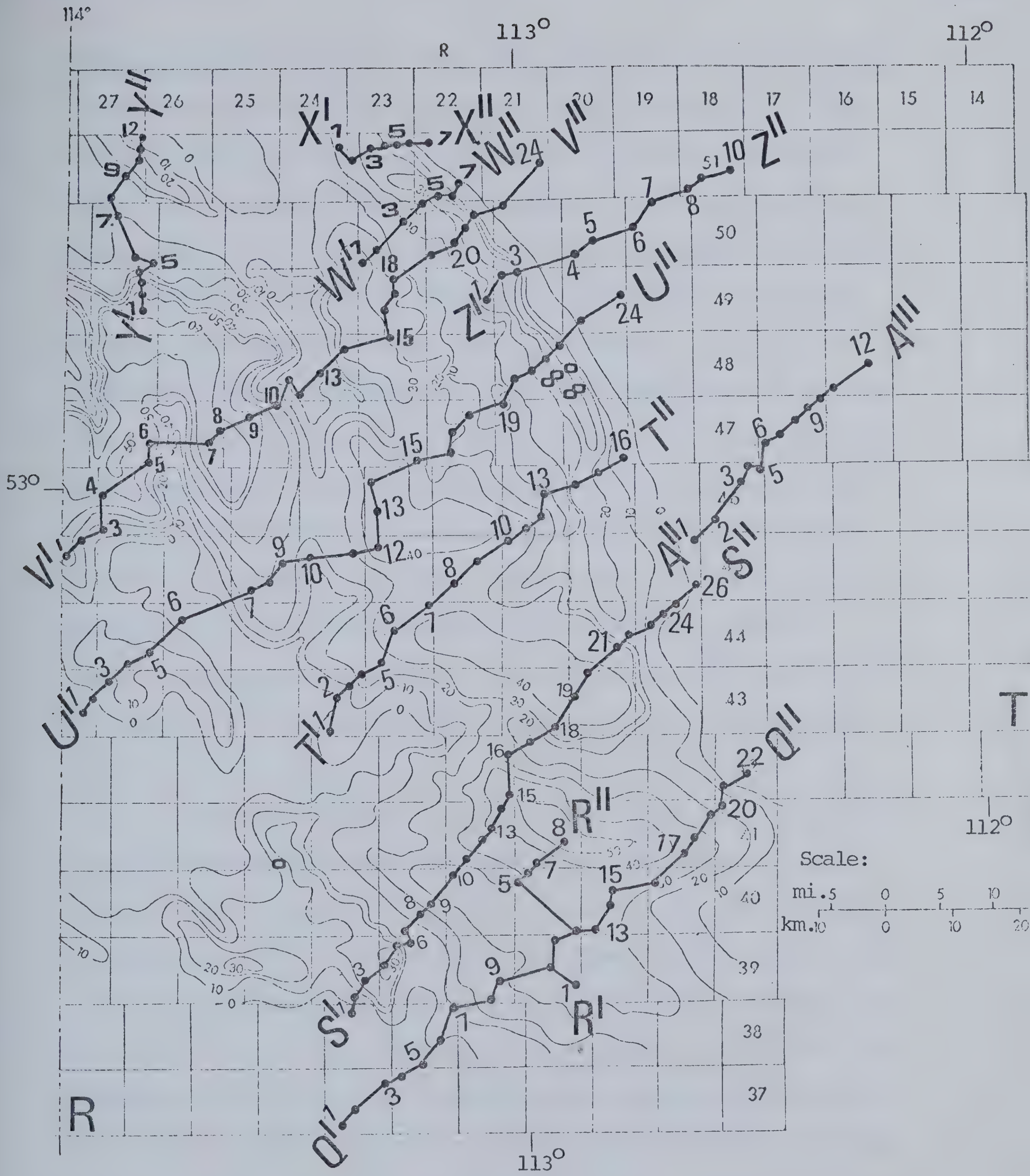

Figure 74. Location of cross-sections Q' to Z' and A" across sand units of the Lower Joarcam complex and cored wells studied.

——————— section lines
o core location
C.I. = 10 ft.

distinguishes the sand ridge complexes of the Lower chronostratigraphic unit (Lower, Joffre, and Joarcam sand ridge complexes). Its trend defines the approximate northeast limit of the Upper chronostratigraphic unit, beyond which no Upper Viking sands were deposited. The unmapped L_9 ridge is correlated between wells 3 and 14. The trace of the axis of maximum thickness of this unit is shown in Figure 56; it trends northwest-southeast. A maximum thickness of 50 feet (15.0 m) is developed in well 8. Relative to the datum, the unit appears relatively static except in the area between wells 3 and 6 where a late migration in a southwesterly direction is indicated. The southwestern, central, and northeastern parts of the unit are capped by laterally restricted thin sand units. Probably these are indicative of the manner in which vertical and lateral ridge growth occurred.

The stratigraphic position of bentonite C in wells 3 to 6, and that of the B_1 sandbody at the base of the Viking (wells 5 to 8, 11 to 12), suggest that the L_9 unit is diachronous from the Basal into the Lower chrono-intervals.

Wells 14 and 15 show that the Joli Fou interval is about 15 feet (4.6 m) thinner than in wells 13 and 16. In the former wells, however, the Viking interval is thicker and muddier. This phenomenon occurs almost at the northeast edge of the B_1 sand unit. When this zone is traced to the southeast, it coincides with the B_1-B_2 swale discussed earlier (Figure 16). The writer is of the opinion that the

loss of upper Joli Fou section is the result of seafloor scouring. However, the scoured trough was later filled with fines--probably during Viking time.

Bentonite A cannot be reliably correlated in this cross-section. However, this horizon should occur slightly above the L_9 sand; thus, the Upper Viking is not present in this area.

The L_9 ridge is, strictly speaking, the southeasternmost ridge member of the Lower Joarcam sand ridge complex to the northwest.

The development of the L_9 sandbody in three dimensions is partly shown in the fence diagram of Figure 19b. Wells 50, 51, 57, 58 and 97 are located in the swale which separates this ridge laterally from those of the Lower sand ridge complex (L_3 and L_5) to the southwest.

In the area occupied by wells 59, 60, 63, 91, 93, 94 and 104, two to three laterally restricted thin sands appear to migrate to the southwest, and probably accreted onto the northeast flank of the L_3-L_4 units. These are the sand units which interrupt the southeast extension of the above swale (well 50, 51, etc.).

Cores from L_9 were studied in four wells aligned nearly parallel to the depositional strike of the ridge (see Figure 56 for locations). A thick coarsening upward sequence of very fine to fine quartz grains characterizes the thickest part of the axis, whereas two similar but thinner sequences characterize the easternmost well, located

on the southwest flank but very near the axis of the ridge. The youngest sequence is capped by a very thin chert pebbly sand bed. This shaly and glauconitic sandbody is very strongly bioturbated throughout. The detailed descriptions of these cores are in Appendix III1.

Section Q'-Q" (Figures 76,85b) is oriented in a southwest-northeast direction from Township 37, Range 24 to Township 42, Range 18 W4M. The datum is a fairly persistent electric log kick near the base of the Formation. However, the bentonite E horizon is shown in wells 1 and 5.

The northeastern edge of the L_7 ridge member of the Lower sand complex (wells 1 to 3) migrated to the southwest relative to the datum and thickened at the same time. These wells lie to the immediate southeast of the Joffre complex. Wells 4 to 6 lie in the swale which distinguishes the Joarcam complex from the Lower sand ridge complex.

Northeast of well 6, the B_3 sand unit lies at the base of the Formation in wells 6 to 14. The overlying LJC_3 unit attains maximum thickness between wells 10 and 11, then thins and pinches out to the southwest before well 6. A thin muddy sand overlies it imbricately and appears to overlap the edge of the L_7 unit. Northeast of well 11, the LJC_3 unit thins and appears continuous with the southeastern margin of the LJC_4 unit in wells 16 and 17. This is due to the almost equal thickness of both units in this area. The latter ridge then thins and grades into mudstone in well 22 above a very thin sandstone (BJC_0) which underlies it

between wells 15 and 22. Between wells 12 and 22 the LJC_3 and LJC_4 ridges are covered by a sandy mudstone which also terminates Viking deposition in the area.

In general, these Joarcam ridges appear to have been static, and the stratigraphic positions of the L_7, LJC_3 and LJC_4 ridges in the section indicate that they are chronotaxial.

The lateral relationship of the LJC_3 and LJC_4 ridges is better shown by section R'-R" (Figures 77,85c) which trends south-north from Townships 39 to 41, Range 21 W4M. This section shows the flanks of the LJC_3 unit to be covered with mudstone, while its northeastern edge (well 6) either coalesced with or was overlapped by the LJC_4 ridge (well 8). The latter interpretation would imply a southwesterly direction of migration for LJC_4.

Section S'-S" (Figures 78,86a) trends southwest-northeast from Township 38, Range 24 to Township 45, Range 19 W4M. The base of the B_3 sand and a fairly persistent electric well log kick in wells 1 to 10, and 10 to 26, respectively, were used as datum horizons. The B_3 sand unit lies at the base of the Formation in wells 1 to 10. Another relatively thin lateral equivalent is correlated at the base of the Formation in wells 24 to 26. Both units are overlain in wells 9 to 26 by the BJC_o unit which thins to the southwest. Well 1 is located in the swale which separates the Joffre complex laterally from the Joarcam complex.

The LJC_2 ridge (wells 2 to 7) migrated to the

southwest relative to the datum and thins in the same direction. The northeastern edge of this sandbody (wells 6 and 7) is possibly overlapped by the northwest margin of the LJC_3 unit. Well 11 is located in the interridge swale between the LJC_3 and LJC_4 ridges. The sandstone is capped by a thin sandy mudstone from wells 10 to 12. The thickly developed LJC_4 sandstone (wells 13 to 15) shares a common sandy swale (wells 16 and 17) with the LJC_5 unit of wells 19 and 20. If the southern edge of the LJC_{12} reservoir sandstone (well 22) is distinct from the LJC_5 unit (well 21), and there is better indication of it elsewhere, LJC_{12} pinches out to the northeast before well 23. Northeast of well 20, these ridges are imbricately overlain by a thin sandy unit which extends as far as well 26.

Section T'-T" (Figures 79,86b) is another southwest-northeast oriented section from Township 43, Range 24 to Township 47, Range 20 W4M. The top of the BJC_o unit is the datum. The BJC_o sandbody, which thins to the southwest, is the first clean sand to be deposited in the area. The overlying LJC_5-LJC_9 complex appears to have migrated to the southwest between wells 1 and 13. This unit pinches out before reaching well 14 to the northeast, and also beyond well 1 to the southwest.

The lateral relationship between the LJC_5-LJC_9 and the LJC_{12} in wells 14 to 16 is not clear. However, the LJC_{12} may overlap the northeastern slope of the former unit up to well 9, and in turn be overlain by muddy sand beds

between wells 13 and 16. Alternatively, the LJC_{12} may pinch out before reaching well 13 to the southwest. In this interpretation, well 13 would be located in an interridge swale which was later filled with muddy sands which also capped both sand ridges between wells 9 and 16. The fairly sharp lower contact and gradational upper contact of the upper sand in well 13 suggest that the second interpretation may be more likely.

Section U'-U" (Figures 80,86c) is oriented southwest-northeast from Township 43, Range 28 to Township 49, Range 20 W4M. Two distinct but laterally restricted electric well log kicks were used as datum planes from wells 1 to 7, and wells 7 to 20, respectively. Bentonite C served as datum for wells 20 to 25. The B_3 sand unit at the base of the Formation between wells 1 and 6 was the first sandbody to be deposited in this area. This was later followed by the BJC_o unit which is better developed in wells 19 and 20, thins and terminates rather abruptly to the northeast before well 22; whereas, to the southwest, it thins gradually and grades into mudstone beyond well 14. The stratigraphic position of BJC_o in wells 21 to 24 indicates its genesis prior to the bentonite C volcanic ashfall.

The thin double, lens-shaped LJC_6 body is correlated between wells 3 and 5, where it developed close to the end of Viking time. The swale at well 6 distinguishes LJC_6 from the southern margin of the LJC_8 sand between wells 7 and 10. The northeastern edge of this unit is overlapped by LJC_9

between wells 11 and 14 where the LJC_9 also becomes a multiple unit.

Well 19 is located within the swale which separates LJC_9 laterally from the LJC_{12} reservoir unit of wells 20 to 23. This sandbody is thickest in wells 22 and 23, and thins to the southwest pinching out before reaching well 19. Another swale at well 24 distinguishes the LJC_{12} sand ridge from the Beaverhill Lake complex ($BBHL_1$) of well 25. The thin Viking interval underneath bentonite C in well 24 suggests scouring or non-deposition beneath the Viking within this part of the swale.

The stratigraphic position of the $BBHL_1$ unit in relation to bentonite C indicates that it began to form earlier than LJC_{12}. The $BBHL_1$, LJC_{12} and northeast margin of the LJC_8 ridges were later capped by sandy mudstones between wells 16 and 25.

Generally, this cross-section shows the Joli Fou interval to be thinner between wells 7 and 10, 14 and 18, and 22 and 23, and that the Lower Viking sandbodies (LJC_8, LJC_9 and LJC_{12}) are arranged in an imbricate pattern.

Section V'-V" (Figures 81,87a) is southwest-northeast oriented section from Township 45, Range 28 to Township 51, Range 21 W4M. An electric well log kick and bentonite C were respectively used for datum lines between wells 1 and 20, and 20 and 24.

The B_3 sand is developed between wells 1 and 4, and was followed by the deposition of the BJC_0 between wells 7

and 21. The base of this unit rises and falls relative to the base of the Formation, suggesting that erosion or non-deposition may have occurred in places. Whereas it thins gradually to the southwest and grades into mudstone beyond well 7, it appears to thin and terminate rather abruptly beyond well 21 to the northeast.

The LJC_7 ridge is recognized between wells 1 and 6. The thinning in the latter well and between wells 6 and 7 (not shown) distinguishes this ridge from the thickly developed LJC_8 from wells 7 to 10. The latter unit also thins to the northeast and pinches out before reaching well 13.

The LJC_{10} body, well developed within the area of wells 14 to 18, thins farther to the southwest and overlaps part of the northeastern flank of the LJC_8 between wells 10 and 13. This sand pinches out toward the northeast before reaching well 19. In well 18 it is in turn overlapped by the LJC_{12} reservoir, which develops maximum thickness in wells 21 and 22. This unit thins gradually and rises to the southwest up to about well 17. Northeast of well 22 it thins rapidly and terminates abruptly southwest of well 23.

The $BBHL_1$ sandbody (well 24) formed before the bentonite C volcanic ashfall. This places the time of formation of this sand within the Basal chronostratigraphic unit. This ridge is laterally distinct from the LJC_{12} unit because of the intervening swale in well 23. The thin Viking interval below bentonite C in the swale suggests seafloor scouring or non-deposition in this part of the swale. A similar

observation was made in the previous cross-section (Figure 80). Finally, sandy mudstone units capped the LJC_{10}, LJC_{12}, and $BBHL_1$ units northeast of well 12.

Generally, the section confirms the imbricate stacking of the LJC_8, LJC_{10}, and LJC_{12} and also shows that the Joli Fou interval is relatively thinner between wells 4 and 15.

Section W'-W" (Figures 82,87b) is a southwest-northeast oriented section from Township 50, Range 23 to Township 51, Range 22 W4M. A distinct and laterally persistent electric well log kick below bentonite C is the datum. This supplimentary section is another view of the lateral relationship between the LJC_{10} and LJC_{12} units.

The Basal (BJC_o) sand rises and falls relative to the datum between wells 1 and 4. This also suggests erosion or non-deposition in places. It finally grades into mudstone in well 5. The LJC_{10} which migrated to the southwest and thickened simultaneously between wells 3 and 1 is imbricately overlain by the southwesterly advancing LJC_{12}, thickly developed between wells 5 and 6. This latter unit thins rapidly in well 7 to the northeast. Two very thin sandbeds cap these ridges between wells 1 and 3, and wells 4 and 7.

Cross-section X'-X" (Figures 83,88a) is oriented in a roughly west-east direction along Township 51, Ranges 24 to 23 W4M. A distinct and persistent electric log signature is datum. This section shows the missing interval at the base of the Viking between wells 5 and 7. The LJC_{12} unit

clearly migrated to the west in this area, according to the datum. The unit thins eastward and grades into mudstone in well 7. The relatively thin sand unit which caps LJC_{12} appears to have migrated to the southwest as well.

A south to north trending section along Range 27W4M, Townships 49 to 50, is shown in Figures 84,88b (section Y'-Y"). The top of the BJC_o unit is the datum. Relative to the base of the formation, the BJC_o appears to have shifted toward the south and thinned in the area of the section. The LJC_8 unit attains maximum thickness development between wells 1 and 4, thins to the northeast of these wells up to well 8. The latter well is located in the swale which distinguishes this unit from the LJC_{11}, which is recognized from wells 9 to 12, develops maximum thickness in wells 10 to 11, thins to the northeast and pinches out immediately beyond well 12. The northern flanks of the LJC_8 and LJC_{11} units are capped by thin sands. Cross-sections P' to Y" are sketched in Figures 85 to 88.

Fence Diagrams

Two fence diagrams (Figures 89a,b) were prepared for the Joarcam and Beaverhill Lake sand ridges. The top of the Formation is datum. Figure 89a covers the southern Joarcam sand ridges within Townships 38 to 44, Ranges 16 to 28 W4M. The identities of wells in the diagram are given in Appendix IId. In this diagram, sands of the Basal chrono-interval include the B_3, restricted to the southwestern half, an undesignated sand in the northeast which is a time equivalent

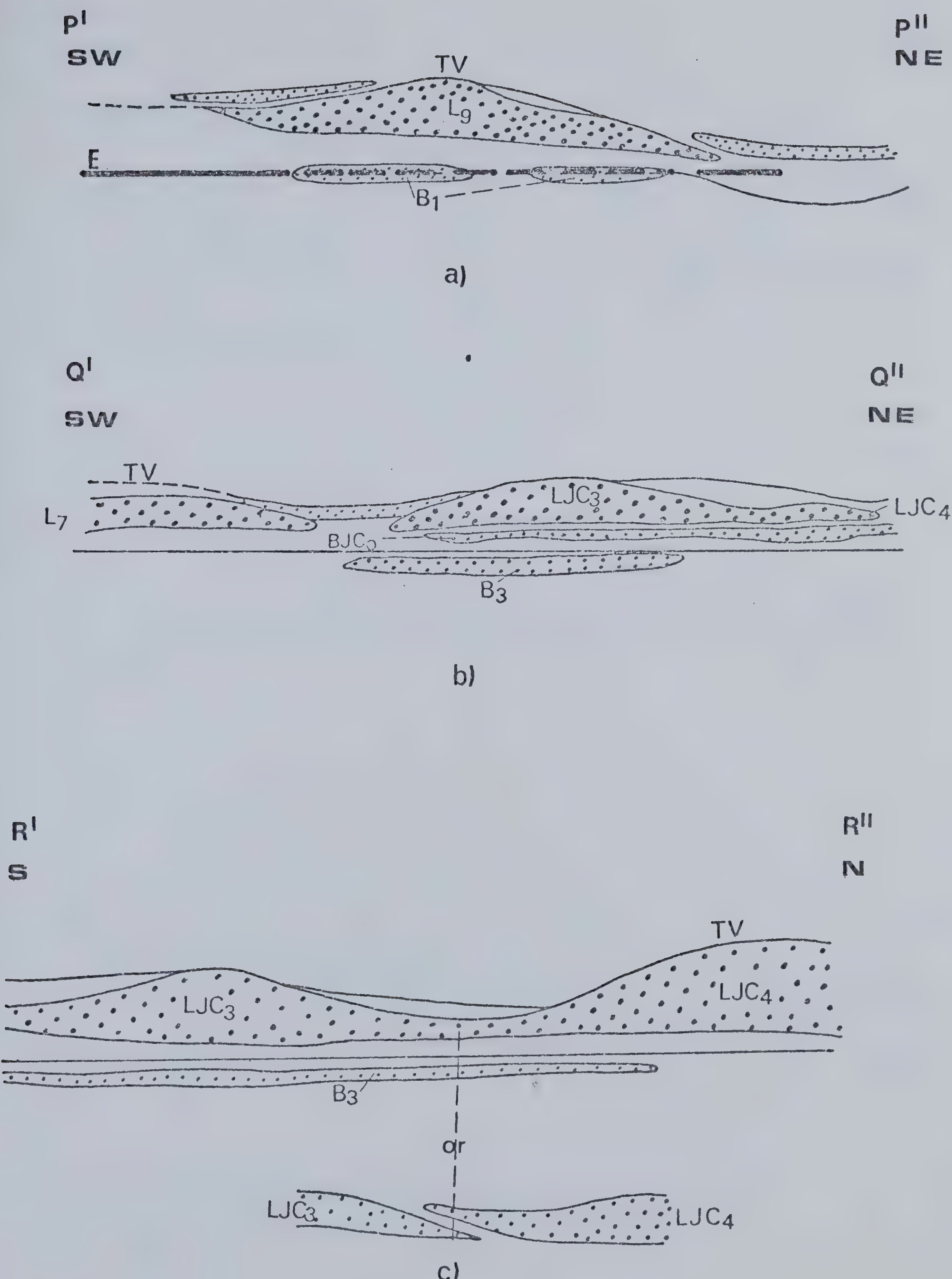

Figure 85. Generalized sketch of gross sand distribution in cross-sections (see fig. 74 for location):
a) P'-P"
b) Q'-Q"
c) R'-R"

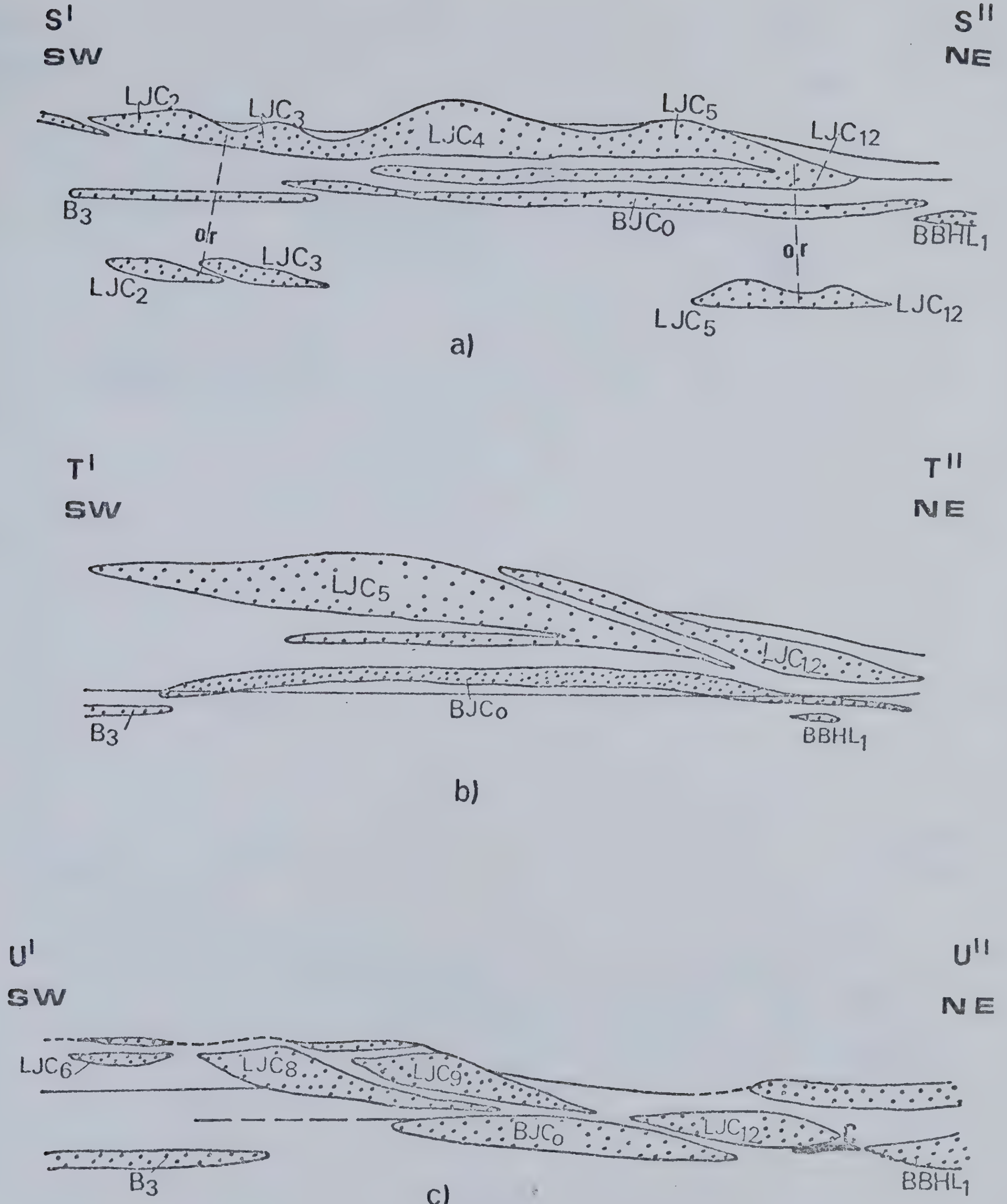

Figure 86. Generalized sketch of gross sand distribution in cross-sections (see fig. 74 for location):
a) S'-S"
b) T'-T"
c) U'-U"

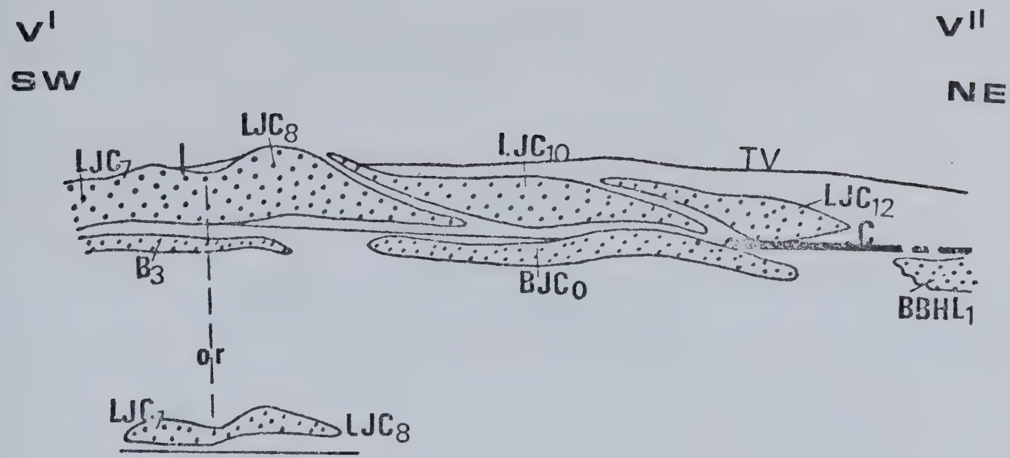

a)

b)

Figure 87. Generalized sketch of gross sand distribution in cross-sections (see fig. 74 for location):
a) V'-V"
b) W'-W"

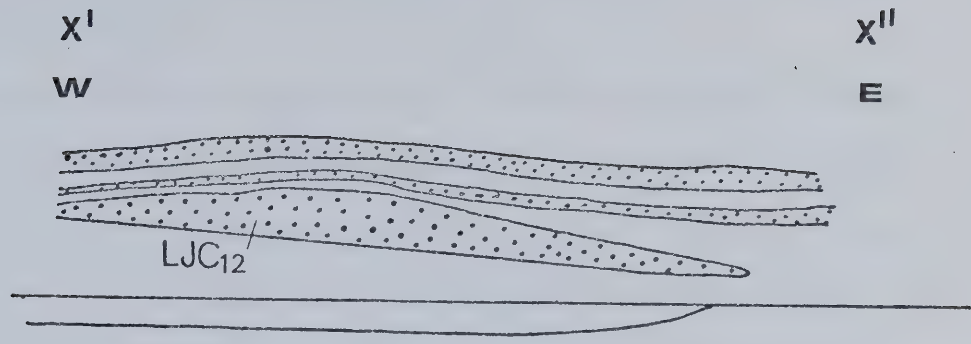

a)

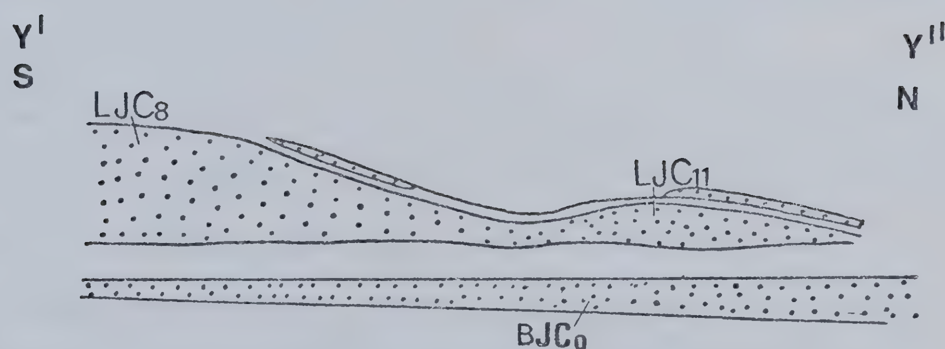

b)

Figure 88. Generalized sketch of gross sand distribution in cross-sections (see fig. 74 for location):
a) X'-X"
b) Y'-Y"

of B_3, and the later BJC_o unit restricted to the northcentral part. All these units are relatively very thin and trend northwest-southeast.

The B_3 sandbody pinches out to the northeast between the following wells: 1 to 3, 18 to 19, 23 to 24, 26 to 45, 42 to 44, 55 to 62, 61 to 77, and 81 to 82. The northeast time equivalent of the B_3 unit pinches out to the west between wells 23 to 48, 47 to 48, 49 to 50, 66 to 67, and 70 to 71. The BJC_o unit pinches out eastward before reaching wells 70, 67, 50, 45 and westward before wells 81, 61, 55, 39 and 40.

The Joarcam ridges of the Lower chrono-interval include the LJC_1 to LJC_8 units, with the exception of LJC_7. Table 1 is a list of the locations of the swales and their general characteristics. This will aid in interpreting the fence diagram of Figure 89a.

Figure 89b covers the northern Joarcam ridges within Townships 45 to 52, Ranges 19 to 28 W4M. It extends farther to the east up to Range 16W4M to include parts of the Beaverhill Lake sandbodies. The diagram shows the B_3 unit to be restricted to the extreme southwest corner and to pinch out to the northeast between wells 16 and 17, 17 to 20, and 18 to 19. The LJC_o unit is better developed in this area. This unit pinches out to the southwest between the following wells: 14 and 15, 17 to 20, 49 and 50, 53 and 54, and 91 and 92; to the northeast it pinches out between wells 4 and 5, 27 and 28, 38 and 39, 61 and 62, 83 and 84, 95 and

Table 1

Locations and Characteristics of Interridge Swales Shown in Figure 89a

	Sand Ridges Limiting Swale	Wells Encountering Swale	Swale Characteristics
1.	LJC_1/LJC_2	9, 12, 31	Poor sand development.
2.	LJC_2/LJC_3	8, 14, 15, 28, 40, 38	Multiple thin and poor sand development.
3.	LJC_2/LJC_6	34, 35, 36, 56, 55, 58	Poor sand development.
4.	LJC_3/LJC_4	24, 25, 26, 42	Mainly thinning.
5.	LJC_5/LJC_{12}	73	Multiple thin sand development.
6.	LJC_5/LJC_8	78, 79, 80	Multiple thin sand development and overlap relationship.
7.	LJC_6/LJC_8	55, 61, 82	Poor sand development.

96, 97 and 98, 119 to 121, and 120 to 129.

As an aid to interpreting the diagram for the northern Lower Joarcam ridges, Table II lists location and characteristics of the swales that separate them laterally.

Core Analysis

Cores recovered from the LJC_2 and LJC_{12} ridges, from one and five wells, respectively, were studied. Their locations are shown in Figure 74, and their descriptions given in Appendix IIIj.

The LJC_2 core, which is cut from the southwestern margin, shows a coarsening upward textural gradient from mudstone to a black and brown chert pebble conglomerate bed which is 7.5 cm thick.

Of the five wells which cored through the LJC_{12} ridge, three are located roughly along the axis, and two are on the northeast flank. The ridge axis appears to be composed of very thin cycles of coarsening upward sequences with sharp contacts in places. Seven such cycles were recognized in one well. A normal cycle begins with bioturbated bentonitic mudstone at the base and ends with coarse sand on top. No pebbles were concentrated in the cores; only isolated black chert pebbles occur here and there in the unit. There is no apparent textural gradient along depositional strike. In contrast, sand units from the northeast flank are thinner and finer grained relative to the axial ones.

Table 2

Locations and Characteristics of Interridge Swales Shown in Figure 89b

	Sand Ridges Limiting Swale	Wells Encountering Swale	Swale Characteristics
1.	LJC_{12}/ Beaverhill Lake units	4, 30, 31, 37, 64, 75, 101, 102, 114, 116, 117	Poor sand development.
2.	LJC_{12}/LJC_{10}	84, 97, 121	Poor sand development.
3.	LJC_{12}/LJC_{9}	26, 41, 60	Poor sand development.
4.	LJC_{12}/LJC_{5}	6 and 9, 7 and 8	Problematic-overlap relationship or undefined poor sand development.
5.	LJC_{8}/LJC_{9}	13, 14, 22, 44 to 46	Thin sand development and overlap relationship.
6.	LJC_{8}/LJC_{10}	56 to 58, 88, 95, 120, 121	Poor sand development.
7.	LJC_{8}/LJC_{11}	93, 94, 121 to 126	Poor and multiple thin sand development.
8.	LJC_{8}/LJC_{7} (northwest)	50 to 52	thin sand development.
9.	LJC_{8}/LJC_{7} (southeast)	partly in 16 and 17	Poor sand development

Summary of the Depositional Development of the Lower Joarcam Sandstone Ridges

Though the diagnostic bentonite controls are weak in the area, where they do occur they show that the Lower Joarcam sand ridges were deposited during the Lower chronostratigraphic interval.

Unlike the other Lower sand ridge complexes, the Joarcam ridges are intimately associated with the Basal sand units (B3 and BJC_o). Missing section at the base of the Viking in places tends to suggest that the top of the Joli Fou was scoured in some areas. Scouring and/or non-deposition may have been contemporaneous with Viking deposition during the Basal chrono-interval in places.

The Lower chrono-interval was a time of major sand deposition, as reflected in the twelve ridges. These ridges migrated in a southwesterly direction. In places, this resulted in an imbricate arrangement, especially for the northern ridges. The swales which surround most of the ridges may have been current paths. The uncertain lateral relationship of the LJC_5 and LJC_{12} ridges around Townships 42 to 45, Ranges 19 to 21 W4M should be resolved by drilling as this may be of economic importance.

Upper Viking sands were not developed in this area.

D. Sandstone Ridge Complexes of the Lower Chrono-Interval: A Summary

During the Lower chrono-interval, areas of sandstone development were generally displaced southwest of those of the Basal chrono-interval. Three major areas of isochronous sand deposition are recognized, and designated Lower, Joffre and Joarcam. From 4 to 12 sand ridges were developed at the same time in these areas, and are thus referred to as sand ridge complexes.

Ridges are generally elongate, linear and parallel; however, single, double, curved and complex shapes are also present. They trend northwest-southeast, with some variation in direction. Most are asymmetric in cross-section with gentle northeast and steep southwest margins. The thickest sand development is in the southeast of the Lower complex. Most ridges migrated toward the southwest (landward), which resulted in an imbricate arrangement of sand ridges in most areas. Swales surrounded the ridges and complexes. The distribution of some chert pebble conglomerate beds is related to these swales.

Missing thickness at the base of the formation and within the Viking in places is indicative of non-deposition and/or scouring before or during Viking deposition.

Sand deposition terminated earlier in the northwest and northeast than to the southeast, and is reflected in the distribution of later Upper Viking sandbodies.

E. The Basal Beaverhill Lake Reservoir Sandbodies

The zero isolith contour northeast and east of the Lower Joarcam sand ridge complex (Figure 74) follows a northwest-southeast trending swale which separates this complex laterally from the southern part of the unmapped Basal Beaverhill Lake gas sands to the northeast. These sandbodies were transected with two cross-sections located in Figure 75. The wells in the sections are identified in Appendix In.

Section Z'-Z" (Figures 90,92a) trends southwest-northeast from Township 49, Range 22 to Township 51, Range 18 W4M. Bentonite C (wells 1 to 4) and a distinct electric log signature (wells 4 to 10) were used as datum horizons. The LJC_{12} ridge attains maximum thickness in wells 2 and 3, thins and rises to the southwest, and overlaps the northeast edge of the underlying BJC_{o} unit in well 1. To the northeast, LJC_{12} pinches out rapidly before reaching well 4. The latter well is located in the swale which distinguishes the above ridge from the Beaverhill Lake sand units (wells 5 to 10).

A poorly developed thin basal unit ($BBHL_1$) overlain by a relatively thick well developed sand unit ($BBHL_2$) constitute the Beaverhill Lake complex. The basal unit thickens and thins and shales out to the southwest near well 3. The $BBHL_2$ unit attains maximum development in well 6 and pinches out to the southwest near well 4. Northeast of well 6, it thins and grades into mudstone beyond well 10. A mudstone

interval, thicker to the northeast, overlies the sands in the section.

Relative to the datum, defined by bentonite C and the top of the Formation, the Beaverhill Lake sand units formed earlier than the LJC_{12} unit, with the $BBHL_2$ unit being chronotaxial with the BJC_o unit. Hence the placement in the Basal chrono-interval.

Section A"-A" (Figures 91, 92b) is oriented southwest-northeast from Township 45, Range 19 to Township 48, Range 16 W4M. A fairly distinct and persistent electric well log kick near the base of the $BBHL_2$ unit is the datum. However, the position of bentonite C is shown in well 1. This section is a northeast extension of section S'-S" (Figure 78). In this cross-section, the $BBHL_1$ unit is restricted to the area between wells 8 and 12. Southwest of the latter well, the interval between the base of the Viking and the datum thins and thickens. This may be indicative of non-deposition and/or scouring before or during Viking deposition. The $BBHL_2$ oversteps the $BBHL_1$ unit in a southwesterly direction between wells 2 and 9. Northeast of the latter well, these units are muddy and poorly developed. A thin muddy sand sheet caps the Formation in this area. Well 1 is located in the swale which separates these units laterally from those of the Lower Joarcam complex to the southwest. The Beaverhill Lake sand units are shown to have developed before the bentonite C volcanic ashfall. Generalized sketches of these cross-sections are shown in Figure 92.

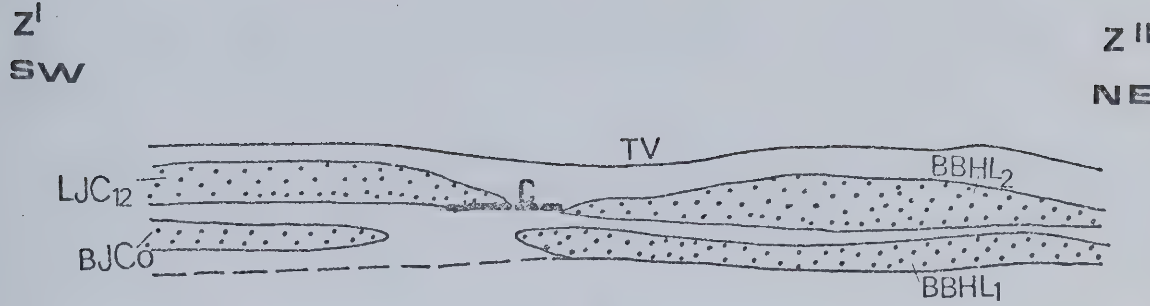

a)

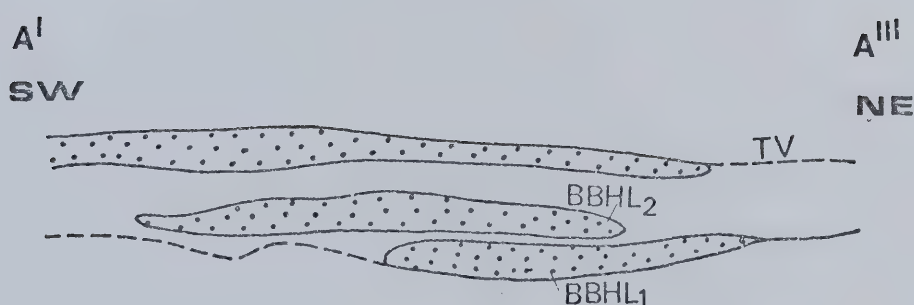

b)

Figure 92. Generalized sketch of gross sand distribution in cross-sections (see fig. 74 for location):
a) Z'-Z"
b) A"-A"'

The three-dimensional development of the Basal Beaverhill Lake sand units is shown in the eastern part of Figure 89b. The fence diagram shows the $BBHL_1$ to be restricted to the central part, while the $BBHL_2$ oversteps it in all directions, but divides into multiple units to the extreme north. These northwest-southeast trending units are confined to the west of wells 1, 34, 68, 70, 107 and 108 and essentially to the east of wells 4, 30, 31, 37, 64, 75, 101, 102, 114, 116 and 117.

A relatively thick muddy interval, better developed in the south, is the top of the Viking in this area and continues into the area of the LJC_{12} member of the Lower Joarcam complex.

CHAPTER VII

SANDSTONES OF THE UPPER CHRONOSTRATIGRAPHIC UNIT

By definition, the Upper chronostratigraphic unit is delimited at the base by bentonite A, and at the top by either bentonite A_O or the top of Viking Formation. Sandstones formed during this period are referred to as Upper Viking sandbodies.

Three major terminal Upper Viking sand complexes were recognized, and designated as Upper Western (UW), Upper Central (UC), and Upper Eastern (UE).

A. Upper Eastern Sandstone Ridge Complex

Isopach Map

The isopach map of the Upper Eastern sand ridge complex is shown in Figure 93. The complex is located approximately within Townships 19 to 31, Ranges 16W4M to 22W3M, and extends in a southeasterly direction beyond the map area. The axis of maximum development trends northwest-southeast for more than 150 miles (242 km). Maximum width and thickness are, respectively, about 48 miles (77 km) and 125 feet (38 m). The latter is developed near the Alberta-Saskatchewan boundary around Townships 23 to 25.

The complex is linear and asymmetric on an isopach

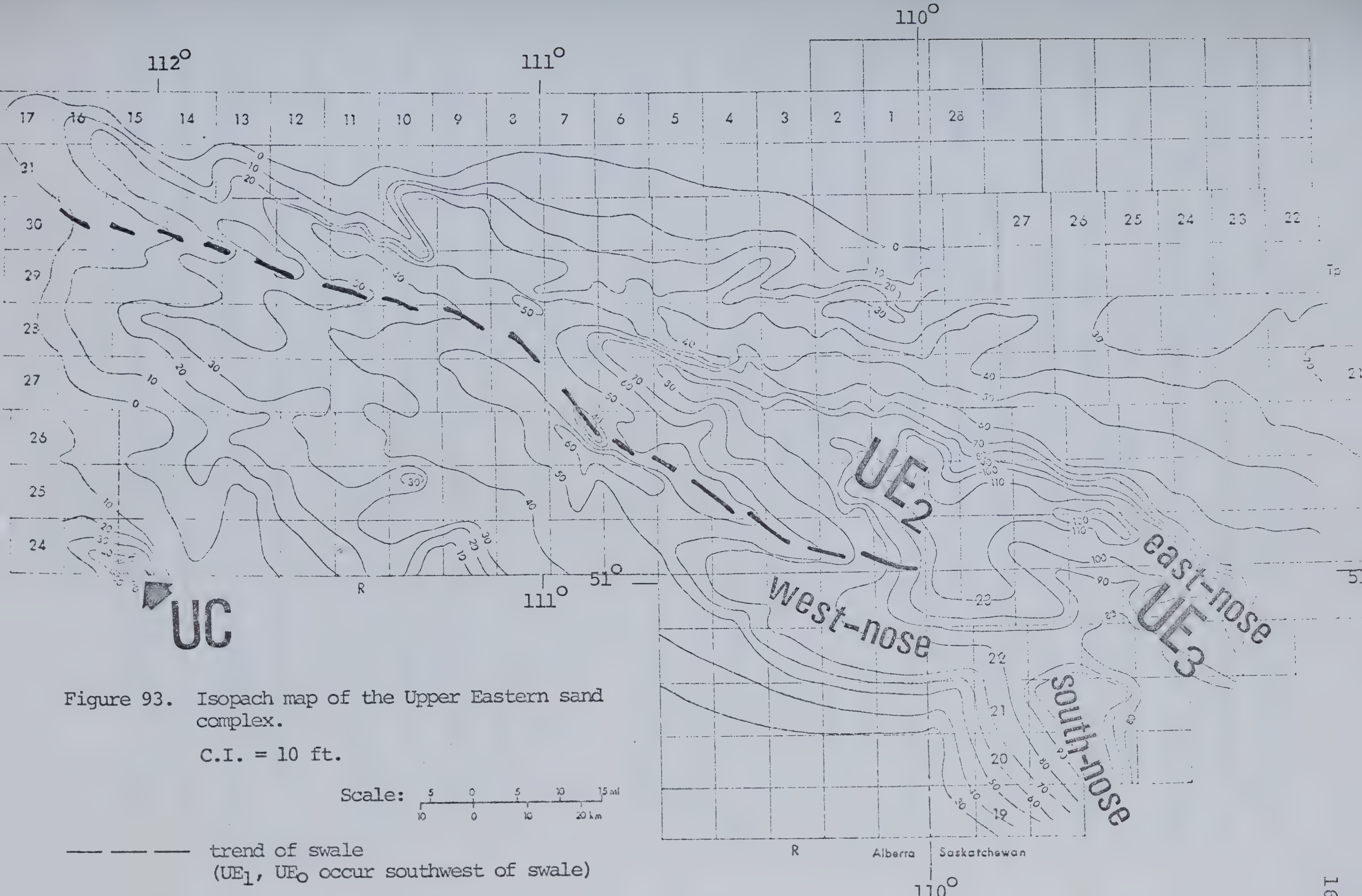

Figure 93. Isopach map of the Upper Eastern sand complex.

C.I. = 10 ft.

Scale: 5 0 5 10 15 mi; 10 0 10 20 km

— — — trend of swale (UE_1, UE_0 occur southwest of swale)

map; the asymmetry being characterized by relatively broad southwestern and fairly steep and indented northeastern margins. The steepest gradient along the northeast margin marks the approximate northeast ridge of the underlying L_3/L_4 ridge members of the Lower sand ridge complex. Three pronounced, thick 'noses' characterize the southeast portion of the complex. Generally, the Upper Eastern sand complex comprises at least three discrete sand ridges.

A northwest-southeast trending line from Township 30, Range 16, through Township 27, Range 7, to Township 24, Range 2W4M (see Figure 94 for location) runs along a swale continuous in places with the underlying L_2/L_4 swale. It is this swale that distinguishes UE_o and UE_1 sand units to the southwest from the UE_2 to the northeast. The stratigraphic relationships between these units are best illustrated in cross-sections.

Cross-Sections

The stratigraphic cross-sections used to study the Upper Eastern complex are located in Figure 94. The identities of wells in the sections are given in Appendix Io. The principal bentonites plus prominent electric log kicks were used as datum horizons.

Section B"-B"' (Figures 95,97a) trends northwest-southeast from Township 32, Range 14 to Township 24, Range 25W3M in southwest Saskatchewan. This orientation follows the axis of maximum sand thickness of the UE_2 sand ridge.

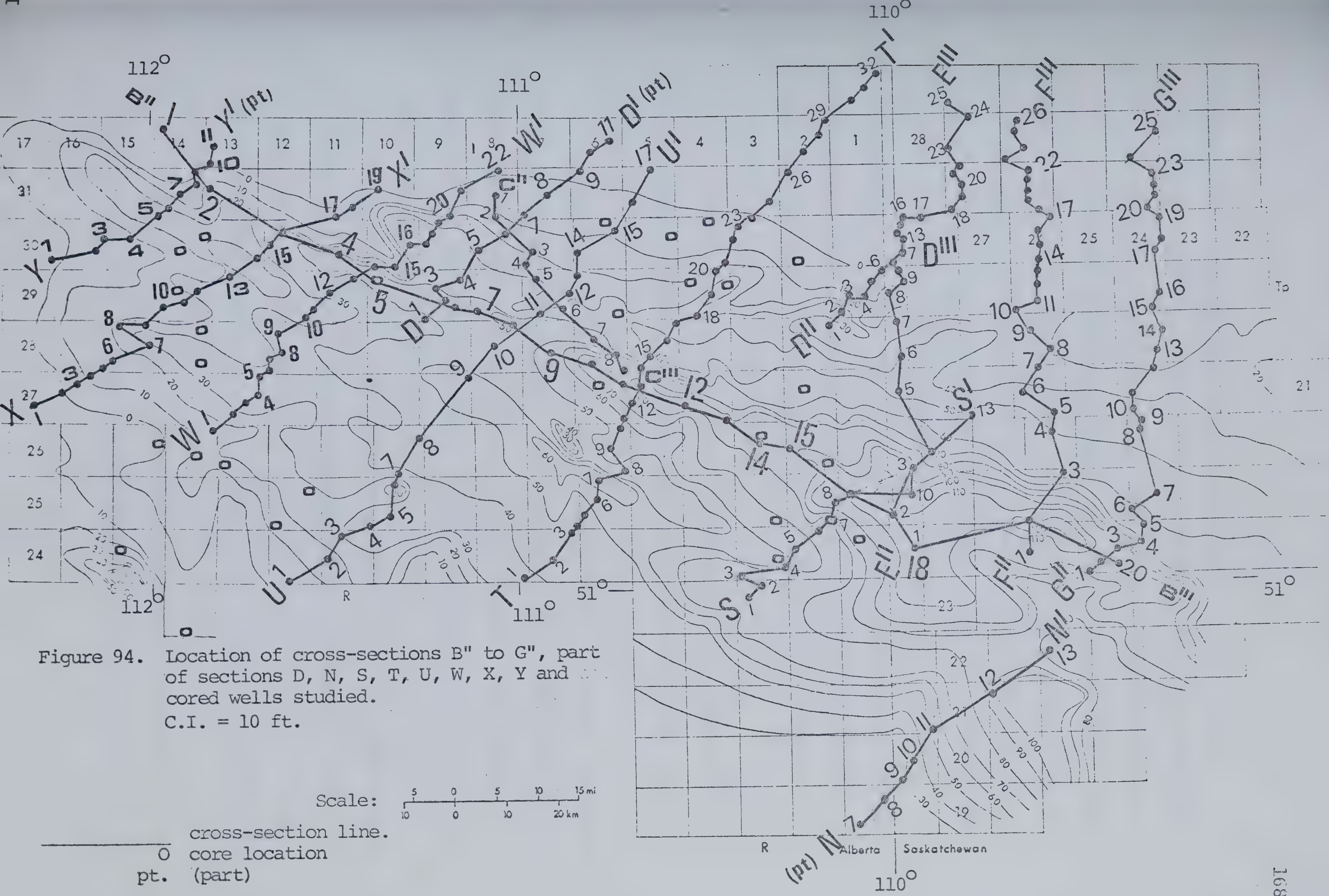

Figure 94. Location of cross-sections B" to G", part of sections D, N, S, T, U, W, X, Y and cored wells studied.
C.I. = 10 ft.

Scale: 5 0 5 10 15 mi; 10 0 10 20 km

——— cross-section line.
O core location
pt. (part)

Bentonite E is the datum though its position is only inferred southeast of well 18. From wells 4 to 8 bentonite A lies near the base of the mudstone overlying the L_4 units.

Maximum sand development in the UE_2 ridge occurred from wells 16 to 18 located near the boundary of Alberta and Saskatchewan. Northwest of this area, the unit thins, overlaps the Lower L_4 units between wells 10 and 11, and finally pinches out before reaching well 1. Fairly clean sand development parallel to the depositional strike also occurred to the southeast between wells 19 and 20. Much of this growth was later in time and constitutes the southeastern nose, herein designated UE_3.

Figure 47 (section Z-Z') shows a fairly similar relationship between the UE_2 unit and the underlying L_4 units.

The Upper Eastern sand complex is correlated between wells 6 and 13 of section N-N' (Figure 31). This portion of the section consists of three fairly distinct and discrete sand units (UE_1, UE_2 and UE_3) stacked one above the other in an imbricate or offlap pattern.

Bentonite A occurs near the top of the L_1 member of the Lower sand ridge complex between wells 1 and 6. The poorly developed southeast margin of the UE_1 unit overlaps the L_1 ridge in wells 9 to 4 as it migrated to the southwest from wells 10 and 11.

The southern nose of the UE_2 sandbody, thickly developed in well 12, thins and overlaps the UE_1 unit in

turn between wells 6 and 11, beyond which it finally pinches out before well 5. Northeast of well 12 it thins rather abruptly and may have essentially shaled out beyond well 13.

The southwesterly migrating UE_3 unit overlaps the UE_2 in turn at well 12 and grades into mudstone at well 11.

Section S-S' (Figure 38) is a northeasterly extension of section O-O' (Figure 32) with wells 1 to 6 in the former section overlapping with wells 16 to 19 of the latter. Bentonite A lies on top of the thin southeast edge of the L_2 member of the Lower sand ridge complex between wells 1 and 4 in Figure 38. The sandy mudstone unit which overlies bentonite A in these wells occupies the position of the UE_1 unit, better developed to the southwest of this section (Figure 32). The well developed sand unit which caps the formation in wells 1 to 3 represents the western nose of the UE_2 (see Figure 93). Wells 4 and 5 are located in a transitional area or swale which separates the western nose of the UE_2 from the main UE_2 unit to the northeast.

The main UE_2 sandstone is best developed between wells 8 and 9, becoming muddy to the northeast. Relative to the datum, the UE_2 sandbody appears to have migrated to the southwest between wells 6 and 8 and possibly overlaps the edge of the L_2 unit between wells 4 and 5. The rather flat base of UE_2 between wells 9 and 13 may indicate that this ridge was fairly static for some time. The UE_3, thickly developed in well 11, caps the UE_2 from wells 8 to 13, and pinches out to the southwest.

Southeast of section S-S', wells 9 to 19 of section O-O' (Figure 32) show the relationship of the UE_1 sand to the western nose of the UE_2. The UE_1, which is thickly developed in well 13, lies on top of bentonite A above the northeast margin of the L_1 member of the Lower sand ridge complex between wells 9 and 15. UE_1 is then overlapped by the western nose of the UE_2 unit, thickest in well 16, from wells 13 to 15. The muddy sands of wells 18 and 19 are located within the swale between the western UE_2 nose and the main UE_2 sandbody.

The sand and muddy sand units at the base of the Formation in wells 1 to 6, and 9 to 13 in Figure 39 (section T-T') are, respectively, the northeast margin of the L_2 and southeast edge of the L_4 ridge members of the Lower sand complex. The units are laterally separated by the L_2/L_4 swale located in wells 7 and 8. Bentonite A lies near the top of these units.

The UE_1 sandbody lies above bentonite A on top of the L_2 unit between wells 1 and 6. The unit is thickly developed in wells 1 and 2 to the southwest, thins to the northeast, and pinches out near well 7. It appears to have migrated to the southwest relative to the time horizon of bentonite A.

Relative to the datum, the thin northeast margin of the main UE_2 body between wells 14 and 24 appears to have shifted fairly rapidly to the southwest and moved over the underlying L_4 unit from wells 13 to 11. Southwest of well

12 the UE_2 breaks into a number of sand units with prominent shale breaks in the swale (wells 3 to 9) and overlaps the UE_1 between wells 3 and 6. The portion of the swale penetrated by wells 7 and 8 is characterized by relatively thin sand development throughout Viking time.

Section T-T' (Figure 39) is roughly a northeast extension of Figure 33 (Section P-P'). In the latter section, another thin sand unit, designated UE_o, forms above bentonite A and is restricted to wells 16 to 22. The thickly developed UE_1 unit in well 24 thins as it rises to the southwest, overlaps the UE_o unit in wells 20 and 21, and pinches out beyond these wells.

In Figure 40 (section U-U') the thin UE_o sand unit overlies bentonite A between wells 1 and 5. Relative to this datum, it appears to have shifted rapidly to the southwest, but did not go much beyond well 1.

The northwestern part of UE_1 is fairly well developed in well 8. This sand also shifted to the southwest, overlapping the UE_o unit in well 5. Northeast of well 8 the unit does not appear to have reached as far as well 9.

The E and A bentonite horizons show the main UE_2 sand unit to have migrated to the southwest. It thickens with multiple shale breaks in well 10 where it overlies the L_4 units. Farther to the southwest it is poorly developed (well 9), but may have overlapped the UE_1 in wells 7 and 8.

The cross-section best demonstrates the diachroneity of the UE_2 unit, its time relationship with the Basal and

Lower sandbodies, and their imbricate pattern of arrangement.

Section C"-C"' (Figures 96, 97b) is oriented approximately north-northwest to south-southeast from Township 31, Range 8 to Township 29, Range 7 W4M. Bentonite E is the datum. The horizons of bentonites D and C are also shown between wells 1 and 5. The southeast margin of the thin B_1 unit shales out before well 6. The sedimentary evolution of the UE_2 sandstone began just before the time of bentonite D as a very thin sand unit in wells 1 and 2. This was subsequently followed by incremental accretion of thin sands which successively overlapped older units to the southeast. Thus, the base of these units is higher and younger to the southeast. The thickest development of UE_2 in well 9 probably occurred in this manner, but was perhaps enhanced by a relatively higher rate of subsidence to the southeast.

A fairly similar growth pattern for the UE_2 ridge in a southwesterly direction is apparent from wells 1 to 6 of Figure 15 (section D-D'), wells 1 to 4 of Figure 16 (section E-E'), Figure 42 (section W-W'), and Figure 43 (section X-X'). In these sections, however, it is thought that the southwesterly incremental growth of the early (time of bentonites D and C) part of the UE_2 ridge was terminated by that of the L_3-L_4 units, which shifted slightly to the northeast just before the bentonite A volcanic ashfall. This was subsequently followed by the deposition of the main UE_2 sandbody.

These sections demonstrate fairly well the

sequential growth stages of the UE_2 sand ridge in the area. The imbricated growth pattern is very similar to that documented and reported by Evans (1970) for the thin Viking sand members of Dodsland-Hoosier areas of southwest Saskatchewan, to be discussed later.

Section R-R' (Figure 37) gives a fairly good indication of the imbricate relationship between the UE_o, UE_1 and the western nose of the UE_2 along the depositional strike of the underlying L_2 sand ridge member of the Lower sand complex.

The thin northwestern edge of the UE_2 sandbody is shown in Figure 48 (section A'-A") to rise to the southwest and thin beyond well 1.

Cross sections B"-B"' and C"-C"' are sketched in Figure 97.

Figure 98 shows the depositional development of the Upper Eastern sand complex and its spatial and time relations to adjacent sandbodies. It covers the area bound approximately by Townships 20 and 32, Ranges 24W3M and 13W4M. The identities of wells in the diagram are given in Appendix IIf.

The southeast margin of the B_1 sand unit occurs in the north-northwest of the diagram in wells 66, 67, 69, 81 to 83, 85 to 87 and 89. The eastern nose of the UE_2 is shown in wells 5 to 15; the southern nose in wells 1 to 14; and the western nose in wells 7, 8 and 12 to 21.

The swale between the western nose and the main UE_2

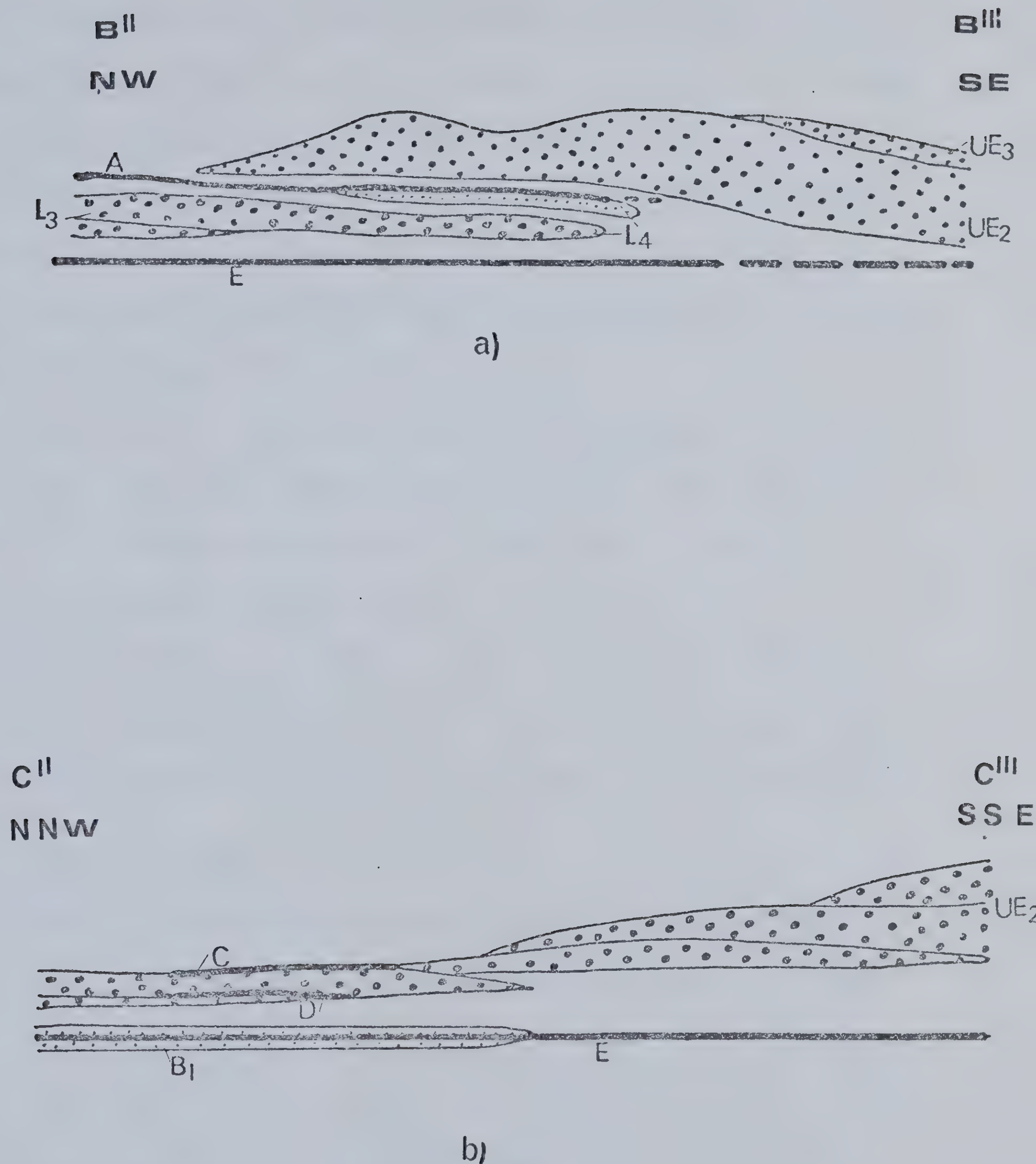

Figure 97. Generalized sketch of gross sand distribution in cross-sections (see fig. 94 for location):
a) B"-B"'
b) C"-C"'

sandstone is located in wells 13, 17 and 22, while that between the UE_1 and UE_2 occurs in wells 21, 36, 37, 48 and 49. These swales are characterized by relatively thin muddy sand development throughout Viking time.

The overlap relationship between the UE_2 and the underlying L_4 units is shown in wells 46, 50, and 61, while that between the UE_1 and UE_2 ridges occurs in wells 2, 8 and 12, and between wells 11 and 21.

Although the imbricate growth pattern of the UE_2 ridge is not very well shown because of the thin units involved, it could be determined in the area of wells 89-85-86-87-88 and/or 82-66-65-64.

The asymmetry of the UE_2 ridge is obvious in the diagram. The base and top of the Viking in the area slope down to the northeast relative to the horizon of bentonite E.

Core Analysis

Data on the internal characteristics of the Upper Eastern sand ridge complex were provided by 26 wells which recovered cores from different parts of the unit in Alberta. The thin UE_o sand unit was cored in 5 wells, 2 of which also recovered cores from the northwest pinch-out edge of the overlying UE_1. Cores from the southwestern and northeastern margins of the main UE_2 sanbody were cut in 7 and 8 wells respectively, while cores from 4 wells were recovered along the ridge axis. One well recovered cores from the swale between the main UE_2 unit and its western nose; while cores from the swale between the Upper Eastern sand complex and

the Upper Central sandbody were recovered from one well. The locations of the cored wells are shown in Figure 95. Detailed core descriptions are in Appendix IIIk.

Cores cut from the UE_0 and overlying UE_1 sandstones indicate that they are each composed of a thin coarsening upward textural sequence. However, only the UE_1 is capped by a thin pebbly sandstone bed which decreases in thickness and size of pebbles to the southeast.

Cores from well 11-24-30-5W4M show the Viking-Joli Fou contact to be fairly sharp, with the upper part of the Joli Fou very calcareous.

A very thin fining upward textural sequence with small black chert pebbles at the base was observed near the zero isopach in well 10-35-30-4W4M. The rest of the northeast margin studied is internally very similar to the Basal and Lower sand units. However, it is capped by a thin black chert pebble conglomerate bed, interlaminated with dark shale and grey mudstone in places. The pebbles decrease in size towards the ridge axis.

The top 5 to 10 feet (1.5-3 m) of the central part of the ridge axis shows no textural variation. However, a very thin black chert fine pebble sandstone bed was observed at the top of the axis in one well. The northwestern part of the axis is composed of 0.2 to 0.6 m thick sand units separated by shale and sandy mudstone intervals 7 to 15 cm thick. The sand units are homogeneously very fine to fine grained. A characteristic fining upward sequence about

60 cm thick from black chert pebble conglomerate at the base to shale at the top lies near the base of the marine Lloydminster shale approximately one meter above the top of the Viking in well 6-23-30-14W4M.

The longer cores from the southwest margin showed no vertical textural variation except that the pebbly sandstone cap is thicker and of larger chert size in the swale than near the axis.

In general, the largest pebble sizes observed were from the northeast flank. The upper part of the UE_2 unit is cleaner than the lower part.

Summary

Upper Eastern sandbodies were deposited east and southeast of the Lower sand ridge complex. Three northwest-southeast trending parallel ridges (UE_o, UE_1, UE_2) constitute the complex from southwest to northeast. However, the thick UE_2 unit developed western, southern, and eastern noses within the southeast part of the map area. The eastern nose, where recognized, is the UE_3 unit.

Whereas the UE_o, UE_1 and UE_3 sandbodies were formed during the Upper chrono-interval, the UE_2 began during the Basal chrono-interval and continued to the end of Viking time in most areas. Thus, the UE_2 ridge is the most diachronous single Viking sandbody encountered in the study area.

The UE_1 unit is separated laterally from the main UE_2 body by a swale continuous, in places, with the

underlying L_2-L_4 swale. In other areas, especially in the southeast and southwest, the two sand units are imbricately stacked. The UE_2 ridge also displays a similar arrangement pattern internally. This imbricate arrangement is consistent with a southwesterly direction of migration deduced for these ridges. It is the shoreward mudstone facies of these units which overlies the Lower sand ridge complex in the area.

The "upslope" decrease in the size of observed chert pebbles at the top of the UE_2 unit supports the interpretation that the distribution of some of these beds was closely related to topographic relief.

B. The Viking Sandmembers in the Dodsland-Hoosier-Smiley Areas of Southwestern Saskatchewan

Evans (1970) recognized six thin sand units in the Dodsland-Hoosier-Smiley areas of southwest Saskatchewan. He designated them O, N, M, LL, LU, and K, in the order of deposition. His nomenclatural system is closely followed in this discussion. He noted that members are thin, linear, subparallel, and trend WSW-ENE, which is at a fairly high angle to the more usual northwest trend of the Viking sandbodies discussed so far. Younger members overlap older units progressively to the south. Multiple diverging axes for a single member are characteristic. Thinning and broadening of the sand units along their axes of maximum thickness development are common features. Chert pebble stringers are present, and a few sand members have pebble

concentrations at the base.

Evans did not show the time and spatial relationships of these sand members to those of the adjacent Upper Eastern sand complex of the present study. To this end five stratigraphic cross-sections oriented in various directions have been constructed using diagnostic electric well log kicks as datum horizons. Locations of these cross-sections are shown in Figure 94, and the identities of some wells in the sections are listed in Appendix Io.

Figure 10 (section A-A') indicates that deposition of these sand units occurred during the Basal chrono-intervals as bentonite C or K (in the terminology of Evans, 1970) lies on top of the 'M' member in wells 7 and 8. Wells 5 and 6 are located in the swale which separates the M and N units laterally from the thin northeast pinchout edge of the UE_2 body of well 4. Well 5 of Figure 99 (section D"-D"') suggests that the swale was scoured in places, as up to 10 feet (3 m) of section is missing at the base of the Viking in this well. The very thin fining upward textural gradient near the northeast zero isopach of the UE_2 unit, reported earlier, is about 20 miles (32 km) northwest of the scoured Viking base in well 5.

The observations of Evans (1970) concerning the depositional pattern and development of the Viking sand members of the Dodsland-Hoosier area are further strengthened by the three south-north trending sections E"-E"' to G"-G"' (Figures 100, 102). However, they show that the imbricating pattern is more complex to the south, thus the

poorly developed younger units (LL, LU, K) are very difficult to differentiate in the area. Most importantly, however, they illustrate how these units migrated onto the northeast edge of the UE_2 sandbody. This relationship can be seen between wells 9 and 10 of Figure 100, 9 and 12 of Figure 101, and 10 and 11 of Figure 102, and is poorly depicted in the north-northeast of Figure 98. Thus, the change from WSW-ENE (N to LL) to WNW-ESE (LU, K) with time, in the trend of the thick axes of the main bodies of members, as shown in Evans' Figure 13, is not surprising. This could be attributed to the impedance of the UE_2 ridge to the youngest members as they migrated closer, probably eventually to be accreted onto the ridge. The three areas of overlap define a northwest-southeast trend which represents the zero isolith for the Upper Eastern sand complex in that area. Figure 102a shows sketches of sections E"-E"' , F"-F"' and G"-G"' .

The extension of Evans' oldest, 'O', member in Alberta is correlated from wells 28 to 32 (Figure 39). This sand unit is about 13.5 miles (22 km) from the northeast edge of the UE_2 sandbody. A swale area (wells 25 to 27) characterized by very minor sand development separates the units laterally from each other. A detailed comparison of the electric logs of wells 27 to 29 suggests that about 4 feet (1.2 m) of section is missing at the base of the 'O' unit in well 28. This area lies to the southeast of the Provost area where similar missing sections were described

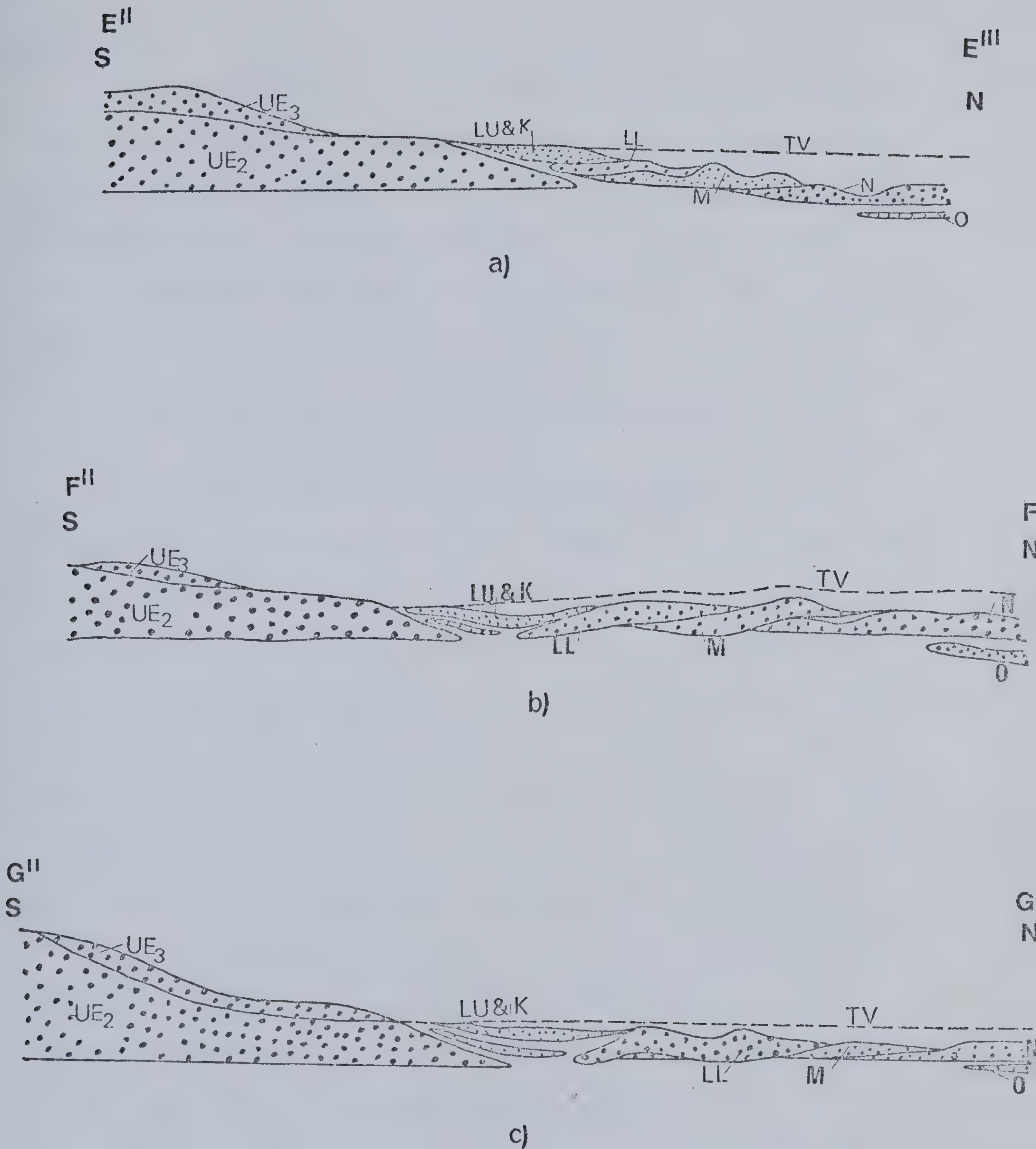

Figure 102a. Generalized sketch of gross sand distribution in
cross-sections (see fig. 94 for location):
a) E"-E"'
b) F"-F"'
c) G"-G"'

earlier.

The writer is of the opinion that the time and spatial relationships of the Dodsland-Hoosier-Smiley sand units to the UE2 unit, coupled with a similar depositional pattern and history, are sufficient evidence to suggest a common genetic mechanism for both units, despite the difference in trend.

C. The Upper Central Sandstone Ridge

The Upper Central sand ridge, designated UC, is located within Townships 22 to 25, Ranges 14 to 17 W4M. The isolith map of part of this sandbody is shown in Figure 93. A maximum thickness of 145 feet (44 m) is attained at the centre of the base of Township 24, Range 15W4M. Thus, it is the thickest single Viking sand unit encountered in the study area. Maximum length and width do not exceed 20 miles (32 km) and 8 miles (13 km), respectively. The sandbody is linear and fairly symmetrical trending northwest-southeast.

A swale characterized by very little sand development surrounds the unit completely, distinguishing it laterally from the Upper Eastern complex to the northeast and the Upper Western complex to the southwest.

Wells 1 to 7 of Figure 34 (section Q-Q') show this sandbody to be best developed near wells 4 and 5, with sharp lower and upper contacts, the former becoming gradational to the southwest in well 3. The unit thins rapidly and pinches out before reaching well 7 in the northeast and

well 2 in the southwest. These wells are located in the surrounding swales.

The UC sandbody is fairly symmetrical, plano-convex upward, and rests on a 15 foot (4.6 m) thick mudstone unit which overlies the southwest edge of the L_1 ridge. The base coincides roughly with the A bentonite horizon. Bentonite A_o occurs at a fairly constant position near the base of the Lloydminster shale approximately 15 feet (4.6 m) above the top of the Viking between wells 3 and 14. Oil is produced from the northern margin of this sandbody.

Core Analysis

Four feet (1.2 m) and 40 feet (12.2 m) of cores were recovered, respectively, from the top of the southeast and northwest margins of the Upper Central sandbody in two wells. The cored wells are located in Figure 94 and fully described in Appendix III1.

No apparent internal textural gradient was observed in the thick core recovered from the northwest margin. A 30 cm thick black and brown chert pebble (1.5 cm longest diameter) conglomerate caps the unit in the southeast. In the northwesterly well, only 1½ inch (3.75 cm) of this bed appears to have been cored. The longest pebble diameter observed is 8 mm, only about one half the size of those in the northwest.

D. The Upper Western Sand Complex

The isopach map of the part of the Upper Western sand complex in the study area is shown in Figure 103. This complex is located in front of the central foothills of Alberta within the area bound roughly by Townships 24 and 36, Ranges 18W4M and 6W5M. The complex trends northwest-southeast and continues beyond the limits of the map area.

Although well coverage in the area is relatively less dense, certain regional trends are discernable. Two linear and parallel northwest-southeast trending sandbodies, designated UW_1 and UW_2, lie along the southwest border of the complex. The northeast apron (UW_3) appears to consist of northeast-southwest trending digitating thin sand units probably continuous with UW_1 and UW_2.

The UW_1 and UW_2 sandbodies are transversed by southwest-northeast trending swales characterized by isopach thinning, two for the former, one for the latter. Thus, the swales impart a chain-like configuration to the units. In the southeast, the 40 foot contour line separates the sandbodies laterally, and no wells are drilled within the swale. Similarly, no wells have been drilled to the immediate northwest of this area. Thus, the northeast and southwest edges of the UW_1 and UW_2 sandbodies, respectively, are not accurately resolved and mapped. The thickly developed UW_1 sand unit attains maximum thickness around Townships 25 and 26, Range 28W4M, just northwest of the city of Calgary.

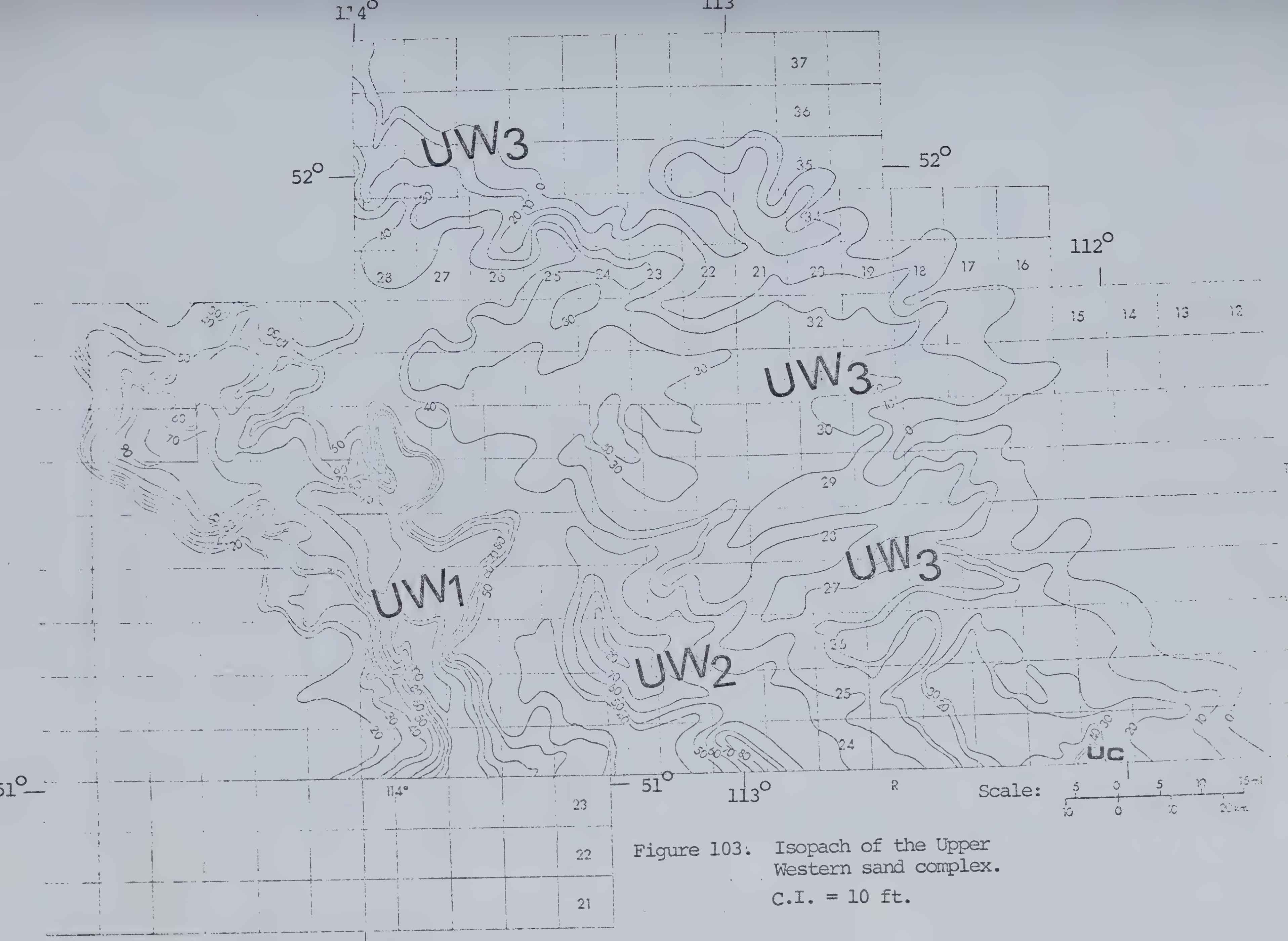

Figure 103. Isopach of the Upper Western sand complex.
C.I. = 10 ft.

This unit extends along strike for more than 72 miles (116 km). Maximum width varies between 15 and 24 miles (24-39 km).

The easterly and northeasterly apron of the complex is constituted by about four relatively thin sand units separated by five swales.

Cross-Sections

Three stratigraphic cross-sections, utilizing fairly distinct and persistent electric well log kicks as datum horizons, were used to study the depositional development of this sand complex. The diagnostic bentonites are very difficult to recognize in much of the area, especially in the southwest where the Joli Fou becomes very sandy and difficult to differentiate from the overlying Viking and underlying Blairmore, probably because of the nearness to the strandline. The poor electric well log resolution in this area further compounds the problem of bentonite recognition. The cross-sections are located in Figure 104, while well identities are given in Appendix Ip.

Section H"-H"' (Figures 105, 108a) is oriented parallel to the depositional strike of the UW_1 sandbody from Township 32, Range 6W5M to Township 23, Range 27W4M. The Base of the Fish Scales marker is the datum. The base of the sandy Joli Fou or top of the Blairmore is difficult to establish and correlate northwest of well 5, where they are only tentatively picked. The three ridges which make up this unit are represented, from northwest to southeast, by wells 2 to 4, 6, and 9 to 11 in the section. The two

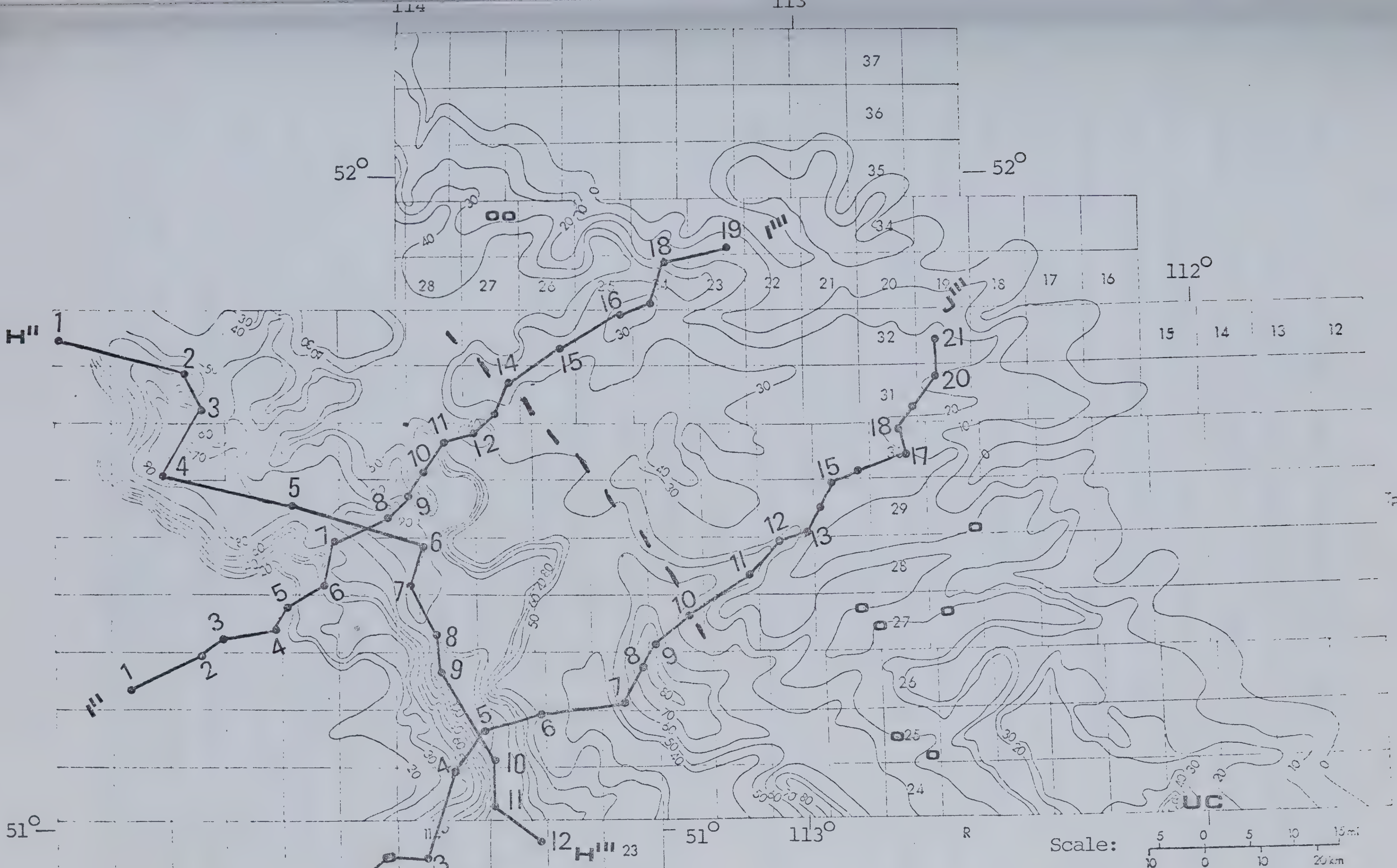

Figure 104: Location of cross-sections H", J" and I" across the Upper Western sand complex and cored wells studied.

—— section lines
o core location
— — — area of change in slope at the base of the Joli Fou.

C.I. = 10 ft.

swales which separate them laterally are penetrated by wells 5 and 8. The funnel-type shape of the spontaneous potential response curve is best shown in the southeast by wells 9 to 11 and, possibly, well 4 in the northwest. The unit may have pinched out to the northwest beyond well 1 and to the southeast beyond well 12, as the sandbody thins and becomes multiple units in these directions. Growth parallel to the depositional strike is more obvious to the southeast. In this area, two upper thin sands cap the sequence between wells 11 and 12, with the youngest rising to the southeast. A similar relationship may occur above the unit in wells 1 and 4. The overlying Lloydminster Shale is thickest between wells 8 and 10 and thins to the southeast and northwest, especially in the latter direction.

Section I"-I'" (Figures 106, 108b) is oriented southwest-northeast from Township 26, Range 5W5M to Township 34, Range 23W4M. Bentonite E is the datum for wells 14 to 19, while another fairly distinct log kick was used for the remaining wells. Relative to the datum, the base of the Joli Fou, which is remarkably flat between wells 14 and 19, slopes to the southwest beyond the former well and then flattens again. Beyond well 8 the base can only be inferred as the area becomes very sandy. These Joli Fou sands behave like regressive-transgressive shoreline sands.

The Upper Western complex, which started developing during the Basal chrono-interval, or even earlier, is correlated between wells 5 and 17. Maximum thickness is

developed near wells 7 and 8. However, the spontaneous pontential curves suggest this may not be coincidental with maximum clean sand thickness. The complex thinned and graded into mudstone above the L_7 ridge member (wells 17 to 19) of the Lower sand complex. Bentonite A seems to have fallen during the development of the Upper Western sand complex in well 17.

The UW_1 unit pinches out southwest of well 5. Except for the formation of two thin sand units, one of which extends up to well 8, no later sand was laid down in this area. The lateral relationships of UW_1, UW_2 and UW_3 are not very clear because of very poor well control. What is clear, however, is that successively younger units rise to the northeast. The Lloydminster Shale thins to the southwest.

Section J"-J"' (Figures 107, 108c) is oriented southwest-northeast from Township 22, Range 2W5M to Township 32, Range 19W4M. Bentonite E is datum for wells 10 to 21, while the base of the Joli Fou or top of the Blairmore was used as datum for the remaining wells. Relative to bentonite E the base of the Joli Fou is nearly flat between wells 10 and 21, slopes to the southwest between wells 9 and 10, and flattens again up to well 4, beyond which it can only be inferred. Northeastward imbricating sand units characterize Joli Fou sand units southwest of well 9.

Sandbodies of the Western sandstone complex are correlated between wells 2 and 17. Maximum sand occurs in

well 5 (UW_1). With contintued northeast progradation, the complex thinned and pinched out before well 18. It overlies the $L5_a$ unit in well 12, and is higher than the L_6 unit which occurs in wells 18 to 21. Both the $L5_a$ and L_6 units are members of the Lower sand ridge complex. A very thick Viking muddy interval (wells 9 to 17) separates the Lower ridges laterally from the Upper Western complex. The problem of the lateral relations between the UW_1, UW_2 and UW_3, encountered in the previous cross-section, re-occurs here. The writer believes that the UW_1 sandbody (well 4) may have thinned from wells 5 to 6 and pinched out before well 7. On the other hand, the UW_2 sandbody overlaps UW_1 in wells 4 to 6, and probably pinches out to the northeast before well 10, while the UW_3 extends beyond this well and grades into mudstone beyond well 17. Bentonite A may have fallen on a sandy bottom at well 17. Little sand deposition (lagoonal) occurred southwest of well 2, except for the overlying highest thin sand units between wells 1 and 3. The overlying Lloydminster Shale thins to the southwest. Cross-sections H"-H"', I"-I"' and J"-J"' are sketched in Figure 108.

Core Analysis

Cores recovered from well 2 of Figure 107, cross-section J"-J"' indicate that the UW_1 is a shoreline sequence. No cores from the UW_2 sandbody were studied. Eight wells recovered cores from different horizons and parts of the UW_3 sand units. Generally, they are characterized by 1 to 4

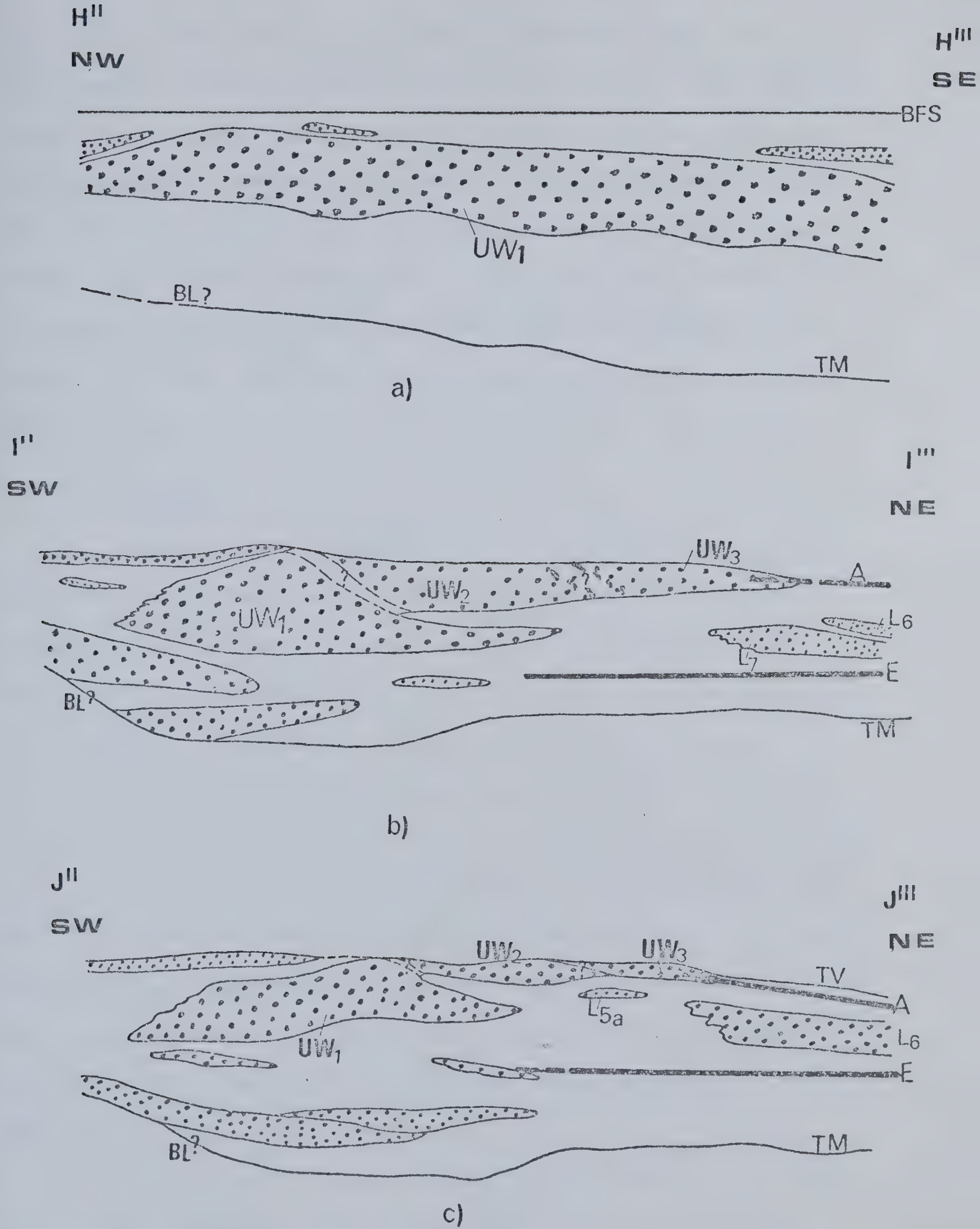

Figure 108. Generalized sketch of gross sand distribution in cross-sections (see fig. 104 for location):
a) H"-H'''
b) I"-I'''
c) J"-J'''

relatively thin coarsening upward sequences, some of which are capped by chert pebble conglomerate beds. The uppermost conglomerate bed, where seen, is underlain by a thin dark fissile shale. Internally, UW_3 cores are radically different from the UW_1 core and are more similar to those from other sand units of the Basal, Lower and Upper chrono-intervals. The locations of cored wells are shown in Figure 104, and detailed descriptions are given in Appendix IIIm.

Summary

Although the relationship of this complex to bentonite A indicates that it formed essentially during the Basal and Lower chrono-intervals, it was placed in the Upper interval because, in places at least, it overlies the L_6, L_7 and L_8 sand ridges of the Lower sand complex.

The Upper Western complex seems to be constituted by two parallel, linear sandbodies (UW_1 and UW_2) which overlap and rise to the northeast, the direction of progradation. The UW_3 may be either the serrated northeast margin of the complex, or may represent yet another series of relatively thin sand units connected, in places, in imbricate fashion to the UW_2 sand unit; hence their trend at right angles to that of the UW_1 and UW_2 sandbodies.

The area of change in slope of the base of the Joli Fou to the southwest defines a northwest-southeast trend which nearly coincides with an imaginary line separating the

UW_3 units from the UW_1 and UW_2 to the southwest. This change in slope may reflect the configuration of the basin, characterizing a more rapidly subsiding southwest and a shallower more stable northeast segment during Viking deposition. However, the Joli Fou is very sandy southwest of the line and shaly to the northeast. The thick muddy interval which separates the Lower sand ridge complex laterally from the Upper Western complex represents the distal and offshore facies of these units, respectively, as they migrated in opposite directions.

The absence of time-equivalent sand units southwest of the UW_1 sandbody, and the presence of a thin Lloydminster Shale unit indicates that the Lloydminster transgression covered the Viking sands in this area and extended beyond them to the southwest. More drilled holes are necessary before the lateral relationships between the UW_1, UW_2 and UW_3 sandbodies can be finally resolved. The northeast edge of the Upper Western sandbody isopach may coincide in places with the northeast margin of the Upper Eastern sand complex.

Upper Viking Sand Complexes: A Summary

The Upper Viking sand complexes are restricted geographically southwest of a northwest-southeast trending line from roughly Township 36, Range 28 through Township 33, Range 15 and Township 30, Range 4W4M in Alberta to Township 24, Range 21W3M in southwest Saskatchewan. In Alberta, this line is defined roughly by the northeast zero isolith contour

of the Lower sand ridge complex in Figure 28.

Classification of the Upper Western and Eastern complexes in the Upper chrono-interval is based mainly on stratigraphic position and only partly on time, because both units seem to have begun during the Basal chrono-interval, and lasted into the Upper, or up to the end of Viking time. Thus, they are the most diachronous Viking units in the study area.

Whereas the Upper Western sand complex prograded to the northeast, the Upper Eastern complex shifted southwesterly, in the opposite direction, but in a different locality. On the other hand, the Upper Central sandbody appears to have been relatively static.

Upper Viking sand complexes are generally younger to the southeast, relative to bentonite A, as deposition of the Upper Western complex in the northwest ceased earlier than did the others.

Internally, the UE_2 sandbody of the Upper Eastern complex consists of relatively thin sand units stacked in an imbricate fashion with each younger unit displaced progressively to the southwest. Similarly, the larger constituent sandbodies of the Upper Eastern complex (UE_o, UE_1, UE_2) also overlap in an imbricate pattern. The same may also be true for the Upper Western sandbodies (UW_1, UW_2, UW_3). The internal imbricate arrangement pattern of the UE_2 sandbody is fairly similar to that described by Evans (1970) for the thin Viking sand members of the Dodsland-Hoosier

area of southwestern Saskatchewan. However, these Basal sand units onlap onto the northeast edge of the UE_2 unit farther to the south.

The distribution of pebbly beds in the UE_2 unit appears to have been related to the topography of the depositional surface. The lack of pebbles in cores from the UW_1 sand unit to the extreme southwest of the study area suggests that pebble transport during Viking deposition occurred mainly well offshore in the area studied.

The internal characteristics of the UW_3 sandbodies while fairly similar to those of the Basal and Lower chronounits, is radically different from that of UW_1.

CHAPTER VIII

SUMMARY OF THE DEPOSITIONAL HISTORY AND PATTERNS OF VIKING SANDBODIES

A northwest-southeast trending line from Township 31, Range 27W4M through Township 27, Range 24 and Township 23, Range 12, to Township 20, Range 8 and Township 17, Range 4, distinguishes the predominantly shaly Joli Fou to the northeast from the very sandy Joli Fou and/or Blairmore to the southwest. Thus, in the latter area the Joli Fou cannot be readily differentiated from either the underlying Blairmore/Mannville or the overlying Viking strictly on the basis of lithology. This line, therefore, is roughly the sand-mud (nearshore-offshore) line during Joli Fou time.

In this study, no indication of a regional unconformity at the Joli Fou-Viking contact was observed either southwest or northeast of this line. In the latter area, however, some stratigraphic section, generally less than 15 feet (4.6 m), is interpreted to be locally missing at the base of the Viking in the following areas: Provost, Hamilton Lake, Joffre, Joarcam, Sibbald and in Township 29, Range 13W4M. This interpretation is based entirely on a comparative analysis of electric well log curves in adjacent wells. Because the missing intervals seem to be laterally discontinuous and restricted, they are regarded as due to scour of

the top of the Joli Fou Shale. The observed sharp lower contacts of the southeast and northeast edges of the L_2 and UE_2 sand units, respectively, is regarded as support for this interpretation. However, some of the areas of reduced section may be simply recording periods of non-deposition.

The areas with missing section are closely associated with the earliest Viking sandbodies northeast of the study area. These were deposited during the Basal chrono-interval, bound time-wise by bentonites E and C at the base and top, respectively. Localized sand development occurred within a northwest-southeast trending area comprising the Dodsland-Hoosier areas of southwestern Saskatchewan, and the Provost, Hamilton Lake, Joarcam and Beaverhill Lake areas of Alberta.

These sandbodies are mostly linear, and sub-parallel. They are characteristically thin, with only a few exceeding 30 feet (9 m) in thickness. They trend NW/SE except for the Dodsland-Hoosier units which trend WSW/ENE. Generally, they lie near the northeast border of the study area. Nearly all of these sand units are presently reservoirs for either oil or gas.

Parts of the L_3, L_5 and L_9 units of the Lower sand ridge complex, including the UE_2 and UW_1 sandbodies, were also nucleated at this time.

During the succeeding Lower chrono-interval, which spans the time from bentonites C to A, the loci of sand deposition shifted to the southwest of the earliest

sandbodies, except for the Joarcam area where Lower Viking sands overlie the Basal sand units directly. Again, localized sand deposition was characteristic, and occurred in three fairly distinct areas (Lower, Joffre and Joarcam). This time, however, from 4 to 12 discrete chronotaxial sandbodies characterized each area. Sand units are linear, fairly parallel, and generally trend NW/SE. Their general configuration at a point in time during deposition is envisaged to be similar to present-day shelf ridge and swale topography, with maximum sand ridge thickness rarely exceeding 60 feet (18 m).

In general, this time interval was that of major Viking sand deposition, and the sand units are very distinct in time and space. Unfortunately, however, only a few have been found to contain oil and/or gas.

The profile defined by bentonite A indicates that deposition of the Upper Western sand complex ceased at about the end of the Lower chrono-interval.

During the terminal Upper chrono-interval, bound at the base by bentonite A, and at the top by bentonite A_o or the top of the Viking, the loci of sand deposition shifted to the southwest and to the southeast of the Lower sand ridge complex. In the former area, the Upper Central ridge developed within Townships 23 and 24, Ranges 14 and 15 W4M, while the major part of the Upper Eastern complex developed across the southern Alberta-Saskatchewan boundary. Three sandbodies (UE_o, UE_1 and UW_2) comprise the Upper Eastern

sand complex. Whereas deposition of the UE_2 was continuous from the Basal to the Upper chrono-intervals, the other two were laid down only during the latter period. The Upper Viking sands are generally linear, parallel to one another, and trend NW/SE. The thickest single Viking sandbody (Upper Central) was laid down at this time.

Most Viking sandbodies have an imbricate stacking pattern. Three variants of this pattern are recognized, and shown schematically in Figure 109. Pattern (a) is the most common. It is believed to have resulted from discrete chronotaxial sandbodies migrating at possibly different rates, but in the same general direction. Good examples of this pattern include the L_0-L_1, L_3-L_5, LJC_8-LJC_9 sand units of the Lower chronostratigraphic unit; and the UE_0-UE_1, UE_1-UE_2 units of the Upper Eastern sand complex.

Pattern (b) is characteristic of the internal geometry of the UE_2 sandbody of the Upper Eastern complex. This pattern of intermittent lateral accretion of thin sand units may have resulted from a current system that was progressively displaced in the direction in which the sand units were migrating. This pattern may have been favoured by a relatively higher rate of subsidence.

Pattern (c) is typical of the thin Viking sandstone members of the Dodsland-Hoosier-Smiley area of southwestern Saskatchewan and is fairly similar to (b), except that the latter shows a larger degree of diachronism, while localized thickening and thinning characterize the former. Evans

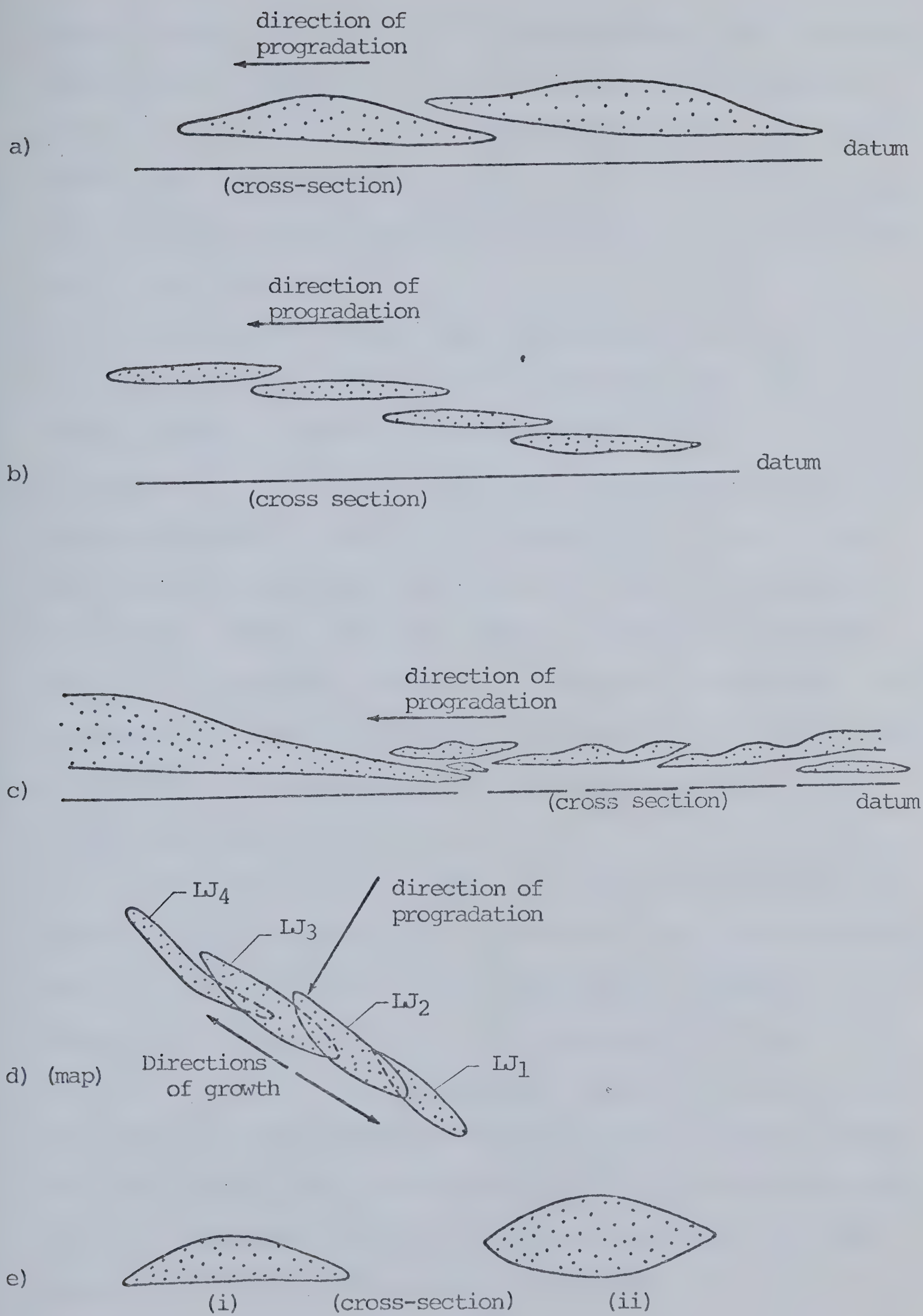

Figure 109. Arrangement patterns of Viking sandbodies.

(1970) related this pattern to east flowing tidal currents migrating in a southerly direction with the sandbodies. Thus, Selley (1976, p. 371, Figure 155) depicted the general pattern Of development for these sandbodies as being similar to the intermittent lateral accretion of a point bar deposit in a fluvial system.

The writer doubts that this interpretation, based on the stratigraphic positions of these sands and their lateral relationships to bentonites MN and K (D and C) is unequivocal. Although pattern (c) could be generated by sands migrating to the SSE as postulated by Evans, a NNW direction of migration also seems possible, in a manner similar to pattern (a). Or perhaps different sandstone members may even have migrated in opposite directions. The absence of a basal bentonite time-control hinders a definite interpretation of the sense of migration of these thin Viking sand members.

However, the localized thickening and thinning of members, their stratigraphic relationship to the bentonites and the UE_2 sandstone, the nearly parallel trend of the youngest K member to the UE_2 and the regional depositional pattern of other Viking sandbodies studied are used to suggest that the Dodsland-Hoosier-Smiley Viking sand members may constitute a large sandwave field, with sands migrating either to the SSE or NNW or in both directions, probably similar to those of the present North Sea.

The North Sea sandwave field trends at high angles

to the tidal sand ridges and comprises sandwaves interpreted to migrate in opposite (SW and NE) directions, as well as some which are static (Terwindt, 1971; McCave, 1971). Close to the tidal sand ridges, the sandwave field grades into mud and sand patches, thinning at the same time (McCave, 1971). This attribute is also exhibited by these Viking sandstone members as they are very poorly developed near the UE_2 sandstone.

Pattern (d) is envisaged for the thin Lower Joffre sandbodies. The four thin sand units may have been nucleated at the same time. Different rates of vertical and lateral growth, probably related to sediment supply and the current flow system may account for the inferred pattern.

A few fairly static sandbodies exhibit different geometric configurations. The Upper Central sandbody is plano-convex shaped, with a flat base and convex top (ei). While the lower contact appears to be sharp to gradational the upper is generally sharp. The $L5_a$ unit, on the other hand, is lens shaped (eii). The spontaneous potential curve of this unit indicates sharp lower and upper contacts. The former may have been scoured in places.

These imbricate arrangement patterns show the direction of migration of the involved sandbodies and may also reflect the shifting pattern of the depositing currents with time. With the exception of the Upper Central sandbody, which was fairly static, and the Upper Western sand complex, which prograded in a northeasterly direction, bentonite

chronostratigraphy indicates that other Viking sandbodies migrated dominantly southwesterly, although those in the Dodsland-Hoosier area appear to have shifted in a SSE direction onto the northeast margin of the UE_2 unit.

These time-spatial distributions deduced for the Viking sandbodies have paleogeographic implications:

1. The Viking Formation is not a simple deposit of a northeasterly or easterly regressing sea. Rather, nearshore and offshore sand deposition was contemporaneous, migrating in opposite directions, seaward for the nearshore sands (UW) and landward for the offshore sands (Basal, Lower and Upper Eastern units).
2. The thick mudstone interval between the nearshore and offshore units is a consequence of this opposed pattern of sand migration and progradation. This pattern explains the northeastward decrease in the thickness of the mudstone interval which separates the Lower from the Upper sandbodies in the northwest. To the southeast, however, this mudstone interval is partly the distal facies of the Upper Eastern sand complex migrating to the southwest. The opposed directions of migration of these sandbodies, coupled with higher rates of subsidence and deposition to the southwest of the study area, plus the regional sediment dispersal pattern, may explain why the Viking Formation is thicker but contains less sand in the southwest, whereas the reverse is true for the northeast, as observed by Boethling (1977b).

3. The Lloydminster transgression probably progressed from the northwest toward the southeast, and if so, was Boreal affiliated.
4. In general, the easterly and northeasterly decrease in thickness of the Formation is not directly related to direction of regression, or distance from shore, but appears to be a consequence of the sediment dispersal mechanisms and patterns.
5. Net opposing directions of sediment movement would suggest two dominant sediment dispersal mechanisms for the Viking sandbodies.

CHAPTER IX

SEDIMENTARY FACIES ANALYSIS

On the bases of lithology, sedimentary structures and textures, and ichnofossils (trace fossils), two quite different facies sequences are recognized in the Viking cores from the study area. Facies were identified either by comparison with possible recent analogs, or on the basis of the predominant physical or biological characteristic. These facies are described and interpreted below from bottom to top.

A. Sedimentary Facies Sequence A

Eleven facies were recognized and identified in cores from the UW_1 sandbody in well A.N.D. No. 1, 10-14-23-1W5M, located approximately 5 miles (8 km) south of Calgary (see Figure 104 for the well location, and Figure 110 for the spontaneous potential curve).

Mudstone Facies (AI)

This facies is about 6 feet (3 m) thick and consists predominantly of dark grey massive mudstone at the base, becoming silty and sandy towards the top. The sand occurs as laminae and lenses, rippled in places (Plate IA). Irregular contorted bedding and nodular pyrite are common

A.N.D. No. I
10-14-23-1W5M
KB 3429 ft.

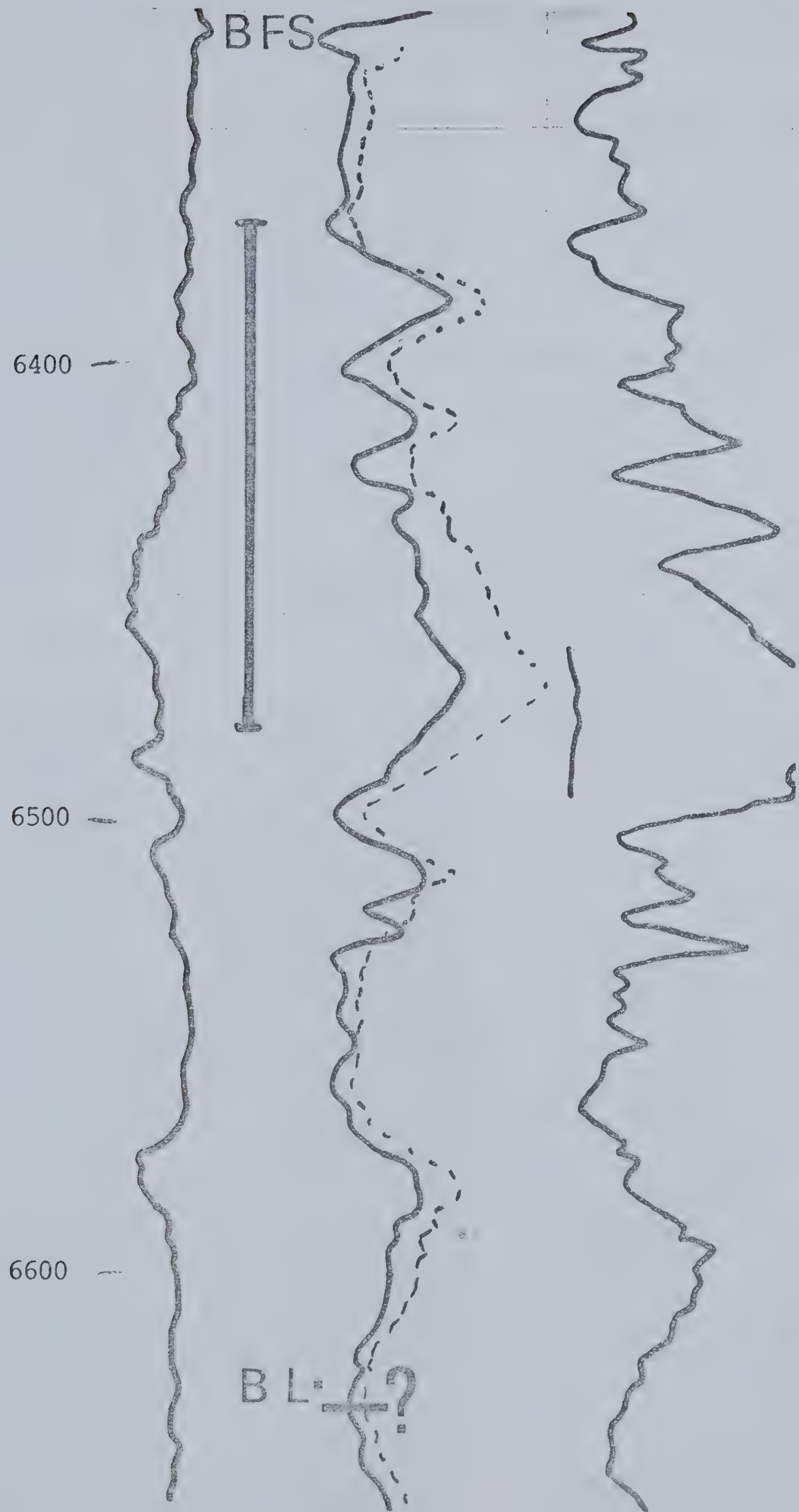

Figure 110. Electric log curve of Viking barrier island (UW_1).

Plate I

Viking facies sequence A: Barrier Island, UW_1 (Ebb Tidal Delta and Transitional Facies) Well A.N.D. No. 1, 10-14-23-1W5M

A. Silt and fine sand laminae, some rippling (a). Upper part of Prodelta mudstone facies; 6477 ft.

B. Contorted bed with sharp base and pyrite nodule (b) with occluded sediment. Prodelta facies; 6475 ft.

C. Sequence of low-angle cross-stratification, bioturbated (*Terebellina* sp. (c)) at base, overlain by ripple trough cross-lamination (d) capped with horizontal lamination, Lower delta front facies; 6470 ft.

D-E Sequence of plane lamination, clay laminae, clay clasts (e), planar low-angle cross-lamination, plane lamination and clay drape. Upper delta front facies; 6465-6464 ft.

F. Weakly bioturbated unit of interbedded sandstone and shale. Transitional (marginal channel) facies; 6462 ft.

PLATE I

features (Plate IB). Bioturbation is generally rare.

Interpretation

The sediments reflect deposition largely from suspension in a relatively low energy environment. As shallowing occurred, the area was occassionally invaded by relatively stronger currents which deposited and rippled the silt and very fine sand laminae and lenses nearer the top. Syndepositional slumping produced the rheotropic structure. Absence of bioturbation may be indicative of rapid deposition. The occurrence of nodular pyrite suggests that this facies was rich in organic matter, and that consolidation occurred in a reducing environment. This transitional facies is thought to have been deposited in a Pro-delta environment but within the Lower shoreface zone, partly because of its relationship to the overlying facies.

Cross-Stratified Fine-Grained Sandstone Facies (AII)

Facies AI grades imperceptibly upward into the cross-stratified facies. This facies is approximately 12 feet (4 m) thick, and comprises clean well sorted cross-stratified sands with dark clay laminae. Average quartz grain size varies from 0.08 mm at the base (Plate IC) to 0.26 mm near the top (Plate IE); that is, very fine to medium sand, showing a coarsening upward size gradient.

Low angle, medium scale cross-stratification is the predominant sedimentary structure. Cross-set thickness varies from 5 to 30 cm. This cross-stratification type is

repetitive and is either succeeded by small scale ripple trough cross-lamination and terminated by a low-angle cross-laminated thin (2.5 cm) sand set, (Plate IC), or capped with dark clay laminae (base of Plate ID). Low-angle cross-stratification may also be succeeded by very thin horizontal lamination and terminated by dark clay laminae (Plate IE). Plate ID also shows clay clasts underlying a cross-stratified unit. In places, foreset laminae are draped with very thin carbonaceous clay. Except for the trace fossil in Plate IC, which is similar to *Terebellina* sp. described from the Lower Cretaceous Dakota Group of Colorado by Chamberlain (1978, p. 175, Plates 109 and 110), ichnofossils are generally rare. This trace fossil is also similar to the "donut burrow" of Boethling (1977b). Pyrite nodules are also occasionally observed (Plate IC).

Interpretation

The gradational and textural relationships between this and the underlying facies suggest a related genetic mechanism. However, deposition of the cross-stratified facies occurred in a shallower and higher energy environment in which traction transport and bed load deposition were the dominant sedimentary processes.

There is a cyclical vertical succession of the sedimentary structures described, indicative of a repetitive decreasing flow regime typical of a wanning unidirectional current. A similar repetitive succession of sedimentary

structures was observed in interpreted tidal sand flat deposits of the Lower Cretaceous Dakota Group near Denver, Colorado, MacKenzie (1975). He attributed their genesis to repeated alternations of tidal currents and wavy slack water. Masters (1967) recognized a similar succession of sedimentary structures in the Mesaverde Formation and interpreted the unit as a flood tidal delta based on its position above the barrier beach facies. The cuspate ebb-tidal delta facies of the Eocene Tordilla Sandstone of Texas, described by White and Galloway (1977), contains discontinous clay lenses and drapes, abundant mud chips and larger clasts, and both disseminated and placer carbonaceous plant debris, besides trough cross-bedding, sandwave bedforms and horizontal stratification.

Based on the succession of sedimentary structures, lithology, coarsening upward textural gradient, similarity to other ancient deposits and stratigraphic position, the writer believes that this facies, together with facies AI, may represent an ebb-tidal delta facies. It is envisaged that during each ebb-tidal flow, sandwaves with superimposed ripples migrated seaward. Suspension deposition of mud and clay resulted under slack water conditions of the tidal cycle. Occasionally the tidal currents were strong enough to scour and redeposit clay clasts in bedform troughs, and at other times they were so weak as to permit deposition of carbonaceous clay drapes on foreset laminae.

The absence of ripple cross-lamination in the

coarser cross-stratification sets higher in the section may be due to the narrow range of velocities in which they form as grain size increases. Flume studies by Southard and Harms (1972) show that ripples give way to lower regime flat bed phase in sands coarser than 0.6 mm.

Interbedded Sandstone, Mudstone and Claystone Facies (AIII)

Facies AII appears to grade upward into the interbedded sandstone-mudstone-claystone facies. This unit is about 3 feet (1 m) thick and consists of sandstone, mudstone and claystone of various thicknesses. Sandstone beds are light grey, fairly well sorted and fine to medium grained. Bed thickness varies from o.6 cm to 7.5 cm. A few beds exhibit a coarsening upward tendency and weak stratification (Plate IF); otherwise, an ungraded appearance is characteristic.

The mudstone and claystone interbeds are generally structureless and less than 2.5 cm thick. Ichnofossils are rare, but where found they affect only the suspension deposits (upper half of Plate IF).

Interpretation

The depositional environment of this facies is one of fluctuating energy conditions with bedload deposition alternating with suspension settlings of fines. The stratigraphic position and relationship to the underlying and overlying units suggest a transitional environment for this

unit, possibly a secondary marginal ebb-tidal channel similar to the "spill-over" ebb-tidal channel of Oertel (1975). It is envisaged that the environment was relatively protected much of the time, but was occasionally invaded by relatively stronger currents.

Bioturbated Sandstone Facies (AIV)

The bioturbated sandstone facies succeeds the underlying interbedded sandstone-mudstone-claystone facies AIII. The basal 7 cm of this unit consists of small mud and clay clasts embedded in a medium to coarse sand and capped by a thin clay laminae. This unit appears to rest on a scoured top of the underlying facies (base of Plate IIA).

The bioturbated sandstone is about 13 feet (4 m) thick and consists of dark grey, moderately well sorted fine to medium grained sand. The average quartz grain size coarsens upward from 0.2 mm near the base to 0.4 mm near the top. Discontinuous wavy clay blebs and wisps are more abundant in the lower part. Irregular bedding and low angle simple cross-stratification are preserved in places (Plate IIB). The degree of bioturbation decreases upward from strong to moderate. Characteristic trace fossils include an unidentified funnel-shaped burrow up to 10 cm deep disrupting lamination (Plate IIA) and fine sand mottles at the base, followed upward by micro-trace fossils (Plate IIB).

Plate II

Viking facies sequence A: Barrier Island,
UW_1 (Middle Shoreface, Shelf, Upper Shoreface-Beach Facies)
Well A.N.D. No. 1, 10-14-23-1W5M

A. Sequence of basal scour (a), clay clasts (basal lag), shale lamina, bioturbation (funnel shaped burrow, disrupted lamination, some mottles of fine sand). Base of Middle shoreface facies; 6457 ft.

B. Horizontal and low-angle cross-stratification types preserved in a bioturbated (micro ichnofossils) unit. Middle shoreface facies; 6453 ft.

C. Pyritic flasers (c,d) and interbedded claystone (e). Transitional (shoreface-offshore) facies; 6451 ft.

D. Sharply based (f), planar, low-angle cross-stratification. Upper shoreface-Beach facies; 6449 ft.

E. Horizontal stratification (beach-type). Upper shoreface-Beach facies; 6447 ft.

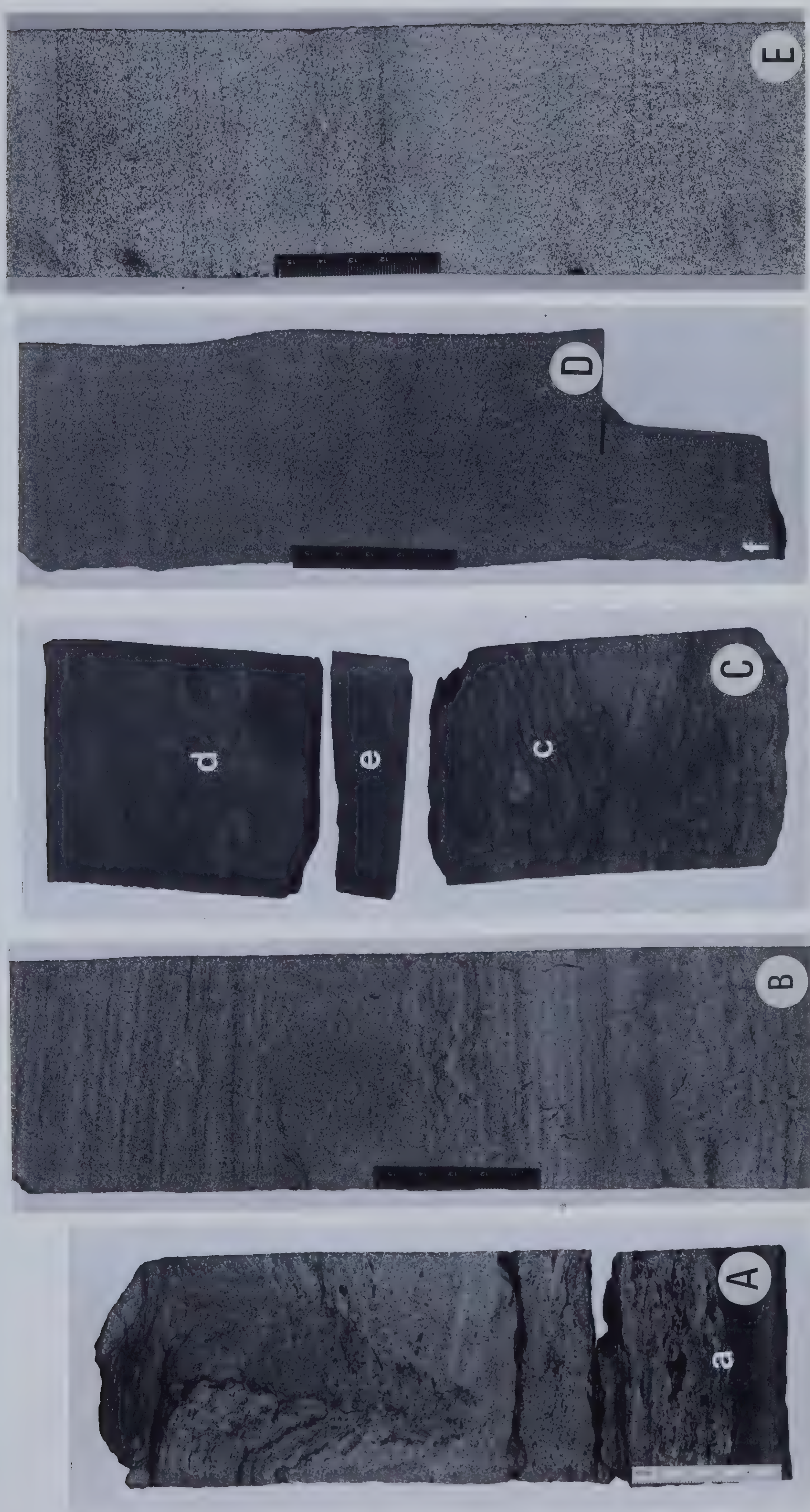

PLATE II

Interpretation

The upward decrease in the degree of bioturbation and clay content are consistent with the coarsening upward textural gradient. These indicate that the subenvironment of this facies was one of high energy level with general increasing competence.

The internal characteristics of this facies are generally similar to those of middle shoreface sediments of the Recent Galveston Barrier Island of Texas described by Bernard *et al.* (1962); and to those of the homotaxial Lower Cretaceous Muddy Barrier Island described by Davies *et al.* (1971). However, stronger currents (storm?) may have scoured or winnowed the top of the underlying unit, accounting for the basal characteristics observed. This basal unit may even be a local phenomenon.

Generally, middle shoreface sediments are deposited in 5 to 30 feet (1.6 to 9 m) of water characterized by shoaling and breaking waves whose energy level increases with decrease in water depth. This inverse relationship (increasing energy level with decreasing water depth) explains the structural and textural gradients observed.

Flaser-Bedded Claystone Facies (AV)

The middle shoreface facies grades upward into a 10 cm thick, pyritic, fine to medium grained sand and mud flaser unit (lower part of Plate IIC), followed by a 45 cm thick, dark massive, claystone (middle part of Plate IIC),

and terminates with another 6.5 cm thick fine sand and mud flaser bedded unit (upper part of Plate IIC). The unit is approximately 62 cm thick.

Interpretation

The sedimentary structures and lithology of this facies indicate a transitional environment in which the predominantly higher energy levels of the underlying unit changed to one with a fluctuating energy level (lower sand-mud flaser unit). This was succeeded by a relatively low energy level (middle claystone), and finally a return to fluctuating energy conditions as reflected in the upper sand-mud flaser unit.

Reineck (1975) observed flaser and lenticular bedding to be characteristic of the shoreface-offshore transition zone in the North Sea. Transgression would allow deposition of marine clay above it, and vice versa. It is therefore thought that the deposition of this transitional facies was related to a minor transgression within a predominantly regressive condition.

Cross-Stratified Sandstone Facies (AVI)

This unit rests sharply (scoured surface?) on the underlying transitional marine facies (left base of Plate IID). It is about 13 feet (4 m) thick, and consists of light grey, clean, very well sorted, medium grained, cross-stratified sand. No apparent grain size variation is

visible except for an occasional lamina or segregation of finer grained heavy opaque minerals shown in Plates IIE and IIIA. These plates also show the characteristic planar low-angle cross-stratification and plane lamination of this unit. Neither shale laminae nor bioturbation is observed.

Similar sedimentary structures and textures have been documented in modern barrier beach environments by Bernard *et al.* (1962), Dickinson *et al.* (1972) and, in ancient deposits by Berg (1976), Davies (1976), Hobday and Tankard (1978), and others. This facies is therefore similarly interpreted as upper shoreface-beach environment characterized predominantly by wave swash and back wash processes. Thus, it represents the highest physical energy level and the shallowest water level in the local depositional milieu.

The sharp (erosive?) basal contact and the absence of middle shoreface sediments beneath this facies suggest a rapid rate of regression following the local transgression. Somewhat similar vertical facies relationships were observed and similarly interpreted by Weber (1971) and Roep *et al.* (1979) for the barrier islands of the Niger delta and Spain, respectively.

Plate III

Viking facies sequence A: Barrier Island.
UW_1 (Upper Shoreface-Beach, Lagoonal, Mixed Tidal Flat Facies)
Well A.N.D. No. 1, 10-14-23-1W5M

A. Heavy mineral band. Upper shoreface-Beach facies; 6442 ft.

B. Root traces (r), pyrite and a coaly horizon (h). Eolian (dune) facies; 6438 ft.

C. Silt and/or very fine sand laminae in weakly bioturbated mudstone, some mudcracks (?) (m). Lagoonal facies; 6430 ft.

D. Peat-like organic accumulation Lagoonal marsh facies; 6420 ft.

E. Plant stem (p). Lagoonal under-marsh clay facies; 6415 ft.

F. Burrow in mudstone filled with coarse sand. Mixed tidal flat facies; 6395 ft.

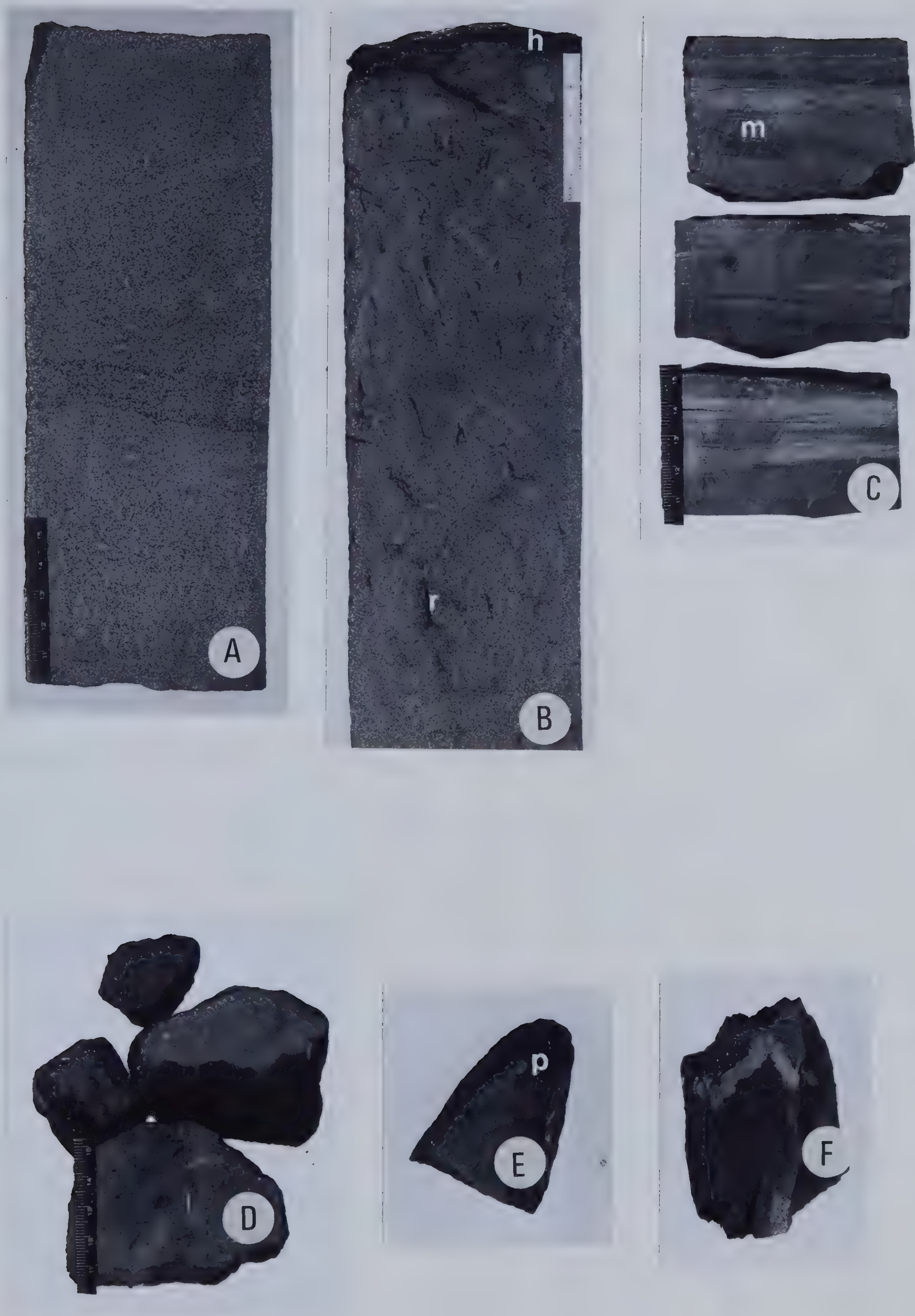

PLATE III

<u>Structureless Sandstone - Facies (AVII)</u>

The upper shoreface-beach facies grades upward into the structureless sandstone facies. This unit is 37.0 cm thick, and consists of relatively clean, fairly well sorted fine to medium-grained sand (0.25 mm).

The unit is generally structureless except for vertical carbonaceous and coaly traces (Plate IIIB) indicative of roots and rootlets. The upper part is pyritic. A very thin coaly bed terminates this facies. No paleosol horizon was recognized.

This facies is interpreted as vegetated eolian dune deposits behind the beach. Modern eolian deposits are characterized by festoon and planar cross-lamination. However, in older analogs, these structures have often been destroyed by roots and groundwater circulation. Their recognition, therefore, relies heavily upon root traces and/or paleosol horizons (Davies *et al.*, 1971).

An observed decrease in quartz grain size from beach to eolian facies is also common to most Gulf of Mexico Holocene barrier islands (e.g.. Mustang and Padre). It also occurs in the interpreted Lower Cretaceous Muddy barrier island at Bell Creek, Montana.

Carbonaceous Mudstone - Facies (AVIII)

The eolian dune facies grades upward into about 5 feet (1.5 m) thick dark carbonaceous mudstone. The carbonaceous materials occur mostly as thin coal streaks and laminae within the basal part of the facies (see Appendix Va for core photograph). This facies is interpreted as poorly vegetated back barrier mud flat deposits.

Lagoonal - Facies (AIX)

The vegetated mud flat facies grades upward into the lagoonal facies, approximately 35 feet (11 m) thick. This facies consists of three cyclically stacked subfacies, and a thin sandfacies of random occurrence. They are discussed from base to top.

a) Lagoonal Dark Grey Mudstone Subfacies (AIXa)

This dark grey mudstone facies occurs three times. The lowest occurrence is directly above the back barrier mudflat facies. The unit consists essentially of dark grey mudstone with very fine silt laminae (Plate IIIC) and rippled fine sand lenses. Bioturbation, carbonaceous traces, and disseminated pyrite are common features of this unit. Thickness ranges from 4 to 10 feet (1.2 to 3.1 m). This subfacies is interpreted as the normal lagoonal subfacies.

b) Lagoonal Muddy Sandstone Subfacies (AIXb)

This muddy sandstone facies is generally less than 2 feet (60 cm) thick. The unit appears to overlie the above lagoonal facies gradationally. It consists of fine to medium grained, poorly sorted, muddy sand. It is generally massive although faint lamination can be seen in a few places; the upper part is bioturbated. These thin sand beds are interpreted as storm generated washover deposits.

c) Lagoonal Rooted Greenish Mudstone Subfacies (AIXc)

The greenish mudstone facies overlies either the washover deposits or the lagoonal deposits. It occurs twice stratigraphically, 1.5 feet (0.45 cm) and 5 feet (1.5 cm) thick, respectively. The rock has varying shades of green coloration with either a fissile or massive character. Carbonaceous streaks of roots and/or stems are common features (Plate IIIE). This facies may represent early marsh or marsh underclay deposits.

d) Lagoonal Peat Subfacies (AIXd)

The peat facies was also recognized at two levels. It always overlies the early marsh or marsh underclay deposits, and ranges in thickness from about 2.5 to 4 feet (0.8 to 1.2 m). The unit consists of dark brown carbonaceous, in part flakey to friable, peat-like material; root traces are common (Plate IIID). This facies is interpreted as marsh deposits.

The vertical succession of these lagoonal facies

from bottom to top is as follows: dune ⟶ vegetated mud flats ⟶ lagoon ⟶ washover ⟶ lagoon ⟶ early marsh/ marsh-underclay ⟶ marsh ⟶ lagoon ⟶ early marsh/ marsh-underclay ⟶ marsh. This cyclic facies succession appears to reflect a fluctuating sea level typical of an unstable tectonic environment. However, also plausible is the occurrence of small islands in the back barrier lagoon. In this case, regression and subsidence alone could explain the observed superposition of the subfacies.

Sandy Mudstone Facies (AX)

The lagoonal-peat subfacies grades upward into this sandy mudstone facies which is about 13 feet (3.0 m) thick. The mudstone beds are dark grey and massive. Lenticular silt laminae are, however, common at some levels. The beds are moderately burrowed in places, and a worm-like burrow filled with coarse sand (Plate IIIF) was observed at one horizon. Coaly laminae and carbonaceous streaks are common features. The sandy beds in the unit are less than 60 cm thick and concentrated at the base and middle. They are medium to coarse grained, muddy and moderately to strongly bioturbated.

This facies is interpreted as lagoonal-mixed tidal flat sediments. The thin sand beds may have been generated by storms or represent micro channel deposits. Reineck and Singh (1975) stated that tidal lagoons are developed more or less like tidal flats; thus, their differentiation may be

difficult. Phleger (1969) included the protected back barrier tidal mudflats and the landward intertidal mudflat deposits as lagoonal deposits.

Cross-Stratified Sandstone Facies (AXI)

This cross-stratified facies begins with a basal scour (Plate IVA) on the underlying tidal mudflat facies. This is followed by a lower clean, fairly well sorted, medium grained (0.33 cm), cross-stratified (trough?) sandstone unit, about 3 feet (1.0 m) thick. Clay clasts up to 2 cm in longest diameter are randomly dispersed near the base. A horizon of imbricated lenticular clay clasts up to 3 cm in longest diameter (Plate IVB) terminates this unit.

A relatively clean, fairly well sorted, finer-grained sand unit, about 30 cm thick and cross-stratified (planar?), succeeds the lower unit. This cross-stratified set, in contact with the clay clast horizon (Plate IVB), has an apparent dip in the opposite direction to that of the next underlying cross-stratified set. The unit is capped by a 2.0 mm thick silty mudstone lamina.

A 40 cm thick micro-trough cross-laminated, finer-grained (0.14 mm), fairly well sorted, muddy sand unit succeeds the second unit.

This facies is finally capped by a 5 foot (1.5 m) thick sandy mudstone bed whose uppermost 15 cm portion consists of medium to coarse grained, poorly sorted sands interbedded with light grey weakly bioturbated mudstone beds

Plate IV

Viking facies sequence: Barrier Island,
Well A.N.D. No. 1, 10-14-23-1W5M, UW_1
(A, B = Tidal creek channel facies);
Shoreface connected sandstone UW_3
(C, D = Bioturbated mudstone, Heterolithic facies);
and Patinated Chert (E).

A. Sharply (scour) based trough cross-stratified unit with clay clasts. Base of Tidal Creek channel facies; 6390 ft.

B. Herringbone-like cross-stratification with clay clasts along set boundaries. Middle part of Tidal Creek channel facies; 6385 ft.

C. Horizontal laminated (l) scoured and overlain by ripple lamination (r), in turn draped with clay (z) with a scoured top and capped by horizontal laminated sand. Bioturbated mudstone facies (UE_3); LALTA C.P.O.G. Wayne 7-21-27-10 W4M; 3805 ft.

D. Tidalite sequence of alternating low-angle sand laminae and thin carbonaceous mud laminae, horizontal laminated sand and mudstone capped by shale. Heterolithic facies (UW_3); C.P.O.G. Clark Hussar 6-17-25-20 W4M; 3972 ft.

E. Patinated Chert: black exterior (a), whitish grey interior with black rim (b). C.P.O.G. W. Hussar 6-18-27-20 W4M; 3853 ft.

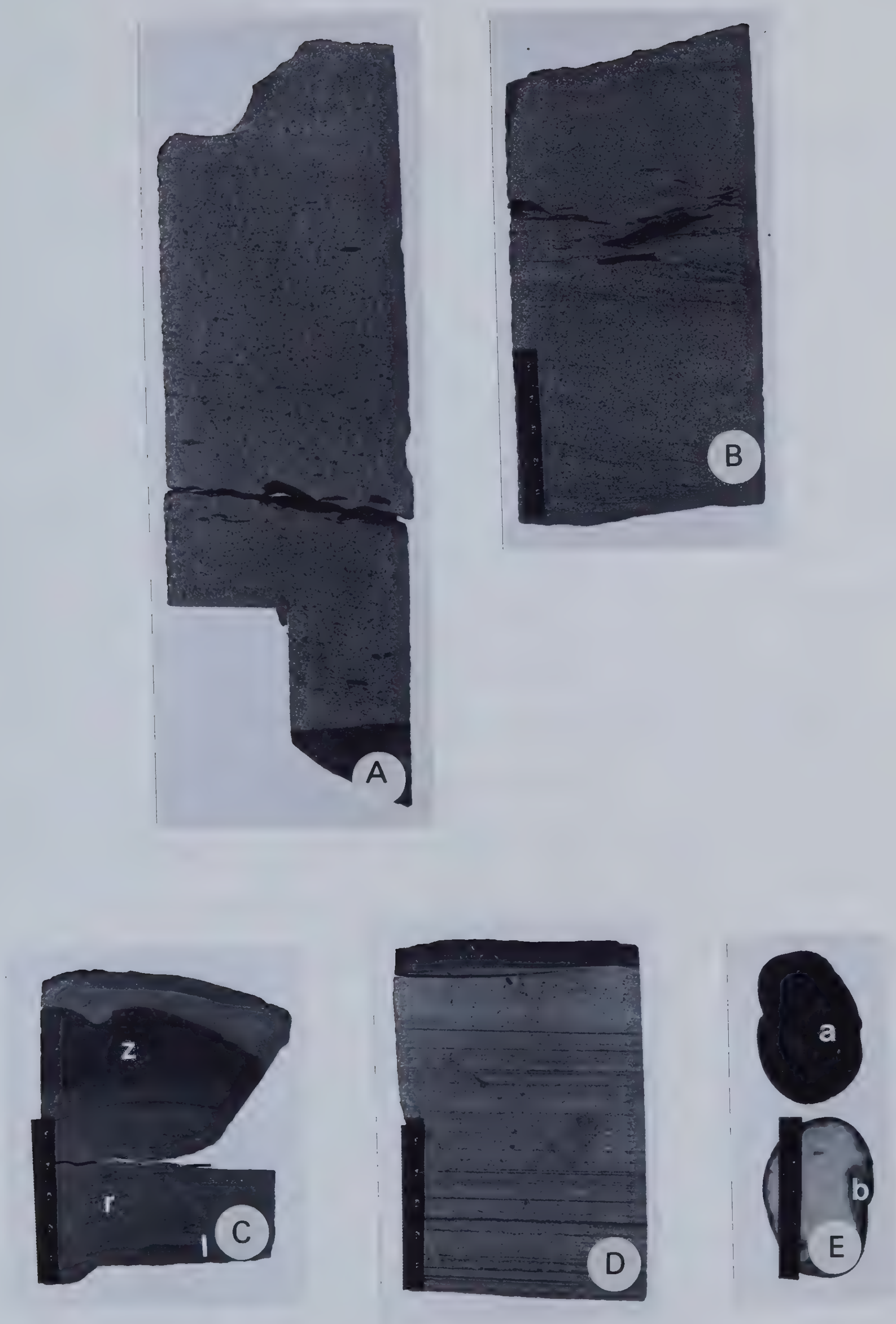

PLATE IV

containing abundant carbonaceous streaks.

Interpretation

The vertical succession of sedimentary structures and the general finning upward textural gradient exhibited by this unit are consistent with a fluvial channel (point bar) deposit probably capped by overbank mudstone containing thin crevasse splay deposits.

However, on the basis of the mudstone laminae, the apparently oppositely dipping cross-strata sets, the thickness of the unit (6 feet--2.0 m), and the overlying facies, the writer is of the opinion that a tidal creek channel on a tidal mudflat is the most likely environmental setting for these deposits. Under this interpretation reversing tidal currents moved bedforms in opposing directions, while the mudstone laminae represent tidal slack water deposits.

A probable modern analog may be found in the tidal mudflat-tidal creek environments of the Netherlands and Germany described by Reineck (1963, 1967); and possibly, the macro-tidal Ord River of western Australia described by Coleman and Wright (1978). In the latter example, isolated tidal creek channel sandbodies are preserved in tidal mudflat deposits with extensive overbank crevassing.

Finally, the Viking succession in this well terminates with a 3 foot (1.0 m) thick green carbonaceous mudstone, followed by 1.5 feet (0.5 cm) of dark brown carbonaceous matter. These deposits are similar to the lagoonal

marsh underclay and marsh deposits described earlier, but are considered to be tidal creek related overbank deposits.

The dark marine shale of the Lloydminster Formation succeeds this unit, bringing Viking time to a close.

Figure 111 is a vertical facies sequence model of the UW_1 sandstone unit. The slabbed core photograph is shown in Appendix Va. The uppermost 8 feet (2.5 m) was not slabbed and therefore is missing from the photograph.

Barrier Island Discussion

The Viking barrier association of lithofacies is broadly similar to that of the Recent prograding Galveston barrier island described by Bernard *et al.* (1962) and to that of the Lower Cretaceous Muddy Formation at Bell Creek Montana, interpreted as a barrier island by Davies *et al.* (1971). However, the Viking sequence differs from the other two in the presence of a thin transgressive marine claystone, and especially, in the sediment characteristics of the lower shoreface zone.

In the Galveston-Muddy regressive facies models, the upper shoreface-beach facies grades uninterruptedly downward into the middle and lower shoreface facies. In the Viking sequence, however, the ebb-tidal delta and the transitional (spill-over channel?) facies lie below the middle and upper shoreface-beach facies. Moreover, marine shelf sediments are interpreted to occur between the middle shoreface and upper shoreface-beach facies.

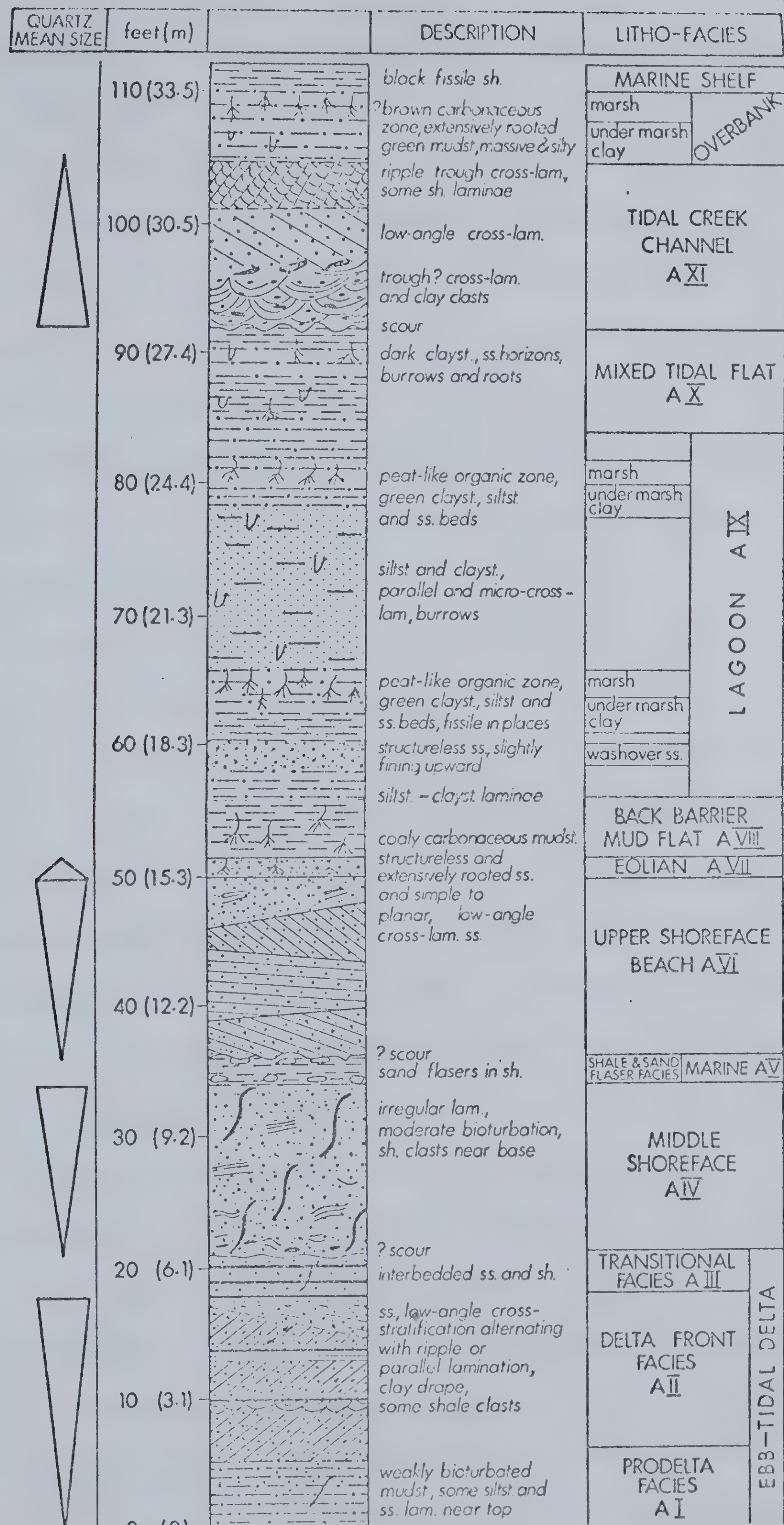

Figure 111. Structure, textures, and lithologies of barrier island associated sediments in core A.N.D. #1 10-14-23-1W5M (see Appendix VI for legend).

This difference stems from the diverse sedimentary processes which may operate in the lower shoreface zone. The middle and lower shoreface zone is seaward of the barrier island below low tide to a depth of about 10 to 20 m. In this depth range waves normally feel bottom. Thus, the predominant depositional process is wave energy, which usually increases with decrease in water depth. This relationship governs the distribution of sedimentary structures and textures observed in the non-barred Galveston Island regressive barrier model.

Where rates of subsidence and/or progradation are high, regressive barriers are known to have little or no middle and lower shoreface sediments, as in the Tertiary Cohansey barrier of New Jersey (Carter, 1978), the Messinian Sorbas barrier of Spain (Roep *et al.*, 1978), and the vertically stacked barrier islands in the Niger delta (Weber, 1971). Transgression may cause the lower shoreface facies to overlie that of the middle shoreface, as in the Recluse field barrier of Wyoming (Davies, 1976).

Storm surge deposits are known to sharply modify modern shoreface sediments (Hayes, 1967; Reineck and Singh, 1972; Swift, 1973; Kumar and Sanders, 1976). Thus, Davidson-Arnott and Greenwood (1976) and Kumar and Sanders (1976) suggested that preserved shoreface sediments in the rock record may essentially comprise storm deposits. The recognition of storm deposits in an ancient shoreface unit by Howard (1972) gives credence to the above suggestion.

Tidal channel (inlet) deposits may displace either the whole shoreface zone, as in the recent Padre barrier island (Hoyt and Henry, 1965) or only the upper part, as in the Lower Eocene Carrizo barrier of Texas (Davies, 1976).

Longshore bars commonly occur within the middle shoreface zone, while ebb-tidal deltas or shoals may occur seaward of barrier island inlets. It would appear that these features are respectively characteristic of micro-tidal wave dominated, and meso-tidal coastlines. However, because longshore currents have been observed to resediment sands from these geomorphic features (Ortel and Howard, 1972), they are commonly thought to have a low preservation potential in the rock record; although Davidson-Arnott and Greenwood (1976) and Van den Berg (1977) are opposed to this view.

Intensive studies of the Recent South Carolina meso-tidal coastal barriers are beginning to shed more light on the high preservation potential of ebb-tidal delta sediments. The degree to which barrier islands and adjacent sub-environments are protected from storms and longshore currents, rates of subsidence, progradation and sediment supply, and possibly depth of water, will affect the preservation potential of ebb-tidal delta deposits in the rock record. In certain parts of the ebb-tidal deltas of Georgia estuaries, wave induced currents are not important sedimentary processes (Oertel, 1975). In the North inlet of South Carolina, Finley (1978) noted the ebb-tidal delta to be an

efficient trap for littoral drift sediments, while low intensity northeast storms which erode beaches have an accretionary effect on the ebb-tidal delta. In the Wadden Sea, narrow tidal inlets funnel ebb-tidal currents to reach depths of up to 90 feet (30 m) where tidal channels bifurcate in relatively deep tidal wedges (De Jong, 1977). Such depths may be beyond effective wave base and possibly beyond the reach of longshore currents. The foregoing cases indicate to the writer that under certain circumstances ebb-tidal deltas will be preserved in the rock record. Inability to recognize them in the rock record may be the principal problem.

The afore-described sedimentary characteristics of facies AI and AII, their stratigraphic positions and the gross similarity between them and those of the Recent described by Oertel (1975) are used to interpret these Viking facies as an ebb-tidal delta or shoal.

The thin overlying transitional interbedded sandstone-mudstone-claystone facies may represent the deposits of a marginal inactive channel similar to that outlined in the ebb-tidal delta morphological model of Hayes (1975), and known as "spill over" channel by Oertel (1975). These transitional deposits are remarkably similar to Oertel's facies III from this sub-environment.

These lines of evidence argue against these facies being wave generated longshore bars as modelled by either Davidson-Arnott and Greenwood (1976) or Van den Berg (1977); and also precludes them being wave generated offshore bars. Finally, Reinson (1979) notes that the identification of

flood- and ebb-tidal delta sandbodies in the rock record may depend mostly on their geometry and stratigraphic position relative to surrounding facies.

If the Viking barrier concept is accepted, the trinity of ebb-tidal delta-shoreface, barrier beach, and lagoon-mudflat-tidal creek channel facies, is evidence in favour of a predominantly regressive barrier island, punctuated by a brief marine incursion, in a probable meso-tidal range Viking sea coast. This environmental setting may have been in some ways similar to the present day South Carolina coast (Lerand, 1979) or the Netherlands-German coast (Reineck, 1975).

Although this interpretation was generated from the cores of only one well, the writer believes that when the core-data information is integrated with sandstone geometry it does provide an adequate amount of significant information which makes it clearer that:

1. The UW_1 and UW_2 sandbodies may be two parallel lines of barrier islands with the UW_2 being younger; and
2. The swales, characterized by isopach thinning, between these units may represent tidal inlets.

Long Island and Fire Island along the coast of New York State (Kumar and Sanders, 1974) are examples of recent parallel barrier islands. The ancient Tordilla sandstone complex of the Eocene Jackson Group of Texas (White and Galloway, 1977) comprises two regressive barrier islands.

B. Sedimentary Facies Sequence B

Five generalized facies, discussed below, were observed to be characteristic of the remaining Viking cored sandbodies.

Bioturbated Mudstone - Facies (BI)

The uppermost part of the Joli Fou Shale is very calcareous in places (Plate VA). The bioturbated mudstone facies succeeds the Joli Fou gradationally or sharply. The thickness of this unit ranges from 3 to 20 feet (1-7 m). Thicker and more diachronous sandbodies are associated with the thickest development of this facies; therefore, its thickness appears to be a function of sand unit thickness and migration distance.

Strongly bioturbated very dark grey mudstone, with very thin wisps, blebs or mottles of silt and very fine sand, is the predominant lithology (Plate VB). Subordinate lithologies include bentonitic clay (Plate VC), and very fine sand (0.1 to 0.12 mm) laminae and lenses (Plate VD).

The nearly equidimensional very fine grained sand lenses, generally less than 3 cm thick, are relatively clean and fairly well sorted. The following stratification types are characteristic: parallel lamination (Plate VD and E), plane and ripple cross-lamination (Plate VIA), herringbone-like cross-lamination with a thin bentonitic clay drape separating glauconitic sets of cross-laminae (Plate VIB), and low-angle cross-limination (Plate VIC and D). Some

Plate V

Viking facies sequence B: Subtidal offshore (tidal current?) sand ridges (Bioturbated mudstone facies).

A. Calcareous shale near Viking - Joli Fou contact. Trecon Sedalia 11-24-30-5W4M; 2388 ft.

B. Wisps and blebs of silt in strongly bioturbated mudstone. Bioturbated mudstone facies; Camac Mavrk Huxley 6-20-34-24 W4M; 4944 ft. (L_7 sand unit).

C. Bioturbated shaly mudstone with silt and sand laminae and *Chondrites?* (u) Bioturbated mudstone facies; Imperial Armena 9-13-48-21 W4M; 3247 ft. (LJC_{12} unit).

D. Horizontal laminated, very fine, clean, well sorted sand lens with sharp upper contact. Bioturbated mudstone facies; Camac Mavrk Huxley 6-20-34-24 W4M; 4942 ft. (L_7 unit).

E. Laminated very fine sand with sharp upper and lower contacts and burrow disrupting laminae; erosional relief? at base. Bioturbated mudstone facies; Dome I.O.E. Wildunn 6-23-30-14 W4M; 3202 ft. (L_3-L_4 junction).

F. U-shaped burrow (*Rhizocorallium* sp.?) disrupting lamination in a fine sand lens. Bioturbated mudstone facies; Camac Mavrk Huxley 6-20-34-24 W4M; 4933 ft. (L_7 unit).

PLATE V

Plate VI

Viking facies sequence B: Subtidal offshore (tidal current?) sand ridges (Bioturbated mudstone facies).

A. Ripple-laminated very fine sand lenses in bioturbated bentonitic mudstone. Bioturbated mudstone facies; Westcoast Sulpetro Smore 11-30-29-10 W4M; 2894 ft. (L_4 unit).

B. Thin clay laminae (w) drape the contacts between cross-laminated sets dipping in oppostie directions (Herring-bone). Unit is glauconitic with some ichnofossils (*Terebellina (T)* sp. or *Siphonities* sp.). Bioturbated mudstone facies; Mobil Oyen 10-4-30-2 W4M; 2579 ft. (UE_2 unit).

C. Planar low-angle cross-laminated glauconitic silty sand. Upper part of bioturbated mudstone facies; H.B. Provost 6-26-34-7 W4M; 2740 ft. (B_1 unit).

D. Low-angle cross-laminated fine sand lens; diffuse top and bottom contacts; vertical burrow disrupts lamination. Bioturbated mudstone facies; Provo Halliday 13-11-28-14 W4M; 3109 ft. (UE_o).

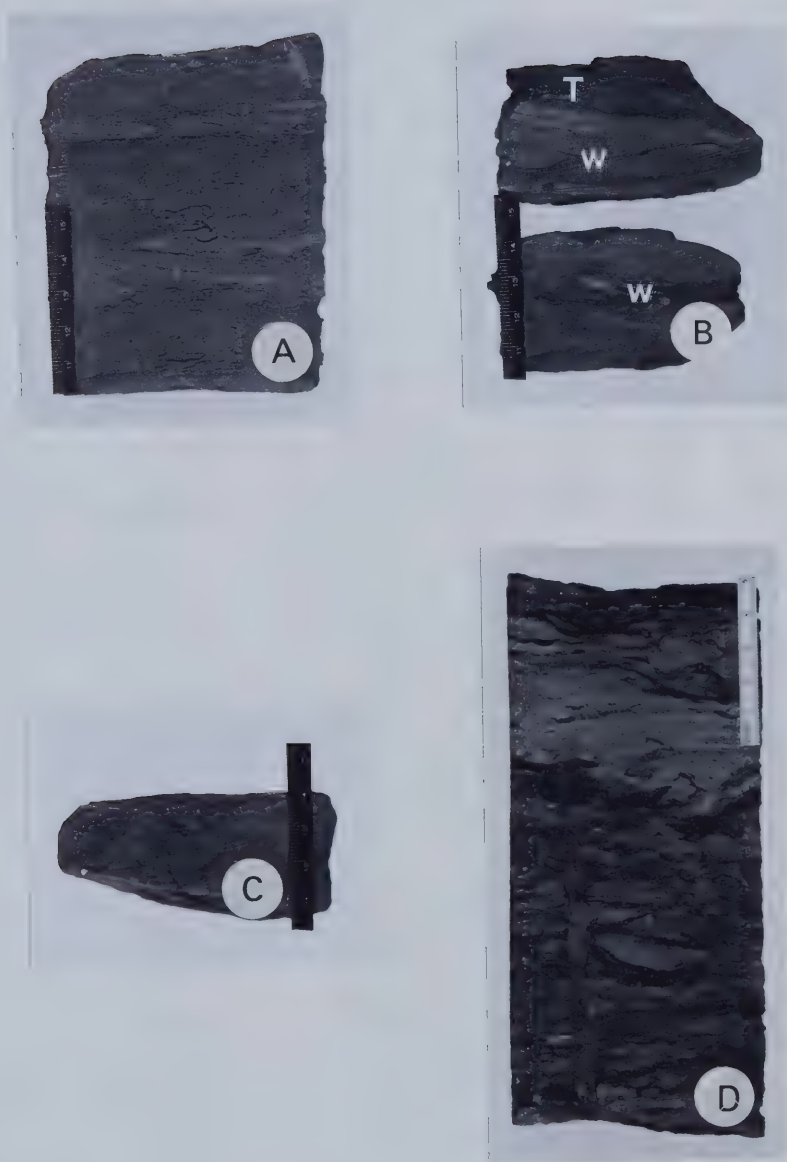

PLATE VI

units are, however, bioturbated and therefore structureless (Plate VC). Contacts may be either sharp or diffuse (Plates VC and VID), or scoured at the upper (Plate VD) or lower (Plate VE) contacts.

Nondescript and poorly preserved burrows obliterate primary sedimentary structures (Plate VE). Indentifiable trace fossils include U-shaped burrows fairly similar to the ichnogenus *Rhizocorallium*(Plate VF), (Risk, personal communication, 1979), and the "doughnut" shaped burrow probably belonging to the ichnogenus *Terebellina* sp. (Plate VIB) (Chamberlain, 1978). An unnamed burrow, 5 cm deep, is shown in Plate VID. In general, the degree of bioturbation and clay content decreases upward as quartz grain size increases. In areas of multiple sand development, this facies overlies the earlier sandbodies, and can be up to 40 feet (12 m) thick. In such cases, the unit may be bioturbated (Plate VIIA and B), or weakly bioturbated with subordinate very fine to fine grained horizontal and cross-laminated sand lenses (Plate VIIC to E) which are pebbly in places (Plate VIIF). Black chert pebble beds are also concentrated in this facies in places. In some areas, these lenses are medium to coarse grained sand and are interbedded with shale laminae (Plate VIIG to I); they also display sharp contacts which appear to be erosional in places (Plates VIIF and H).

Vertical burrows are predominant. Identifiable trace fossils include: *Arenicolites* (Plate VIIA), *Zoophycus* (Plate VIIC,E), *Asterosoma?* (Plate VIIE). In

Plate VII

Viking facies sequence B: Subtidal offshore (tidal current?) sand ridges (Upper bioturbated mudstone facies).

A. Vertical burrows. Upper-bioturbated mudstone facies; Dome I.O.E. Wildunn 6-23-30-14 W4M; 3135 ft. (UE_2).

B. Intense reworking by organisms. Upper bioturbated mudstone facies; Provo Halliday 13-11-28-14 W4M; 3130 ft. (UE_0).

C. Ripple-laminated fine sand lenses; *Zoophycus* sp. (z) and vertical burrow distupting lamination. Upper bioturbated mudstone facies; Dome I.O.E. Wildunn 6-23-30-14 W4M; 3142 ft. (UE_2).

D. Preserved thinly laminated sand lenses in bioturbated mudstone facies; Imperial Armena 9-13-48-21 W4M; 3206.5 ft. (LJC_{12}).

E. Horizontal laminated sandstone lens with vertical burrow and horizontal *Zoophycus* trace fossil (z). Upper bioturbated mudstone facies; Dome I.O.E. Wildunn 6-23-30-14 W4M; 3134 ft. (UE_2).

F. Planar, low-angle cross-stratification with sharp upper and lower contacts; some pebbles on foreset bedding planes. Upper bioturbated mudstone facies; Provo Halliday 13-11-28-14 W4M; 3131 ft. (UE_2).

G. Medium to coarse grained sand lenses interbedded with shale laminae. Upper bioturbated mudstone facies; Imperial Armena 1-13-48-21 W4M; 3210 ft. (LJC_{12}).

H. Medium to coarse sand lenses interbedded with shale and/or mudstone laminae; sand lenses with sharp wavy lower and upper contacts; some vertical burrows. Upper bioturbated mudstone facies; Imperial Armena 9-13-48-21 W4M; 3220 ft. (LJC_{12}).

I. Sharp contact between medium to coarse sand lens and silty shale. Upper bioturbated mudstone facies; Imperial Armena 9-13-48-21 W4M; 3211.5 ft. (LJC_{12}).

PLATE VII

general, the degree of bioturbation varies from weak to moderate; the lower and upper parts are sandier.

Interpretation

The above facies characteristics indicate that these deposits formed from suspension settling in a predominantly low energy marine environment occasionally invaded by relatively higher energy currents capable of moving sand and gravel by traction. The herringbone-like structure indicates that these currents flowed in opposing directions at certain times, at least in some places.

Heterolithic - Facies (BII)

The bioturbated mudstone facies grades upward into the heterolithic facies. This unit varies from about 2 to 30 feet (0.6 to 10 m) in thickness, and consists of very thin to medium bedded (terminology of Ingram, 1954), sand, interbedded with thin laminae of dark shale, dark grey to maroon mudstone, and silt (Plates VIII and IX).

The sand beds are light grey, very fine to fine grained (0.12 to 0.18 mm), muddy but fairly well sorted. Matrix-framework ratio varies between 0.25 and 0.6. These sand beds rarely exceed 6 cm in thickness. Most are structureless (Plate VIII), whereas, a few are parallel to low-angle cross-laminated (Plate IXB to E). Contacts may be diffuse to irregular (Plates VIIIE and IXA) or sharp and erosional (Plates VIIID and IXE). Some sands are

Plate VIII

Viking facies sequence B: Subtidal offshore (tidal current?) sand ridges (Heterolithic facies).

A. Interlaminated fine sand and shale, burrows and mottles of sand in shale laminae. Heterolithic facies; Chevron Handhills 10-36-28-14 W4M; 3154 ft. (L_3).

B. Interlaminated fine sand and shale with indistinct boundaries due to reworking by organisms. Heterolithic facies; Chevron Handhills 10-36-28-14 W4M; 3156 ft. (L_3).

C. Interlaminated fine sand and shale; indistinct litho-boundaries, weak to moderate bioturbation. Typical Heterolithic facies; Camac Chevron Huxley 10-4-34-24 W4M; 4885 ft. (L_7).

D. Relatively thicker, parallel laminated, fine to medium sand bed with a sharp (scoured) base and diffuse top. Heterolithic facies; Chevron Handhills 10-36-28-14 W4M; 3150 ft. (L_3).

E. *Zoophycus* sp. (v) in reworked lower section of Heterolithic facies. Sand and clay laminae more completely mixed at base then at top. Chevron Handhills 10-36-28-14 W4M; 3161 ft. (L_3).

F. Interlamination of sand and mud; deep vertical burrow (*Arenicolites* sp.?). Heterolithic facies; Chevron Handhills 10-36-28-14 W4M; 3138 ft. (L_3).

PLATE VIII

Plate IX

Viking facies sequence B: Subtidal offshore (tidal current?) sand ridges (Heterolithic facies).

A. Interlaminated sandstone-mudstone-shale unit. Wavy lower and upper contacts of lower sand lens, fairly distinct. Sand mottles due to burrowing near top. Heterolithic facies; Provo Halliday 13-11-28-14 W4M; 3157 ft. (L_3).

B. Funnel-shaped trace fossil (*Rosselia* sp.?) disrupting lamination. Heterolithic facies; Provo Halliday 13-11-28-14 W4M; 3155 ft. (L_3).

C. Interlamination of fine sand and shale. Heterolithic facies; H.B. Provost 6-26-34-7W4M; 2935 ft. (B_1).

D. Interbedded fairly laminated sand and muddy shale. Bioturbation (*Chondrites*) confined more to the finer sediment. Heterolithic facies; Fina Handhills 7-22-29-14 W4M; 3073 ft. (UE_1).

E. Homogenization of sandstone and shale laminae by bioturbation. However, cross-laminated sandstone lens with sharp upper contact; upper lens with scoured basal contact. Heterolithic facies; Provo Halliday 13-11-28-14 W4M; 3065 ft. (UE_1).

PLATE IX

glauconitic (Plate IXC).

The thin suspension deposits of clay, mud and silt, or a combination of these, are rythmically interbedded with the sand beds. Generally, these laminae are less than 2 mm thick, but where a thicker bed occurs it is mainly a homogenized mixture of these sediments, due to bioturbation (Plate IXA, D and E).

Laminae of these suspension deposits, where preserved, may be irregularly distorted but continuous (Plate VIIIA, B), indistinct (Plate VIIIC), diffuse (Plate VIIID), or wavy (Plate IXA). Often, they show a dish-like structure, particularly near the lower contacts of sand beds (Plate VIIIE).

Recognizable trace fossils include horizontal (Plate VIIIE) and vertical (Plate VIIIF) burrows. Augen-like bioturbate structures filled with sand (Plates VIIIA and IXA) are common. Identifiable ichnogenera include *Rosselia* (Plate IXB) and *Chondrites* (Plate IXD). Generally, suspension sediments are more apt to be organically reworked.

In general, average quartz grain size increases upward from very fine sand at the base to fine near the top. Correspondingly, the proportion of clay, mud and silt, and the degree of bioturbation decrease upwards. Consequently, color is lighter than for the underlying bioturbated mudstone facies. In cases where the heterolithic facies is strongly bioturbated, and therefore difficult to distinguish from the underlying bioturbated mudstone, the above

characteristics were useful in differentiating the units.

Interpretation

The facies characteristics indicate a depositional environment dominated by two hydraulic regimes. A higher energy regime of traction transport and bedload deposition of sand alternated regularly with a low energy regime of suspension settling of clay, mud and silt. This depositional setting is envisaged to be broadly similar to that of the underlying bioturbated mudstone facies except that the currents which deposited the heterolithic facies attained a higher energy level, persisted for longer periods, and alternated more regularly with low energy suspension deposition than in the former case.

Cross-Stratified Sandstone Facies (BIII)

Facies BII grades imperceptibly upward into the cross-stratified sandstone facies. This unit ranges from 2 to 30 feet (0.6 to 10 m) in thickness, and consists essentially of sand, with minor clay, mud and silt laminae and lenses.

The sand beds are generally light to greenish grey, muddy with well sorted quartz grains. Measured average quartz grain size varies from fine to medium sand (0.15 to 0.3 mm), but some beds are coarser. Framework minerals are predominantly quartz and chert grains that are fairly well rounded, with minor amounts of feldspar and rock fragments. The matrix is made up of clay and silt. Matrix-framework

ratio ranges from 0.20 to 0.5. Secondary quartz overgrowths along with continuous to patchy calcite cements predominate in places.

Cross-stratified sets range from 2 cm to 45 cm in thickness. Cross-stratification varies from low-angle (Plate XA to E) to planar high angle (Plate XD); that shown in Plate XI(C,E,F) may be the "herringbone"-type. Cross-stratification set boundaries are sharp and may be erosional (Plate XIC). Some of the bedding surfaces shown in Plate XI (B to F) are probably reactivation surfaces; in (B) and (D) these surfaces are draped with a thin film of clay or carbonaceous mudstone. Low-angle cross-lamination is succeeded by ripple cross-lamination in Plate XIH.

Shale and mudstone occur occasionally as interlaminae, mostly less than 3 mm thick (Plates XII and XIII), clay clasts (Plate XA), and as drapes on foreset laminae (Plates XB to F and XIF, H and I). In some samples these clay drapes act as cleavage planes along which the forset sand laminae separate easily. Glauconite is ubiquitous and also drapes foreset laminae in places (Plates XA, and D; XIA, B, D, E, G, and H; XIIA, and E). Where glauconite grains are abundant they impart a greenish hue to the core and, in places, emphasize the stratification visually.

The facies is weakly bioturbated. Suspension sediments (Plate XIIIC) and sand beds (Plate XIIID) are alike affected by burrows which disrupt lamination. Sand mottles are common.

Plate X

Viking facies sequence B: Subtidal offshore (tidal current?) sand ridges (Cross-stratified sandstone facies).

A. Low-angle cross-stratification, glauconite (g) and shale on foreset laminae clay clasts. Cross-stratified facies; Chevron Handhills 10-36-28-14W4M; 3127 ft. (L_3).

B. Horizontal to low-angle cross-stratification, shale on foreset laminae. Cross-stratified facies; Dec Alta. CDR Huxley 6-36-34-25 W4M; 4968 ft. (L_7).

C. Horizontal to low-angle cross-stratification with shale(s) on foreset laminae. Cross-stratified facies. Camac Mavrk Husley 6-20-34-24 W4M; 4900 ft. (L_7).

D. Medium to High-angle cross-stratification, with glauconite (g) on foreset laminae. Cross-stratified facies; Imperial Dinant 16-6-48-20 W4M; 3198 ft.; (LJC_{12}).

E-F. Low-angle cross-stratification with carbonaceous mudstone on foreset laminae. Cross-stratified facies; Anglo Royalite Kroy Acadia 6-28-24-1W4M; 2521 ft.; (UE_2).

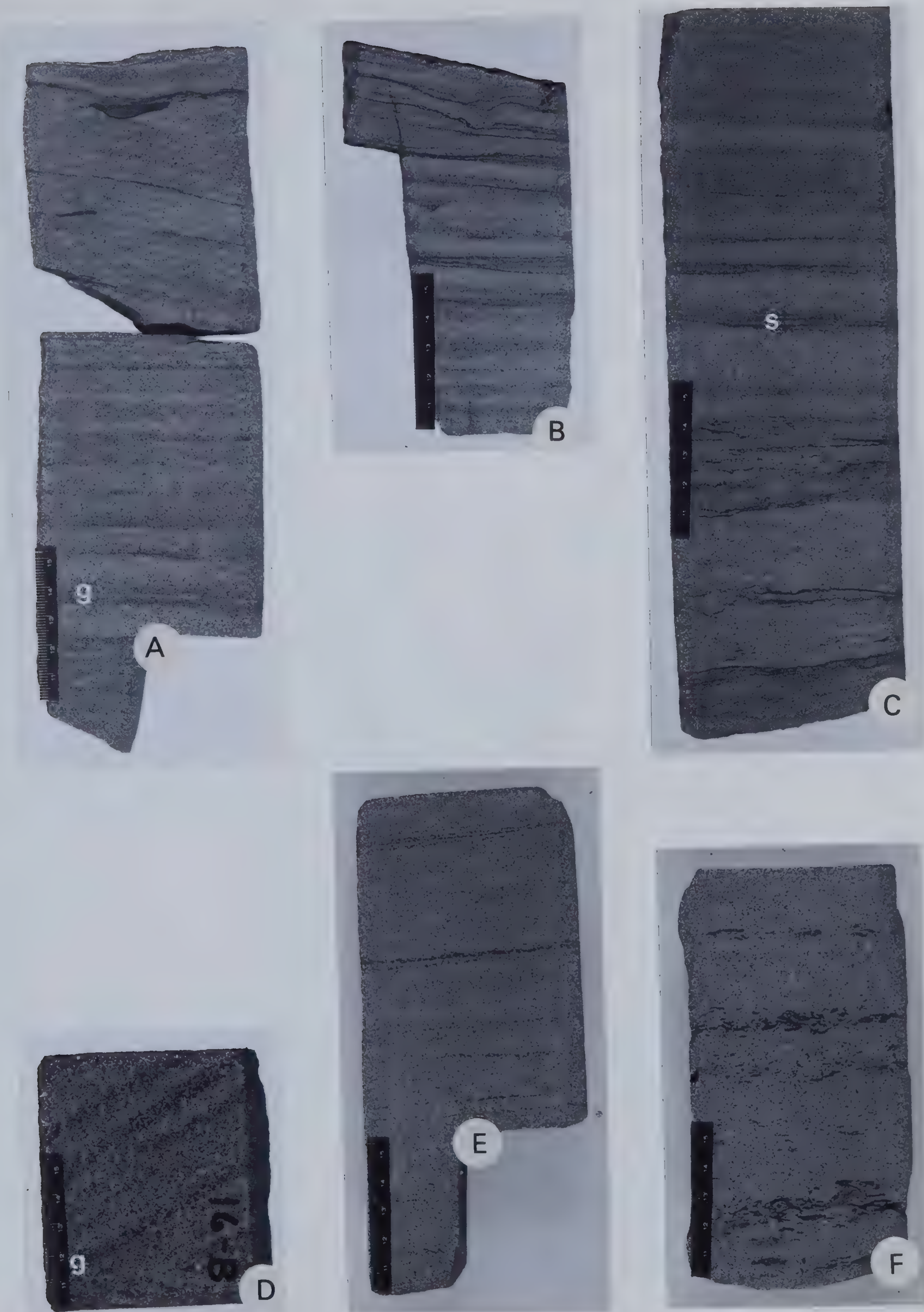

PLATE X

Plate XI

Viking facies Sequence B: Subtidal offshore
(tidal current?) sand ridges
(Cross-stratified sandstone facies).

A. Glauconite on foreset cross-laminae cross-stratified facies; H.B. Provost 6-26-34-7 W4M; 2933.5 ft. (B_1).

B. Horizontal (a) to (b) low-angle cross-lamination with carbonaceous mud drape on foreset laminae. (c) thin carbonaceous mud drape below cross-set. (d) low-angle cross-bedding, glauconite drape on foreset laminae. Cross-stratified facies; Chevron Handhills 10-36-28-14 W4M; 3132 ft. (L_3).

C. Sharp (erosive?) cross-set boundary; cross-stratified facies; Westcoast Sulpetro Smore 11-30-29-10 W4M; 2815 ft. (UE_2).

D. Boundaries of thin cross-laminated and glauconitic sets draped by thin shale laminae (s). Cross-stratified facies; Imperial Unit Johmin 10-8-48-20 W4M; 3184 ft. (LJC_{12}).

E. Herringbone-type cross-stratification with sharp set boundary. Sandstone is glauconitic. Cross-stratified facies; Imperial Armena 9-13-48-21 W4M; 3232 ft. (LJC_{12}).

F. Herringbone-type cross-stratification with sharp set boundary. Carbonaceous material on foreset laminae in upper part of upper set. Cross-stratified facies; Provo Halliday 13-11-28-14 W4M; 3064 ft. (UE_1).

G. Thin cross-laminated sets with sharp set boundaries and glauconite on some foreset laminae. Cross-stratified facies; Gulf N.C.O. Provost 12-17-36-12 W4M; 3126 ft. (L_9).

H. Low-angle cross-lamination with glauconite on foreset laminae, capped by flasered ripple cross-lamination cross-stratified facies; Chevron Handhills 10-36-28-14 W4M; 3124 ft. (L_3).

I. Low-angle cross-stratification at base is capped with low-angle cross-lamination with some carbonaceous mud drape on foreset laminae. Some weak bioturbation. Cross-stratified facies; P.C.P. and O. Acadia 11-21-26-3 W4M; 2455 ft. (UE_2).

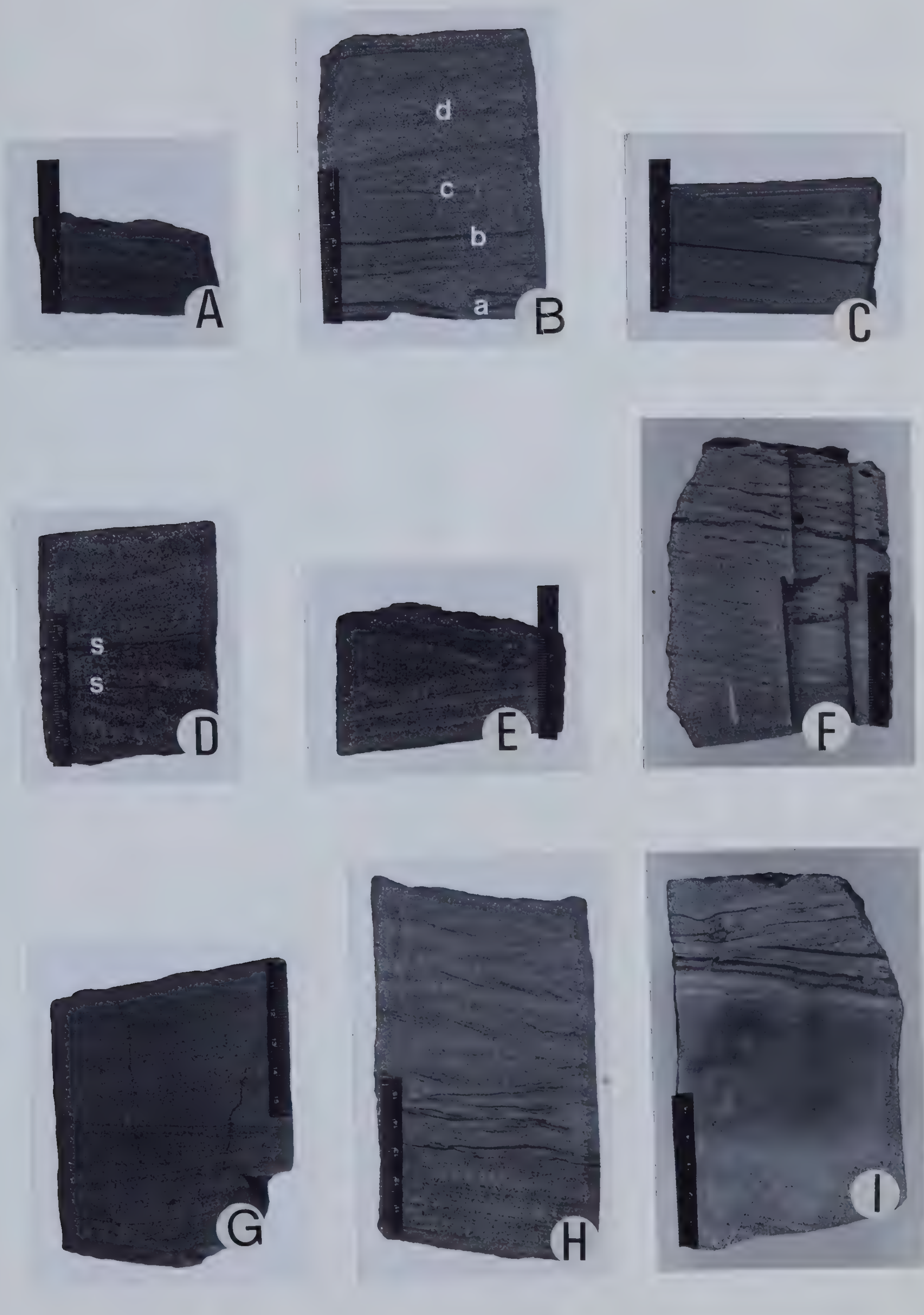

PLATE XI

Plate XII

Viking facies sequence B: Subtidal offshore
(tidal current?) sand ridges
(Cross-stratified sandstone facies).

A. Cross-stratified set boundary draped with thin shale laminae carrying mottles of sand. Cross sets are glauconitic and calcareous. Cross-stratified facies; Dome I.O.E. Wildunn 6-23-30-14 W4M; 3180 ft. (L_3-L_4 junction).

B. High angle, planar cross-stratification (r) sharply overlain by low-angle cross-stratification (bioturbated in places) (t) and draped by shale (u). Cross-stratifie facies; Chevron Handhills 10-36-28-14 W4M; 3122 ft. (L_3)

C. Interbedded sand and shale unit. Cross-stratified facie Dome I.O.E. Wildunn 6-23-10-14 W4M; 3098 ft. (UE_2).

D. Thin inter-laminated sandstone-mudstone and shale at base is bioturbated and overlain sharply by low-angle cross-laminated sand capped with dark shale on top. Cross-stratified facies; Provo Halliday 13-11-28-14 W4M; 3065 ft. (UE_1).

E. Sharply based shale laminae in glauconite cross-stratifi facies; Imperial Armena 13-19-48-20 W4M; 3235 ft. (LJC_{12}

F. Shale laminae and streak in cross-stratified facies. A few sand mottles in shale. Cross-stratified facies; Imperial Dinant 16-6-48-20 W4M; 3194 ft.; (LJC_{12}) center

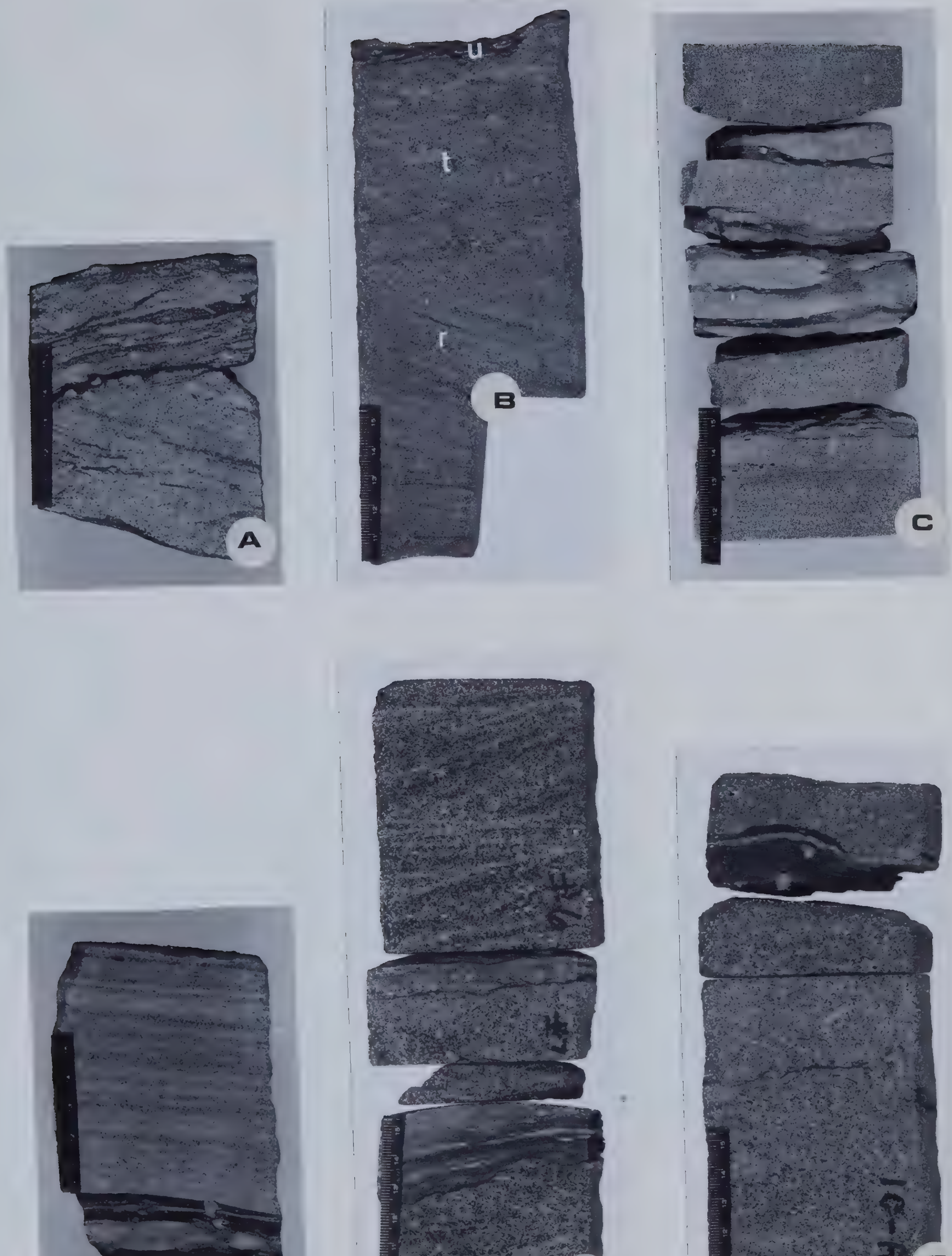

PLATE XII

Plate XIII

Viking facies sequence B: Subtidal offshore
(tidal current?) sand ridges
(Cross-stratification sandstone and Conglomerate facies)

A. Diffuse and continuous shale streaks in glauconitic sandstone; cross-stratified facies; Imperial Armena 9-13-48-21 W4M; 3231.5 ft. (LJC_{12}).

B. White, grey and black chert pebbles cross-stratified with brown mud clasts. Conglomerate facies; Camac Mavrk Huxley 6-20-34-24 W4M; 4899 ft. (L_7).

C. *Chondrite* sp. trace fossils in shale laminae. Cross-stratified facies; Chevron Handhills 10-36-28-14 W4M; 3124 ft. (L_3).

D. Vertical burrow disrupts sand and glauconite laminae; bioturbated sand-shale interlaminae near top. Cross-stratified facies; Chevron Handhills 10-36-28-14 W4M; 3118 ft. (L_3).

PLATE XIII

Generally, the textural gradient of this facies is variable. Most Basal, Lower, and Upper sandbodies show a coarsening upward textural sequence from fine at the base to medium sand at the top. Exceptions are the LJC_{12} and UE_2 units which show no preferred vertical textural gradient. Furthermore, the clay-mud content is higher in the Basal and Lower sandbodies than in the Upper sand units. Coarser sands of this facies contain a still lesser proportion of fines. Thus, the clay-mud content of the cross-stratified sandstone facies is dependent on grain size of the framework.

Tan siderite nodules and pyritic horizons are common elements of this facies.

Interpretation

The characteristics of the facies indicate that it was deposited in an environment broadly similar to that of the underlying heterolithic facies. However, the energy level was relatively higher, and traction transport-bedload deposition of sand predominated over suspension settling of clay and silt. Both depositional settings appear to have fluctuated immensely between suspension deposition and vigorous flow, and may have locally reached the upper flow regime.

Bioturbated Sand - Facies (BIV)

The just described cross-stratified facies grades upward into a bioturbated surface facies made up of bioturbated dark grey shaly sand or light grey sandstone. Where the degree of bioturbation is strong, the unit is almost structureless (Plates XIV and XV). However, with moderate bioturbation, fairly clean and well sorted, plane laminated, very fine to medium grained sand lenses with sharp bases are occasionally preserved (Plate XIVB and C). Such sand lenses may be up to 7 cm thick, and glauconitic (Plate XIVC). Generally, the quartz grain size varies between very fine and coarse sand, and occasionally small chert pebbles are dispersed in a shaly sand matrix (Plate XVB).

The very dark color of this unit is due to the presence of shale laminae originally interbedded with sand but now homogenized in places by organisms; remnants of shale laminae occur throughout the unit in most areas (Plate XIVA and B).

Most burrows are nondescript and poorly preserved. Identifiable ichnofossils are predominantly simple vertical tubes (worm?) (Plate XVC), U-shaped tubes of *Asterosoma* sp. (Plate XVD), and the funnel shaped tube of *Rosselia* sp. (Plate XIVA); the latter disrupts lamination. Sand mottles are also common. This unit may be up to 10 feet (3.0 m) thick.

Plate XIV

Viking facies sequence B: Subtidal offshore (tidal current?) sand ridges (Bioturbated Sandstone Facies).

A. Bioturbated sandstone, some burrows, wavy continuous shale streaks, and sharply based sandstone lens. Bioturbated sandstone facies; Chevron Handhills 10-36-28-14 W4M; 3112 ft. (L_3).

B. Bioturbated interlamination of sandstone and shale. Bioturbated sandstone facies; Chevron Handhills 10-36-28-14 W4M; 3119 ft. (L_3).

C. Clean, finely laminated, sharply based sand lens in bioturbated sandstone facies; Fina Handhills 7-22-29-14 W4M; 3104 ft. (L_3).

PLATE XIV

Plate XV

Viking facies sequence B: Subtidal offshore (tidal current?) sand ridges (Bioturbated Sandstone facies).

A. Sandstone and shale laminae fairly well homogenized by bioturbation. Bioturbated sandstone facies; Camac Chevron Huxley 10-4-34-24 W4M; 4868 ft. (L_7).

B. Small chert pebbles dispersed in glauconitic shaly sand by bioturbation. Bioturbated sandstone facies; Dome I.O.E. Wildunn 6-23-30-14 W4M; 3177 ft. (L_3-L_4 junction).

C. Deep burrow lined with small black chert grains. Bioturbated sandstone facies; Westcoast Sulpetro Smore 11-30-29-10W4M; 2885 ft. (L_{4a}).

D. U-shaped burrow (*Asterosoma* sp.?) and vertical tubes in Bioturbated sandstone facies; Chevron Handhills 10-36-28- W4M; 3112 ft. (L_3, back of core).

PLATE XV

Interpretation

Characteristics suggest deposition of this unit in an environment similar to that of either the heterolithic or the cross-stratified facies. However, the rate of sedimentation of the Bioturbated Sand facies may have been slower, as bioturbation kept pace with sedimentation in most areas.

Chert Pebble Conglomerate - Facies (BV)

This facies consists of varicolored light grey, brown and black chert pebbles that are fairly well rounded (Plate XVI). Plate IVE shows that the so-called 'black' chert pebbles may actually be patinated chert with an internal light grey color and an external black rind. Mud clasts are rare but occasionally encountered (Plate XIIIB). Quartzite and plagioclase feldspar (Jones, 1961), nodular phosphate clasts and phosphatized wood (Simpson, 1975), and carbonate pebbles (Boethling, 1977b) have been reported. Largest pebble diameter found in the present study is 35 mm.

The pebble conglomerate beds are mostly matrix supported (Plate XVIA). The matrix materials varies from dark mud through muddy sand to very coarse sand. Sorting is generally poor. Phenoclast supported pebbles are rare.

Most commonly, the chert pebble conglomerate beds are interbedded with shale, mudstone and siltstone (Plate XVIB). Although the pebbles may be concentrated in units up to 15 feet (4.6 m) thick, they more frequently occur in beds

Plate XVI

Viking facies sequence B: Subtidal offshore (tidal current?) sand ridges (Conglomerate facies).

A. Sequence from base:
   a) Dark fissile shale
   b) massive, grey and black chert pebbles in a poorly sorted medium to coarse grained sand matrix. Unit is inversely graded except for interruption by shale laminae (sh).
   c) Parallel laminated sand
   d) Capping of dark fissile shale (not well shown).
   Conglomerate facies; Dome I.O.E. Wildunn 6-23-30-14 W4M; 3093 - 3095 ft. (post-UE_2).

B. Chert pebble conglomerate beds with sharp contacts interbedded with sandy mudstone and interlaminae of fine sand and shale. Conglomerate facies; Provo Halliday 13-11-28-14 W4M; 3133 ft. (post L_3).

C. Light and dark chert pebbles in shaly sand capped by sandy mudstone and followed by pebbly sandstone. Conglomerate facies; Provo Halliday 13-11-28-14 W4M; 3063 ft. (UE_2).

D. Pebbly sandstone lens, with sharp contacts and concentration of pebbles at base, in moderately reworked pebbly mudstone unit. Conglomerate facies; Camac Mavrk Huxley 6-20-34-24 W4M; 4896 ft. (post L_7).

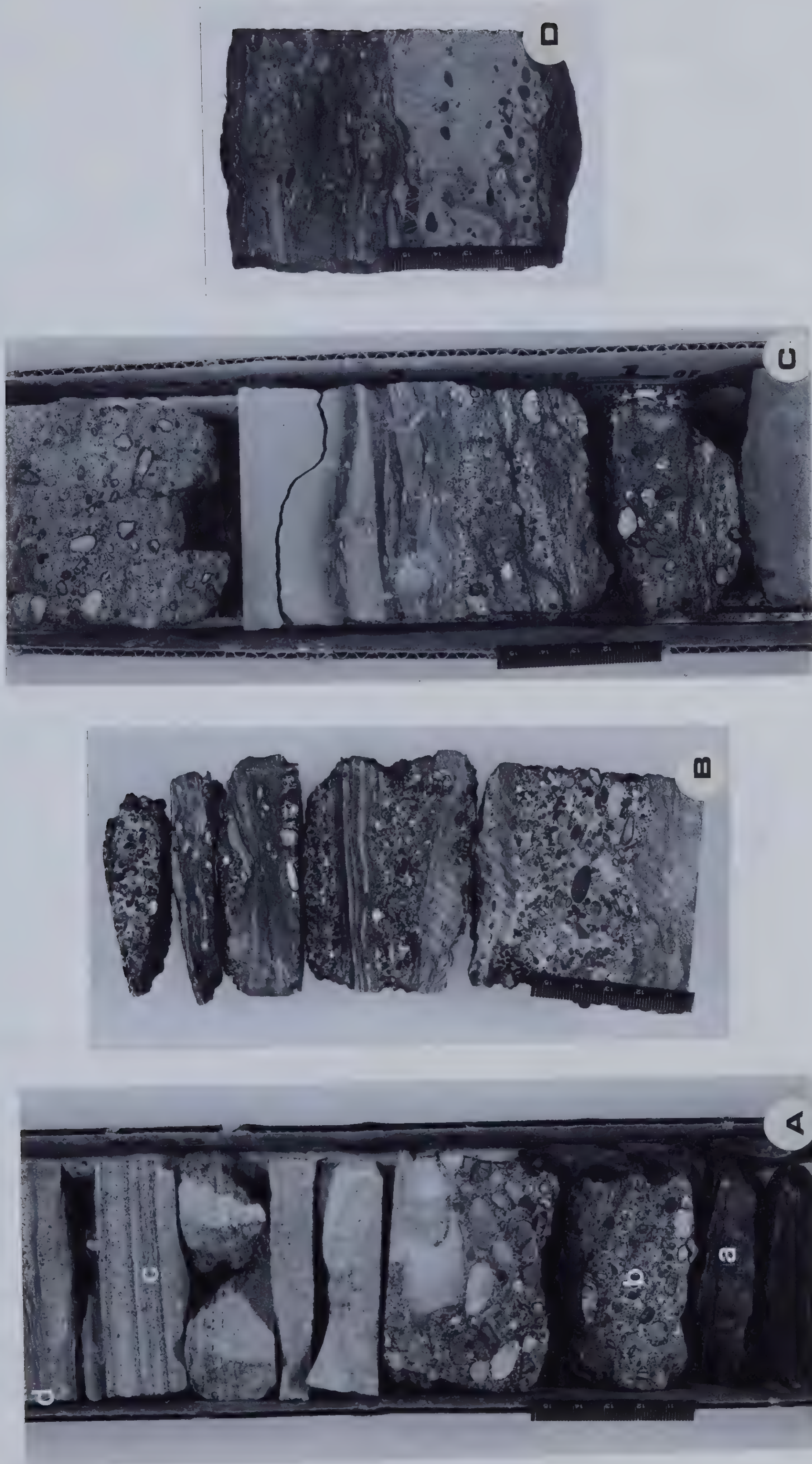

PLATE XVI

3 to 6 inches (7.5 cm to 15 cm) thick. In some places they are only pebbly sandstone beds (Plate XVIC and D), or even pebbly mudstone beds. A few are weakly stratified and bioturbated.

The thickest occurrence of this facies within the study area is in the Lower Joffre sandbodies (LJ_3) where the unit is up to 15 feet (4.6 m) thick. Jones (1961) also observed a 9 foot (3.0 m) thick conglomerate bed in well Imperial Centrefield 13-10-26-21W3M at the eastern extreme in southwest Saskatchewan. Between these areas, the observed conglomerate beds or pebbly horizons rarely exceeded 30 cm in thickness. The contacts of the thinner beds are sharp and often erosional while those of the thicker units appear gradational.

Generally, the stratigraphic position and distribution of this facies is the most variable and erratic, as it occasionally occurs in virtually all the aforementioned facies.

Interpretation

This facies was deposited by the highest energy hydraulic regime operating during Viking time. In places, however, it alternated regularly with low energy suspension deposition; in others, it appeared only sporadically and catastrophically.

Facies Relationships

A typical vertical arrangement of the facies constitutes a facies sequence model. Core data indicate that five generalized facies sequences (a to e) are recognizable in these Viking sandbodies. The most complete and typical facies sequence is 'a', represented schematically in Figure 112, and characteristic of the axes of the sand ridges. In this facies model, however, facies BIII may be wholly replaced by the conglomerate facies as in the LJ_3 unit at Joffre, or, facies I and II may be undifferentiable due to bioturbation as in the LJC_{12} unit at Joarcam, or, the sequence may in places be capped by a thin pebbly sand bed as along parts of the axis of the UE_2 sandbody of the Upper Eastern sand complex. This facies sequence is also typical of parts of the northeast flank of the thin B_1 (Hamilton Lake) reservoir sandstone.

The following vertical successions of facies were observed to be characteristic of certain ridges or parts of ridges:

1. Southwest flanks of ridges -

   $1 \longrightarrow 2 \longrightarrow 4$ (b)

   This facies sequence may, however, be capped by pebbly sandbeds or very coarse sand, especially if near swales. It is also characteristic of the axis of the thin B_1 unit.

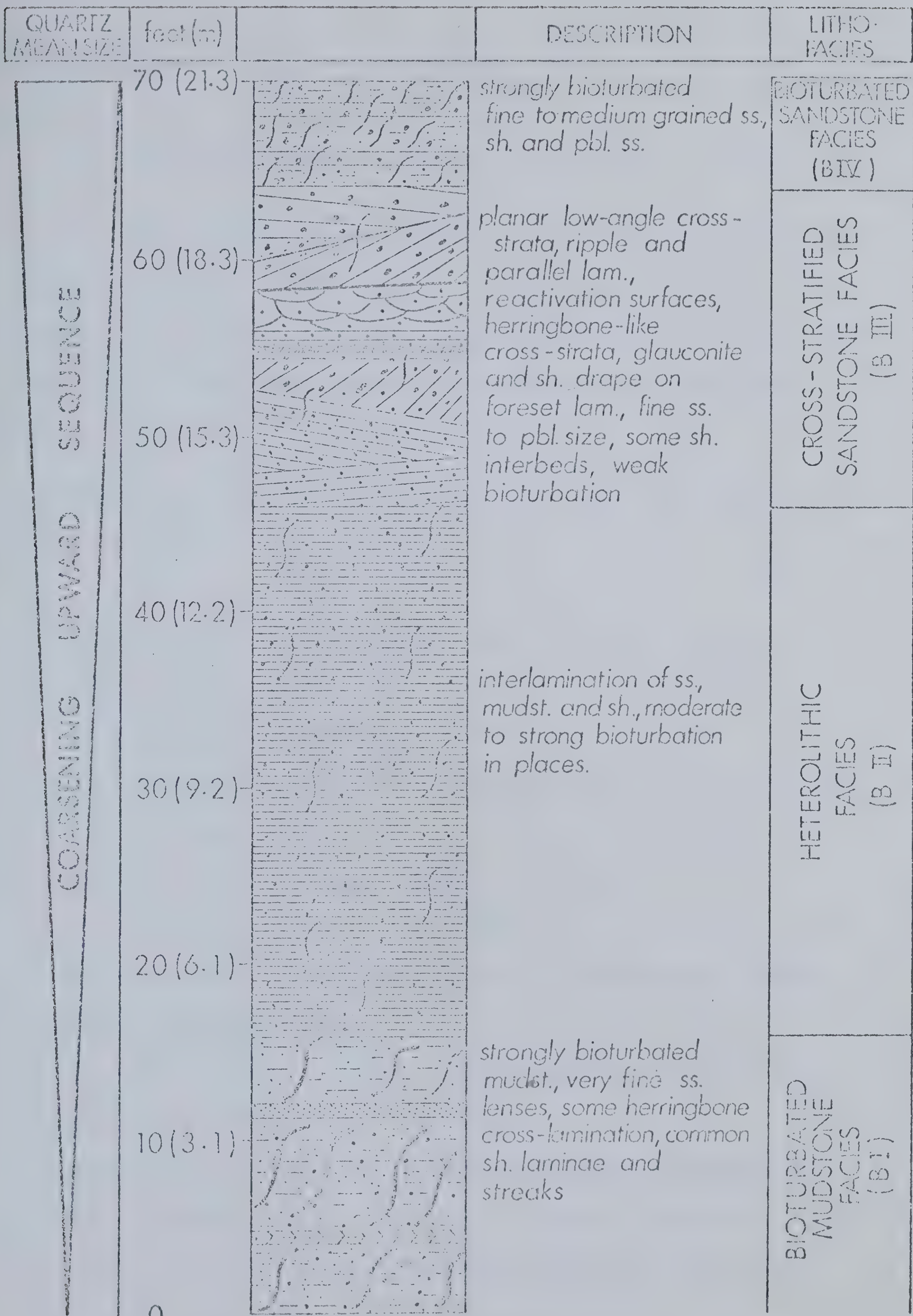

Figure 112. Typical sedimentary structures, textures, and lithologies of an offshore, subtidal, tide generated Viking sand ridge (see Appendix VI for legend).

2. Northeast flanks of ridges -

   1 ⟶ 2 ⟶ 4 ⟶ 5 (c)

   In the Joarcam area, however, subfacies 5 is absent.

The swales are not characterized by any of the above facies sequences, which appear to vary with location in the swale. In general, however, facies sequences in swales are very thin, shaly and coarser grained or even conglomeratic and bioturbated.

3. Northeast edge of the UE_2 unit of the Upper Eastern sand complex -

   5 ⟶ 4 ⟶ 2 (d)

   This fining upward sequence may also be typical of parts of the Viking sand members of the Dodsland-Hoosier-Smiley areas of southwest Saskatchewan (Evans, 1970; Reasoner and Hunt, 1954), and parts of the Provost sand units (Thomas, 1977).

4. UW_3 unit of the Upper Western complex -

   1 ⟶ 2 ⟶ 3 ⟶ 5 (e)

   This sequence lacks the Bioturbated Sandstone facies, which makes it unique.

The following observations regarding the facies sequences were made:

1. Coarsening upward facies sequences are predominant; a few, however, have no apparent textural variation (e.g., UE_2). They may be erosively or gradationally based.

2. In general, sequences exhibit marked variations in thickness and grain size distribution; however, most individual ridges are coarser to the northeast than southwest.
3. Multiple stacking of facies sequences is very common. In places, the intervening fine facies BI is absent. The vertical superposition of facies may be due to progressive and/or episodic basinal subsidence in relation to tectonism to the west and southwest of the study area.
4. Sequences may be completely bioturbated and therefore difficult to subdivide; e.g. the L4 and L9 sand units. In such cases, however, they do show the coarsening upward textural gradient.
5. Sequences are overlain either by bentonitic and conglomeratic mudstone or marine shale.
6. Missing facies in sequences are attributed to one or more of the following: bioturbation, sea floor topography, water depth and flow velocity gradient.

Photographs of some typical facies sequences are shown in Appendix Vb.

Comparison with Previous Facies Subdivisions of the Viking Sandbodies

The studies of Tizzard and Lerbekmo (1975) and Simpson (1975) are two which utilized the process-response concept for interpreting the depositional environments of the Viking sandbodies. Tizzard and Lerbekmo (1975) recognized three subfacies (Lower shoreface, Middle shoreface and

Upper shoreface-Beach) in the Suffield area of Alberta, and considered them to be similar to those of the Galveston barrier Island of Texas.

Facies BI to BIII in this text may be generally similar to their subfacies. However, detailed examination of their facies in slabbed cores indicates that their interpretation may be in doubt. Recognition of facies BIV and a comparative study of facies BI to BIII with those of the interpreted southwest barrier Island, supports the present facies interpretation rather than theirs. On the other hand, my facies subdivisions are generally fairly similar to the general facies recognized by Simpson (1975).

The gross similarity of facies sequence developments in space and time, coupled with the characteristic southwesterly direction of ridge migration and the imbricate linear arrangement pattern of these sandbodies, indicate a recurring pattern of depositional processes and responses.

C. Depositional Environments and Sediment Dispersal Mechanisms

The characteristic lithologic association, common occurrence of glauconite, moderate to very strong degree of bioturbation, presence of Ctenoid fish scales, and the foraminiferal biostratigraphy (Bullock, 1950; North and Caldwell, 1975) of the studied Viking sandbodies indicate their deposition under marine conditions. Chronologic and areal relationships with the southwestern barrier island(s)

indicate that the majority formed roughly 80 to 250 km offshore.

Relying on the principle of uniformitarianism for interpreting and reconstructing paleogeography, an attempt will be made to compare modern shelf depositional responses, whose processes are known and relatively well understood, to those of the Viking, in order to assess the most probable sediment dispersal hydraulic regime in the Lower Cretaceous Viking Sea.

Offshore sedimentary processes have been extensively reviewed by Shephard (1948), Allen (1970b), and Swift *et al.* (1971). The following four main current systems with their energy sources are recognized:

1. Turbidity currents are downslope, mostly deep sea, currents kept in motion by gravity acting on relatively small differences in density due to dispersed sediment in the fluid medium.
2. Semi-permanent or Intruding ocean currents are large scale currents, e.g. the Gulf Stream or Agulhas Current. The stress of the prevailing winds and the differences in temperature and salinity between the poles and the equator are the driving mechanisms.
3. Meteorological (wind-wave) currents embrace oscillatory motion, wave-drift, and storm surge caused by meteorological disturbances.
4. Tidal currents are produced by the attraction of the moon and sun on the surface waters of the earth.

Turbidity Currents

Beach (1955) and Roessingh (1959) advocated turbidity currents as a transport mechanism for some Viking sediments, especially the distribution of the conglomerate beds. However, the writer has seen no convincing evidence favouring this mechanism. The characteristic succession of sedimentary structures and textures typical of the classical Bouma model, and/or variations thereof, Walker (1979), were nowhere observed in the cores studied.

Semi-Permanent Currents

Known present-day semi-permanent currents are mostly either continuous (Flemming, 1978) or discontinuous (Werner and Newton, 1975) undirectional flows. In the latter case, sufficient velocity to move sediment occurs only every few years over short periods of time. Large scale meandering is common, and seasonal directional reversals are frequently experienced (Kulm *et al.*, 1975). However, where they interact with periodic counter currents or strong tidal currents (tidal range 6 m) their effects are suppressed and unimportant (Flemming, 1978).

On the narrow continental shelf of southeast Africa, Flemming (1978) noted that surface velocities of the Agulhas current reach 2.5 m/sec., and that a bedform sequence ranging from gravels to ribbons and dunes and/or sandwaves forms in response to these currents. The bedforms migrate in water depths of up to 80 m. He noted, however, that the deposits are physiographically distinct from those of the

wave dominated nearshore and inner shelf zones.

Under similar conditions, the Viking sand facies, which show repeated evidence of waning flow, could have been deposited by semi-permanent currents. However, facies III would require periodic boosting by tide and/or storm generated currents. Since these currents vary in strength normal to the flow direction and are weaker with increasing depth in the continental shelf (Banks, 1973b), facies I would reflect the deepest water, and facies III the shallowest.

In the Viking case, the semi-permanent currents could have been a southerly flowing cold boreal current, opposed perhaps by a northerly flowing warm gulfian counter current, as envisaged by Kauffman (1975) and Boethling (1977b).

Although deposits of semi-permanent currents are very poorly known, and consequently no compelling evidence in their favour is recognized here, the writer is of the opinion that they may have been a significant sediment dispersal mechanism during Viking deposition. This feeling is based on: (a) the large dimensions of the well defined Viking sandbodies and interridge swales; (b) their far offshore positions; (c) their time and spatial distribution; and (d) the uncommon occurrence of such large scale, far offshore deposits on present-day shelves which do not have such currents.

Meteorological Currents

Meteorological disturbances generate oscillatory wave motion and a variety of unidirectional currents, including wave drift, storm surge and storm generated currents.

a) Wave energy

The absence of symmetrical wave-type ripples and beach-type stratification in facies BIII coupled with the stratigraphic position of facies BIV suggest that wave activity may not have been a major sediment dispersal mechanism, at least on a regional scale in the offshore zone. Suspension deposits (clay, glauconite, and mud) in facies BIII would not likely remain in the energetic wave breaker zone. Therefore, the sandbodies are not likely to be wave generated offshore bars.

Facies BI, however, closely resembles Lower shoreface sediments of regressive shoreline sequences (e.g., barrier island). This should be expected because both shoreline and offshore massive sandbodies are shoaling geomorphic units.

b) Storm surge ebb currents

This is a large unidirectional backflow of water in a seaward direction after the passing of a storm. Present day responses to this process are characterized by graded bedding with sharp facies boundaries (Hayes, 1967; Rodolfo *et al.*, 1971; Kumar and Sanders, 1976; Morton, 1978; and Pickey *et al.*, 1978). Paleocurrent directional modes should

be directed offshore, perpendicular to shoreline (Banks, 1973b). Some ancient analogs have been reported by Brenner and Davies (1973), and Brenchley *et al.* (1979).

Although paleocurrent measurements are not normally possible on core and were not made on the Viking sandbodies, isopach-isolith maps indicate that none of the units trend perpendicular or highly oblique to the strandline except the northeast apron (UW_3) of the Upper Western sand complex and the thin Viking sandstone members of Dodsland-Hoosier area of southwest Saskatchewan. The large scale and absence of graded bedding in these units suggest that they are not genetically related to storm surge ebb currents.

The only graded deposit seen in the study area which might represent storm surge currents is shown in Plate XVIA. The unit is about 2 feet (0.6 m) thick and occurs near the base of the Lloydminster Shale, approximately 3 feet (1.0 m) above the top of the Viking Formation. Strictly speaking, this deposit may have been associated with the Lloydminster transgression rather than with Viking deposition.

Storm Generated Currents

Along the eastern seaboard of the United States, characterized by intermittent intense storms and abundant supply of sand, both small and large scale bedforms in the shoreface and inner shelf environments are responses to this process. However, the large scale ridge and swale topography

is perhaps the best studied and documented (Swift *et al.*, 1971, 1972a,b, 1973; Swift, 1974, 1975; Duane *et al.*, 1972; Stubblefield *et al.*, 1975; Swift *et al.*, 1977, 1978). The review below is based on these studies.

The sand ridges are tens of kilometres long, less than 3 km wide, about ten or more meters above adjacent swales, and spaced 2 to 5 km apart. Ridge flanks slope at a degree or less, but the seaward slope is usually steeper. Grain size ranges from fine to coarse sand (Swift *et al.*, 1973; Duane *et al.*, 1972).

Linear, and comma shaped sand ridges are common. They are nearly parallel to one another and trend either diagonally across the shelf or perpendicularly to the coast. Many are attached to the shoreface at acute angles of 20-40^{o}, opening preferentially upwind or downwind the prevalent storms. Swales or troughs separate them laterally. Migrating directions are predominantly in the downcurrent and seaward directions (Swift *et al.*, 1978; Stahl *et al.*, 1974).

The ridge and swale topography rests on a lagoonal substrate and is maintained by the present day hydraulic regime dominated by periodic southward directed unidirectional storm generated currents. Thus, fair weather and storm processes interact very intimately (Swift *et al.*, 1978; Stubblefield and Swift, 1976; Swift *et al.*, 1973).

During major storms, large scale secondary circulation develops, currents descend into the swales and scour

the bottom. Sand is shifted up ridge flanks and onto the crestal region in the form of sandwaves. Southwest advancing waves winnow fines from the crest. The net textural result is one of a coarsening upward gradient, with coarse sediment lags in the crestal zones and swales. Overall, gentle landward flanks, ridge crests and swales are coarser while finer sediments are trapped on the steeper seaward flanks of the ridges (Swift *et al.*, 1978; Stubblefield *et al.*, 1975).

Fairweather process include normal processes and less intense storms. During such storms, wave surge winnows fines from ridge crests. These are resedimented on the flanks and in the swales. Normal oscillatory wave processes may generate small scale symmetrical ripples on sandwaves, or crests of sandwaves may be bioturbated while troughs are filled with mud up to 10 cm thick (Swift *et al.*, 1978; Stubblefield *et al.*, 1975). Generally, though, fairweather processes are completely erased by subsequent storms (Pickey *et al.*, 1978).

A shoreface-connected ridge may be truncated by longshore currents at its neck, and be isolated on the shelf following a transgression (Duane *et al.*, 1972). Ridge maintenance subparallel to the strandline is due to wave processes; however, their long term effect is destructional, particularly if the ridge crest builds up above wave base, where crestal aggradation by storm flows is balanced by crestal erosion due to wave surge (Stubblefield and Swift,

1976; Stubblefield *et al.*, 1975).

Although no sedimentary facies model has been formally proposed for storm generated sand ridges, it is envisaged from the above considerations that such deposits should reflect both storm and fairweather processes. Thus, they should contain horizons of relatively coarse sand as lag, and/or cycles of finning upward textural gradients, as hypothesized by Davies (1976), due to the waning storm flow system succeeded by fairweather suspension settling of clays.

Although facies BI, BII and some occurrences of facies BV in the offshore Viking sandbodies may be responses to storm generated currents, it is felt that the characteristics of facies BIII places limits on the application of a storm generated hydraulic model to the development of these sandbodies. Suspension drapes (clay, mud, glauconite) on foreset laminae, herringbone cross-stratification and discontinuity or reactivation surfaces described in facies BIII are often associated with tidal deposits (Klein, 1977). In general, however, cross-stratification resulting from storm and tide generated currents are difficult to distinguish (Walker, 1979). Hummocky cross-stratification (Walker, 1979) was not recognized, but even if present would not be easily recognized in core. This structure appears to be the response to storm waves below normal wave base. Its absence might suggest that storms did not represent the major transport process. The general absence of coarse sediment lags in these ridges also argues against an interpretation of

major influence by storms on the sedimentary record. Furthermore, the ridge and swale topography of the West Atlantic shelf rests on lagoonal substrates and is intimately associated with the nearshore zone and the Pleistocene rise in sea level. The offshore Viking sandbodies, on the other hand, were generated up to 250 km offshore (Evans, 1970; Boethling, 1977b), and rest on the marine Joli Fou Shales, the upper part of which has been demonstrated to be scoured and possibly physically reworked in places.

It is difficult to dismiss storm generated currents as a possible major regional Viking sediment dispersal mechanism; the writer believes that they may have been important in the development of the northeast apron (UW_3) of the Upper Western nearshore sandstone complex.

Tidal Currents

Although tide generated mud, silt and sand ridges have been noted by Off (1963) on a significant portion of the world's continental shelves and marginal environements, the tidal sand ridges of the North Sea are the best understood, and have been described by Stride (1963), Jones *et al.* (1965), Harvey (1965), Belderson and Stride (1966), Robinson (1966), Houbolt (1968), Kenyon (1970), Kenyon and Stride (1970), Caston and Stride (1970), MaCave (1970, 1971, 1979), Terwindt (1971), Stride and Chesterman (1973), and Kenyon and Belderson (1973). The brief review which follows draws mainly from these works.

The North Sea tidal sand ridges are up to 65 km long, 10 to 40 m high, 1 to 5 km wide, and are spaced 1 to 9 km apart. They are predominantly linear, but S-shaped and other curved ridges occur in places. Topographically symmetric and asymmetric sand ridges are both common, but the latter are predominant and are characterized by a steeper offshore slope (1^{o} to 4^{o}). While most adjacent ridges show a strong degree of parallelism, others are connected in a complicated pattern.

The sand ridges occur offshore as far as 120 km. Water depth ranges from 16 m to 6o m, but most commonly is near 30 m. Ridge crests reach into the zone of normal wave base and are, therefore, exposed to nearly continuous wave action.

Inter-ridge channels (swales) are 27 to 42 m deep, but their western sides are generally deeper; width varies from 1 to 9 km. Nearshore swales are wedge shaped, and "interfingering" is common; offshore, they are usually devoid of transverse obstructions. In general, the channels parallel ridge trend.

These North Sea sand ridges are large scale mobile bedforms in dynamic equilibrium with the present day hydraulic regime dominated by diurnal and semi-diurnal rectilinear and partially rotary tidal flow. The ebb and flood currents, which flow in opposite directions, follow separate but well defined paths in the interridge channels (Caston and Stride, 1970). These currents drive sandwaves and ripples along the channels and deflect them upslope with crests aligned normal

to the main current flow direction. These bedforms finally converge on the crestline of the ridges, which is periodically affected by wave processes.

Where the ridge is asymmetric (e.g., Wells Bank) due to the dominance of the ebb flow, more sandwaves are driven up the gentle landward flank and over the crest, to be deposited on the steep offshore slope. Waves also move sand periodically from the ridge crest and this is resedimented on the steeper slope. Sand is also believed to circulate around the ridge under the influence of what Houbolt (1968) thought to be a helical secondary flow structure. (McCave (1979), however, observed that tidal current directions do not conform to this flow pattern but agree with the pattern expected for Ekman veering.) In this manner, vertical and lateral ridge growth is accomplished, and ridge asymmetry is continuously perpetuated (Stride, 1963; Houbolt, 1968; and Caston, 1972). Caston (1972) suggested that as the sand ridges migrate, they should tend to merge into sinuous bars and finally into a sheet-like sandbody.

Like their storm generated counterparts, not much is known about the internal characteristics of these sandwaves except for the following observations of Houbolt (1968) from cores. The sands are clean, well sorted, and show no vertical textural gradient. Fine grained sand occurs on the slopes while coarser sand and gravel occur in swales. Occasionally small pebbles, some up to 1 cm in diameter, are scattered here and there within some sand

ridges (West Dyck and Outer Gabbard). In parts of the steep slope of the Well Bank, short clay laminae drape foreset beds. He interpreted these clay laminae to represent suspension deposits during slack or high water of a tidal cycle. Absence of internal structures, erratic foreset bedding directions, and herringbone cross-stratification characterize different parts of this sand ridge. Generally the sand ridges rest on a thin pebble lag deposit.

Based on the asymmetry of Well Bank, and the sand transport and grain distribution patterns, Houbolt (1968, p. 257) proposed a hypothetical model consisting of offshore dipping thick sets of cross strata for this ridge.

In the absence of a diagnostic facies model for these tidal ridges, Klein (1977, p. 94, Figure 80) proposed an integrated hypothetical model for the vertical sequence of preserved coalescing, subtidal, tide-dominated sandbodies, based on the works of Reineck (1963), Houbolt (1968), Evans (1970), McCave (1971), and Caston (1972). He characterized each sand ridge with three subfacies, thus:

1. A basal thick cross-bedded subunit overlain by
2. A reworked thin cross-bedded subunit capped by
3. A thin clay drape.

Walker (1979), however, suggests that the internal structure of tidal sand ridges should be complex medium scale cross-beds with sets less than 1 m thick, based on the gentle dip (5^{o}) of the steep face and types of bedforms (sandwaves and ripples) on ridges. The writer is in agreement with this suggestion based on the

observations made in this study.

The foregoing indicate the general poor state of our knowledge on the internal attributes of these shelf tidal current response deposits. In general, however, tidal current generated deposits should be expected to reflect tidal characteristics, at least to some extent, irrespective of the depositional setting. Tidal characteristics are best documented in intertidal sandbodies (Klein, 1970a, 1970b, 1977). Tidal current bedload transport with bipolar or bimodal reversals of flow direction is reflected in sharp boundaries between sets of cross-strata, and herringbone cross-stratification. Reactivation surfaces reflect time-velocity asymmetry of tidal current traction transports. Although they are to be expected in tidal deposits, they are by no means confined to them (Collinson, 1970; McCabe and Jones, 1977). Alternation of tidal current bedload transport with suspension deposition during slack water periods is reflected in flaser bedding, cross-stratification with clay-mud drapes on foreset laminae, and tidal bedding (alternation of thin sandbeds with thin clay and/or mud laminae). Mud chips, shell lag, and intraformational conglomerates reflect tidal scour.

However, the occurrence of these sedimentary structures and features in facies BIII of Sequence B in the Viking sandbodies may indicate their genesis in a subtidal, tide-dominated offshore hydraulic regime.

Under this interpretation, facies BI and BII would represent deposits of waning tidal currents. The very fine to fine sand laminae and lenses in facies BI would reflect periodic influx of relatively coarser sediments into an area dominated by suspension deposition. Although it is tempting to interpret them as responses to storms (Simpson, 1975), the absences of grading (Kumar and Sanders, 1976), escape burrows (Reineck and Singh, 1975); restriction of bioturbation to the upper part (Chamberlain, 1978), and symmetrical wave ripples (Johnson, 1977), which are storm indicators, argue against a storm origin for these sand laminae and lenses. Goldring and Bridges (1973) believe such beds could equally be formed by turbidity currents, tsunamis and tidal currents. Although the role of storms cannot be overlooked, the writer feels that these features seen in Viking sands may be responses to spring tides alone. Alternatively, semi-permanent currents, and/or wave input from storms and/or earthquakes may enhance tides to cause short-lived periods of very strong currents. Johnson and Stride (1966) noted that when storms enhance spring tides, one hundred times more sediment is transported than during neap tides in fair weather. Thus, each of the sand beds in facies BI is thought to represent a single tidal event in the manner envisaged by Stride (1965). The occurrence of glauconitic herringbone cross-stratification with a thin clay drape between cross-stratified sets in this facies strengthens the tidal origin interpretation for these sand layers. Singh

(1969) believes this type of herringbone cross-stratification to be fairly diagnostic of tidal currents.

The interstratification of suspension and traction deposits in facies BII indicates that sand was transported periodically, probably as thin sheets. Clay, mud and silt were deposited during periods of low velocity and/or non-existent flow which would be at either low or high water slack periods of a tidal cycle. Re-establishment of biologic activity, plus the variability in thickness of the suspension deposits, indicates that low energy conditions must have lasted longer at times. Muddy deposits may also be due to lack of availalbe sand. On the other hand, traction transport and bedload deposition would occur during higher velocity phases of the tidal cycle. Tidal bedload and suspension depositional models have been described by Reineck (1963) and Klein (1977).

The characteristic and rather complex superposition of low to high angle, medium scale cross-stratification (some of which is herringbone-like), the common occurrence of sharp discontinuity surfaces (some draped by carbonaceous mud film), clay glauconite as drapes on foreset laminae, and mud clasts, all of which typify facies BIII (Cross-stratified sandstone facies) suggest tidal currents moving sand, and occasionally pebbles, in the form of dunes and/or sandwaves. The presence of ripple lamination in this facies indicates that at times sand was moved in the form of ripples. Mudclasts may be indicative of tidal scour. The marked textural variation of this facies from fine sand to pebbles

shows that the tidal velocity fluctuated greatly; however, availability of sediment sizes may have played a part in the final size distribution pattern. Organisms tolerant to relatively high energy levels probably produced the disruptive burrows of this facies.

The position of facies BIV in the sequence suggests that for those sand ridges without overlying sand units (e.g., UE_2), it may be the organically reworked surface of the tidal sand ridge. After formation of some of the ridges, benthonic organisms recolonized the substrate and reworked the surface of the stagnated sand ridge. For those ridges overlain by another sandstone unit(s) facies BIV may represent the basal part of some swale deposits. If these interpretations are correct, the absence of wave-formed structures in facies BIII, the common occurrence but varying degrees of bioturbation in all the facies, and the terminal position of facies BIV, may indicate that these offshore Viking sandbodies, especially those of the Basal and Lower chrono-intervals, formed below normal effective wave base. The common occurrence of primary glauconite in these sands suggests water depths between 30 to 2000 m (Porrenga, 1967).

Where sandbodies are vertically stacked in imbricate fashion, the intercalated moderately bioturbated mudstone interval represents facies BI of the overlying sandbody. In other areas, particularly near the Upper Western sand complex, the mudstone interval above the L_6 and L_7 ridges is predominantly the offshore mudstone facies of the

northeasterly prograding Upper Western sand complex. In some other areas (e.g., Joffre, Joarcam) the overlying mudstone is transitional into the deeper water facies of the Lloydminster Shale transgression.

The four gradational facies (BI to BIV) are thought to reflect different parts of a tidal current velocity gradient such as described and mapped by Stride (1963) and Belderson and Stride (1966), and applied to coarsening upward textural gradients of ancient subtidal tidal current sandstone ridges by (Banks, 1973b; Anderton, 1976). In this model facies BI would represent the lowest energy medium, characterized by suspension deposition and sand patches. Facies BII would represent the zone of continuous sand and muddy sand; and facies BIII, the zone of moving sandwaves. The position of the transitory sand ribbon zone is occupied by facies BIV. Facies BV may represent the zone of erosion. Bank (1973b) suggested that the zone of erosion may not exist if there is abundant coarse sediment available.

The gradual lateral displacement of facies down sediment transport paths under conditions of net deposition may explain the predominant coarsening upward textural gradient of these sandbodies. Although a coarsening upward sequence is commonly related to shallowing of the sea, Johnson and Belderson (1969) suggest this need not be a function of depth, as it could occur under constant water depth conditions, especially in tide-dominated shelf environments. Thus, these sandbodies may have formed under

either fairly constant or shallowing depths.

The sharp lower contacts of the Viking, and the thin Upper Joli Fou sections beneath the Viking in places, may reflect tidal scours after Joli Fou deposition and before or during Viking deposition. Tidal currents are known to scour the seabed in up to 600 feet (180 m) of water depth (Cartwright and Stride, 1958; Stride, 1963; Harvey, 1965). The filling of such scours is likely to have produced the fining upward textural gradient observed in the Provost area and along the northeast edge of the UE_2 unit.

The morphology of these sandbodies (which may have been similar to present day ridge and swale topography) suggests that the tidal current transport paths were along the swales. The presence of coarser sands in some of the swales studied, and the topographic control on the distribution of some of the pebble beds support this interpretation.

The characteristic asymmetry of most ridges, which is consistent with the direction of ridge migration, and the lateral textural gradients (in the places studied) indicate that one of the tidal phases (ebb or flood) was dominant. A similar consistency between texture, ridge asymmetry, direction of ridge migration and the dominance of the ebb tidal currents, was observed by Caston and Stride (1970) and Houbolt (1968) for some of the Norfolk tidal sand ridges of the southern North Sea. The Viking sandbodies may have been subjected to the same type of sand transport and

grain circulation patterns described for the North Sea tidal ridges.

The probable syndepositional modifications of the L_2, L_3-L_4, L_5, UE_2 and the LJC_5-LJC_{12} ridges may have been partly accomplished by impinging tidal currents in a manner fairly similar to the growth and development stage models of the North Sea linear sandbeds proposed by Caston (1972). He suggested further that migration of the Norfolk tidal ridges would result in their merging into sinuous bars and finally into a sheet-like body. Thus Klein (1977) hypothesized that the internal anatomy of such a sand sheet complex should show a series of imbricated sandbodies similar to those described by Evans (1970). The Viking imbricate depositional patterns discussed earlier herein are generally similar to those of Evans (1970), for which a tidal origin is being advocated.

Other Evidence Favouring Tidal Origin

1. The association of an ebb tidal delta, fairly large tidal inlets?, an extensive mixed tidal mudflat and tidal creek channel facies with the Viking barrier island suggests at least a meso-tidal (2 to 4 m tidal range)(Davis, 1964; Hayes, 1976) Viking coast pervaded by wave and tidal current processes. Although macro-tidal (> 4 m tidal range) coastline barrier islands are rare (Hayes, 1976) 10% of the world's (poorly understood) barrier islands exist in such settings (Glaeser, 1978). Therefore, Viking

coastline may have been characterized by macro-tidal range.

2. Facies BI to BIII have many features in common with some other ancient sandbodies of inferred tidal current origin, such as: the Lower Cambrian Duolbasgaissa Formation of northern Norway (Banks, 1973b); the Late Precambrian Jura Quartzite of Scotland (Anderton, 1976); the Late Precambrian Upper Quartzitic Sandstone member of north Norway described by Hobday and Reading (1972) and re-interpreted by Johnson (1977). These outcrop studies relied heavily on facies analyses, but more on paleocurrent patterns in their interpretations. Examples from the Cretaceous Interior Seaway include the Upper Cretaceous (Santonian) Shannon Sandstone in the Powder River Basin of Wyoming (Spearing, 1976; and Seeling, 1979); the Upper Cretaceous (Campanian) Sussex Sandstone of Wyoming (Berg, 1975; Klein, 1977; Brenner, 1978). However, elements of storm-generated currents were incorporated in some interpretations. In general, only Brenner (1978) recognized the surface bioturbated sandstone facies BIV.

3. Klein and Ryer (1978) suggested that the Cretaceous Interior seaway was characterized by exceedingly high velocity tidal currents, based on sedimentologic and paleontologic lines of evidence. They used the positive correlation between shelf width, tidal range, and tidal current velocity on Holocene continental shelves to

strengthen their interpretation, as the widest shelves are characterized by the greatest tidal ranges and current velocities. This correlation has been tested by Cram (1979) and found to be correct. Paleogeographic reconstruction (Figure 4) indicates that the width of the Lower Cretaceous (Viking) epeiric sea may have been in excess of 300 km. It therefore seems reasonable that the Viking Sea would have been characterized by a high tidal range.

4. Johnson and Belderson (1969) suggested that shallow epicontinental seas open to an ocean or oceans will most likely be strongly influenced by tidal currents. They reasoned that if the independent tides of such a sea are negligible, changes in the configuration of the basin, particularly those caused by major diastrophism and/or continental drift will produce greatly magnified co-oscillating tides from the well developed external (oceanic) tides. The Viking Sea fits very well into the above geologic setting. Tidal exchanges are likely to have occurred between the Viking Sea and the northern Boreal and/or the southern Gulfian oceans in the manner postulated by Kauffman (1975). The many occurrences of bentonite beds in the Formation is indicative of volcanism, possibly related to plutonic-diastrophic activities in the Cordillera at about this time (Rudkin, 1964). These in turn may have been due to subduction of the Pacific Plate beneath the North American continent

(Figure 3).

The combination of a very wide epeiric Viking sea, connections with the Boreal and/or Gulfian oceans, and Cordilleran diastrophism are appealing lines of evidence in favour of high velocity tidal currents during Viking deposition. The results of the present study are in harmony with this tenet.

Viking Sand Members of the Dodsland-Hoosier-Smiley Areas of Southwest Saskatchewan

Evans (1970) attributed the deposition of these thin sand units to east flowing tidal currents, mainly on the basis of the following characteristics:

1. Interbedding of bedload and suspension deposits (clay, mud, sand and pebbles) supposedly laid down during high and low energy phases of a tidal cycle.
2. An unusual WSW-ENE trend which is nearly perpendicular to the normal NW/SE trend of the Viking sandbodies covered in this study.
3. The imbricate pattern of arrangement, with younger units progressively displaced southwards.

He also assumed the following:

1. That the Viking Sandstone is a clastic wedge; hence he lumped the Hamilton Lake (B_1), Provost and parts of the Lower sand and Upper Eastern sand complexes together (see his Figure I);
2. The clastic wedge thins and fines to the northeast and east;

3. The sandbodies are shoreline and offshore bars which represent successive Viking shoreline deposits, and the northeast limit of the seaward advance of the clastic wedge was just south of the Dodsland-Hoosier area.

The paleogeographic picture that comes to mind is that of a regressive Viking clastic wedge, or successively younger clastic wedges prograding to the northeast and east, just up to the Dodsland-Hoosier area. East flowing tidal currents generated the WSW-ENE trending and southerly imbricating thin sand units immediately seaward of the regressive clastic wedge. This was depicted by Simpson (1975, Figure 4C and E, p. 567). The most obvious stratigraphic implications of this paleogeographic model are:

1. These tidal current sandbodies should be stratigraphically younger and higher in the section;
2. The depositional strike of the tidal sand ridge should be parallel to that of the regressive clastic wedge and more importantly, their directions of migration should be opposed.

The results of the present study, as earlier discussed, constrast markedly to Evans' paleogeographic assumptions and the implications therefrom regarding the expected stratigraphic relationships of his sand members to the so-called regressive Viking clastic wedge. Thus, weaknesses in his paleogeographic picture make aspects of his environmental interpretation vulnerable because the latter leans heavily on the former. Moreover, the imbricated pattern of these sand members is more complex than portrayed, especially

south of Township 30. Also, the WSW-ENE trend of the axes of maximum thickness development of his members (see his Figure 13) changes gradually but systematically with time, becoming nearly NW/SE for the youngest shaly 'K' member. This member was shown in the present study to overlap the thin northeast edge of the UE_2 sandbody. When these observations are integrated with the time-relations of the thin sand members to the UE_2 sandbody, it appears to the writer that the former thin units were being driven in a southerly direction, probably destined to be accreted onto the UE_2 sandbody.

If this interpretation is further coupled with the configuration of these thin sand members in stratigraphic cross-sections, which compares favourably with the hypothetical sandwave slope facies (C) in the model of Nio (1976), the writer wonders whether these sand units did not indeed comprise an offshore sandwave field. This interpretation would go a long way toward explaining the systematic change in their axial trend with time, the overlap relationship with the UE_2 sandbody, the multiple axial characteristics of members, the typical erratic thinning and thickening, the characteristic flattening and broadening exhibited by members in an easterly direction, and the southerly complicated imbricated pattern of arrangement of these sand units.

Tide generated sandwave fields with heights up to 15 m and more are common on most present-day continental

shelves (Off, 1962). They may be isolated, as in the Taiwan strait (Bogg, 1974) and the Irish sea (Harvey, 1965), or occur adjacent to tidal sand ridges, as near the Le Chapelle bank off the west coast of France (Cartwright and Stride, 1958), and the tidal sand ridges of the southern North Sea (McCave, 1971; and Terwindt, 1971). The latter field is more than 200 km long. The depth of water in which sandwaves occur may reach 200 m (Cartwright and Stride, 1958; Harvey, 1965). Gravel, granules and shell fragments have been reported in sandwave troughs (Carruther, 1963; Drapeau, 1970).

Although not enough is known about the geometry and internal anatomy of sandwaves to arrive at reliable conclusions regarding possible ancient analogs, the writer believes that the possibility of the rather anamolously oriented Dodsland-Hoosier thin sand members being a tidal sandwave field associated with the tidal sand ridges previously described and interpreted in this study should be seriously considered.

D. Conclusions

Although storm and tide generated currents are contrasting hydraulic regimes, the present level of our knowledge of these processes indicates that their sedimentary responses are very similar. Thus, there seems to be no unequivocal evidence at present in favour of the development of the offshore Viking sandbodies by the one mechanism as

opposed to the other. However, the characteristics of facies BIII, the stratigraphic position of facies BIV, the time and spatial relations of the sandbodies, coupled with the meso tidal coastal barrier island and the distance of occurrence offshore are features that appear most compatible with a tidal current hydraulic regime, and therefore most appealing to the writer.

Deposition of these offshore sandbodies probably occurred mostly below normal wave-base in a subtidal tide-dominated offshore environment in a manner fairly similar to that of the present-day tidal sand ridges of the southern North Sea, which is characterized by a rectilinear tidal current flow system and storms. During Viking deposition, however, the tidal currents may have been boosted periodically by semi-permanent currents, as well as storms. The thin sand members of the Dodsland-Hoosier areas of southwest Saskatchewan may represent a far from shore tide-generated sandwave field. In general, the offshore environmental setting was distinct and separate from the wave and/or storm dominated shore and nearshore barrier island depositional environments.

CHAPTER X

PALEOGEOGRAPHY AND HYDROCARBON DISTRIBUTION

A. Paleogeography

The Foothills region of Alberta has generally been regarded as the major sediment source-area for the Viking Formation (Rudkin, 1964). Sediment contributions from the Precambrian Shield to the northeast was minimal.

More specific locations and stratigraphic positions of the source area(s) were indicated by Stelck (1958, 1975). He suggested that the Viking is equivalent to part of an erosional hiatus between the following successions in the Foothills of Alberta and northeastern British Columbia:

1. Lower and Upper Blairmore Formation of the southern Alberta Foothills;
2. Mountain Park and Blackstone Formations of the central western Alberta Foothills;
3. Cadotte and Paddy Members of the Peace River Formation of the Peace River area; the latter member represents in part the shoreline facies of the Joli Fou and Viking Formations;
4. Within the Hasler Shale and the Buckinghorse Formation of northeast British Columbia. Stelck believes that the regional hiatus provided a proximate and adequate source for the Viking sediments, which were deposited during

a temporary still-stand of the *Haplophragmoides gigas* (Joli Fou) sea.

In the Peace River area where much work on the Lower Cretaceous formations has been carried out, the Cadotte-Paddy-Viking relationship has been supported by Oliver (1960), May (1967), and Koke (1979). The latest worker used the distribution of *Haplophragmoides gigas* to suggest that the Peace River Arch was expressed as a peninsula at that time. If this interpretation is correct, the adjacent Hasler (north) and Joli Fou (south) embayments would have been favourable sites for tide-dominated and/or balanced deltas. The 'Lower Viking' delta northeast of the present Jasper National Park area may be of either type according to Amoco (1976). Stelck (personal communication, 1979) is in agreement with the presence of a delta in this area during Viking deposition.

Although no similarly detailed studies have been conducted in southern or southwestern Alberta, the writer is of the opinion that another, perhaps somewhat later, major source may have been located in this region. This would help to explain the restricted deposition of Upper Viking sandbodies (UE) around the southern border between Alberta and Saskatchewan and into southwest Saskatchewan. Thus, two major Viking source areas may have been located in southern and western central Alberta. This interpretation appears consistent with the thickest Lower Colorado deltaic sandstone developments being in the Grande Prairie-Peace River-

northeastern British Columbia region; and near the Alberta-Saskatchewan-Montana boundaries (Figure 5). The apparent restricted occurrence of thickest known chert pebble conglomerate beds in the Joffre-Gilbey (Twp. 39, Rge. 26W4M) and southwestern Saskatchewan (Twp. 26, Rge. 21W3M) areas, may be further evidence in support of this interpretation. If we accept a predominant western sediment-source for the Viking Formation, one must fit the opposed directions of progradation and migration deduced for the shoreline and offshore Viking sandbodies, respectively, into this setting. Two alternate explanations are advanced to explain the observed phenomena:

1. Deltas located in western central and southern Alberta may have funneled sediments offshore where they were redistributed and shaped into sand ridges by principally northwest-southeast oriented tidal current flow in a subtidal tide-dominated environment. The sediment dispersal mechanism envisaged is partially similar to that which obtains in the Yellow Sea of China (Niino and Emery, 1961) and the coast of Oregon (Schneidergger and Kulm, 1971), where rivers transport sediments into the shelf environment.
2. Some Viking sand may have been derived from deltaic deposits laid down during earlier stages of lower sea level; at least in the Peace River area where the Joli Fou equivalent is mostly missing (Stelck, 1958; Koke, 1979). These sands could have been later redistributed and reshaped by tidal currents with a rise in the sea

level, in a manner similar to the recent sands of the Flemish, Hinder, Falls, and Sandellite tidal current ridges of the southern North Sea, which were derived from Rhine River sands deposited in the area during stages of lower sea level (Houbolt, 1968).

If we regard the missing upper Joli Fou sections in the Provost (BP_1 and BP_2), Hamilton Lake (B_1), Joffre (LJ_4), Joarcam (LJC_{12}) Beaverhill Lake ($BBHL_I$ and $BBHL_{II}$) and basal part of the Upper Eastern sandstone (UE_2) area as subsea scours, then it appears reasonable to regard these sandbodies as being partly derived from reworked upper Joli Fou sediments by tidal current scouring. Depending upon the configuration of the Peace River Arch peninsula, it may have accentuated tidal current velocities, and thereby enhanced the redistribution and shaping of some of the offshore tidal current and ridges. A generalized possible paleogeographic setting is depicted in Figure 113.

Boethling (1977b) used the absence of a middle foreshore to eolian facies to suggest that Viking sandbodies were deposited in water depths ranging from 30 to 150 feet (10 to 50 m), and certainly greater than wave base. The stratigraphic position of facies IV causes the present writer to agree that most Viking sand units were probably deposited below wave base. The association of *Zoophycus*, *Rosselia* and *Terebellina* ichnofacies also probably indicate water depths in excess of 60 feet (20 m) (Chamberlain, 1978), while the ubiquitous occurrence of glauconite may suggest water depths between 30 to 2000 m (Porrenga, 1967).

The maximum northeasterly and/or easterly extent of

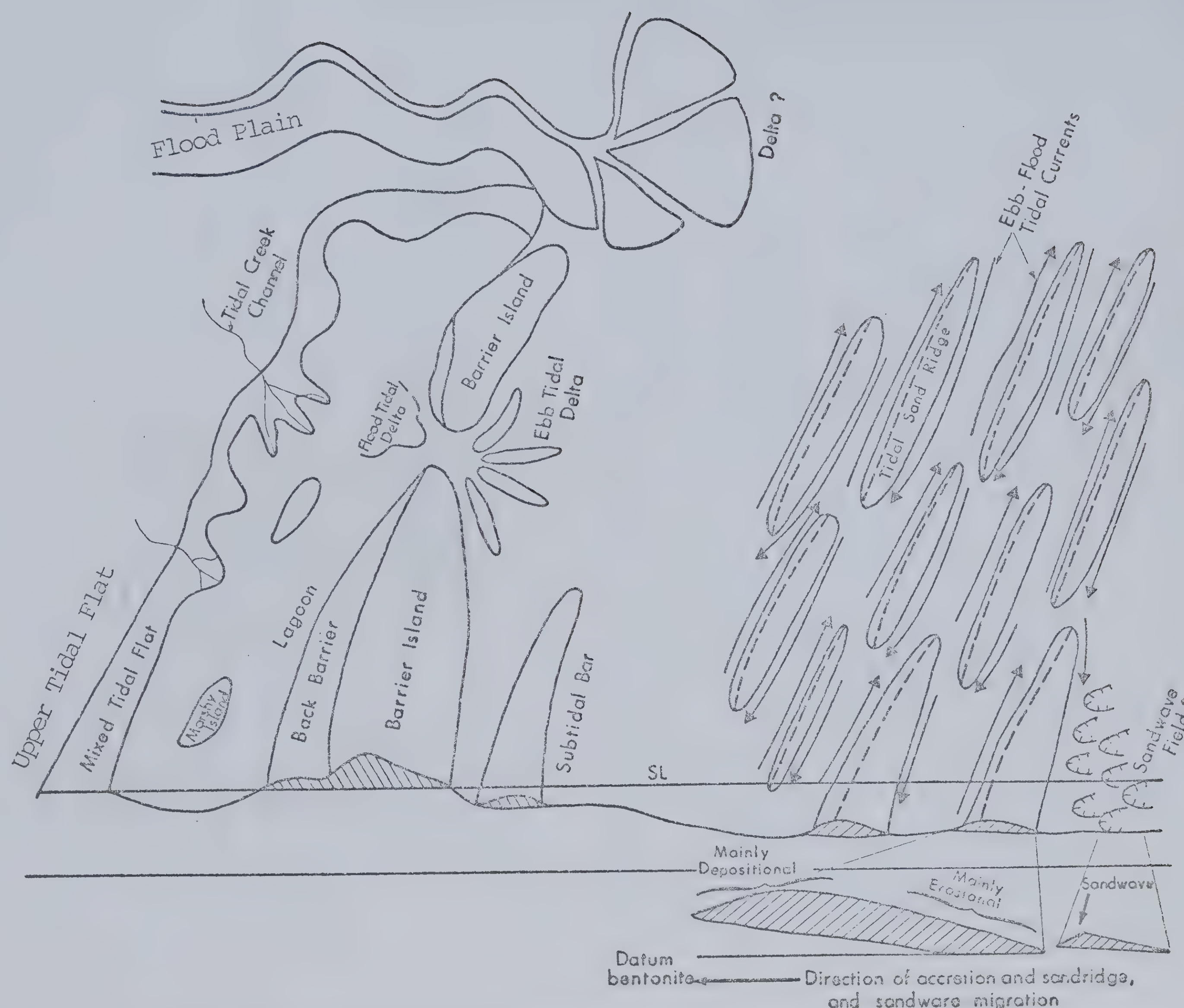

Figure 113. Schematic reconstruction of probable Viking Formation depositional milieu

the regressive Viking shoreline is roughly delimited by a northwest-southeast trending line from Township 35, Range 28 through Township 31, Range 22 and Township 28, Range 20 to Township 24, Range 18 and Township 21, Range 16 W4M. North of Township 24, this limit was reached at about the time of bentonite A. Thus, Viking deposition occurred during what was essentially a still-stand of the Joli Fou sea, as suggested by Stelck (1958). The minor regression which took place was mostly a function of coastal outbuilding (progradation). The earlier termination of Viking deposition in the northwest of the study area may mean that the *Miliammina manitobensis* (Lloydminster Shale) transgression was Boreal related. Alternatively, delta outbuilding ceased earlier in the north.

B. Relationship of Petroleum Occurrences to Stratigraphy and Depositional Environment

Some Viking sandbodies produce oil and/or gas in the study area (Figure 2). As an outcome of this study, it is possible to group some of the oil and gas occurrences in time equivalent reservoir units, and to broadly relate them to depositional milieu.

Presently known reservoirs in each chrono-interval are listed below.

<u>1. Basal reservoir units</u>: (a) Beaverhill Lake ($BBHL_I$ and $_{II}$), gas pool; (b) Donalda and Red Willow, gas

pool; (c) Hamilton Lake (B_1), oil pool; (d) Provost (BP_1, BP_2, BP_3), oil and gas pools; and (e) Dodsland-Hoosier-Smiley (M and LL), oil and gas pools, southwestern Saskatchewan.

2. Lower reservoir units: (a) Joarcam (LJC_{12}), oil and gas pools; (b) Joffre (LJ_1, LJ_2, LJ_3), oil pools; (c) Huxley (L_7), gas pool; (d) Cessford (L_1-L_2), gas pool; and (e) Sedalia-Sibbald-Oyen (UE_2), gas pools.

3. Upper reservoir units: (a) Bindloss (UE_2), gas pool; (b) Atlee-Buffalo (UE_1), gas pool; (c) Cessford (UC), oil pool; and (d) Wayne-Rosedale (UW_3), gas pool.

Generally, oil reservoirs of the Lower chrono-interval are the most economic, followed by the Basal and then the Upper chrono-units. The reverse seems true for gas distribution. However, most sand units of the Lower chrono-interval (lower Joffre and Joarcam complexes) are presently unproductive.

The far offshore sandbodies have been found to date to be more petroliferous than their shoreline and nearshore counterparts which have not been fully explored. All known oil reservoirs in the study area are believed to belong to the former depositional milieu.

In some of the discrete and fairly isolated reservoirs (e.g., Hamilton Lake (B_1), Joarcam (LJC_{12}), and Cessford (UC)), oil and/or gas are trapped up-dip at the northeasterly or easterly margins of the reservoirs

(Figure 114b). This part of the reservoirs is also relatively coarser and cleaner, probably in response to stronger current flow. Moreover, this part of the units developed early, as migration was to the southwest (Figure 114a). Thus, the trap type is combination stratigraphic-structural.

The productive multiple thin sand units (Beaverhill Lake, Joffre, Provost, Dodsland-Hoosier) most commonly occur at the northeasterly or easterly edges of complexes where units are older and relatively coarser and cleaner, as in the more discrete reservoir units. Thus, the northeastern or easterly margins of northwest-southeast trending units tend to be more favourable sites of hydrocarbon accumulation. This location appears to be more a function of depositional environment than structure, although the combination trap-type coincidentally provides an optimal situation. The shoreline and nearshore sand units and the sandbodies west of the Joarcam reservoir unit have not been intensely explored by drilling and coring.

a)

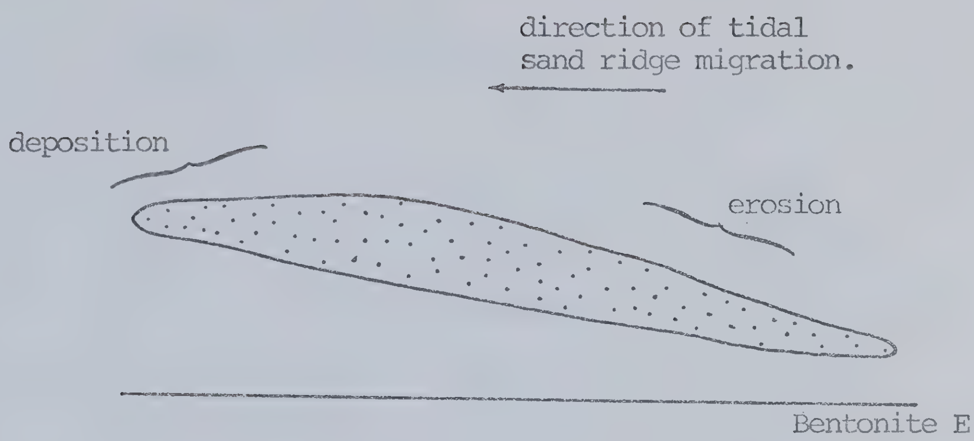

b)

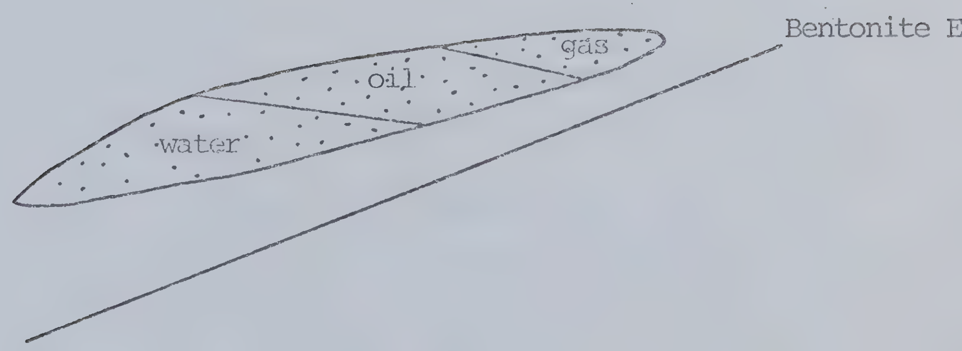

Figure 114. a) Depositional history of reservoir unit.
b) Post-depositional regional tilting and oil and gas entrapment (e.g., B_1 and LJC_{12}).

CHAPTER XI

SUMMARY AND CONCLUSIONS

An integration of core, electric well log and chemical data indicate that five (E, D, C, A, A_O) of the many bentonite beds in the Lower Cretaceous Viking Formation of southeast-central Alberta are regionally widespread. Some reached into southwestern Saskatchewan, where bentonites D and C may be, respectively, the same as the "MN" and "K" bentonitic shales of Evans (1970).

Because bentonites are excellent time horizons, and the stratigraphic positions of the ones under study range from the base to the top of the Viking, they have been used to subdivide the formation into three chrono-units. Thus, the Basal, Lower and Upper chrono-stratigraphic intervals are respectively bound by bentonites E and C, C and A, and A and A_O. This time framework facilitated the examination of the depositional development of the Viking sandbodies in time and space within each time interval through extensive utilization of stratigraphic cross-sections, isopach-isolith maps, and fence diagrams and cores. Integrated analysis of the depositional relations of the sandbodies lead to a more unified picture of the depositional pattern(s) and history of these sandbodies, as summarized below.

Following the widespread, predominantly suspension

deposition of the marine Joli Fou muds in parts of Alberta and Saskatchewan, sands of the Basal chrono-interval were laid down largely in four distinct areas, namely: Beaverhill Lake, Hamilton Lake and Provost, in Alberta and the Dodsland-Hoosier-Smiley area of southwest Saskatchewan. The characteristic multiple thin sand development of this period appears to be gradational with the underlying Joli Fou. However, localized missing section (thinned Joli Fou) at the base of the sand units suggests basal scour before and/or during Viking deposition. Some may, however, be simply areas of non-deposition. These sand units define a northwest-southeast trend and lie at the northeasterly and easterly boundaries of the study area. Sandstone development during the somewhat later Lower stratigraphic interval occurred in the Joarcam, Joffre, and Huxley-Watts-Cessford areas (Lower), generally displaced slightly to the southwest of the main areas of Basal sand deposition. This was the period of maximum Viking sand development. From 4 to 12 fairly discrete, moderately thick, chronotaxial sand units developed in each of these areas, and are regarded as complexes. Sand deposition in this time interval stopped earlier in the northwest, but continued in the southeast until very close to the time of bentonite A. Some Upper Viking sandbodies were deposited to the southwest (Upper Central), but most are to the southeast (Upper Eastern) of the Lower sand units. The thickest single Viking sandbody (UC) formed at this time. The UE_2 member evolved from the

Basal through the Lower chrono-intervals, but mostly during the Upper. The Upper Western (UW) sand units may have evolved in a similar fashion, but deposition appears to have ceased at about the time of bentonite A.

Sand units trend northwest-southeast parallel to the paleostrandline except for the unusual WSW-ENE trend of the Dodsland-Hoosier sands of southwest Saskatchewan. Most ridges are elongate, asymmetrical and arranged in parallel fashion. The superficially sheet-like distribution of most sandbodies is a result of coalescence and/or overlap of discrete sand units. Imbricate stacking of sandbodies is the most common arrangement.

Two opposed main directions of sandbody migration were noted for these sandstones. The Upper Western sand units prograded in a northeasterly and easterly direction while the rest of the Viking sandbodies migrated predominantly landward in a southwesterly direction. The opposed sense of sand movement indicates that:

1. The Viking Formation is not a simple clastic wedge or successions of clastic wedges younging in a northeasterly or easterly direction as has been previously stated in the literature.
2. The Viking sandbodies exhibit different degrees of diachronism in different directions. Perpendicular to the depositional strike, the Upper Western unit youngs to the northeast, while others young slightly toward the southwest, the UE_2 being the most diachronous Viking

unit in the study area. Parallel to the depositional strike, the sandbodies also young in a southeasterly direction; consequently, the Lloydminster Shale transgression in this area is thought to be Boreal related.

The opposed directions of ridge migration also explains the genesis of the mudstone unit which bears bentonite A, and separates the Upper from the Lower sand units in the area of Huxley-Watts-Cessford and Bindloss (i.e., the area of the Lower sand ridge complex). The mudstone facies represents, respectively, the seaward and the shoreward mud facies of the northeasterly prograding Upper Western unit and the southwesterly migrating Upper Eastern units. It is not the product of a separate marine transgression, as suggested by Tizzard (1974).

Most importantly, the opposed directions of sand movement suggests two major sand dispersive mechanisms during Viking deposition. The northeasterly and/or easterly prograding Upper Western sand complex is probably a complex of regressive meso-tidal barrier islands (UW_1 and UW_2) with associated shoreface or nearshore units (UW_3) of wave-tide and/or storm origin. The barrier islands along the coast of Georgia are considered close modern analogs.

The southwesterly (landward) migrating units are predominantly offshore, subtidal, tide-dominated sand ridges laid down below normal wave base. However, semi-permanent currents of either Boreal and/or Gulfian origin, and/or storm currents, are considered to have boosted the tidal

regime; hence, the large scale of these sand ridges. A few thin units (e.g., in the Provost area) may represent subsea tidal scour fill deposits. It is quite possible that the thin sand members of the Dodsland-Hoosier area of southwest Saskatchewan represent an offshore tide-generated sandwave complex. The present day tidal sand ridges, sandwaves and scours in the North Sea are fairly reasonable analogs.

It is thought that much of the offshore sand was derived from the Foothills region through major deltas, located in the present Jasper National Park area, and, possibly, the region of the Alberta-Montana border. Minor contributions may have been furnished by sea floor scouring and reworking of Upper Joli Fou sediment. The distribution of at least some chert pebble conglomerate beds was controlled by seafloor topography, with thicker and more beds in the swales. Such control indicates that relatively stronger currents flowed in the swales and around the edges of the ridges than over ridge crests.

Paleogeographically, Viking deposition occurred essentially during a vertical still stand of the *Haplophragmoides gigas - Innoceramus comancheanus* tidal sea. Minor regression in a northeasterly direction was mostly a function of coastal outbuilding. The northeast limit of this progradation does not appear to have reached as far as the position of the zero isopach of the Upper Western sand unit. Continued regression would have produced the superposition of shoreline facies over offshore sand units.

Individual offshore sandbodies are relatively cleaner and coarser along their northeast margins than their southwest margins. This lateral textural gradient is consistent with the direction of ridge migration and decrease in flow energy. It is reflected vertically in the coarsening upward grain size sequence which is typical of these sandbodies. The greater accumulation of oil and gas on the northeastern or eastern margins of the sand units is possibly as much the primary influence of the depositional environment producing better reservoir rock as the later regional southwest dip.

More work on the Viking sandbodies of adjacent regions is necessary for an overall definitive regional interpretation of depositional environments and paleogeographic setting of the Viking Sea.

BIBLIOGRAPHY

Alho, L.O., Gray, F.F., and Kassube, J.R., 1977. The Provost Viking 'C' oil pool east-central Alberta: Can. Soc. Petroleum Geologists, Bull., V. 25(3), pp. 396-409.

Allen, J.R.L., 1970b. Physical Processes of Sedimentation. London: Allen and Unwin, 240 pp.

Amajor, L.C., 1977. Some Viking bentonites, south-central Alberta; Unpub. M.Sc. thesis, University of Alberta, 104 pp.

Amoco Canada Petroleum Company Limited, 1976. 1976-1977 thesis topics.

Anderton, R., 1976. Tidal shelf sedimentation: an example from the Scottish Dalradian: Sediment., V. 23, pp. 429-458.

Badgley, P.C., 1952. Notes on the subsurface stratigraphy and oil and gas geology of the Lower Cretaceous Series in central Alberta: Geol. Surv. Canada, paper 52-11.

Bahan, W.G., 1951. Microfauna of the Joli Fou Formation in north-central Alberta: Unpub. M.Sc. thesis, University of Alberta.

Banks, N.L., 1973b. Tide dominated offshore sedimentation, Lower Cambrian, North Norway: Sediment., V. 20, pp. 213-228.

Beach, F.K., 1955. Cardium, a turbidity current deposit: Alberta Soc. Petroleum Geologists, Bull., V. 3(8), pp. 123-125.

__________, 1956. Reply to De Wiel on Turbidity current deposits: Alberta Soc. Petroleum Geologists, Bull., V. 4(8), pp. 175-177.

__________, 1972. Viking deposition (discussion): Alberta Soc. Petroleum Geologists, Bull., V. 10(4), pp. 210-212.

Belderson, R.H., and Stride, A.H., 1966. Tidal current fashioning of a basal bed: Marine Geol., V. 4, pp. 237-257.

Berg, R.R., and Davies, D.K., 1968. Origin of Lower Cretaceous Muddy Sandstone at Bell Creek field, Montana: Am. Assoc. Petroleum Geologists, Bull., V. 52, pp. 1888-1898.

__________, 1975. Depositional environment of Upper Cretaceous Sussex Sandstone, House Creek field, Wyoming: Am. Assoc. Petroleum Geologists, Bull., V. 59, pp. 2099 - 2110.

Berg, R.R., 1976. Highlight Muddy Field, Lower Cretaceous transgressive deposits in the Powder River Basin, Wyoming: Mtn. Geol., V. 13(2), pp. 33-45.

Bernard, H.A., Le Blanc, R.J., and Major, C.F., 1962. Recent and Pleistocene geology of southeast Texas, field excursion no. 3: In Geology of the Gulf Coast and central Texas and Guide book of excursions: Geol. Soc. America Ann. Mtg., Houston, Texas: Houston Geol. Soc., pp. 175-225.

Boethling, Jr., F.C., 1977a. Increase in gas prices rekindles Viking-sandstone interest: Oil and Gas Jour., V. 75(12), pp. 196-200.

__________, 1977b. Typical Viking sequence: A marine sand enclosed with marine shales: Oil and Gas Jour., V. 75(13), pp. 172-176.

Boggs, Sam. Jr., 1974. Sand-wave fields in Taiwan Strait: Geology, V. 2, pp. 251-253.

Brenchley, P.J., Newell, G., and Stanistreet, I.G., 1979. A storm surge origin for sandstone beds in an epicontinental platform sequence, Ordovician, Norway: Sediment Geol., V. 22, pp. 185-217.

Brenner, R.L., 1978. Sussex sandstone of Wyoming - Example of Cretaceous offshore sedimentation: Am. Assoc. Petroleum Geologists, Bull., V. 62(2), pp. 181-200.

__________, and Davies, D.K., 1973. Storm generated Coquinoid Sandstone: Genesis of high energy marine sediments from the Upper Jurassic of Wyoming and Montana: Geol. Soc. America., Bull., V. 84, pp. 1685-1698.

Bullock, D.B., 1950. A microfaunal study of the Basal Lloydminster Shale: Unpub. M.Sc. thesis, University of Alberta, 43 pp.

Caldwell, W.G.E., North, B.R., Stelck, C.R., Wall, J.H., 1978. A foraminiferal zonal scheme for the Cretaceous System in the Interior Plains of Canada: In Stelck, C.R. and Chatterton, B.D.E. (Eds.), Western and Arctic Canadian Biostratigraphy, Percival Sydney Warren Memorial Volume, G.S.C. Spec. Paper No. 18, p. 495-575.

Carter, C.H., 1978. A regressive barrier and barrier-protected deposit: Depositional environment and geographic setting of the Late Tertiary Cohansey Sand: Jour. Sediment. Petrol., V. 48, pp. 933-950.

Carruthers, J.N., 1963. History, sandwaves and near-bed currents of La Chapelle Bank: Nature, V. 197 (4871), pp. 942-946.

Cartwright, D.E., and Stride, A.H., 1958. Large sandwaves near the edge of the continental shelf: Nature, V. 181(4601), p. 41.

Caston, V.N.D., 1972. Linear sand banks in the southern North Sea: Sediment., V. 18, pp. 63-78.

__________, and Stride, A.H., 1970. Tidal sand movements between some linear sand banks in the North Sea off northeast Norfolk: Marine Geol., V. 9, M_{38} - M_{42}.

Chamberlain, C.K., 1978. Recognition of trace fossils in cores: In Basan P.B. (ed.), Trace fossil concepts, S.E.P.M. short course No. 5, pp. 133-184.

Coleman, J.M., and Wright, L.D., 1978. Sedimentation in an arid macrotidal alluvial river system; Ord River, western Australia: Jour. Geol., V. 86, pp. 621-642.

Collinson, J.D., 1970. Bedforms of the Tana River, Norway: Geogr. Annlr., V. 52, pp. 31-55.

Cram, J.M., 1979. The influence of continental shelf width on tidal range: Paleoceanographic implications: Jour. Geol., V. 87, pp. 441-447.

Davidson-Arnott, R.G.D., and Greenwood, B., 1976. Facies relationship on a barred coast, Kouchibouguac Bay, New Brunswick, Canada: in Davis Jr., R.J. (ed.), Beach and Nearshore sedimentaton: Soc. Econ. Paleont. Mineral. Spec. Publ. No. 24, pp. 149-168.

Davies, D.K., Ethridge, F.G., and Berg, R.R., 1971. Recognition of barrier environments: Am. Assoc. Petroleum Geologists, Bull., V. 55, pp. 550-565.

Davies, D.K., 1976. Models and concepts for exploration in Barrier Islands, in Saxena, R.S. (ed.), Sedimentary environments and hydrocarbons, AAPG and NOGS short course, pp. 77-115.

Davis, J.L., 1964. A morphogenetic approach to world shorelines: Zeites fur Geomorph., V. 8, pp. 127-142.

De Jong, J.D., 1977. Dutch tidal flats: Sediment. Geol., V. 18, pp. 13-23.

De Wiel, J.E.F., 1956. Viking and Cardium not turbidity current deposits: Alberta Soc. Petroleum Geologists, Bull., V. 4(8), pp. 173-174.

Dickenson, W.R., 1971. Plate tectonic models of geosynclines: Earth Plan. Sci. lett., V. 10, pp. 165-174.

__________, 1976. Sedimentary basins developed during evolution of Mesozoic-Cenozoic arc trench system in western North America: Can. Jour. Earth Sci., V. 13(9), pp. 1268-1287.

Dickinson, K.A., Berryhill Jr., H.L., and Holmes, C.W., 1972. Criteria for recognizing ancient barrier coastlines: in Rigby, J.K., and Hamblin, Wm. K., (eds.), Recognition of ancient sedimentary environments: Soc. Econ. Paleont. Mineral Spec. Publ. No. 16, pp. 192-214.

Douglas, R.J.W., Gabrielse, H., Wheeler, J.O., Stott, D.F., Belyea, H.R., 1970. Geology of western Canada: Geol. Surv. Can. Econ. Geol. Rept. No. I, pp. 367-488.

Drapeau, G., 1970. Sandwaves on Browns bank observed from the shelf diver: Maritime Sediments, V. 6(3), pp. 90-101.

Duane, D.B., Field, M.E., Meisberger, E.P., Swift, D.J.P., and Williams, S.J., 1972. Linear shoals on the Atlantic continental shelf, Florida to Long Island: In Swift, D.J.P., Duane, D.B., and Pilkey, O.H. (eds.), Shelf sediment transport: Process and pattern: Dowden, Hutchinson and Ross Inc., Stroudsburg, pp. 447-498.

Ealph, E.W., 1955. The inclined oil-water contact at the Joarcam field: Alberta Soc. Petroleum Geologists, Bull., V. 3(7), pp. 99-103.

Eicher, D.L., 1960. Stratigraphy and micropaleontology of the Thermopolis Shale: Peabody Mus. Nat. Hist., Yale Univ., Bull., 15, 126 pp.

Eisbacher, G.H., 1977. Mesozoic-Tertiary basin models for the Canadian Cordilleran and their geological constraints: Can. Jour. Earth Sci., V. 14(10), pp. 2414-2417.

Evans, W.E., 1970. Imbricate linear sandstone bodies of the Viking Formation in Dodsland-Hoosier area of southwestern Saskatchewan: Am. Assoc. Petroleum Geologists, Bull., V. 54(3), pp. 469-486.

Eysinga, F.W.B., 1975. Geological Time Table, Elservier Scientific Publ. Comp., 3rd Edit.

Finley, R.J., 1978. Ebb-tidal delta morphology and sediment supply in relation to seasonal wave energy flux, North Inlet, South Carolina: Jour. Sediment Petrol., V. 48(1), pp. 227-238.

Flemming, B.W., 1978. Underwater sand dunes along the southeast African Continental Margin - observations and implications: Marine Ecol., V. 26, pp. 177-198.

Gammell, H.G., 1955. The Viking Member in central Alberta: Alberta Soc. Petroleum Geologists, Bull., V. 3(5), pp. 63-69.

Glaeser, J.D., 1978. Global distribution of Barrier Islands in terms of Tectonic setting: Jour. Geology, V. 86(3), pp. 283-297.

Glaister, R.P., 1958. Petrology of the Blairmore sandstone: Alberta Soc. Petroleum Geologists, Bull., V. 6(2), pp. 43-49.

__________, 1959. Lower Cretaceous of southern Alberta and adjoining areas: Am. Assoc. Petroleum Geologists, Bull., V. 43(3), pp. 590-640.

Goldring, R. and Bridges, P., 1973. Sublittoral sheet sandstones: Jour. Sediment Petrol., V. 43, pp. 736-747.

Gopinath, T.R., 1978. Depositional environments of the Muddy Sandstone (Lower Cretaceous) Wind River Basin, Wyoming: Mtn. Geol., V. 15(1), pp. 27-47.

Harvey, J.G., 1965. Large sandwaves in the Irish Sea: Marine Geol.

Hayes, M.O., 1967. Hurricanes as geological agents, South Texas coast: Am. Assoc. Petroleum Geologists, Bull., V. 51(6), pp. 937-956.

__________, 1975. Morphology of sand accumulations in estuaries: In Cronin, L.E. (ed.), Estuarine research, V. 2, Geology and Engineering: New York, Academic Press, pp. 3-22.

Hitchon, B., 1964. The effect of differences in interpretation on the lithological evaluation of electric log: Alberta Soc. Petroleum Geologists, Bull., Vol. 12(3), pp. 754-769.

Hobday, D.K., and Reading, H.G., 1972. Fair weather versus storm processes in shallow marine sandbar sequences in the Late PreCambrian of Finmark, North Norway: Jour. Sediment Petrol., V. 42, pp. 318-324.

__________, and Tankard, A.J., 1978. Transgressive-barrier and shallow-shelf interpretation of the Lower Paleozoic Peninsula Formation, South Africa: Geol. Soc. America Bull., V. 89, pp. 1733-1744.

Houbolt, J.J.H., 1968. Recent sediments in the southern Bight of the North Sea: Geol. en Mijn., V. 47, pp. 245-273.

Howard, J.D., 1972. Trace fossils as criteria for recognizing shorelines in stratigraphic record: In Rigby, J.K. and Hamblin, Wm. K. (eds), Recognition of ancient sedimentary environments: Soc. Econ. Paleont. Mineral Spec. Publ. No. 16, pp. 215-225.

Hoyt, J.H., and Henry Jr., V.J., 1965. Significance of inlet sedimentation in the recognition of ancient Barrier islands: Geol. Assoc. Wyoming, 19th Field Conference Guidebook, pp. 190-194.

Hunt, W.C., 1954. The Joseph Lake-Armena-Camrose producing trend, Alberta: in Clark, L.M. (ed.), Western Canada Sedimentary Basin, pp. 452-463.

Ingram, R.L., 1954. Terminology for the thickness of stratification and parting units in sedimentary rocks: Geol. Soc. America Bull., V. 65, pp. 937-938.

Iwuagwu, C.J., 1979. Diagenesis of the Basal Belly River Sandstone: Unpub. M.Sc. thesis, University of Alberta, 175 pp.

Jardine, D., 1954. The Joarcam-Viking Oil Field: Oil in Canada, Aug. 16, 1954, pp. 22-30.

Johnson, H.D., 1977. Shallow marine sand bar sequences: an example from the late PreCambrian of North Norway: Sediment, V. 24, pp. 245-270.

Johnson, M.A., and Belderson, R.H., 1969. The tidal origin of some vertical sedimentary changes in epicontinental seas: J. Geol., V. 77, pp. 353-357.

__________, and Stride, A.H., 1969. Geological significance of North Sea sand transport rates: Nature, London, V. 224, pp. 1016-1017.

Jones, H.L., 1961a. The Viking Formation in southwestern Saskatchewan: Dept. Min. Resources, Saskatchewan Rept. No. 65, 79 pp.

__________, 1961b. Viking deposition in southwestern Saskatchewan with a note on the source of the sediments: Alberta Soc. Petroleum Geologists, Bull., V. 9(8), pp. 231-244.

__________, 1962. Viking deposition (discussion): Alberta Soc. Petroleum Geologists, Bull., V. 10(4), p. 212.

Jones, N.S., Kain, J.M., and Stride, A.H., 1965. The movement of sandwaves on Warts Bank, Isle of Man: Marine Geol., V. 3(5), pp. 329-337.

Kauffman, E.G., 1973a. Stratigraphic evidence for Cretaceous eustatic changes (abstr.): Abstr. Vol., 1973 Ann. Mtg., Geol. Soc. America, p. 687.

__________, 1975. Dispersal and biostratigraphic potential of Cretaceous benthonic bivalvia in the western Interior: In Caldwell, W.G.E. (ed.), The Cretaceous system in the western Interior of North America: Geol. Assoc. Can. Spec. paper No. 13, pp. 163-194.

__________, 1977. Geological and biological overview: Western Interior Cretaceous Basin: Mtn. Geol. V. 14(3 and 4), pp. 75-97.

Klein, G.D., 1970a. Tidal origin of a PreCambrian quartzite - the Lower fine grained quartzite (Middle Dalradian) in Islay, Scotland: Jour. Sediment Petrol., V. 40, pp. 973-985.

__________, 1970b. Depositional and dispersal dynamics of intertidal sand bars: Jour. Sediment Petrol., V. 40(4), pp. 1095-1127.

__________, 1977. Tidal circulation model for deposition of clastic sediment on epeiric and mioclinal shelf seas: Sediment Geol., V. 18, pp. 1-12.

__________, 1977. Clastic tidal facies, Continuing Educ. Publ. Comp., Illinois, 149 pp.

__________, and Ryer, T.A., 1978. Tidal circulation patterns in PreCambrian, Paleozoic, and Cretaceous epeiric and mioclinal shelf seas: Geol. Soc. America Bull., V. 89, pp. 1050-1058.

Kenyon, N.H., 1970. Sand ribbons of European tidal seas: Marine Geol., V. 9(1), pp. 25-39.

__________, 1970. The origin of some transverse sand patches in the Celtic Sea: Geol. Mag., V. 107(4), pp. 389-393.

__________, and Stride, A.H., 1970. The tide-swept continental shelf sediments between the Shetland Isles and France: Sediment., V. 14 (3-4), pp. 159-173.

__________, and Belderson, R.H., 1973. Bedforms of the Mediterranean undercurrent observed with side-scan sonar: Sediment., Vol., V. 9(2), pp. 77-79.

Koldijk, W.S., 1976. Gilby Viking 'B': A storm deposit: in Lerand, M.M. (ed.), The sedimentology of selected clastic oil and gas reservoirs in Alberta: Can. Soc. Petroleum Geologists, pp. 62-77.

Krumbein, W.B. and Sloss, L.L., 1963. Stratigraphy and sedimentation: W.H. Freeman Co., San Francisco, 660 pp.

Krynine, P.D., 1948. The megascopic study and field classification of sedimentary rocks: Jour. Geol., V. 56, pp. 130-165.

Kulm, L.D., Rousch, R.C., Harlett, J.C., Neudeck, R.H., Chambers, D.M., and Runge, E.J., 1975. Oregon continental shelf sedimentation: Interrelationships between facies distribution and sedimentary processes: Jour. Geol., V. 837, pp. 145-176.

Kumar, N., and Sanders, J.E., 1976. Characteristics of shoreface storm deposits: Modern and Ancient examples: Jour. Sediment Petrol., V. 46, pp. 145-162.

Larson, L.H., 1960 (ed.). Gas fields of Alberta: Alberta Soc. Petroleum Geologists, 407 pp.

Lerand, M., 1979. Modern clastic depositional environments and processes, South Carolina Coast: An overview and travelog, Edm. Geol. Soc. seminar.

Lowman, S.W., 1949. Sedimentary facies in Gulf Coast: Am. Assoc. Petroleum Geologists Bull., V. 33, pp. 1939-1997.

Love, M., 1955. The Joffre oil field, geology and development: Oil in Canada, V. 7(38), pp. 12884-12890.

MacKenzie, D.B., 1975. Tidal sand flat deposits in Lower Cretaceous Dakota Group near Denver, Colorado: In Ginsburg, R.N. (ed.), Tidal deposits, a casebook of recent examples and fossil counterparts, Springer Verlag, pp. 117-125.

Magdich, F.S., 1955. The Viking Formation in Saskatchewan: Unpub. M.Sc. Thesis, University of Saskatchewan, Saskatoon.

Masters, C.D., 1967. Use of sedimentary structures in determination of depositional environments, Mesaverde Formation Williams Fork Mountains, Colorado: Am. Assoc. Petroleum Geologists, Bull., V. 5(10), pp. 2033-2043.

May, R., 1967. Geology of the Peace River, Viking, Joli Fou and Notikewin Formations, Kaybob area, N. Alberta, Unpub. M.Sc. Thesis, University of Calgary.

McCabe, P.J., and Jones, C.M., 1977. Formation of reactivation surfaces within superimposed deltas and bedforms: Jour. Sediment. Petrol., V. 47, pp. 707-715.

McCave, I.N., 1970. Deposition of fine-grained suspended sediment from tidal currents: Jour. Geophys. Res., V. 75, pp. 4151-4159.

__________, 1971. Sandwaves in the North Sea off the coast of Holland: Marine Geol., V. 10(3), pp. 199-225.

__________, 1979. Tidal currents at the North Hinder lightship, southern North Sea: Flow directions and turbulence in relation to maintenance of sand banks: Marine Geol., V. 31, pp. 101-114.

McPherson, Wm. J., 1955. Thin sand completions at Hamilton Lake field: Alberta Soc. Petroleum Geologists, Bull., V. 3(3), pp. 34-35, 40.

Morton, R.A., 1978. Large scale rhomboid bedforms and sedimentary structures associated with hurricane washover: Sediment., V. 25 (2), pp. 183-204.

Nauss, A.W., 1945. Cretaceous stratigraphy of Vermillion area, Alberta, Canada: Am. Assoc. Petroleum Geologist, Bull., V. 39, pp. 1605-1629.

__________, 1947. Cretaceous microfossils of the Vermillion area, Alberta: Jour. of Paleont., Vol. 21(4), pp. 329-343.

Niino, H., and Emery, K.O., 1961. Sediments of shallow portions of East China sea and South China sea: Geol. Soc. America, Bull., V. 72(5), pp. 731-762.

Nio, S.D., 1976. Marine transgression as a factor in the Formation of sandwave complexes: Geol. en Mijnb., V. 55, pp. 18-40.

Norgaard, G.A., 1954. Viking Formation, Colorado Group, Lower Cretaceous: In Lexicon of Geologic names in the western Canadian sedimentary basin and Arctic Archipelago: Alberta Soc. Petroleum Geologists, Calgary, pp. 360-361.

North, B.R. and Caldwell, W.G.E., 1975. Foraminiferal faunas in the Cretaceous system of Saskatchewan: In Caldwell, W.G.E. (ed.), The Cretaceous system in the Western Interior of North America, Geol. Assoc. Can. Spec. paper, No. 13, pp. 303-332.

Oertel, F.G., and Howard, J.D., 1972. Water criculation and sedimentation at estuary entrances on the Georgia Coast, pp. 411-428: In (Swift, D.J.P., Duane, D.B., and Pilkey, O.H.)(eds.), Shelf sediment transport; Stroudsburg, Dowden, Hutchinson, and Ross, 656 pp.

__________, 1975. Ebb-tidal deltas of Georgia Estuaries: In Cronin, L.E. (ed.), Estuarine research, Vol. II, Geology and Engineering: New York, Academic Press, pp. 267-276.

Off, T., 1963. Rythmic linear sandbodies caused by tidal currents: Am. Assoc. Petroleum Geologists, Bull., V. 47(2), pp. 324-341.

Oliver, T.A., 1960. The Viking-Cadotte relationship: Alberta Soc. Petroleum Geologists, Bull., V. 8(9), pp. 247-253.

Phleger, F.B., 1969. Some general features of coastal lagoons: In Castanares, A.A., and Phleger, F.B. (eds.), Coastal lagoons, a symposium, Mexico: Universidad Nacional-Autonoma, pp. 5-26.

Pilkey, O.H., Trumbull, J.V.A., and Bush, D.M., 1978. Equilibrium shelf sedimentation, Rio de La Plata shelf, Puerto Rico: Jour. Sediment. Petrol. V. 48(2), pp. 389-400.

Porrenga, D.H., 1967. Glauconite and chamosite as depth indicators in the marine environments: Mar. Geology, Vol. 5, pp. 495-501.

Potter, P.E., 1967. Sandbodies and sedimentary environments: A review: Am. Assoc. Petroleum Geologists, Bull., V. 51(3), pp. 337-365.

Price, L.L., 1962. Lower Cretaceous rocks of southeastern Saskatchewan: Geol. Soc. Can., paper 62-69, 55 pp.

Reasoner, M.A., and Hunt, A.D., 1954a. Smiley Oil Field, Saskatchewan: Can. Min. and Metall. Bull., V 47(509), pp. 612-617.

Reineck, H.E., 1963. Sedimentgefuge in Bereich der sudliche Nordsee: Senckengergische Natorf. Gesell. Abh., No. 505, pp. 1-138.

__________, 1967. Layered sediments of tidal flats, beaches and shelf bottoms: In Lauff, G.H. (ed.), Estuaries: Am. Assoc. Advan. Sci. Publ. 83, pp. 191-206.

__________, 1975. German North Sea Tidal flats: In Ginsburg, R.N. (ed.), Tidal Deposits, a casebook of recent examples and fossil counterparts: Springer Verlag, New York, pp. 5-12.

__________, and Singh, I.B., 1975. Genesis of laminated sand and graded rhythmites in storm-sand layers of shelf mud: Sediment., V. 18, pp. 123-128.

__________, 1975. Depositional sedimentary environments with reference to Terrigenous clastics: Berlin, Springer Verlag, 439 pp.

Reinert, S.L., and Davies, D.K., 1976. Third Creek field, Colorado: A study of sandstone environments and diagensis: Mtn. Geologists, V. 13(2), pp. 47-60.

Reinson, G.E., 1979. Barrier island systems: Geo. Sci. Cana., V. 6(2), pp. 51-68.

Robinson, A.H.W., 1966. Residual currents in relation to shoreline evolution of the East Anglian Coast: Marine Geol., V. 4, pp. 57-84.

Rodolfo, K.S., Buss, B.A., and Pilkey, O.H., 1971. Suspended sediment increase due to hurricane Gerda in continental shelf waters off Cape Lookout, North Carolina: Jour. Sediment. Petrol., Vol. 41(4), pp. 1121-1125.

Roep, T.H.B., Beets, D.J., Dronkert, H., and Pagnier, H., 1979. A prograding coastal sequence of wave built structures of Messinian age, Sorbas, Almeria, Spain: Sediment. Geol., V. 22, pp. 135-163.

Roessingh, H.K., 1959. Viking deposition in the southern Alberta Plains: Alberta Soc. Petroleum Geologists, 9th Annual field Conf., pp. 130-137.

Rudkin, R.A., 1964. Lower Cretaceous, Chapter II: In McCrossan, R.G., and Glaister, R.P. (eds.), Geological History of Western Canada: Alberta Soc. Petroleum Geologists, Calgary, pp. 156-168.

Schneidegger, K.F. and Kulm, L.D., Runge, E.J., Sediment sources and dispersal patterns of Oregon continental shelf sands: Jour. Sediment. Petrol., V. 41(4), pp. 1112-1120.

Scott, R.W., 1970. Stratigraphy and sedimentary environments of Lower Cretaceous rocks, southern Western Interior: Am.Assoc. Petroleum Geologists Bull., V. 54., pp. 1225-1244.

Seeling, A., 1979. The Shannon sandstone, a further look at the environment of deposition at Heldt Draw field, Wyoming: Mtn. Geologist, V. 15(4), pp. 133-144.

Selley, R.C., 1976. An introduction to sedimentology: Academic Press, 408 pp.

Shelton, J.W., 1973. Models of sand and sandstone deposits: a methodology for determining sand genesis and trend: Viking Sandstone, Cretaceous, Joffre Field, Alberta: Oklahoma Geol. Surv. Bull., V. 118, pp. 91-94.

Shephard, F.P., 1948. Submarine Geology, New York: Harper and Brothers, 348 pp.

Simpson, F., 1975. Marine Lithofacies and Biofacies of the Colorado Group (Middle Albian to Santonian), in Saskatchewan: In Caldwell, W.G.E. (ed.), The Cretaceous system in the Western Interior of North America: Geol. Assoc. Can. Spec., paper No. 13, pp. 553-587.

Singh, I.B., 1969. Primary sedimentary structures in PreCambrian Quartzites of Telemark, Southern Norway, and their environmental significance: Norsk Geol. Tidsskr., Vol. 49, pp. 1-31.

Slipper, S.E., 1918. Viking gas field, Structure of Area: Geol. Surv. Summ. Rept., 1917, Part C, p. 8C.

Southard, J.B., and Harms, J.C., 1972. Sequence of bedform and stratification in silts, based on flume experiments (abst.): Am. Assoc. Petroleum Geologists, Bull., V. 56, pp. 654-655.

Spearing, D.R., 1976. Upper Cretaceous Shannon Sandstone: An offshore shallow marine sandbody: Wyoming Ecol. Assoc. 28th Ann. Guidebk., pp. 65-72.

Stahl, L., and Koczam, J., and Swift, D., 1974. Anatomy of a shoreface-connected sand ridge on the New Jersey shelf: Implications for the genesis of the shelf surficial sand sheet: Geol. V. 2, No. 3, pp. 117-120.

Stansberry, G.F., 1957. The Viking Formation, Central Alberta: Unpubl. M.Sc. Thesis, University of Alberta, 124 pp.

Stapp, R.W., 1967. Relationship of Lower Cretaceous depositional environments to oil accumulation, Northeast Powder River Basin, Wyoming: Am. Assoc. Petroleum Geologists, Bull., V. 51(10), pp.

Stelck, C.R., 1958. Stratrigraphic position of Viking sand: Alberta Soc. Petroleum Geologists, Bull., V. 6(1), pp. 2-7.

__________, 1975. The Upper Albian *Miliammina manitobensis* zone in northeastern British Columbia: In Caldwell, W.G.E. (ed.), The Cretaceous system in the Western Interior of North America: Geol. Assoc. Can. Spec. paper No. 13, pp. 253-275.

Stride, A.H., 1963. Current swept sea floors near the southern half of Great Britain: Quart. Jour. Geol. Soc. , V. III, pp. 175-199.

__________, b965. Preservation of some marine current bedding: Nature Lond., V. 206, pp. 498-499.

__________, 1970. Shape and size trends for sandwaves in a depositional zone of the North Sea: Geol. Mag., V. 1970, pp. 469-477.

__________, A.H., and Chesterman, W.D., 1973. Sedimentation by non-tidal currents around northern Denmark: Marine Geol., V. 15., pp. M53-M58.

Stubblefield, W.L., Lavelle, J.W., Swift, D.J.P., and McKinney, T.F., 1975. Sediment response to the present hydraulic regime on the Central New Jersey shelf: Jour. Sediment. Petrol., V. 45, pp. 337-358.

__________, and Swift, D.J.P., 1976. Ridge development as revealed by sub-bottom profile on the Central New Jersey shelf: Marine Geol., V. 20, pp. 315-334.

Swift, D.J.P., Stanley, D.J., and Curay, J.R., 1971. Relict sediments on continental shelves: A reconsideration: Jour. Geol., V. 79, pp. 322-346.

__________, D.J.P., Holliday, B., Avignone, N., and Shideler, G., 1972a. Anatomy of a shoreface ridge system, False Cape, Virginia: Marine Geol., V. 12, pp. 59-84.

__________, Kofoed, J.W., Saulsbury, F.P., and Sears, P., 1972b. Holocene evolution of the shelf surface, Central and Southern Atlantic shelf of North America: In Swift, D.J.P., Duane, D.B., Pilkey, O.H. (eds.), Shelf sediment transport: Process and pattern, pp. 499-574. Dowden Hutchinson and Ross, Inc., Stroudsburg.

__________, Duane, D.B., and McKinney, T.F., 1973. Ridge and swale topography of the Middle Atlantic Bight: Scalar response to Holocene hydraulic regime: Marine Geol., V. 15, pp. 227-247.

__________, 1974. Continental shelf sedimentation: In Burke, C.A., and Drake, C.L. (eds.), The Geology of continental margins, Springer Verlag, pp. 117-124.

__________, 1975. Barrier Island genesis: Evidence from the Central Atlantic shelf, eastern U.S.A.: Sediment Geol., V. 14, pp. 1-43.

__________, 1975. Tidal sand ridges and shoal retreat massifs: Marine Geol., V. 18, pp. 105-134.

__________, Nelson, T., Mchone, J., Holliday, B., Palmer, H., Shideler, G., 1977. Holocene evolution of the inner shelf of southern Virginia: Jour. Sediment. Petrol., V. 47(4), pp. 1454-1474.

__________, Sears, P.C., Bohlke, B., and Hunt, R., 1978. Evolution of a shoal retreat massif, North Carolina shelf: Inferences from areal geology: Jour. Sediment. Petrol., V. 27, pp. 19-42.

__________, Parker, G., Lanfredi, N.W., Perillo, G., Figge, K., 1978. Shoreface-connected sand ridges on American and European shelves: A comparison: Estuarine and Coastal Mrine Sci., V. 7, pp. 257-273.

Thomas, M.B., 1977. Depth-Porosity relationships in the Viking and Cardium Formations of Central Alberta: Unpub. M.Sc. thesis, University of Calgary, 147 pp.

Terwindt, J.H.J., 1971. Sandwaves in the southern bight of the North Sea: Marine Geol., V. 10, pp. 51-68.

Tizzard, P.G., 1974. Viking deposition in the Suffield area, Alberta: Unpub. M.Sc. thesis, University of Alberta, 126 pp.

__________, and Lerbekmo, J.F., L975. Depositional history of the Viking Formation, Suffield area, Alberta Canada: Can. Soc. Petroleum Geologists, Bull., V. 23(4), pp. 715-752.

Van den Berg, J.H., 1977. Morphodynamic development and preservation of physical sedimentary structures in two prograding recent ridge and runnel beaches along the Dutch coast: Geol. En. Mijn., V. 56(3), pp. 185-202.

White, W.A., and Galloway, W.E., 1977. Guide to modern Barrier environments of Mustang and North Padre Islands and Jackson (Eocene) Barrier-Lagoon facies of South Texas Uranium district: Bur. Econ. Geol., Univ. Texas, Austin. Res. Note 7, 51 pp.

Wickenden, R.T.D., 1949. Some Cretaceous sections along Athabasca River from the mouth of Calling River to below Grand Rapids, Alberta: Geol. Surv. Can. Paper, 49-15, pp. 3, 16.

Williams, G.D., and Stelck, C.R., 1975. Speculations on the Cretaceous Paleogeography of North America: In Caldwell, W.G.E. (ed.), The Cretaceous system in the Western Interior of North America: Geol. Assoc. Can. spec. paper No. 13, pp. 1-7.

Walker, R.G., 1979. Turbidites and associated coarse clastic deposits: In Walker, R.G. (ed.), Facies models: Geo Sci. Can. Repr. Ser. I, pp. 91-104.

Weber, K.J., 1971. Sedimentological aspects of oil fields in the Niger Delta: Geol. en Mijnb., V. 50, pp. 559-576.

Werner, F., and Newton, R.S., 1975. The pattern of large-scale bed forms in the large land belt (Baltic Sea): Marine Geol., V. 19, pp. 29-59.

Wheeler, J.O., Aitken, J.D., Berry, M.J., Gabrielse, H., Hutchison, W.W., Jacoby, W.R., Monger, J.W.H., Niblett, E.R., Norris, D.K., Price, R.A., and Stacey, R.A., 1972. The Cordilleran structural Province, in Price, R.A., and Douglas, J.W. (eds.), Variations in tectonic styles in Canada: Geol. Assoc. Can. Spec. Paper No. 11, pp. 1-82.

White, R.J., 1960 (ed.). Oil fields of Alberta: Alberta Soc. Petroleum Geologists, pp. 22-23.

APPENDICES

APPENDIX Ia

Cross-Section A-A' (Figure 10)

Well No.	Name	Well Location	K.B. Elev. (ft.)
1	West Coast Sulpetro Smore	7-10-30-11W4M	
2	Unigas *et al.* Chinook	10-34-30-8W4M	
3	Eden Sedgas Chinook	10-19-30-6W4M	
4	Trecon Sedalia	11-14-30-5W4M	
5	Siebens *et al.* Hudson	10-17-30-2W4M	
6	Petrodyne Mobile Hudson	11-16-30-2W4M	
7	Husky I.N.C. K.R. Oyen	7-17-30-1W4M	
8	W.R.M. Matadore Gulf Antlop	7-25-30-1W4M	
9	Husky Phillips Greene	10-32-30-28W4M	

APPENDIX Ib

Cross-Section B-B' (Figure 11)

Well No.	Name	Well Location	K.B. Elev. (ft.)
1	L & M Canpet C.P.O.G. Redland	11-16-27-22W4M	
2	C.P.O.G. Hussar	10-12-26-20W4M	
3	Delta *et al.* Connors	10-17-25-14W4M	
4	P.C.P. *et al.* Winterh	6-14-24-15W4M	
5	Mobil Oil C.P.R. Hutton	3-19-24-15W4M	
6	Banff *et al.* Matziwin	11-4-23-14W4M	

APPENDIX Ic

Cross-Section C-C' (Figure 12)

Well No.	Name	Well Location	K.B. Elev. (ft.)
1	N.U.L. Beaverhill Lake	7-17-52-19W4M	
2	Anglo Home C and E Camrose	8-16-47-20W4M	
3	B.A. Richards Stet. W.	2-6-37-20W4M	
4	Ceja P.C.P. Leo	6-21-36-17W4M	
5	Can Oxy *et al.* Garden	7-13-34-13W4M	
6	C.P.O.G. Dowling	10-29-32-14W4M	
7	Provident Wainoco Hanna	10-22-30-15W4M	
8	Chevron Handhills	10-36-28-14W4M	
9	H.F. Heathdale	11-31-25-7W4M	

APPENDIX Id

Cross-Section D-D' (Figure 15)

Well No.	Well Location	K.B. Elev.(ft.)
1	11-6-29-9W4M	2643
2	10-16-29-9W4M	2642
3	10-21-29-9W4M	2636
4	7-26-29-9W4M	2552
5	6-18-30-8W4M	2497
6	7-27-30-8W4M	2503
7	6-6-31-7W4M	2617
8	10-22-31-7W4M	2613
9	10-33-31-6W4M	2510
10	11-9-32-6W4M	2499
11	11-15-32-6W4M	2465
12	7-12-33-6W4M	2531
13	6-29-33-5W4M	2586
14	7-22-34-5W4M	2291
15	11-2-35-5W4M	2317
16	7-21-35-4W4M	2275

Cross-Section E-E' (Figure 16)

Well No.	Well Location	K.B. Elev.(ft.)
1	6-6-31-13W4M	2735
2	6-8-31-13W4M	2752
3	11-14-31-13W4M	2662
4	10-24-31-13W4M	2672

Cross-section D-D' (Figure 16) (cont'd)

Well No.	Well Location	K.B. Elev.(ft.)
5	6-5-32-11W4M	2562
6	11-16-32-11W4M	2578
7	10-36-32-11W4M	2560
8	10-20-33-10W4M	2538
9	4-33-33-10W4M	2548
10	2-23-34-10W4M	2552
11	13-6-35-9W4M	2535
12	13-17-35-9W4M	2569
13	11-27-35-9W4M	2630
14	7-6-36-8W4M	2580
15	11-28-36-8W4M	2690
16	11-35-36-8W4M	2649
17	7-1-37-8W4M	2638
18	10-7-37-7W4M	2499
19	4-14-37-7W4M	2549
20	7-25-37-7W4M	2488
21	11-32-37-6W4M	2343

Cross-Section F-F' (Figure 17)

1	3-8-33-16W4M	2762
2	10-20-33-15W4M	2866
3	11-31-33-14W4M	2684
4	11-15-34-14W4M	2703
5	11-23-34-14W4M	2712
6	11-5-35-13W4M	2708

Cross-Section F-F' (Figure 17) (Cont'd)

Well No.	Well Location	K.B. Elev.(ft.)
7	11-9-35-13W4M	2666
8	7-27-35-13W4M	2680
9	7-11-36-13W4M	2689
10	12-17-36-12W4M	2693
11	12-27-36-12W4M	2657
12	7-36-36-12W4M	2658
13	1-6-37-11W4M	2646
14	11-10-37-11W4M	2510
15	6-18-37-10W4M	2475
16	10-20-37-10W4M	2478
17	11-2-38-10W4M	2510
18	10-16-38-9W4M	2534

APPENDIX Ie

Cross-Section G-G' (Figure 21)

Well No.	Well Location	K.B. Elev.(ft.)
1	11-16-34-7W4M	2508
2	10-36-34-7W4M	2442
3	10-6-35-6W4M	2560
4	10-16-35-6W4M	2485
5	12-27-35-6W4M	2530
6	11-34-35-6W4M	2623
7	10-7-36-5W4M	2476
8	10-17-36-5W4M	2410
9	7-23-36-5W4M	2436
10	10-25-36-5W4M	2214
11	11-31-36-4W4M	2178
12	10-6-37-4W4M	2177
13	7-21-37-4W4M	2193
14	3-27-37-4W4M	2220
15	7-6-38-3W4M	2254
16	6-16-38-3W4M	2254

Cross Section H-H' (Figure 22)

1	10-6-35-7W4M	2539
2	10-15-35-7W4M	2599
3	10-23-35-7W4M	2604
4	10-36-35-7W4M	2512
5	11-5-36-6W4M	2512
6	5-14-36-6W4M	2543
7	13-24-36-6W4M	2317
8	7-33-36-5W4M	2485

Cross-Section I-I' (Figure 23)

Well No.	Well Location	K.B. Elev.(Ft.)
1	11-7-35-8W4M	2631
2	7-27-35-8W4M	2695
3	7-12-36-8W4M	2547
4	5-7-36-7W4M	2550
5	11-15-36-7W4M	2460
6	6-23-36-7W4M	2448
7	10-24-36-7W4M	2471
8	14-31-36-6W4M	2496
9	13-9-37-6W4M	2691
10	10-23-37-6W4M	2326

Cross-Section J-J' (Figure 24)

1	13-6-35-9W4M	2535
2	9-15-35-9W4M	2623
3	6-25-35-9W4M	2627
4	10-32-35-8W4M	2592
5	10-4-36-8W4M	2656
6	7-12-36-8W4M	2647
7	6-18-36-7W4M	2551
8	10-20-36-7W4M	2514
9	12-34-36-7W4M	2479

Cross-Section K-K' (Figure 25)

Well No.	Well Location	K.B. Elev.(ft.)
1	11-10-33-7W4M	2425
2	7-34-33-7W4M	2491
3	11-2-34-7W4M	2504
4	10-25-34-7W4M	2491
5	10-6-35-7W4M	2539
6	10-15-35-7W4M	2599
7	11-22-35-7W4M	2660
8	10-32-35-7W4M	2599
9	10-9-36-7W4M	2472
10	11-15-36-7W4M	2460
11	12-34-36-7W4M	2479
12	7-3-37-7W4M	2431
13	12-11-37-7W4M	2482
14	4-14-37-7W4M	2549
15	10-22-38-7W4M	2368
16	6-36-38-7W4M	2443

Cross Section L-L' (Figure 26)

1	11-6-35-5W4M	2456
2	10-4-35-4W4M	2206
3	10-3-35-4W4M	2252
4	10-5-35-3W4M	2445
5	10-1-35-2W4M	2367

APPENDIX If

Cross-Section M-M' (Figure 30)

Well No.	Well Location	K.B. Elev.(ft.)
1	10-17-25-14W4M	2496
2	10-2-25-14W4M	2441
3	3-4-25-13W4M	2423
4	4-36-24-13W4M	2394
5	4-5-24-12W4M	2370
6	7-26-23-12W4M	2322
7	11-9-23-11W4M	2326
8	11-33-22-11W4M	2354
9	11-18-22-10W4M	2361
10	10-2-22-10W4M	2487
11	10-36-21-9W4M	2476
12	11-19-21-7W4M	2563
13	6-36-20-7W4M	2644
14	7-29-20-5W4M	2490
15	6-2-19-3W4M	2403
16	10-21-18-2W4M	2496
17	10-34-17-1W4M	2487

Cross-Section N-N' (Figure 31)

1	11-20-16-4W4M	2472
2	7-19-17-3W4M	2431
3	6-34-17-3W4M	2463
4	7-3-18-2W4M	2542
5	6-13-18-2W4M	2473
6	7-9-19-1W4M	2477

Cross-Section N-N' (Figure 31) (cont'd)

Well No.	Well Location	K.B. Elev.(ft.)
7	7-22-19-1W4M	2484
8	10-26-19-1W4M	2450
9	7-5-20-29W3M	--
10	10-21-20-29W3M	2366
11	1-1-21-29W3M	2388
12	7-30-21-27W3M	2340
13	4-20-22-26W3M	2210

Cross-Section O-O' (Figure 32)

1	6-11-19-8W4M	2551
2	6-30-19-7W4M	2650
3	6-33-19-7W4M	2532
4	6-4-20-7W4M	2538
5	6-10-20-7W4M	2480
6	6-30-20-6W4M	2706
7	6-6-21-6W4M	2712
8	6-16-21-6W4M	2579
9	6-23-21-6W4M	2437
10	10-25-21-6W4M	2319
11	3-5-22-5W4M	2248
12	6-8-22-5W4M	2003
13	10-22-22-5W4M	2480
14	10-6-23-4W4M	2398

Cross-Section O-O' (Figure 32) (cont'd)

Well No.	Well Location	K.B. Elev.(ft.)
15	7-17-23-4W4M	2434
16	11-28-23-3W4M	2398
17	10-10-24-3W4M	2416
18	10-14-24-3W4M	2390
19	11-31-24-2W4M	2315

Cross-Section P-P' (Figure 33)

1	10-5-19-16W4M	2552
2	6-16-19-16W4M	2528
3	2-22-19-16W4M	2514
4	6-27-19-16W4M	2506
5	6-4-20-15W4M	2537
6	11-11-20-15W4M	2539
7	10-20-20-14W4M	2493
8	10-28-20-14W4M	2461
9	10-5-21-13W4M	2396
10	10-8-21-13W4M	2386
11	14-14-21-13W4M	2377
12	7-19-21-12W4M	2362
13	11-35-21-12W4M	2322
14	11-2-22-12W4M	2312
15	4-18-22-11W4M	2320
16	11-20-22-11W4M	2355
17	11-28-22-11W4M	2325

Cross-Section P-P' (Figure 33) (cont'd)

Well No.	Well Location	K.B. Elev.(ft.)
18	6-11-23-11W4M	2344
19	10-18-23-10W4M	2368
20	10-21-23-10W4M	2381
21	12-35-23-10W4M	2413
22	11-6-24-9W4M	2384
23	10-12-24-9W4M	2428
24	6-30-24-8W4M	2499

Cross-Section Q-Q' (Figure 34)

1	6-6-23-16W4M	2499
2	10-16-23-16W4M	2522
3	6-25-23-16W4M	2442
4	10-31-23-15W4M	2434
5	7-5-24-15W4M	2398
6	10-9-24-15W4M	2430
7	5-27-24-15W4M	2448
8	6-7-25-14W4M	2466
9	10-17-25-14W4M	2496
10	6-32-25-14W4M	2542
11	6-9-26-14W4M	2586
12	10-16-26-14W4M	2573
13	10-13-26-14W4M	2560
14	11-18-26-13W4M	2555
15	6-29-26-13W4M	2560

APPENDIX Ig

Cross-Section R-R' (Figure 37)

Well No.	Well Location	K.B. Elev.(ft.)
1	10-1-28-16W4M	2934
2	11-14-27-15W4M	2725
3	10-18-27-14W4M	2675
4	6-30-26-13W4M	2579
5	6-27-26-12W4M	2433
6	10-32-25-11W4M	2473
7	6-33-24-10W4M	2414
8	6-30-24-8W4M	2489
9	10-16-24-7W4M	2528
10	11-12-24-6W4M	2599
11	4-10-24-5W4M	2412
12	7-7-24-4W4M	2594

Cross-Section S-S' (Figure 38)

1	11-29-23-3W4M	2639
2	6-33-23-3W4M	2427
3	11-6-24-3W4M	2456
4	7-12-24-3W4M	2307
5	10-19-24-2W4M	2292
6	7-33-24-2W4M	2347
7	10-2-25-2W4M	2386
8	10-13-25-2W4M	2450
9	7-29-25-1W4M	2492
10	10-27-25-29W3M	2626

Cross-Section S-S' (Figure 38) (cont'd)

Well No.	Well Location	K.B. Elev.(ft.)
11	6-2-26-29W3M	2512
12	4-17-26-28W3M	2437
13	1-5-27-27W3M	2281

Cross-Section T-T' (Figure 39)

1	10-1-24-8W4M	2481
2	10-16-24-7W4M	2528
3	10-35-24-7W4M	2427
4	7-1-25-7W4M	2505
5	10-7-25-6W4M	2623
6	7-20-25-6W4M	2608
7	10-33-25-6W4M	2566
8	11-2-26-6W4M	2585
9	11-15-26-6W4M	2555
10	7-35-26-6W4M	2553
11	6-1-27-6W4M	2564
12	10-19-27-5W4M	2594
13	7-29-27-5W4M	2598
14	10-5-28-5W4M	2645
15	7-10-28-5W4M	2630
16	15-23-28-5W4M	2586
17	6-36-28-5W4M	2602
18	10-4-29-4W4M	2615
19	11-15-29-4W4M	2535

Cross-Section T-T' (Figure 39) (cont'd)

Well No.	Well Location	K.B. Elev.(ft.)
20	7-35-29-4W4M	2485
21	11-1-30-4W4M	2372
22	6-19-30-3W4M	2349
23	6-29-30-3W4M	2376
24	6-33-30-3W4M	2239
25	7-11-31-3W4M	2398
26	6-32-31-2W4M	2249
27	6-10-32-2W4M	2207
28	11-23-32-2W4M	2241
29	11-36-32-2W4M	2389
30	16-9-33-1W4M	2302
31	1-22-33-1W4M	2338
32	6-26-33-1W4M	2315

Cross-Section U-U' (Figure 40)

1	10-4-24-12W4M	2384
2	10-19-24-11W4M	2378
3	6-33-24-11W4M	2360
4	12-1-25-11W4M	2402
5	10-17-25-10W4M	2469
6	11-28-25-10W4M	2541
7	10-4-26-10W4M	2587
8	11-25-26-10W4M	2630
9	10-36-27-9W4M	2612

Cross-Section U-U' (Figure 40) (cont'd)

Well No.	Well Location	K.B. Elev.(ft.)
10	15-22-28-8W4M	2573
11	6-5-29-7W4M	2613
12	10-13-29-7W4M	2525
13	10-31-29-6W4M	2460
14	7-18-30-6W4M	2417
15	6-26-30-6W4M	2498
16	11-9-31-5W4M	2532
17	11-34-31-5W4M	2598

Cross-Section V-V' (Figure 41)

1	3-4-25-13W4M	2423
2	6-10-25-13W4M	2446
3	7-14-25-13W4M	2425
4	10-24-25-13W4M	2383
5	3-30-25-12W4M	2428
6	6-29-25-12W4M	2411
7	3-32-25-12W4M	2427
8	5-5-26-12W4M	2419
9	14-9-26-12W4M	2418
10	11-16-26-12W4M	2491
11	6-22-26-12W4M	2439
12	6-27-26-12W4M	2433
13	6-35-26-12W4M	2477
14	7-6-27-11W4M	2572
15	11-29-27-10W4M	2573

Cross-Section W-W' (Figure 42)

Well No.	Well Location	K.B. Elev.(ft.)
1	11-36-26-14W4M	2561
2	7-9-27-13W4M	2595
3	6-22-27-13W4M	2622
4	10-23-27-13W4M	2626
5	7-35-27-13W4M	2674
6	11-1-28-13W4M	2689
7	13-7-28-12W4M	2758
8	7-17-28-12W4M	2664
9	10-29-28-12W4M	2757
10	6-2-29-12W4M	2564
11	7-12-29-12W4M	2558
12	6-20-29-11W4M	2554
13	11-35-29-11W4M	2521
14	11-6-30-10W4M	2515
15	7-3-30-10W4M	2495
16	6-23-30-10W4M	2508
17	11-19-30-9W4M	2503
18	11-29-30-9W4M	2505
19	10-33-30-9W4M	2498
20	7-3-31-9W4M	2506
21	6-24-31-9W4M	2517
22	11-35-31-8W4M	2554

Cross-Section X-X' (Figure 43)

Well No.	Well Location	K.B. Elev.(ft.)
1	6-15-27-17W4M	2691
2	7-20-27-16W4M	2993
3	7-28-27-16W4M	2970
4	6-34-27-16W4M	2952
5	10-1-28-16W4M	2934
6	16-7-28-15W4M	2933
7	11-23-28-15W4M	2871
8	10-33-28-15W4M	2973
9	6-35-28-15W4M	2926
10	6-7-29-14W4M	2856
11	3-15-29-14W4M	2584
12	6-23-29-14W4M	2588
13	10-33-29-13W4M	2863
14	11-12-30-13W4M	2691
15	7-19-30-12W4M	2627
16	10-28-30-12W4M	2561
17	6-3-31-11W4M	2601
18	10-11-31-11W4M	2550
19	11-20-31-10W4M	2523

APPENDIX Ih

Cross-Section Y-Y' (Figure 46)

Well No.	Well Location	K.B. Elev.(ft.)
1	12-16-34-18W4M	2797
2	6-12-34-17W4M	2713
3	6-21-33-16W4M	2701
4	3-8-33-16W4M	2762
5	10-32-32-15W4M	2701
6	7-17-32-15W4M	2663
7	11-5-32-15W4M	2633
8	12-34-31-15W4M	2655
9	2-6-31-14W4M	2672
10	6-7-30-14W4M	2654
11	6-28-29-14W4M	2593
12	10-36-28-14W4M	2591
13	6-10-28-13W4M	2675
14	11-1-28-13W4M	2689
15	6-31-27-12W4M	2636
16	6-22-27-12W4M	2464
17	7-3-27-11W4M	2586
18	6-32-26-11W4M	2512
19	11-28-26-11W4M	2534
20	6-3-26-11W4M	2476

Cross-Section Z-Z' (Figure 47)

Well No.	Well Location	K.B. Elev.(ft.)
1	10-16-31-14W4M	2692
2	10-12-31-14W4M	2725
3	7-33-30-13W4M	2717
4	10-26-30-13W4M	2680
5	7-16-30-12W4M	2595
6	6-30-29-11W4M	2569
7	11-16-29-10W4M	2492
8	10-10-29-9W4M	2630
9	15-22-28-8W4M	2573
10	10-22-27-7W4M	2567
11	6-7-27-6W4M	2494
12	6-1-27-6W4M	2564
13	7-13-26-5W4M	2626
14	7-9-26-4W4M	2556

Cross-Section A'-A" (Figure 48)

1	11-12-30-17W4M	3538
2	10-23-30-16W4M	2905
3	10-24-30-16W4M	2887
4	10-22-30-15W4M	2790
5	2-6-31-14W4M	2672
6	9-8-31-14W4M	2690
7	10-16-31-14W4M	2692
8	7-26-31-14W4M	2777

Cross-Section A'-A" (Figure 48) (Cont'd)

Well No.	Well Location	K.B. Elev.(ft.)
9	7-35-31-14W4M	2837
10	10-1-32-14W4M	2774
11	6-18-32-13W4M	2760
12	6-22-32-13W4M	2689
13	10-35-32-13W4M	2662
14	6-12-33-13W4M	2656
15	10-24-33-12W4M	2582
16	6-24-34-11W4M	2557
17	10-36-34-11W4M	2557

APPENDIX Ii

Cross-Section B'-B" (Figure 52)

Well No.	Well Location	K.B. Elev.(ft.)
1	1-9-32-19W4M	2823
2	9-2-32-19W4M	2813
3	4-29-31-18W4M	2847
4	6-15-31-18W4M	2901
5	6-3-31-18W4M	2908
6	6-34-30-18W4M	2886
7	4-11-30-18W4M	2865
8	11-12-30-17W4M	3538
9	7-31-29-16W4M	3441
10	10-31-28-15W4M	3007
11	11-23-28-15W4M	2871
12	11-19-28-14W4M	2819

Cross-Section C'-C" (Figure 53)

1	13-5-29-18W4M	2725
2	8-10-29-18W4M	2837
3	7-13-29-18W4M	3000
4	4-32-29-17W4M	3467
5	11-12-30-17W4M	3538
6	7-35-30-16W4M	2819
7	6-5-31-15W4M	2853
8	10-3-31-15W4M	2742

Cross-Section D'-D" (Figure 54)

Well No.	Well Location	K.B. Elev.(ft.)
1	6-9-27-23W4M	2932
2	7-30-27-22W4M	2852
3	6-2-28-22W4M	2896
4	14-11-28-22W4M	2865
5	11-7-28-21W4M	3008
6	6-17-28-21W4M	2906
7	6-3-29-20W4M	2650
8	4-18-29-19W4M	2797
9	7-6-30-18W4M	2731
10	4-11-30-18W4M	2865
11	14-29-30-17W4M	3041
12	6-12-31-17W4M	2998
13	6-29-31-16W4M	2875
14	10-36-31-16W4M	2665
15	11-5-32-15W4M	2633
16	10-9-32-15W4M	2661

APPENDIX Ij

Cross-Section E'-E" (Figure 57)

Well No.	Well Location	K.B. Elev.(ft.)
1	10-6-34-22W4M	2890
2	10-21-33-22W4M	2944
3	11-1-33-22W4M	2702
4	10-29-32-21W4M	2732
5	12-22-32-21W4M	2758
6	4-13-32-21W4M	2777
7	4-21-32-20W4M	2723
8	11-15-32-20W4M	2728
9	10-10-32-20W4M	2741
10	11-36-31-20W4M	2791
11	10-13-31-20W4M	2752
12	10-7-31-19W4M	2738
13	6-10-31-19W4M	2809

Cross-Section F'-F" (Figure 58)

1	7-19-31-22W4M	2762
2	6-6-32-21W4M	2728
3	10-24-32-21W4M	2774
4	11-28-32-20W4M	2705
5	11-36-32-20W4M	2808
6	6-7-33-19W4M	2808
7	12-35-33-19W4M	2857
8	10-5-34-18W4M	2826
9	7-32-34-17W4M	2789
10	2-20-35-16W4M	2874

Cross-Section G'-G" (Figure 59)

Well No.	Well Location	K.B. Elev.(ft.)
1	11-19-32-23W4M	2944
2	6-30-32-22W4M	2765
3	6-4-33-22W4M	2943
4	6-11-33-22W4M	2800
5	10-13-33-22W4M	2691
6	10-32-33-21W4M	2831
7	11-17-34-21W4M	2963
8	2-24-34-21W4M	2697
9	6-22-34-20W4M	2806
10	7-27-34-20W4M	2750
11	15-3-35-19W4M	2732

APPENDIX Ik

Cross-Section H'-H" (Figure 62)

Well No.	Well Location	K.B. Elev.(ft.)
1	6-12-34-29W4M	3317
2	5-14-34-28W4M	3276
3	6-25-34-27W4M	3066
4	7-21-34-26W4M	3285
5	10-32-34-25W4M	3037
6	6-36-34-25W4M	3051
7	11-32-34-24W4M	2990
8	6-16-34-24W4M	3038
9	10-12-34-24W4M	2826
10	11-2-34-23W4M	3019
11	10-6-34-22W4M	2890
12	6-3-34-22W4M	2717
13	10-5-34-21W4M	2815

Cross-Section I'-I" (Figure 63)

1	7-20-32-27W4M	3166
2	1-4-33-26W4M	3027
3	6-31-33-25W4M	3080
4	6-3-34-25W4M	2916
5	2-18-34-24W4M	3094
6	11-32-34-24W4M	2990
7	10-16-35-23W4M	3109
8	11-27-35-23W4M	3097
9	7-2-36-23W4M	2921
10	7-23-36-23W4M	3009

Cross-Section I'-I" (Figure 63) (cont'd)

Well No.	Well Location	K.B. Elev. (ft.)
11	3-31-36-22W4M	3003
12	2-9-37-22W4M	2849
13	10-19-37-22W4M	3009
14	13-26-37-21W4M	2768
15	14-9-38-20W4M	2735
16	5-15-38-20W4M	2727
17	4-27-38-20W4M	2720

Cross-Section J'-J" (Figure 64)

1	2-6-33-28W4M	3247
2	7-15-33-28W4M	3223
3	7-34-33-28W4M	3289
4	6-5-34-27W4M	3270
5	12-1-35-27W4M	3185
6	7-8-35-26W4M	3402
7	10-35-35-26W4M	3064
8	6-26-36-25W4M	3050
9	9-7-37-24W4M	2995
10	10-16-37-24W4M	2957
11	15-22-37-24W4M	2811
12	11-24-37-24W4M	2817
13	3-31-37-23W4M	2816
14	5-5-38-23W4M	2779
15	4-15-38-23W4M	2799

APPENDIX I1

Cross-Section K'-K" (Figure 67)

Well No.	Well Location	K.B. Elev.(ft.)
1	10-33-39-28W4M	3006
2	7-25-39-28W4M	3104
3	11-20-39-27W4M	2931
4	8-20-39-27W4M	2905
5	11-12-39-27W4M	2762
6	16-6-39-26W4M	2925
7	6-4-39-26W4M	2701
8	13-33-38-26W4M	3218
9	7-33-38-26W4M	3110
10	5-34-38-26W4M	3041
11	4-35-38-26W4M	3046
12	3-35-38-26W4M	3117

Cross-Section L'-L" (Figure 68)

1	11-17-37-25W4M	3208
2	10-34-37-25W4M	2837
3	1-11-38-25W4M	2795
4	6-12-38-25W4M	2816
5	12-12-38-25W4M	2818
6	11-12-38-25W4M	2857
7	16-12-38-25W4M	2897
8	4-18-38-24W4M	2916
9	11-17-38-24W4M	2900
10	16-16-38-24W4M	2885
11	3-25-38-24W4M	2706

Cross-Section M'-M" (Figure 69)

Well No.	Well Location	K.B. Elev.(ft.)
1	2-6-37-27W4M	2948
2	6-5-37-27W4M	2995
3	6-16-37-27W4M	2981
4	4-23-37-27W4M	2959
5	9-25-37-27W4M	2954
6	4-5-38-26W4M	3052
7	4-14-38-26W4M	3072
8	6-24-38-26W4M	2942
9	10-24-38-26W4M	2950
10	16-24-38-26W4M	2988
11	4-30-38-25W4M	3012
12	6-30-38-25W4M	2958
13	11-30-38-25W4M	2943

Cross-Section N'-N" (Figure 70)

1	4-33-38-27W4M	2877
2	9-2-39-27W4M	2782
3	3-12-39-27W4M	2775
4	7-12-39-27W4M	2762
5	9-12-39-27W4M	2767
6	16-12-39-27W4M	2758
7	13-7-39-26W4M	2761
8	3-18-39-26W4M	2733
9	1-18-39-26W4M	2731

Cross-Section N'-N" (Figure 70) (cont'd)

Well No.	Well Location	K.B. Elev.(ft.)
10	11-17-39-26W4M	2845
11	3-21-39-26W4M	2939
12	11-22-39-26W4M	2963
13	12-26-39-26W4M	3047
14	12-5-40-25W4M	3138
15	1-9-40-25W4M	2953
16	13-36-40-25W4M	2806

Cross-Section O'-O" (Figure 71)

1	7-9-39-28W4M	3039
2	7-25-39-28W4M	3104
3	1-7-40-27W4M	3067
4	6-12-40-27W4M	2809
5	10-18-40-26W4M	2792
6	10-32-40-26W4M	2780
7	13-11-41-26W4M	2886
8	11-29-41-25W4M	3039
9	1-22-42-25W4M	2868
10	2-32-42-24W4M	2871

APPENDIX Im

Cross-Section P'-P" (Figure 75)

Well No.	Well Location	K.B. Elev.(ft.)
1	11-28-35-18W4M	2724
2	9-23-35-18W4M	2715
3	10-31-35-17W4M	2748
4	6-5-36-17W4M	2730
5	10-10-36-17W4M	2733
6	10-14-36-17W4M	2755
7	11-24-36-17W4M	2779
8	6-31-36-16W4M	2790
9	7-17-37-16W4M	2753
10	10-27-37-16W4M	2724
11	13-11-38-16W4M	2750
12	6-33-38-15W4M	2717
13	6-2-39-15W4M	2608
14	10-23-39-15W4M	2352
15	11-35-39-14W4M	2400
16	6-14-42-12W4M	2245

Cross-Section Q'-Q" (Figure 76)

1	10-8-37-24W4M	2962
2	10-16-37-24W4M	2957
3	11-25-37-24W4M	2836
4	3-31-37-23W4M	2816
5	6-3-38-23W4M	2820
6	6-14-38-23W4M	2800

Cross-Section Q'-Q" (Figure 76) (cont'd)

Well No.	Well Location	K.B. Elev.(ft.)
7	7-36-38-23W4M	2696
8	14-2-39-22W4M	2575
9	15-11-39-22W4M	2607
10	11-21-39-21W4M	2754
11	2-34-39-21W4M	2685
12	13-1-40-21W4M	2680
13	10-6-40-20W4M	2717
14	7-16-40-20W4M	2682
15	7-21-40-20W4M	2647
16	6-30-40-19W4M	2664
17	6-10-41-19W4M	2582
18	3-14-41-19W4M	2569
19	11-25-41-19W4M	2565
20	7-31-41-18W4M	2559
21	6-7-42-18W4M	2565
22	16-16-42-18W4M	2523

Cross-Section R'-R" (Figure 77)

1	10-12-39-21W4M	2689
2	11-21-39-21W4M	2754
3	2-34-39-21W4M	2685
4	13-1-40-21W4M	2680
5	3-30-40-21W4M	2597

Cross-Section R'-R" (Figure 77) (cont'd)

Well No.	Well Location	K.B. Elev.(ft.)
6	4-32-40-21W4M	2621
7	12-4-41-21W4M	2628
8	9-14-41-21W4M	2597

Cross-Section S'-S" (Figure 78)

1	10-33-38-24W4M	2867
2	16-3-39-24W4M	2772
3	4-11-39-24W4M	2779
4	4-19-39-23W4M	2842
5	14-29-39-23W4M	2844
6	10-33-39-23W4M	2697
7	1-4-40-23W4M	2769
8	9-11-40-23W4M	2644
9	6-13-40-23W4M	2748
10	10-31-40-22W4M	2595
11	10-8-41-22W4M	2595
12	6-16-41-22W4M	2676
13	12-22-41-22W4M	2853
14	6-35-41-22W4M	2730
15	11-1-42-22W4M	2621
16	14-24-42-22W4M	2614
17	5-29-42-21W4M	2644
18	10-2-43-21W4M	2544
19	7-18-43-20W4M	2502

Cross-Section S'-S" (Figure 78) (cont'd)

Well No.	Well Location	K.B. Elev.(ft.)
20	10-32-43-20W4M	2586
21	11-11-44-20W4M	2622
22	16-13-44-20W4M	2501
23	13-20-44-19W4M	2475
24	10-28-44-19W4M	2414
25	6-34-44-19W4M	2387
26	12-11-45-19W4M	2359

Cross-Section T'-T" (Figure 79)

1	2-4-43-24W4M	2855
2	10-22-43-24W4M	2646
3	7-26-43-24W4M	2595
4	11-36-43-24W4M	2592
5	5-5-44-23W4M	2559
6	7-21-44-23W4M	2559
7	10-36-44-23W4M	2478
8	3-8-45-22W4M	2524
9	10-22-45-22W4M	2472
10	3-31-45-21W4M	2457
11	6-5-46-21W4M	2460
12	4-10-46-21W4M	2271
13	1-23-46-21W4M	2446
14	10-30-46-20W4M	2483
15	8-33-46-20W4M	2444
16	5-1-47-20W4M	2460

Cross-Section U'-U" (Figure 80)

Well No.	Well Location	K.B. Elev. (ft.)
1	6-14-43-28W4M	2864
2	16-24-43-28W4M	2992
3	6-29-43-27W4M	2836
4	11-3-44-27W4M	2689
5	10-11-44-27W4M	2860
6	1-29-44-26W4M	2787
7	10-8-45-25W4M	2690
8	6-15-45-25W4M	2768
9	4-23-45-25W4M	2648
10	4-20-45-24W4M	2555
11	10-24-45-24W4M	2509
12	11-29-45-23W4M	2535
13	9-17-46-23W4M	2484
14	10-30-46-23W4M	2481
15	10-1-47-23W4M	2445
16	7-8-47-22W4M	2543
17	10-21-47-22W4M	2487
18	8-27-47-22W4M	2458
19	10-31-47-21W4M	2476
20	6-8-48-21W4M	2519
21	3-15-48-21W4M	2486
22	14-23-48-21W4M	2481
23	2-25-48-21W4M	2485
24	11-8-49-20W4M	2628
25	7-25-49-20W4M	2647

Cross-Section V'-V" (Figure 81)

Well No.	Well Location	K.B. Elev.(ft.)
1	16-21-45-28W4M	2858
2	10-34-45-28W4M	2824
3	2-6-46-27W4M	2818
4	12-19-46-27W4M	2865
5	13-2-47-27W4M	2714
6	2-12-47-27W4M	2689
7	10-11-47-26W4M	2566
8	4-13-47-26W4M	2627
9	7-28-47-25W4M	2584
10	10-35-47-25W4M	2537
11	7-12-48-25W4M	2513
12	16-6-48-24W4M	2475
13	16-16-48-24W4M	2547
14	6-26-48-24W4M	2527
15	7-33-48-23W4M	2523
16	10-16-49-23W4M	2482
17	14-22-49-23W4M	2501
18	7-27-49-23W4M	2509
19	15-7-50-22W4M	2503
20	11-16-50-22W4M	2522
21	9-22-50-22W4M	2539
22	3-26-50-22W4M	2553
23	4-31-50-21W4M	2546
24	4-14-51-21W4M	2471

Cross-Section W'-W" (Figure 82)

Well No.	Well Location	K.B. Elev.(ft.)
1	7-6-50-23W4M	2467
2	6-8-50-23W4M	2433
3	4-26-50-23W4M	2506
4	10-36-50-23W4M	2499
5	10-5-51-22W4M	2491
6	14-4-51-22W4M	2555
7	6-9-51-22W4M	2533

Cross-Section X'-X" (Figure 83)

Well No.	Well Location	K.B. Elev.(ft.)
1	4-25-51-24W4M	2391
2	10-19-51-23W4M	2442
3	7-28-51-23W4M	2399
4	7-27-51-23W4M	2374
5	10-26-51-23W4M	2449
6	6-25-51-23W4M	2474
7	12-29-51-22W4M	2500

Cross-Section Y'-Y" (Figure 84)

Well No.	Well Location	K.B. Elev. (ft.)
1	11-14-49-27W4M	2428
2	1-23-49-27W4M	2423
3	12-26-49-27W4M	2411
4	15-35-49-27W4M	2378
5	11-1-50-27W4M	2369
6	10-10-50-27W4M	2372
7	12-28-50-27W4M	2307
8	10-4-51-27W4M	2314
9	2-14-51-27W4M	2328
10	5-24-51-27W4M	2329
11	6-25-51-27W4M	2325
12	6-36-51-27W4M	2324

APPENDIX In

Cross-Section Z'-Z" (Figure 90)

Well No.	Well Location	K.B. Elev.(ft.)
1	10-24-49-22W4M	2541
2	6-31-49-21W4M	2558
3	10-32-49-21W4M	2562
4	4-8-50-20W4M	2612
5	7-15-50-20W4M	2503
6	4-19-50-19W4M	2460
7	6-32-50-19W4M	2375
8	7-6-51-18W4M	2276
9	6-8-51-18W4M	2220
10	13-14-51-18W4M	2204

Cross-Section A"-A'" (Figure 91)

1	10-36-45-19W4M	2341
2	11-8-46-18W4M	2341
3	10-27-46-18W4M	2367
4	10-35-46-18W4M	2357
5	6-36-46-18W4M	2356
6	7-7-47-17W4M	2370
7	7-17-47-17W4M	2395
8	11-21-47-17W4M	2376
9	10-27-47-17W4M	2344
10	11-36-47-17W4M	2376
11	11-6-48-16W4M	2339
12	10-15-48-16W4M	2225

APPENDIX Io

Cross-Section B"-B"' (Figure 95)

Well No.	Well Location	K.B. Elev.(ft.)
1	10-29-32-14W4M	2742
2	7-19-31-13W4M	2769
3	10-28-30-12W4M	2561
4	7-16-30-11W4M	2569
5	11-30-29-10W4M	2508
6	6-14-29-9W4M	2585
7	7-7-29-8W4M	2554
8	11-35-28-8W4M	2581
9	10-16-28-7W4M	2610
10	10-8-28-6W4M	2452
11	10-25-27-6W4M	2482
12	11-18-27-4W4M	2620
13	6-1-27-4W4M	2473
14	11-21-26-3W4M	2397
15	7-19-26-2W4M	2477
16	1-20-25-1W4M	2490
17	7-9-25-29W3M	2452
18	1-23-24-29W3M	2220
19	4-6-25-26W3M	2275
20	9-11-24-25W3M	--

Cross-Section C"-C"' (Figure 96)

Well No.	Well Location	K.B. Elev.(ft.)
1	1-22-31-8W4M	2547
2	7-3-31-8W4M	2529
3	7-17-30-7W4M	2496
4	11-6-30-7W4M	2476
5	10-29-29-7W4M	2605
6	8-11-29-7W4M	2585
7	6-21-28-6W4M	2493
8	10-14-28-6W4M	2555
9	6-1-28-6W4M	2531

Cross-Section D"-D"' (Figure 99)

1	6-36-28-2W4M	2351
2	7-5-29-1W4M	2438
3	7-17-29-1W4M	2403
4	10-16-29-1W4M	2457
5	11-26-29-1W4M	2360
6	11-36-29-1W4M	2347
7	11-12-30-29W3M	2260

Cross-Section E"-E"' (Figure 100)

1	1-23-24-29W3M	2220
2	7-9-25-29W3M	2452
3	6-2-26-29W3M	2512
4	4-17-26-28W3M	2437
5	6-22-27-29W3M	2298

Cross-Section E"-E"' (Figure 100) (cont'd)

Well No.	Well Location	K.B. Elev. (ft.)
6	11-12-28-29W3M	2313
7	11-35-28-29W3M	2329
8	6-15-29-29W3M	2347
9	7-25-29-29W3M	2284
10	10-35-29-29W3M	2305
11	16-3-30-29W3M	2371
12	11-12-30-29W3M	2260
13	3-24-30-29W3M	2214
14	10-24-30-29W3M	2174
15	6-25-30-29W3M	2213
16	1-36-30-29W3M	2214
17	10-32-30-28W3M	2310
18	10-6-31-27W3M	2215
19	7-9-31-27W3M	2268
20	7-16-31-27W3M	2296
21	13-29-31-27W3M	2373
22	7-32-31-27W3M	2363
23	10-7-32-27W3M	2311
24	10-33-32-27W3M	2377
25	6-6-33-27W3M	2354

Cross-Section F"-F"' (Figure 101)

Well No.	Well Location	K.B. Elev. (ft.)
1	10-18-24-26W3M	2264
2	4-6-25-26W3M	2275
3	10-35-25-26W3M	2302
4	1-27-26-26W3M	2460
5	7-2-27-26W3M	2442
6	11-17-27-26W3M	2326
7	1-34-27-26W3M	2374
8	11-11-28-26W3M	2388
9	11-28-28-26W3M	2445
10	10-6-29-26W3M	2380
11	8-10-29-26W3M	2468
12	4-22-29-26W3M	2447
13	7-27-29-26W3M	2359
14	15-3-30-26W3M	2367
15	1-15-30-26W3M	2358
16	11-22-30-26W3M	2375
17	15-35-30-26W3M	2325
18	7-2-31-26W3M	2357
19	10-10-31-26W3M	2308
20	10-15-31-26W3M	2329
21	8-22-31-26W3M	2331
22	7-27-31-26W3M	2349
23	7-6-32-26W3M	2366
24	9-10-32-26W3M	2378

Cross-Section F"-F"' (Figure 101) (Cont'd)

Well No.	Well Location	K.B. Elev. (ft.)
25	11-20-32-26W3M	2380
26	6-29-32-26W3M	2333

Cross-Section G"-G"' (Figure 102)

Well No.	Well Location	K.B. Elev. (ft.)
1	8-5-24-25W3M	2212
2	7-9-24-25W3M	2226
3	11-14-24-25W3M	2262
4	11-20-24-24W3M	2283
5	6-32-24-24W3M	2360
6	6-7-25-24W3M	2324
7	6-22-25-24W3M	2274
8	4-29-26-24W3M	2407
9	4-32-26-24W3M	2444
10	3-4-27-24W3M	2385
11	7-16-27-24W3M	2327
12	11-35-27-24W3M	2254
13	16-14-28-24W3M	2273
14	11-25-28-24W3M	2252
15	6-2-29-24W3M	2233
16	6-14-29-24W3M	2256
17	4-11-30-24W3M	2260
18	15-13-30-24W3M	2260
19	7-36-30-24W3M	2291
20	9-2-31-24W3M	2353

Cross-Section G"-G"' (Figure 102) (cont'd)

Well No.	Well Location	K.B. Elev. (ft.)
21	8-12-31-24W3M	2312
22	9-13-31-24W3M	2350
23	3-24-31-24W3M	2349
24	5-3-32-24W3M	2339
25	6-24-32-24W3M	2326

APPENDIX Ip

Cross-Section H"-H" (Figure 105)

Well No.	Well Location	K.B. Elev.(ft.)
1	6-18-32-6W5M	4140
2	1-29-31-4W5M	3630
3	7-10-31-4W5M	3845
4	12-2-30-5W5M	3945
5	7-20-29-2W5M	3768
6	6-31-28-28W4M	3370
7	10-10-28-29W4M	3701
8	10-8-27-28W4M	3655
9	11-19-26-28W4M	3658
10	6-6-25-27W4M	3340
11	10-7-24-27W4M	3353
12	10-25-23-27W4M	3300

Cross-Section I"-I"' (Figure 106)

1	8-16-26-5W5M	3922
2	10-34-26-4W5M	4268
3	10-12-27-4W5M	4202
4	10-14-27-3W5M	4154
5	6-30-27-2W5M	4081
6	10-10-28-2W5M	3977
7	6-36-28-2W5M	3808
8	8-11-29-1W5M	3481
9	6-23-29-29W4M	3407
10	10-5-30-28W4M	3282

Cross-Section I"-I"' (Figure 106) (cont'd)

Well No.	Well Location	K.B. Elev.(ft.)
11	10-22-30-28W4M	3211
12	6-25-30-28W4M	3158
13	10-4-31-27W4M	3082
14	11-26-31-27W4M	3102
15	13-14-32-26W4M	3036
16	11-35-32-25W4M	2954
17	6-5-33-24W4M	2848
18	10-34-33-24W4M	3060
19	11-2-34-23W4M	3019

Cross-Section J"-J"' (Figure 107)

1	2-14-22-2W5M	3803
2	10-14-23-1W5M	3429
3	4-13-23-29W4M	3384
4	10-33-24-28W4M	3472
5	10-23-25-28W4M	3448
6	11-36-25-27W4M	3147
7	6-4-26-25W4M	3176
8	7-27-26-25W4M	3082
9	11-6-27-24W4M	3054
10	6-26-27-24W4M	2942
11	10-13-28-23W4M	2881
12	10-33-28-22W4M	2770
13	7-1-29-22W4M	2727

Cross-Section J"-J"' (Figure 107) (cont'd)

Well No.	Well Location	K.B. Elev.(ft.)
14	10-18-29-21W4M	2663
15	11-32-29-21W4M	2662
16	6-2-30-21W4M	2652
17	6-16-30-20W4M	2749
18	7-34-30-20W4M	2712
19	11-12-31-20W4M	2737
20	15-29-31-19W4M	2781
21	7-20-32-19W4M	2853

APPENDIX IIa

Well Locations for Figure 19

Well No.	Well Location	K.B. Elev.(ft.)
1	12-4-30-8W4M	2552
2	7-17-31-1W4M	2315
3	10-7-31-2W4M	2462
4	6-10-31-3W4M	2399
5	7-6-31-6W4M	2550
6	7-8-31-7W4M	2561
7	10-31-31-7W4M	2664
8	9-16-31-8W4M	2548
9	6-24-31-9W4M	2517
10	6-1-31-9W4M	2510
11	15-14-31-10W4M	2507
12	10-11-31-11W4M	2550
13	6-3-31-11W4M	2601
14	7-6-31-12W4M	2652
15	10-32-32-15W4M	2701
16	6-22-32-14W4M	2748
17	7-11-32-14W4M	2841
18	10-29-32-12W4M	2610
19	11-11-32-11W4M	2544
20	6-29-32-9W4M	2528
21	11-35-32-8W4M	2480
22	11-32-32-7W4M	2476
23	7-2-32-7W4M	2560
24	11-2-32-5W4M	2630
25	11-11-32-4W4M	2371

Well No.	Well Location	K.B. Elev. (ft.)
26	10-10-32-3W4M	2307
27	7-1-32-2W4M	2280
28	7-12-32-1W4M	2359
29	8-12-33-2W4M	2396
30	6-6-33-2W4M	2207
31	10-32-33-2W4M	2387
32	10-16-33-3W4M	2217
33	16-1-33-4W4M	2304
34	11-3-33-5W4M	2643
35	11-3-33-6W4M	2494
36	11-13-33-7W4M	2480
37	10-1-33-9W4M	2537
38	11-30-33-10W4M	2545
39	10-24-33-12W4M	2582
40	11-33-33-13W4M	2721
41	10-9-33-13W4M	2699
42	10-1-33-14W4M	2699
43	11-22-33-14W4M	2742
44	4-23-33-15W4M	2751
45	11-10-33-15W4M	2775
46	10-20-33-15W4M	2866
47	6-21-33-16W4M	2701
48	16-5-33-16W4M	2754
49	7-13-33-17W4M	2725
50	8-7-34-19W4M	3765

Well No.	Well Location	K.B. Elev.(ft.)
51	4-30-34-18W4M	2776
52	10-5-34-18W4M	2826
53	7-2-34-18W4M	2710
54	7-32-34-17W4M	3412
55	6-12-34-17W4M	2713
56	10-10-34-16W4M	2837
57	6-25-34-16W4M	2853
58	14-17-34-15W4M	2810
59	11-15-34-14W4M	2703
60	7-13-34-13W4M	2664
61	7-4-34-12W4M	2588
62	11-7-34-11W4M	2586
63	6-20-34-11W4M	2614
64	4-27-34-10W4M	2555
65	2-6-34-9W4M	2535
66	10-2-34-9W4M	2561
67	7-25-34-8W4M	2532
68	10-36-34-7W4M	2442
69	7-33-34-6W4M	2514
70	7-36-34-5W4M	2238
71	7-33-34-4W4M	2254
72	10-20-34-2W4M	2371
73	7-3-34-2W4M	2437
74	15-15-34-1W4M	2400
75	10-20-35-1W4M	2362

Well No.	Well Location	K.B. Elev.(ft.)
76	6-31-35-2W4M	2551
77	10-26-35-4W4M	2380
78	6-30-35-5W4M	2482
79	12-27-35-6W4M	2530
80	7-30-35-6W4M	2509
81	10-6-35-6W4M	2560
82	10-15-35-7W4M	2599
83	10-32-35-7W4M	2599
84	7-27-35-8W4M	2695
85	11-7-35-8W4M	2631
86	13-6-35-9W4M	2535
87	11-27-35-9W4M	2630
88	6-33-35-9W4M	2627
89	1-26-35-10W4M	2544
90	4-18-35-10W4M	2619
91	7-27-35-13W4M	2680
92	1-30-35-13W4M	2701
93	11-28-35-14W4M	2656
94	10-4-35-15W4M	2734
95	2-20-35-16W4M	2874
96	10-3-36-18W4M	2780
97	6-20-36-19W4M	2842
98	10-21-36-18W4M	2756
99	6-21-36-17W4M	2719
100	6-17-36-16W4M	2799

Well No.	Well Location	K.B. Elev.(ft.)
101	11-20-36-15W4M	2746
102	6-27-36-15W4M	2689
103	10-22-36-13W4M	2692
104	7-11-36-13W4M	2689
105	10-14-36-12W4M	2630
106	7-36-36-12W4M	2658
107	2-13-36-11W4M	2606
108	6-18-36-9W4M	2575
109	6-20-36-9W4M	2587
110	7-6-36-8W4M	2580
111	11-28-36-8W4M	2690
112	11-35-36-8W4M	2649
113	7-12-36-8W4M	2547
114	11-15-36-7W4M	2466
115	6-23-36-7W4M	2448
116	11-33-36-6W4M	2524
117	11-5-36-6W4M	2512
118	10-35-36-6W4M	2447
119	11-12-36-6W4M	2382
120	10-17-36-5W4M	2410
121	10-25-36-5W4M	2214
122	6-4-36-3W4M	2447
123	11-32-36-2W4M	2197
124	6-16-36-1W4M	2284
125	2-30-37-1W4M	2294

Well No.	Well Location	K.B. Elev.(ft.)
126	6-2-37-4W4M	2189
127	11-13-37-5W4M	2248
128	10-17-37-5W4M	2425
129	11-29-37-5W4M	2289
130	10-18-37-6W4M	2455
131	7-25-37-7W4M	2488
132	7-3-37-7W4M	2431
133	7-24-37-8W4M	2673
134	10-7-37-8W4M	2698
135	10-36-37-9W4M	2317
136	11-6-37-9W4M	2499
137	10-29-37-9W4M	2483
138	7-14-37-11W4M	2468
139	1-28-37-11W4M	2461
140	6-17-37-12W4M	2624
141	11-36-37-13W4M	2541
142	10-30-37-13W4M	2746
143	6-18-37-13W4M	2697
144	10- 5 -37-14W4M	2685
145	11-31-37-14W4M	2699
146	10-10-37-16W4M	2798
147	6-4-37-18W4M	2775
148	11-19-37-18W4M	2758
149	5-33-37-18W4M	2729
150	10-34-37-19W4M	2742

APPENDIX IIb

Well Locations for Figure 50a

Well No.	Well Location	K.B. Elev. (ft.)
1	1-5-29-9W4M	2689
2	10-18-29-9W4M	2612
3	10-18-29-10W4M	2490
4	10-13-29-11W4M	2489
5	10-5-29-11W4M	2532
6	10-23-29-12W4M	2607
7	7-1-29-13W4M	2770
8	7-11-29-14W4M	2596
9	7-27-29-14W4M	2603
10	11-14-29-15W4M	3104
11	6-11-29-17W4M	3423
12	11-29-29-16W4M	3380
13	4-6-29-17W4M	2851
14	10-1-30-18W4M	3036
15	10-30-30-18W4M	2822
16	10-28-30-18W4M	2828
17	14-29-30-17W4M	3041
18	11-12-30-17W4M	3538
19	12-2-30-16W4M	3049
20	10-27-30-16W4M	2851
21	10-22-30-15W4M	2790
22	6-7-30-14W4M	2654
23	10-30-30-14W4M	2640
24	10-26-30-14W4M	2670
25	11-12-30-14W4M	2710

Well No.	Well Location	K.B. Elev.(ft.)
26	11-20-30-13W4M	2790
27	11-12-30-13W4M	2691
28	7-33-30-13W4M	2717
29	10-14-30-12W4M	2546
30	7-18-30-11W4M	2574
31	6-14-30-11W4M	2551
32	6-19-30-10W4M	2527
33	10-20-30-10W4M	2510
34	10-11-31-11W4M	2550
35	6-3-31-11W4M	2601
36	7-35-31-11W4M	2547
37	10-18-31-11W4M	2544
38	16-15-31-12W4M	2533
39	7-6-31-12W4M	2652
40	11-12-31-13W4M	2675
41	6-8-31-13W4M	2752
42	11-17-31-13W4M	2779
43	6-1-31-14W4M	2733
44	6-3-31-14W4M	2712
45	2-6-31-14W4M	2672
46	10-3-31-15W4M	2741
47	12-34-31-15W4M	2655
48	6-32-31-15W4M	2793
49	6-12-31-16W4M	2748
50	6-28-31-17W4M	2967

Well No.	Well Location	K.B. Elev.(ft.)
51	6-1-31-18W4M	2930
52	4-10-31-18W4M	2920
53	2-6-31-18W4M	2801
54	11-17-32-18W4M	2867
55	6-30-32-18W4M	2850
56	8-34-32-17W4M	2783
57	10-14-32-17W4M	2721
58	10-9-32-16W4M	2743
59	1-14-32-16W4M	2811
60	10-29-32-14W4M	2742
61	6-22-32-14W4M	2749
62	6-22-32-13W4M	2689
63	2-6-32-14W4M	2626
64	10-1-32-14W4M	2774
65	10-4-32-13W4M	2723
66	7-15-32-12W4M	2556
67	11-1-32-12W4M	2534
68	11-24-32-12W4M	2550
69	1-13-32-11W4M	2551
70	6-31-32-12W4M	2622
71	6-33-32-11W4M	2575
72	10-36-32-11W4M	2561
73	6-34-32-10W4M	2522

APPENDIX IIc

Well Locations for Figure 50b

Well No.	Well Location	K.B. Elev.(ft.)
1	10-12-26-11W4M	2488
2	10-7-26-11W4M	2504
3	6-22-26-11W4M	2571
4	10-36-26-11W4M	2545
5	11-24-26-12W4M	2491
6	6-35-26-12W4M	2477
7	6-33-26-12W4M	2425
8	2-31-26-12W4M	2479
9	7-13-26-13W4M	2485
10	6-30-26-13W4M	2579
11	10-30-26-14W4M	2630
12	10-29-26-15W4M	2732
13	10-29-26-16W4M	2718
14	11-19-26-17W4M	3054
15	6-30-27-16W4M	3056
16	7-20-27-16W4M	2980
17	10-24-27-16W4M	2825
18	7-17-27-15W4M	2776
19	6-15-27-15W4M	2765
20	6-32-27-14W4M	2721
21	10-34-27-14W4M	2611
22	6-8-27-14W4M	2647
23	11-15-27-14W4M	2628
24	6-22-27-13W4M	2622
25	10-23-27-13W4M	2626

Well No.	Well Location	K.B. Elev.(ft.)
26	6-25-27-13W4M	2640
27	10-20-27-12W4M	2515
28	6-22-27-12W4M	2464
29	6-11-27-12W4M	2471
30	10-18-27-11W4M	2546
31	15-29-27-11W4M	2541
32	7-10-27-11W4M	2566
33	1-12-27-11W4M	2563
34	6-12-28-11W4M	2600
35	10-34-28-11W4M	2467
36	11-32-28-11W4M	2519
37	6-21-28-11W4M	2471
38	10-7-28-11W4M	2489
39	10-11-28-12W4M	--
40	13-7-28-12W4M	2758
41	10-29-28-12W4M	2757
42	6-10-28-13W4M	2675
43	6-27-28-14W4M	2633
44	11-19-28-14W4M	2819
45	11-23-28-15W4M	2871
46	10-9-28-15W4M	2883
47	6-35-28-15W4M	2926
48	10-31-28-15W4M	3007
49	6-33-28-16W4M	3157
50	6-6-28-16W4M	3028

Well No.	Well Location	K.B. Elev.(ft.)
51	11-29-28-17W4M	2927
52	4-32-29-17W4M	3467
53	7-31-29-16W4M	3442
54	11-30-29-15W4M	3111
55	7-16-29-15W4M	3146
56	6-7-29-14W4M	2856
57	6-28-29-14W4M	2593
58	10-2-29-14W4M	2584
59	6-4-29-13W4M	2727
60	10-33-29-13W4M	2863
61	10-15-29-13W4M	2739
62	7-1-29-13W4M	2770
63	6-29-29-12W4M	2659
64	10-23-29-12W4M	2607
65	7-12-29-12W4M	2558
66	6-20-29-11W4M	2554
67	10-13-29-11W4M	2487

APPENDIX IId

Well Locations for Figure 89a

Well No.	Well Location	K.B. Elev.(ft.)
1	7-32-38-16W4M	2700
2	7-26-38-18W4M	2687
3	7-16-38-18W4M	2779
4	10-29-38-19W4M	2720
5	4-27-38-20W4M	2720
6	14-7-38-20W4M	2714
7	10-35-38-21W4M	2669
8	2-15-38-22W4M	2574
9	16-10-38-24W4M	2830
10	6-3-39-26W4M	3237
11	10-8-39-25W4M	2909
12	8-15-39-24W4M	2928
13	13-17-39-23W4M	2739
14	2-13-39-23W4M	2758
15	7-9-39-22W4M	2880
16	11-25-39-22W4M	2700
17	10-26-39-21W4M	2679
18	10-23-39-20W4M	2679
19	10-24-39-18W4M	2556
20	11-31-39-16W4M	2542
21	10-32-39-16W4M	2525
22	11-29-39-15W4M	2369
23	6-19-40-18W4M	2588
24	7-16-40-20W4M	2682
25	6-18-40-21W4M	2590

Well No.	Well Location	K.B. Elev.(ft.)
26	11-24-40-22W4M	2577
27	12-16-40-22W4M	2642
28	1-7-40-23W4M	2998
29	9-10-40-24W4M	2960
30	11-8-40-24W4M	2926
31	11-2-40-26W4M	3266
32	11-35-40-25W4M	2829
33	10-25-40-26W4M	3021
34	6-12-41-28W4M	3032
35	14-20-41-27W4M	3032
36	14-28-41-26W4M	2773
37	2-15-41-25W4M	2889
38	8-7-41-24W4M	2767
39	4-32-41-24W4M	2877
40	2-5-41-24W4M	2768
41	2-11-41-24W4M	2868
42	10-7-41-23W4M	2839
43	1-32-41-23W4M	2978
44	12-22-41-22W4M	2853
45	4-13-41-21W4M	2586
46	11-19-41-18W4M	2556
47	10-20-41-17W4M	2458
48	4-15-41-16W4M	2394
49	5-20-42-17W4M	2472
50	11-25-42-19W4M	2385

Well No.	Well Location	K.B. Elev.(ft.)
51	6-15-42-20W4M	2673
52	6-15-42-21W4M	2650
53	15-5-42-21W4M	2598
54	5-29-42-21W4M	2644
55	10-36-42-24W4M	2829
56	3-1-42-25W4M	2913
57	3-26-42-26W4M	2679
58	7-35-42-28W4M	2929
59	11-27-43-27W4M	2811
60	7-1-43-26W4M	2733
61	11-8-43-25W4M	2708
62	7-2-43-22W4M	2594
63	10-2-43-21W4M	2544
64	7-18-43-20W4M	2502
65	2-26-43-20W4M	2566
66	10-28-43-19W4M	2608
67	6-35-43-18W4M	2369
68	10-21-43-16W4M	2358
69	6-33-44-17W4M	2313
70	12-33-44-18W4M	2350
71	6-32-44-19W4M	2336
72	4-31-44-19W4M	2426
73	11-30-44-20W4M	2533
74	11-7-44-20W4M	2614
75	1-35-44-22W4M	2575

Well No.	Well Location	K.B. Elev.(ft.)
76	10-1-44-23W4M	2561
77	11-2-44-24W4M	2598
78	8-24-44-24W4M	2581
79	10-22-44-24W4M	2620
80	7-20-44-24W4M	2642
81	10-23-44-25W4M	2714
82	10-29-44-26W4M	2787
83	10-34-44-27W4M	2789
84	5-2-44-28W4M	2994

APPENDIX IIe

Well Locations for Figure 89b

Well No.	Well Location	K.B. Elev.(ft.)
1	7-14-45-16W4M	2355
2	7-18-45-16W4M	2322
3	7-16-45-17W4M	2348
4	10-17-45-18W4M	2324
5	10-7-45-19W4M	2365
6	16-11-45-20W4M	2390
7	3-35-45-20W4M	2380
8	7-35-45-21W4M	2447
9	6-2-45-21W4M	2524
10	1-1-45-22W4M	2493
11	3-8-45-22W4M	2524
12	10-22-45-22W4M	2472
13	10-24-45-24W4M	2509
14	4-20-45-24W4M	2555
15	10-8-45-25W4M	2690
16	10-9-45-26W4M	2730
17	7-15-45-27W4M	2829
18	7-26-46-28W4M	2829
19	10-11-46-27W4M	2788
20	10-11-46-26W4M	2633
21	10-11-46-25W4M	2582
22	10-30-46-23W4M	2481
23	11-30-46-22W4M	2462
24	6-5-46-21W4M	2460
25	1-23-46-21W4M	2446

Well No.	Well Location	K.B. Elev.(ft.)
26	6-34-46-21W4M	2486
27	10-30-46-20W4M	2483
28	10-28-46-20W4M	2458
29	14-36-46-20W4M	2465
30	10-26-46-19W4M	2413
31	1-11-46-19W4M	2379
32	7-14-46-18W4M	2341
33	11-24-46-17W4M	2324
34	6-24-46-16W4M	2329
35	10-20-47-17W4M	2387
36	10-8-47-18W4M	2402
37	6-11-47-19W4M	2445
38	6-35-47-20W4M	2441
39	13-32-47-20W4M	2450
40	15-33-47-21W4M	2522
41	10-31-47-21W4M	2476
42	10-21-47-22W4M	2487
43	10-12-47-23W4M	2473
44	15-21-47-23W4M	2470
45	1-21-47-24W4M	2453
46	10-13-47-25W4M	2616
47	10-11-47-26W4M	2566
48	11-18-47-26W4M	2617
49	5-21-47-27W4M	2804
50	7-31-47-27W4M	2729

Well No.	Well Location	K.B. Elev.(ft.)
51	12-13-48-28W4M	2615
52	8-17-48-27W4M	2601
53	2-15-48-27W4M	2589
54	5-19-48-26W4M	2522
55	8-16-48-25W4M	2506
56	7-12-48-25W4M	2513
57	16-16-48-24W4M	2547
58	10-8-48-23W4M	2491
59	13-30-48-22W4M	2487
60	1-35-48-22W4M	2514
61	11-33-48-21W4M	2509
62	2-34-48-21W4M	2528
63	14-23-48-21W4M	2481
64	6-8-48-19W4M	2486
65	6-5-48-18W4M	2420
66	11-12-48-18W4M	2384
67	11-12-48-17W4M	2350
68	11-1-48-16W4M	2335
69	10-33-48-18W4M	2409
70	10-1-49-16W4M	2270
71	6-8-49-16W4M	2274
72	6-16-49-17W4M	2368
73	10-17-49-18W4M	2340
74	12-9-49-18W4M	2426
75	11-8-49-20W4M	2628

Well No.	Well Location	K.B. Elev.(ft.)
76	7-25-49-20W4M	2647
77	3-29-49-19W4M	2505
78	11-27-49-19W4M	2393
79	7-28-49-18W4M	2296
80	11-36-49-17W4M	2257
81	10-32-49-21W4M	2562
82	10-31-49-21W4M	2542
83	4-36-49-22W4M	2540
84	11-29-49-22W4M	2504
85	10-31-49-23W4M	2495
86	7-33-48-23W4M	2523
87	10-3-49-24W4M	2502
88	1-23-49-25W4M	2439
89	9-13-49-26W4M	2386
90	11-6-49-26W4M	2466
91	2-23-49-28W4M	2453
92	1-22-49-27W4M	2428
93	7-20-50-27W4M	2323
94	13-15-50-26W4M	2359
95	9-16-50-25W4M	2330
96	9-26-50-24W4M	2383
97	12-29-50-23W4M	2447
98	11-19-50-22W4M	2514
99	8-22-50-22W4M	2560
100	2-23-50-22W4M	2550

Well No.	Well Location	K.B. Elev.(ft.)
101	6-17-50-21W4M	2527
102	4-8-50-20W4M	2612
103	16-30-50-19W4M	2364
104	11-27-50-19W4M	2361
105	6-30-50-18W4M	2298
106	10-15-51-17W4M	2221
107	10-34-50-16W4M	2252
108	11-33-51-16W4M	2236
109	10-25-51-19W4M	2257
110	10-33-51-19W4M	2338
111	6-23-52-19W4M	2401
112	9-36-51-20W4M	2445
113	4-14-51-21W4M	2471
114	10-12-51-22W4M	2438
115	10-36-52-21W4M	2444
116	6-19-52-21W4M	2436
117	12-34-52-22W4M	2408
118	16-13-51-23W4M	2530
119	6-34-51-23W4M	2390
120	9-30-52-23W4M	2293
121	10-31-51-24W4M	2232
122	10-2-51-25W4M	2306
123	13-33-51-25W4M	2248
124	5-36-51-26W4M	2258
125	16-28-51-26W4M	2328

Well No.	Well Location	K.B. Elev.(ft.)
126	3-18-51-26W4M	2314
127	7-8-52-27W4M	2367
138	6-34-52-27W4M	2348
129	15-35-52-26W4M	2350

APPENDIX IIf

Well Locations for Figure 98

Well No.	Well Location	K.B. Elev.(ft.)
1	7-20-20-28W3M	2406
2	10-27-20-2W4M	2461
3	10-28-20-4W4M	2388
4	6-6-20-6W4M	2716
5	5-32-21-24W3M	--
6	11-16-21-26W3M	--
7	7-9-21-1W4M	2320
8	11-33-21-3W4M	2195
9	6-10-21-5W4M	2456
10	7-15-22-7W4M	2316
11	11-30-22-5W4M	2327
12	11-17-22-4W4M	2410
13	6-21-22-1W4M	2304
14	13-25-22-28W3M	2240
15	6-25-23-25W3M	1955
16	10-23-23-29W3M	2252
17	6-16-23-2W4M	2077
18	7-13-23-9W4M	2322
19	6-16-23-11W4M	2338
20	6-25-24-8W4M	2460
21	7-7-24-4W4M	2594
22	11-31-24-2W4M	2316
23	11-19-24-25W3M	2223
24	11-20-24-24W3M	2283
25	6-7-25-24W3M	2324

Well No.	Well Location	K.B. Elev.(ft.)
26	6-12-25-27W3M	--
27	3-27-25-28W3M	--
28	5-22-25-1W4M	2342
29	11-22-25-2W4M	2350
30	7-2-25-10W4M	2344
31	6-7-25-11W4M	2419
32	6-23-26-13W4M	2484
33	6-30-26-10W4M	2531
34	11-28-26-9W4M	2518
35	7-1-26-8W4M	2631
36	10-34-26-7W4M	2499
37	11-2-26-6W4M	2585
38	7-22-26-4W4M	2553
39	6-2-26-29W3M	--
40	4-17-26-28W3M	2437
41	1-27-26-26W3M	2460
42	16-29-26-25W3M	--
43	4-29-26-24W3M	2407
44	10-29-27-1W4M	2372
45	4-3-27-3W4M	2568
46	7-19-27-6W4M	2390
47	7-17-28-12W4M	2664
48	7-15-28-11W4M	2552
49	6-27-28-9W4M	2620
50	10-2-28-7W4M	2560

Well No.	Well Location	K.B. Elev.(ft.)
51	10-17-28-5W4M	2673
52	10-16-28-2W4M	2265
53	7-20-28-1W4M	2325
54	11-12-28-29W3M	--
55	4-22-28-28W3M	--
56	11-28-28-26W3M	2445
57	11-25-28-24W3M	2252
58	7-6-29-23W3M	2233
59	11-29-29-25W3M	2361
60	6-15-29-6W4M	2484
61	11-30-29-10W4M	2508
62	11-12-30-13W4M	2691
63	6-15-30-11W4M	2574
64	11-6-30-10W4M	2515
65	7-15-30-9W4M	2516
66	10-13-30-8W4M	2465
67	10-21-30-6W4M	2531
68	7-1-30-7W4M	2449
69	10-18-30-5W4M	2415
70	10-6-30-4W4M	2521
71	10-11-30-3W4M	2322
72	6-27-30-2W4M	2433
73	10-12-30-1W4M	2353
74	11-12-30-29W3M	--
75	11-29-30-28W3M	--

Well No.	Well Location	K.B. Elev.(ft.)
76	12-34-30-27W3M	--
77	6-12-31-27W3M	--
78	10-1-31-29W3M	--
79	11-10-31-1W4M	2331
80	6-32-31-3W4M	2351
81	7-8-31-4W4M	2458
82	11-21-31-6W4M	2553
83	11-28-31-7W4M	2609
84	6-4-31-9W4M	2509
85	10-33-31-9W4M	2513
86	4-25-31-10W4M	2505
87	6-3-31-11W4M	2601
88	11-12-31-13W4M	2675
89	11-34-32-7W4M	2484
90	6-31-32-6W4M	2493
91	10-34-32-3W4M	2231
92	7-25-32-1W4M	2334
93	7-24-32-29W3M	2357
94	7-6-32-26W3M	--
95	10-17-32-25W3M	2299
96	1-4-32-23W3M	2317

APPENDIX III

Interpretation of Lithofacies Sequence B in Viking Cores

Legend:

Facies BI	- Bioturbated mudstone facies
Facies BII	- Heterolithic facies
Facies BIII	- Cross-stratified sandstone facies
Facies BIV	- Bioturbated sandstone facies
Facies BV	- Chert pebble conglomerate facies

E-log Curves
- left - Spontaneous potential
- right - Resistivity

APPENDIX IIIa

Basal Sandstone

B_1 (Hamilton Lake reservoir) member

PONDERAY ET AL YOUNGSTOWN

12-19-31-9W4M

K.B. 2503'

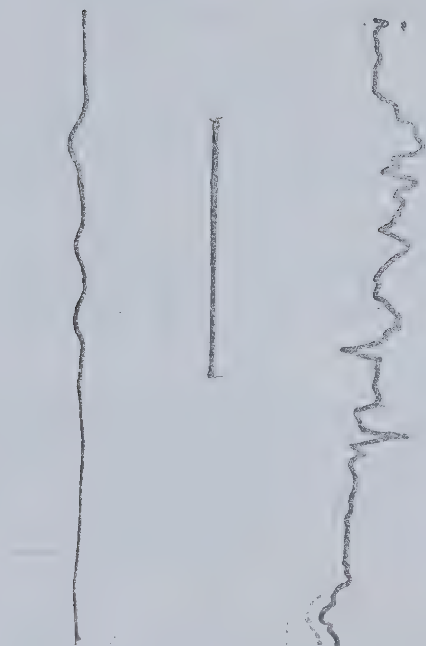

Core: 3"; good recovery

Depth (ft.) | Description

2860-2864 (facies BIII)
Sandstone: medium to coarse grained, moderate sorting; low-angle planar cross-stratification with shale laminae on foreset bedding; intervals of moderate to strong bioturbation; black chert pebbles (4 mm - 5 mm) dispersed throughout interval.

2864-2868 (facies BII)
Sandstone: fine to medium grained; ripple cross-stratification; moderate to strongly bioturbated; shale and mudstone interbeds.

2868-2883 (facies BI)
Mudstone: dark grey, regular fine sandstone laminae and lenses; moderate to strong bioturbation; bentonites, grey, fine to medium grained, 2" to 3" thick at 2871' and 2883'.

Depth (ft.)	Description

2883-2890

Sandy mudstone: dark grey, some cross-laminated and horizontal laminated siltstone and fine sandstone laminae and lenses; scour surfaces; almost completely homogenized by very strong bioturbation.

2890-2897

Claystone: dark grey, common siltstone to fine sandstone laminae and lenses; weak bioturbation; bentonite, light grey, 1" thick at 2893'.

2897-2899 (facies BIV)

Sandstone (B_1): fine grained; shale streaks common, unit strongly bioturbated.

2899-2907 (facies BII)

Sandstone: dark grey, fine grained, moderate sorting; abundant bioturbated shale and mudstone laminae; glauconite; moderate to strong bioturbation, some burrows; bentonite E, light to dark grey, medium to coarse grained biotite, graded, 15" to 18" thick at 2907'.

2907-2912 (facies BI)

Mudstone: dark grey, inclined and horizontal laminated siltstone and very fine sandstone laminae and lenses; moderate to strong bioturbation.

DOME KIRKPATRICK

10-18-33-9W4M

K.B. 2558'

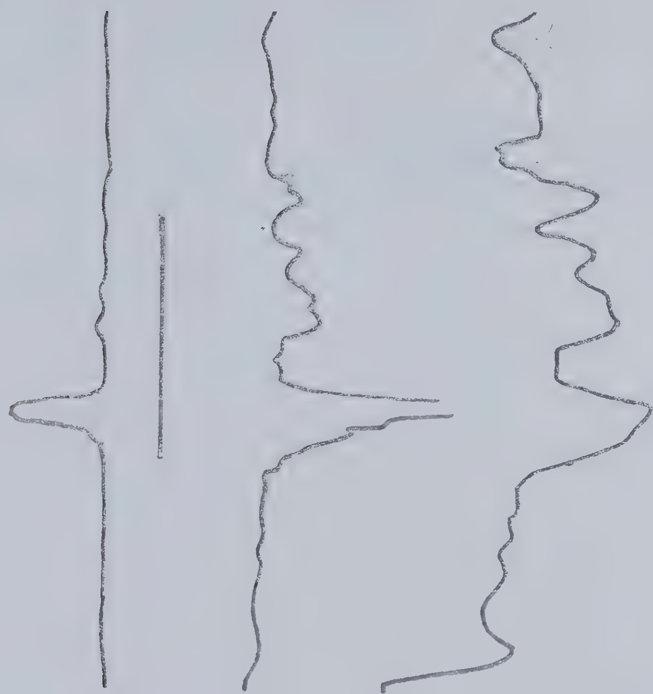

Core: 3"; good recovery

Depth (ft.)	Description

2925-2941
Mudstone: dark grey, bentonite; few siltstone and sandstone laminae; moderate bioturbation; bentonite, light grey, fine grained, thin at 2928'.

2941-2952
Sandy Mudstone: dirty, dark grey, very fine to fine grained sand; strongly bioturbated; bentonite, dark grey, fine grained, thin at 2945'.

2952-2962
Claystone: dark, massive; occasional siltstone and sandstone laminae and lenses; weak bioturbation; bentonite, light grey, fine grained, ½" thick at 2956'.

2962-2965 (facies BIV)
Shaly Sandstone (B_1): dark grey, fine grained; few sandstone lenses; unit nearly homogenized by bioturbation.

Depth (ft.)	Description

2965-2970 (facies BIII)

Sandstone: light grey, dark grey, greenish in places; fine to medium grained, friable; fairly well sorted; medium angle, planar cross-lamination, shale and glauconite drapes on foreset laminae, scour contacts; weak bioturbation.

2970-2975 (facies BI ± BII)

Mudstone: dark grey, sandy upwards, few siltstone and sandstone lenses, moderate to strong bioturbation.

2975-2977

Shale: dark, fissile.

MAPLO KIRKPATRICK

2-28-33-9W4M

K.B. 2546'

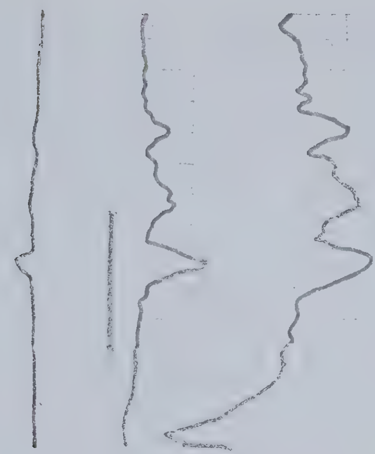

Core: 2"; fair recovery

Depth (ft.)	Description

2915-2928
Claystone: dark, massive; occasional siltstone and sandstone lenses; sandier and more bioturbated near top and base.

2928-2930 (facies BIV)
Shaly sandstone (B_1): dark grey, few fine grained sharply based sandstone lenses; nearly homogenized by bioturbation.

2930-2935 (facies BIII)
Sandstone: light grey, greenish in places, fine to medium grained, friable; low angle, planar cross- and horizontal laminations, glauconite and shale laminae on foreset laminae; weak bioturbation.

2935-2940 (facies BI $\pm$ BII)
Mudstone: dark grey; sandy upwards; occasional siltstone and sandstone lenses; strongly bioturbated.

2940-2960
Shale: dark and fissile.

TENN. H.B. PROVOST

10-4-34-9W4M

K.B. 2551'

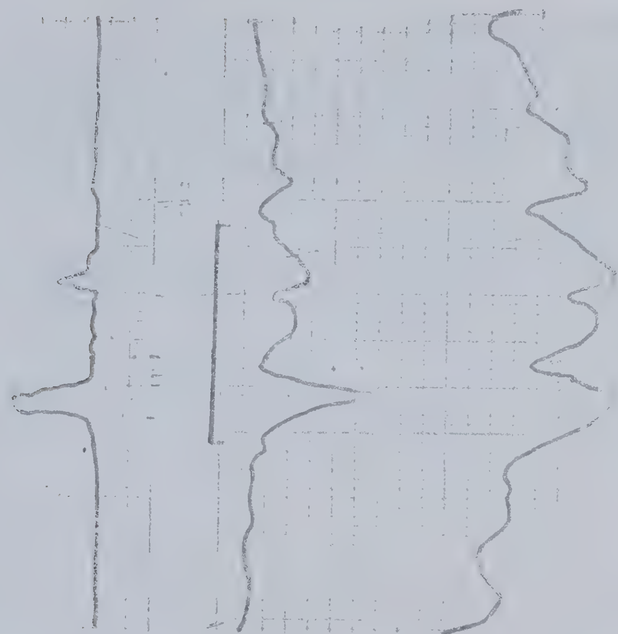

Core: 2"; fair recovery

Depth (ft.)	Description

2905-2911 (facies BI)
Mudstone: dark grey, regular sandstone laminae and lenses; weak bioturbation; bentonite, light grey, fine grained, thin at 2911'.

2911-2916 (facies BIV)
Sandstone: dark grey, fine grained; shale interbeds; highly bioturbated, vertical burrows.

2916-2921 (facies BIII)
Sandstone: grey to greenish, fine to medium grained; fair sorting, low to medium angle, planar cross-lamination; shale and glauconite on foreset laminae, shale laminae; vertical and inclined burrows; sharp lower contact; bentonite, light grey, fine grained, 6" thick at 2921'.

2921-2934 (facies BI)
Mudstone: dark grey, some siltstone and sandstone laminae and lenses, bioturbated horizons.

2934-2938
Shale: dark and fissile.

Depth (ft.)	Description
2938-2941	(facies BIV)
	Sandstone (B_1): dark grey, fine grained; shaly; moderate to strong bioturbation.
2941-2946	(facies BIII)
	Sandstone: light grey, fine to medium grained, friable, clean and well sorted; low angle, planar cross-stratification, shale on foreset laminae; several bioturbated horizons.
2946-2950	(facies BI $\pm$ BII)
	Mudstone: dark grey, sandy upwards, shalier downwards; bioturbated.
2950-2952	
	Shale: black and fissile.

MAPCO PROVOST

2-8-34-9W4M

K.B. 2552'

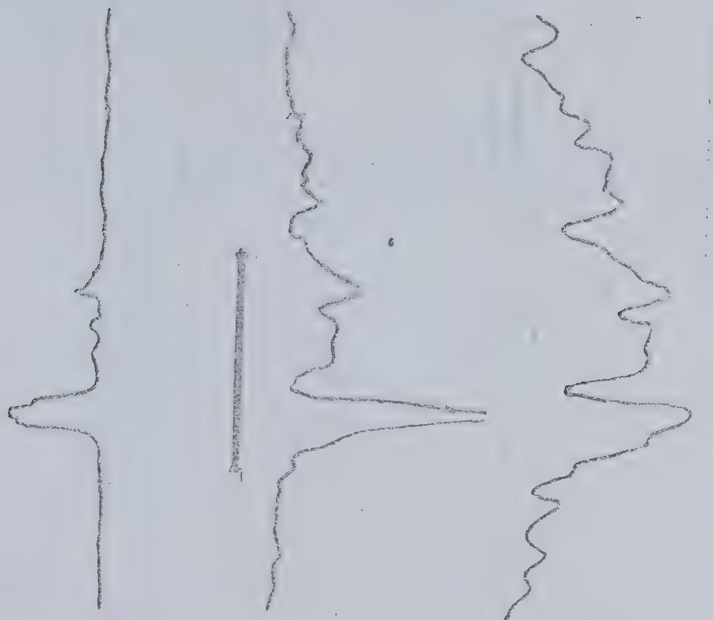

Core: 3"; fair recovery

Depth (ft.)	Description
2910-2916	(facies BIV) Sandstone: dark grey, fine to medium grained, shale interbeds; strong bioturbation.
2916-2919	(facies BIII) Sandstone: dark grey, fine to medium grained, dirty; low to medium angle, planar cross-stratification; shale interlaminae; moderate bioturbation, some vertical burrows; indurated calcareous band.
2919-2934	(facies BI) Mudstone: dark grey, very sandy between 2924'-2934'; moderate to strong bioturbation; bentonite, light grey, fine grained, 6" thick at 2921'.
2934-2938	Shale: dark and fissile.
2938-2942	(facies BIV) Sandstone (B_1): dark grey, fine grained; scours; shaly; moderate to strong bioturbation.

Depth (ft.)	Description

2942-2947 (facies BIII)

Sandstone: light grey, fine to medium grained, friable, clean, well sorted; low to medium angle, planar cross-stratification, horizontal lamination, sharp set boundaries, scours, shale on foreset laminae; weak bioturbation.

2947-2951 (facies BI)

Mudstone: dark grey, few sandstone lenses, sandier near top; moderate to strong bioturbation.

CANADIAN CHIEFTAIN PROVOST

7-14-34-7W4M

K.B. 2589'

Core: 3"; fair recovery

Depth (ft.) Description

2820-2835 (facies BI)
Mudstone: dark grey; siltstone and fine sandstone lenses and laminae, more near base; bentonite, light grey, fine grained, thin, at 2835'; weak to moderate bioturbation.

2835-2842
Sandstone: dark grey, very fine to fine grained; muddy, shaly; homogenized by bioturbation.

2842-2850
Shale: dark, fissile marine shale; thin pebbly mudstone lens at 2845'; pebbles up to 1.25 cm long diameter; sharp lower contact.

2850-2852 (facies BIV)
Sandstone (B_1): dark grey, fine to medium grained; shale interlaminae, strongly bioturbated horizons.

2852-2855 (facies BIII)
Sandstone: light grey, fine to medium grained, friable, fair sorting; low angle, planar corss-stratification, glauconite and shale on foreset laminae; shale interlaminae; moderately bioturbated horizons; indurated calcareous band at 2852'.

Depth (ft.)	Description
2855-2863	(facies BI)

Silty mudstone: dark grey; siltstone and sandstone lenses and laminae; more upwards, shalier at base; weak to moderate bioturbation; bentonite, light grey, fine grained, thin at 2860'.

H.B. PROVOST

6-26-34-7W4M

K.B. 2476'

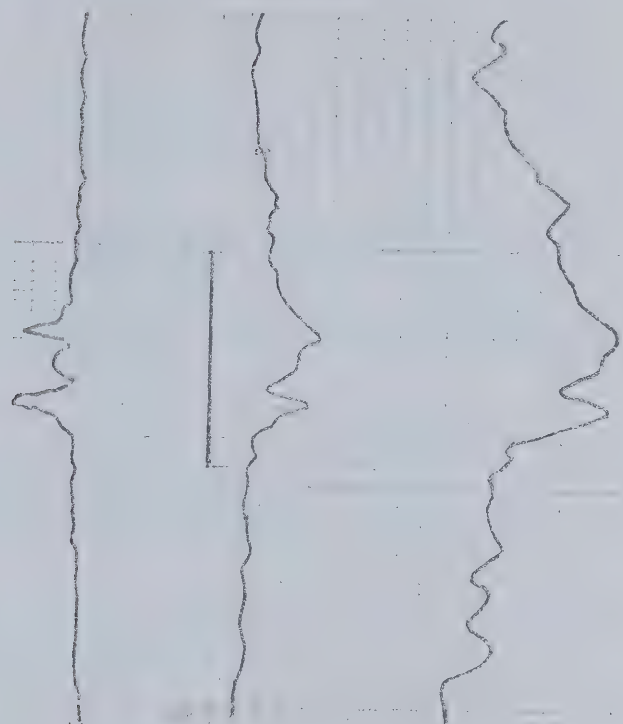

Core: 3"; good recovery

Depth (ft.)	Description

2701-2713 (facies BI)

Mudstone: dark grey; siltstone, fine to medium grained sandstone laminae and lenses; moderate bioturbation; bentonite, light grey, fine grained, thin at 2702' and 2713'.

2713-2720

Sandstone: light grey, fine to medium grained at base and very fine grained on top, clean, well sorted; low angle, planar cross-stratification; weak bioturbation.

2720-2723 (facies BI)

Mudstone: dark grey, regular siltstone and sandstone laminae and lenses; strong bioturbation.

2723-2727

Muddy sandstone: dark grey; homogenized by bioturbation.

Depth (ft.)	Description

2727-2731
Shale: dark, fissile; pebbly mudstone lens; bentonitic shale, dark grey, coarse biotite rich, 3" thick at 2730'.

2731-2732 (facies BIV)
Sandstone (B_1): dark grey, fine to medium grained; shaly; weak bioturbation.

2732-2736 (facies BIII)
Sandstone: light grey to greenish, fine to medium grained, friable, clean, well sorted; low angle, planar cross-stratification, horizontal lamination, sharp cross-set boundaries, scours; indurated calcareous band.

2736-2741 (facies BII)
Sandstone: dark grey to greenish, very fine to fine grained; shale laminae and lenses abundant; moderate bioturbation; glauconite.

2741-2743 (facies BI)
Mudstone: dark green, siltstone laminae common, moderate bioturbation.

2743-2746
Shale: dark, fissile.

GULF N.C.O. PROVOST

12-17-36-12W4M

K.B. 2694'

Core: 3"; good recovery

Depth (ft.)	Description

3094-3096 (facies BIII)
Sandstone: dark grey, fine to medium grained, moderate sorting; low angle, planar cross-stratification, shale laminae on foreset bedding; bioturbated horizons.

2096-3100 (facies BII)
Sandstone: dark grey, silt to very fine grained; sharply based sandstone lenses; bioturbated shaly horizons; shalier towards base; moderate bioturbation.

3100-3110 (facies BI)
Mudstone: dark grey; silt and fine sand laminae and lenses; moderate bioturbation.

3110-3114 (facies BIV)
Sandstone: dark grey, fine to medium grained; shale laminae; moderate to strong bioturbation.

Depth (ft.)	Description

3114-3121 (facies BIII)

Sandstone: light grey, fine to medium grained; fair sorting; low angle, planar cross-stratification; weak bioturbation.

3121-3126 (facies BI ± BII)

Sandstone: dark grey, silt to very fine grained; muddy; shale laminae; strongly bioturbated.

3126-3133

Claystone: dark, massive; silt and fine sand laminae and lenses, some glauconitic and cross-laminated.

3133-3140 (facies BIII)

Sandstone (B_1): light grey, fine to medium grained, clean, well sorted; low angle, planar cross-stratification, shale and glauconite on foreset laminae; bioturbation, more near top and base.

3140-3145 (facies BII)

Sandstone: dark grey, silt to fine grained; shale interlaminae; bioturbation.

3145-3155 (facies BI)

Mudstone: dark grey; shalier near base; weak bioturbation; bentonite, light grey, coarse biotite grained, 3" thick at 3150'.

3155-3183

Not examined.

C.S. CASTOR

6-11-39-14W4M

K.B. 2494'

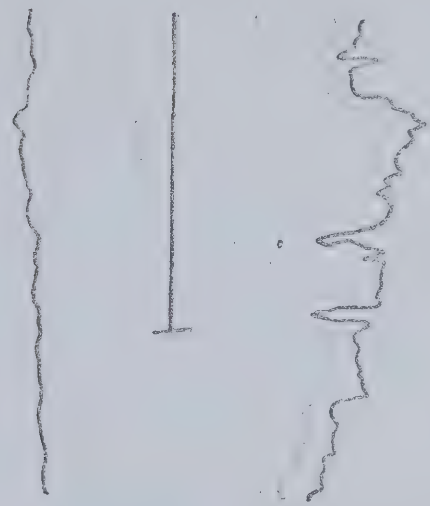

Core: 2"; good recovery

Depth (ft.) | Description

2990-2995
Shale: dark, fissile, marine.

2995-3010
Sandstone: dark grey, silt to very fine grained; ripple lamination; scours, shale laminae; moderate bioturbation.

3010-3040
Mudstone: dark grey; siltstone and sandstone laminae and lenses; weak to strong bioturbation in places; bentonite, light grey, fine to medium grained, greater than 12" and 15" thick at 3023' and 3040'.

APPENDIX IIIb

Basal Provost Sandstone Ridges
(BP_3 Member)

FINA PROVOST

10-9-36-7W4M

K.B. 2472'

Core: 3"; poor recovery

Depth (ft.) Description

2635-2646
Claystone: dark, massive; sandier near top and bottom.

2646-2652 (facies BIV)
Sandstone: light grey, friable, fine to medium grained; low angle, planar cross-stratification, shale lamine on foreset laminae; shale laminae; moderate bioturbation, 12" vertical burrow; bentonitic; oil stains near base.

APPENDIX IIIc

Lower Sandstone Ridge Complex

(L_1 Member)

H.B. CESSFORD

11-6-25-12W4M

K.B. 2373'

Core: 1"; fair recovery.

Depth (ft.)	Description
2636-2642	Shale: dark, fissile; sandstone lenses near base.
2642-2644	(facies BII) Sandstone (UE_O): dark grey, fine to medium grained; shale laminae; bioturbated.
2644-2648	(facies BIII) Sandstone: light grey, fine to medium grained; shale laminae; bioturbated; siderite concretions.
2648-2653	(facies BII) Sandstone: dark grey, very fine to fine grained; shale laminae; moderate to strong bioturbation.
2653-2680	No cores cut.
2680-2686	(facies BI) Mudstone: dark grey, siltstone laminae; weak bioturbation.
2686-2688	(facies BIV) Sandstone (L_1): dark grey, fine to medium grained, scour and fill structures; shale laminae; strong bioturbation.
2688-2694	(facies BIII) Sandstone: light grey, fine to medium grained; shale laminae; bentonitic.
2694-2699	(facies BI $\pm$ BII) Mudstone: dark grey, bentonitic; fine sand lenses; shaly horizons; strong bioturbation.

Depth (ft.)	Description

2699-2702 (facies BIV)

Sandstone: dark grey, medium to coarse grained; shaly; strong bioturbation.

APPENDIX IIId

Lower Sandstone Ridge Complex
(L_2 Member)

11-12-24-6W4M

K.B. 2599'

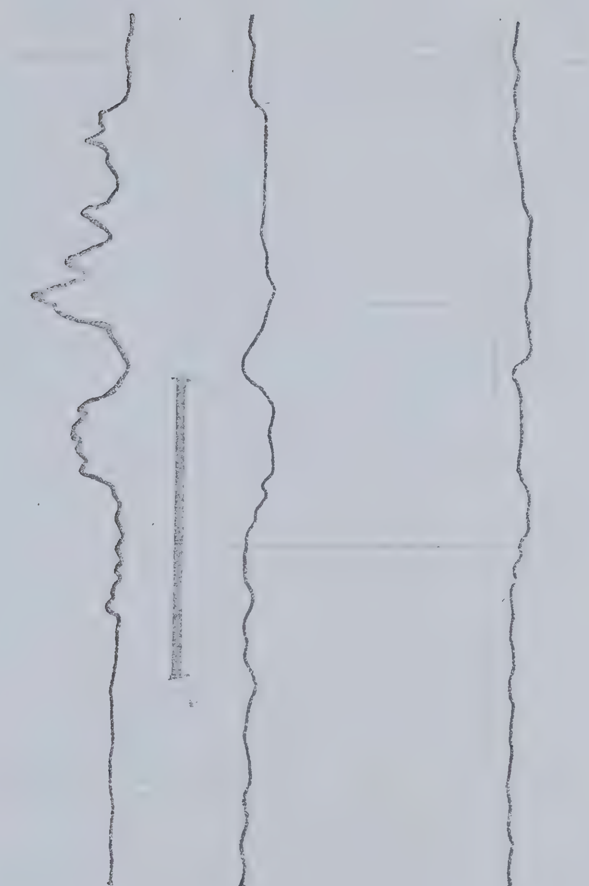

Core: ~1"; Wireline; good recovery

Depth (ft.)	Description

2715-2718
Mudstone: dark grey, bentonitic, moderate bioturbation.

2718-2736
Sandstone (L_2): dark grey, fine to medium grained, friable; abundant shale streaks and laminae; strongly bioturbated.

2736-2765
Mudstone: dark grey, abundant siltstone and very fine sandstone laminae; bentonite, light grey, fine to medium grained, 2 to 4" thick at 2737', 2749', 2754' 2758'; fairly homogenized by strong bioturbation; sharp (erosional) basal contact.

Depth (ft.)	Description

2765-2776

Shale: black, fissile; bentonite, light grey, fine to medium grained, biotite rich, 5" thick at 2767'.

2776-2778

Siltstone: dark, completely reworked by bioturbation.

H.B. CESSFORD

14-26-25-12W4M

K.B. 2452'

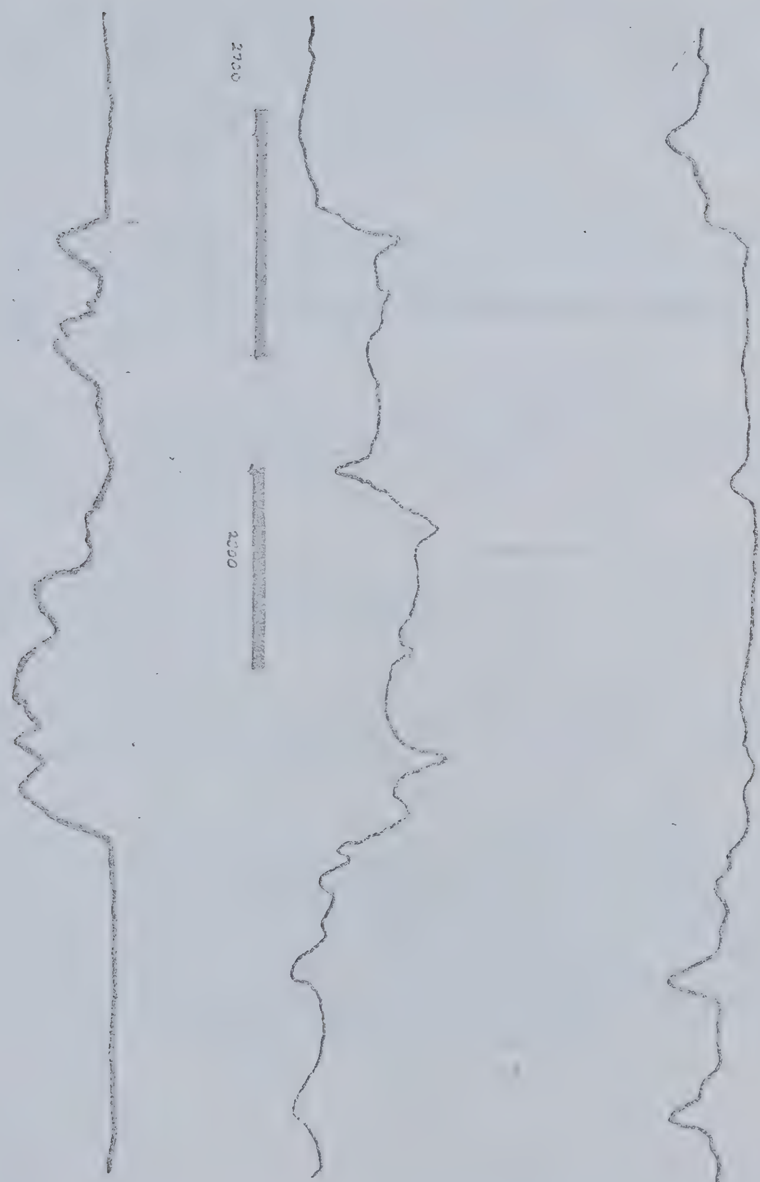

Core: 2"; good recovery

Depth (ft.)	Description

2710-2734

Shale: dark, fissile; bentonite, light grey, fine grained, 12" thick at 2715'; siltstone and sandstone laminae near base.

2734-2734.5 (facies BV)

Pebble Conglomerate (UE_1): black and white chert pebbles up to 12 mm long, fairly rounded; matrix supported, poorly sorted medium to coarse grained sand; shale interlaminae; thin mudstone base; calcareous cement.

2734.5-2740 (facies BIII)

Sandstone: light grey, fine to medium grained, fair sorting; low angle, planar cross-stratification, shale laminae on foreset bedding; bioturbated horizons.

2740-2745 (facies BII)

Sandstone: very fine to fine grained sandstone alternating with shale and mudstone laminae; moderate bioturbation.

2745-2752 (facies BI)

Mudstone: dark grey; siltstone and very fine grained sandstone laminae; strong bioturbation.

2752-2754 (facies BIV)

Sandstone (UE_o): fine grained sandstone alternate with mudstone and shale; moderate bioturbation.

2754-2760 (facies BIII)

Sandstone: dark grey; fine to medium grained sandstone, 12" to 15" thick, alternate with 2" to 4" thick shale-mudstone-siltstone laminae; medium to high angle, planar cross-stratification, shale laminae on foreset laminae; scoured contacts, reactivation surface, herringbone-like cross-stratification near top; bioturbated horizons.

2760-2784

No cores cut.

2784-2793 (facies BI)

Mudstone: dark grey, minor siltstone and very fine sandstone lenses; bentonite, light grey, coarse biotite rich, 12" thick at 2785'.

2793-2800

Pebbly Sandstone(L_2): dark grey, very fine to fine grained, fine chert pebbles in a poorly sorted coarse grained sandstone matrix at 2793'; fairly well homogenized by strong bioturbation.

Depth (ft.)	Description

2800-2805 (facies BI)

Mudstone: dark grey, siltstone and sandstone laminae; strong bioturbation; darker and shalier near base.

2805-2815

Sandstone: dark grey, very fine to fine grained; structureless due to strong bioturbation; darker and shalier near base.

2815-2822 (facies BI)

Mudstone: dark grey, shale, silt and fine sand laminae; bioturbated horizons.

2822-2825

Pebbly Sandstone: dark grey, fine to medium grained, black chert pebbles dispersed in poorly sorted, medium grained sandstone; homogenized by very strong bioturbation.

11-7-26-13W4M

K.B. 2531'

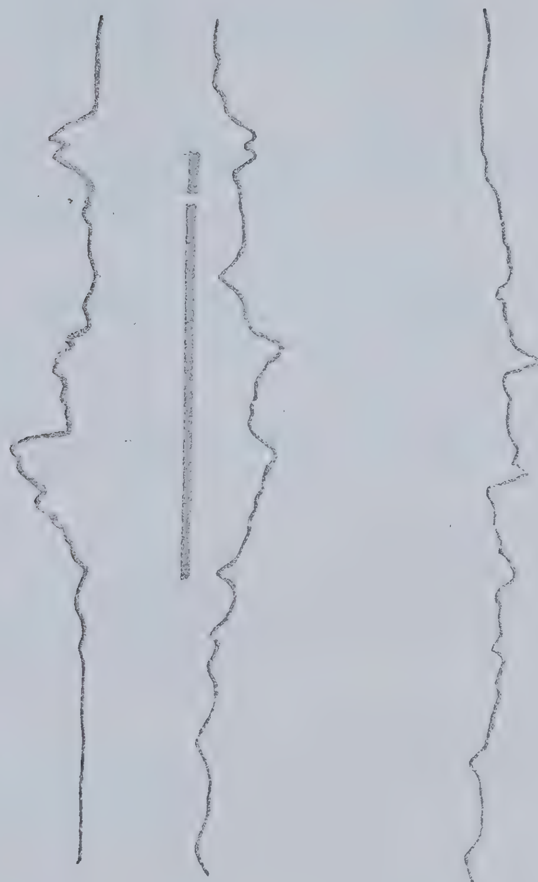

Core: 1"; good recovery

Depth (ft.) Description

2910-2914 (facies BIII)

Sandstone (UE_O): dark grey, fine to medium grained, fair sorting; some shale laminae; scour surfaces; weak bioturbation.

2914-2918 (facies BI ± BII)

Mudstone: darker grey; sandier near top and base; strongly bioturbated.

2918-2921

No cores cut.

Depth (ft.)	Description

2921-2947 (facies BI)

Mudstone: dark grey, siltstone and very fine grained sandstone lenses common, sandier near top and bottom; moderately bioturbated; bentonite, dark grey, medium to coarse grained biotite grains, greater than 6" thick at 2936'.

2947-2950 (facies BIV)

Sandstone (L_2): dark grey, fine to medium grained; two black chert pebbles; shale laminae; strong bioturbation.

2950-2958 (facies BIII)

Sandstone: dark grey, fine to medium grained; abundant shale laminae and streaks; weak bioturbation.

2958-2969 (facies BI ± BII)

Sandstone: dark grey, silt to fine grained; darker and shalier toward base; strong bioturbation.

2969-2981.5 (facies BIII)

Sandstone: light grey, medium to coarse grained, pebbly on top; planar cross-stratified; scour surfaces; weak bioturbation; bentonitic shale, 18" thick at 2980'.

2981.5-2985 (facies BIII)

Sandstone: light grey, coarse to very coarse grained, fairly well sorted; bentonite, light grey, fine grained, 6" thick at 2985'.

2985-2996 (facies BI ± BII)

Muddy Sandstone: light grey, very fine to fine grained; muddy and shalier toward base; pebbly near top; strongly bioturbated; bentonitic at 2996'.

14-23-26-14W4M

K.B. 2550'

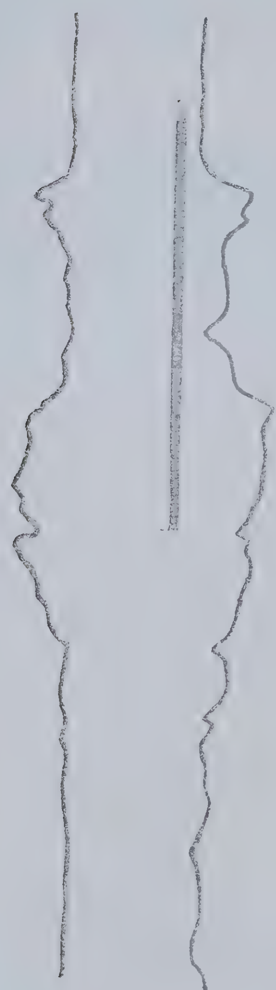

Core: 1"; good recovery

Depth (ft.)	Description

2938-2952
Shale: dark, fissile and massive in places; sandy toward base.

2952-2955 (facies BIV)
Sandstone (UE_o): fine grained, shaly; strongly bioturbated, some burrows.

2955-2964 (facies BIII)
Sandstone: light grey, very fine to fine grained, fairly well sorted; low angle, planar cross-lamination; shale laminae; weak bioturbation.

Depth (ft.)	Description

2964-2998 (Facies BI $\pm$ BII)

Mudstone: dark grey, abundant siltstone laminae and fine grained sandstone lenses; sparingly bioturbated in places; bentonite, dark grey, coarse biotite grains, graded, shaly, greater than 6" thick at 2986'.

2998-3025

Sandstone: light grey, greenish in places, medium to coarse grained, a black chert pebble on top; muddy and shalier toward base; bioturbated, stronger on top and base; glauconitic; bentonitic near base; siderite concretions; oil stain.

AMERADA CROWN

7-25-26-15W4M

K.B. 2634

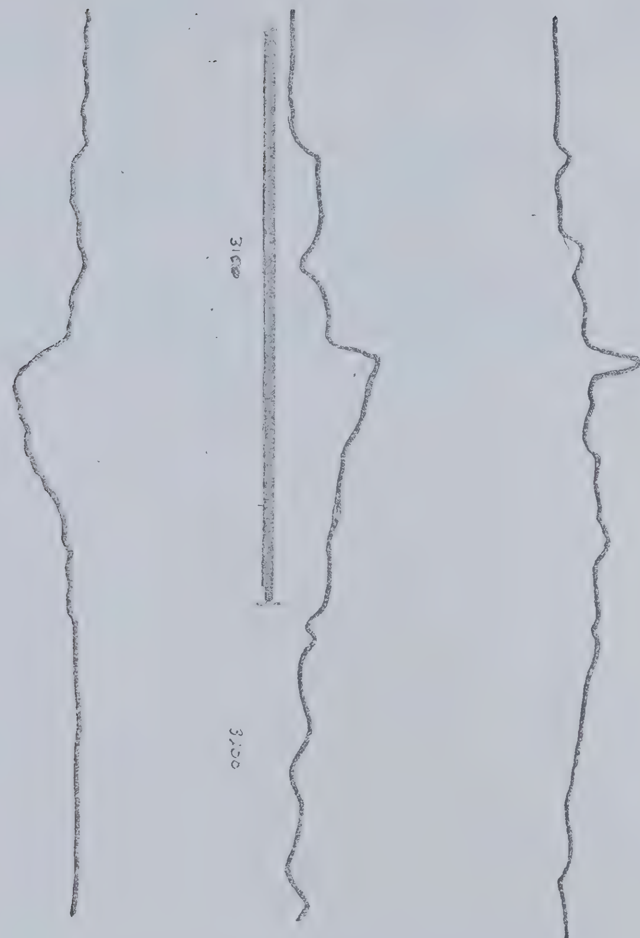

Core: 1"; sidewall samples; fair recovery

Depth (ft.)	Description
3054-3080	Shale: black, fissile, sharp basal contact.
2080-3090	Siltstone: dark grey; abundant shale laminae; scour surfaces; weak bioturbation, more at base.
3090-3118	(facies BI) Mudstone: dark grey, horizontally laminated siltstone laminae, cross-stratified very fine sandstone lenses; moderate bioturbation in places; bentonite, light grey, medium to coarse biotite grains, greater than 6" thick at 3101'.

Depth (ft.)	Description

3118-3145 (facies BIII ± BIV)

Sandstone (L_2): dark grey, fine to medium grained, fairly well rounded chert pebbles 10 mm long diameter, dispersed in sand on top; abundant shale laminae and streak; nearly homogenized by bioturbation.

3145-3155 (facies BII)

Sandstone: dark grey, very fine to fine grained; shale and mudstone interlaminae, bioturbated horizons.

3155-3170 (facies BI)

Mudstone: dark grey, siltstone laminae, fine sandstone lenses; bentonitic interval at 3155'-3160'; siderite concretions; strongly bioturbated.

KEWANEE A CESS

6-12-27-15W4M

K.B. 3815'

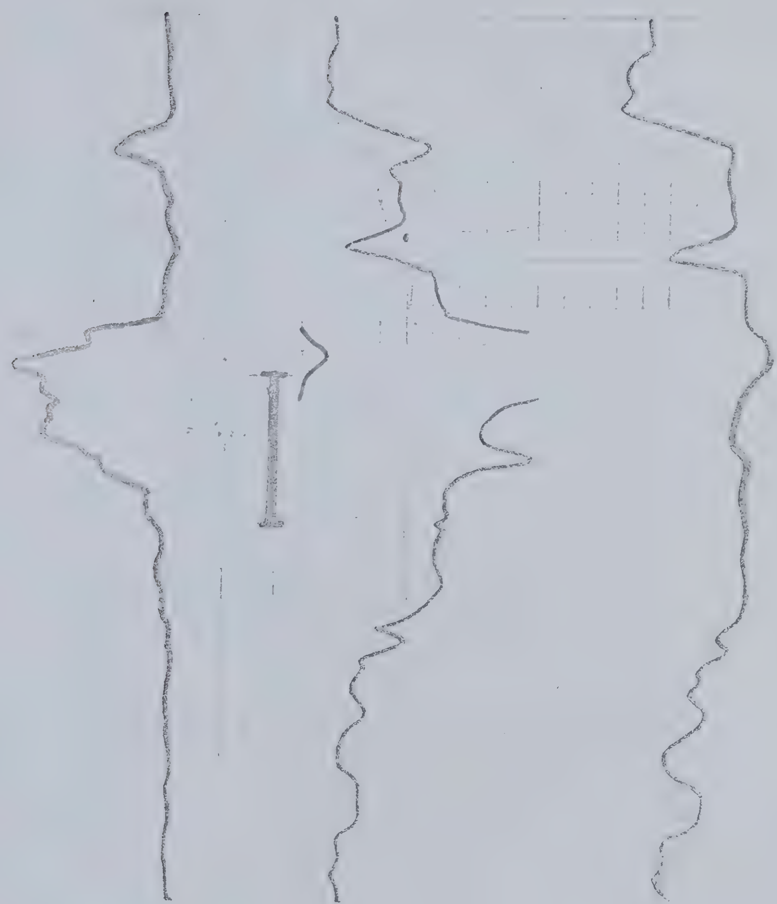

Core: 3"; good recovery

Depth (ft.) Description

3225-3255

Sandstone (L_2): dark grey, fine to medium grained; abundant shale partings and laminae; scour surfaces; darker and shalier near base; homogenized by strong bioturbation.

APPENDIX IIIe

Lower Sandstone Ridge Complex
(L_3 and L_4 members)

PROVO (GULF) HALLIDAY

13-11-28-14W4M

K.B. 2608'

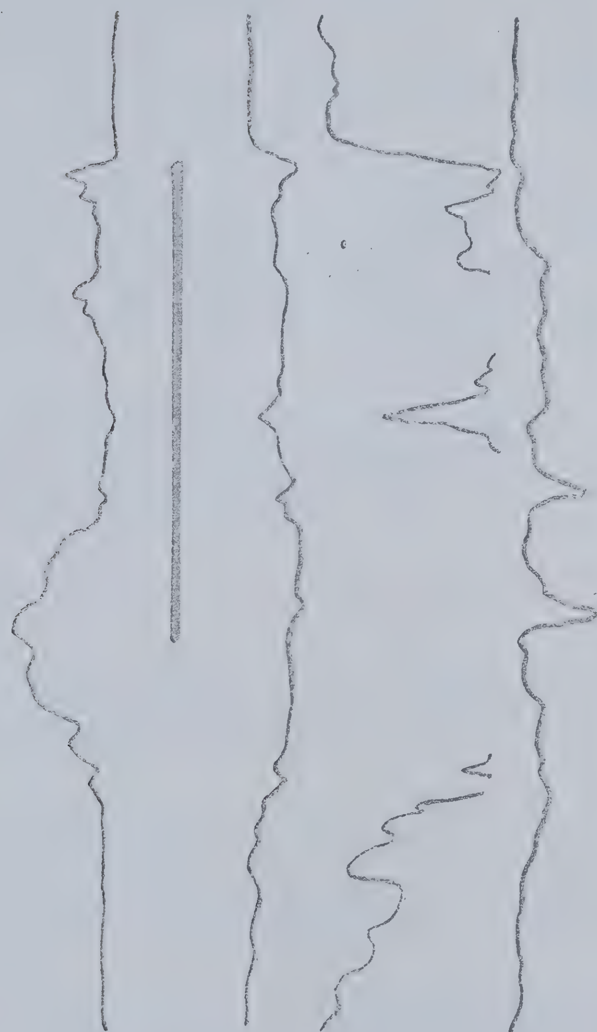

Core: 3"; fair recovery (slabbed)

Depth (ft.) — Description

3063-3063.9 (facies BV)

Pebble Conglomerate: black chert pebbles, fairly well rounded; poorly sorted very coarse sand matrix, matrix support; shale and mudstone interlaminae.

3063.9-3065 (facies BI ± BII)

Mudstone: dark grey, massive, siltstone and fine sandstone laminae, some cross-laminated; moderate bioturbation.

Depth (ft.)	Description

3065-3070 (facies BIII)

Sandstone (UE_1): light grey, fine grained, clean, well sorted; planar and ripple cross-lamination, shale and carbonaceous mudstone on foreset laminae, sharp contacts, reactivation surfaces, granule horizon at 3067'; siderite concretions; bioturbated horizons; bentonite, light grey, fined grained, less than 2" thick at 3070'.

3070-3072 (facies BII)

Sandstone: light grey, very fine to fine grained, clean, cross-laminated sandstone laminae; alternate regularly and sharply with dark grey, shaly and muddy horizons, often strongly bioturbated in places.

3072-3080 (facies BI)

Mudstone: dark grey, massive; siltstone and fine sandstone laminae and lenses, clean, well sorted, inclined and horizontal lamination; moderate bioturbation, *Chondrites* sp.

3080-3088

Missing cores.

3088-3089 (facies BIII)

Sandstone (UE_0): light brown, fine grained; low angle, planar cross-stratification, sharp set boundaries.

3089-3095 (facies BII)

Sandstone: dark grey, very fine to fine grained, well sorted sandstone thin beds; in regular alternation with bioturbated shaly, muddy and silty horizons; moderate to strong bioturbation, horizontal burrows.

3095-3137 (facies BI)

Mudstone: dark grey; siltstone and sandstone lenses, more at top and bottom, some pebbly at 3106' and 3132'; chert pebble conglomerate bed, fair rounding, poorly sorted very coarse sand matrix, sharp erosional lower contact, shale and mudstone interlaminae, 9" thick at 3127'; bentonite, light grey, coarse biotite rich, 12" and 3" thick at 3114' and 3130'; bioturbation, weak to moderate, vertical burrows 3" deep at 3096'; *Zoophycus* sp.

Depth (ft.)	Description

3137-3152 (facies BIV)

Sandstone (L_3): dark, medium to coarse grained, dirty, poor sorting; shale laminae, more at base; top pebbly; glauconitic; structureless due to very strong bioturbation.

3152-3160 (facies BII)

Sandstone: shades of grey; medium to coarse grained, pebbly on top; clean well sorted thin sandstone beds alternate regularly and sharply with bioturbated shaly, muddy, and silty horizons; bioturbation, moderate to strong; funnel shaped burrows, *Rosselia* sp.

CALSTAN (CHEVRON) HANDHILLS

10-36-28-14W4M
K.B. 2591'

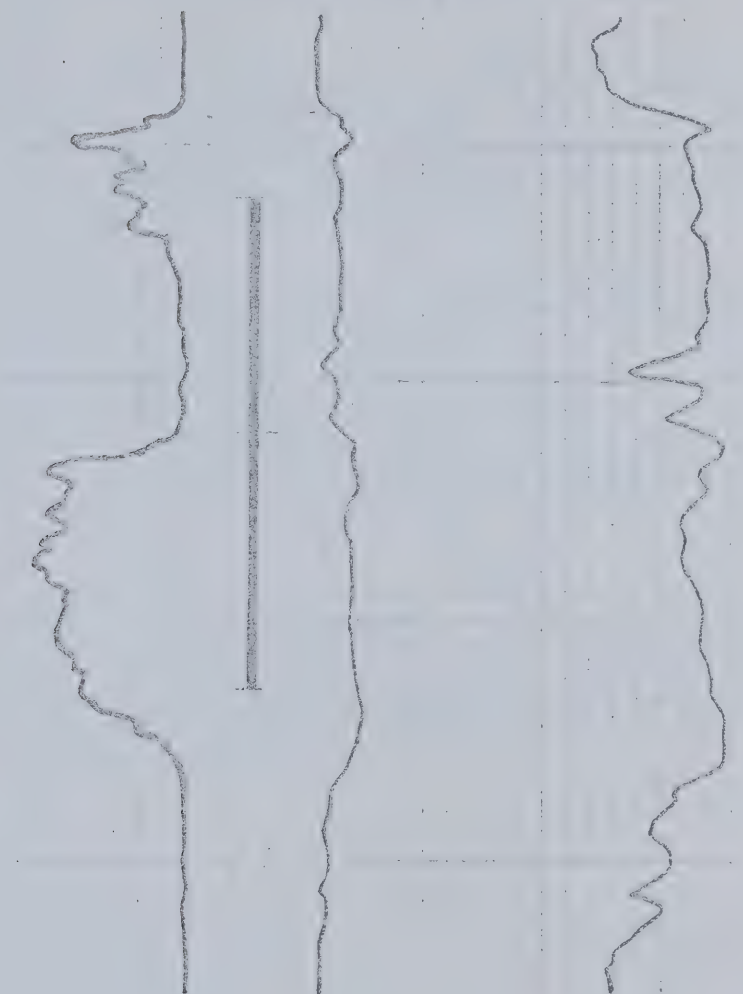

Core: 3"; good recovery (partly slabbed)

Depth (ft.) | Description

3062-3069 (facies BII)

Sandstone (UE_2): fine grained, well sorted; shale and mudstone interlaminae; scour contacts; bioturbation, more at top and base; planar cross- and horizontal stratification; siderite concretions.

3069-3111 (facies BI)

Mudstone: dark grey; abundant siltstone and very fine sandstone lenses, some horizontal and cross-stratified; sandy towards base and top; weak to moderate bioturbation; bentonites, light grey, coarse biotite rich, about 6" and 4" thick at 3097' and 3107'; black chert pebble conglomerate, fairly well rounded, poorly sorted very coarse sand matrix,

Depth (ft.) Description

shale and mudstone interlaminae, about 8", 2", and 4" thick horizons at 3106', 3110', 3111'.

3111-3122 (facies BIV)
Sandstone (L_3): shades of grey; fine to medium grained sandstone lenses alternate with shale laminae; strong bioturbation, deep burrows up to 14 cm, U-shaped burrow *Asterosoma* sp.; glauconitic; black chert pebbles at 3114'.

3122-3134 (facies BIII)
Sandstone: greenish grey, fine to medium grained, well sorted; low angle, planar cross- and horizontal lamination, ripple cross-lamination, sharp contacts, reactivation surfaces, some draped by carbonaceous mudstone; shale and glauconite on foreset laminae; shale laminae, shale clasts; bioturbation, weak, some funnel-shaped burrows; siderite concretions.

3134-3164 (facies BII)
Sandstone: dark grey, very fine to fine grained sandstone laminae; regularly interstratified with shale, mudstone and siltstone laminae; sharp contacts; bioturbation, moderate, vertical tubes, shale more affected, decreases upwards, *Zoophycus* sp. and *Arenicolites* sp.

FINA HANDHILLS

7-22-29-14W4M
K.B. 2588'

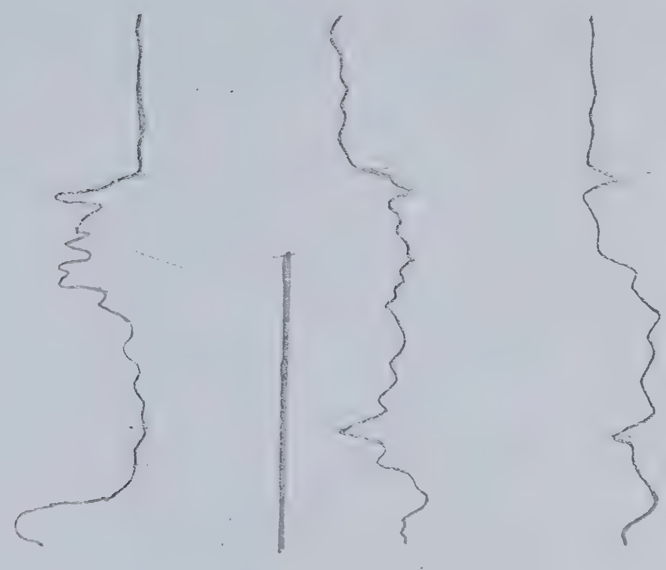

Core: 3"; good recovery (slabbed)

Depth (ft.)	Description

3051-3055 (facies BIII)
Sandstone (UE_2): light grey, fine grained, well sorted, clean; low angle, planar cross-stratification; some shale laminae; bioturbated horizons alternate with non-bioturbated inrervals toward base.

3055-3059 (facies BIII)
Sandstone: light grey, fine grained, clean, well sorted, low angle, planar cross-lamination, some herring-bone-like, sharp set contacts; mudstone inter-laminae; weak bioturbation.

3059-3061 (facies BII)
Sandstone: light grey, very fine grained, clean, well sorted, planar and simple cross-laminated sandstone lenses; alternate regularly with dark grey, bio-turbated shale, siltstone and mudstone laminae.

3061-3104 (facies BI)
Mudstone: dark grey, massive; horizontal and ripple cross-laminated sandstone lenses abundant near base and top; bioturbation, weak to moderate, more toward base and top; bentonite, light grey, coarse biotite rich, 12" and 3" thick at 3088' and 3094'.

Depth (ft.)	Description

3104-3113 (facies BIV)

Sandstone (L_3): greenish grey, fine to medium grained, clean, well sorted, cross-stratified and glauconitic sandstone thin beds; in regular alternation with dark green, strongly bioturbated shaly, muddy and silty intervals; sharp contacts, some erosional.

ATKINSON ET AL HANNA

7-16-30-14W4M
K.B. 2622'

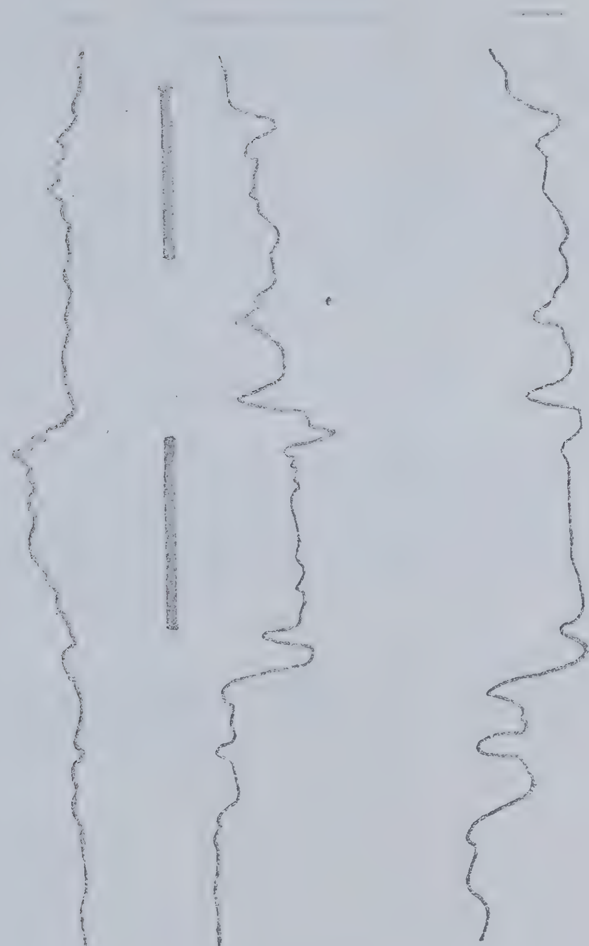

Core: 3"; good recovery

Depth (ft.) Description

3065-3068
Claystone: dark, massive; fine to coarse grained sandstone lenses at base; no bioturbation.

3068-3069 (facies BV)
Pebble Conglomerate: black and varicolored chert pebbles, fairly well rounded, up to 3 cm long diameter; poorly sorted coarse grained sandstone and mudstone matrix; shale, silt and mud interlaminae; scoured basal contact.

3069-3073
Shale: black, fissile, fine to medium grained sandstone lenses; moderate bioturbation at base.

Depth (ft.) Description

3073-3092
Sandstone (UE_2): dark grey; thin sandstone beds, light grey, fine to medium grained, clean, well sorted, cross- and horizontal stratification, sharp set boundaries, alternate with bioturbated laminae of shale, mudstone and siltstone; shalier downward.

3092-3101 (facies BI)
Mudstone: dark grey; fine to medium grained sandstone lenses, more towards top, some cross-stratified; moderate bioturbation, vertical and horizontal burrows.

3101-3140
No cores cut, or missing.

3140-3168 (facies BIII ± BIV)
Sandstone (L_3): dark grey, fine to medium grained, dirty, muddy and shaly; structureless due to very strong bioturbation, vertical burrows up to 3" deep at top; siderite concretions.

3168-3180 (facies BII)
Sandstone: dark grey, very fine to fine grained; shalier and darker downwards; homogenized by very strong bioturbation.

DOME I.O.E. WILDUNN

6-23-30-14W4M

K.B. 2663'

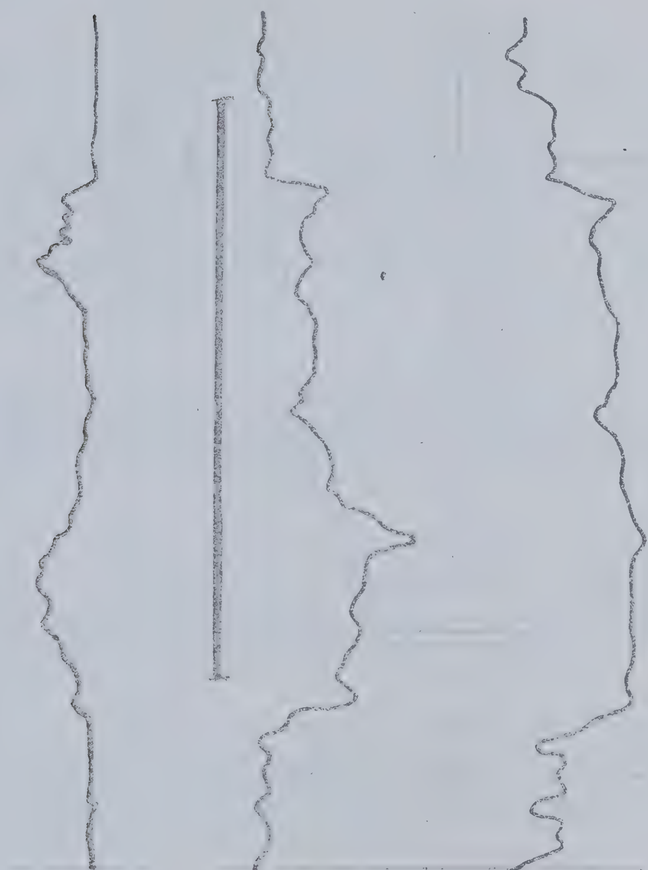

Core: 3"; good recovery (slabbed)

Depth (ft.) — Description

3088-3103
Shale: dark, fissile; highly radioactive; few coarse sandstone lenses near base.

3103-3104
Sandstone: medium to coarse grained, fines upward, fairly well sorted, horizontal laminated; some shaly horizons; bioturbation in places.

3104-3104.5 (facies BV)
Pebble Conglomerate: black and varicolored chert pebbles, well rounded; poorly sorted very coarse sand matrix; dark fissile shale interlaminae; appears reversely graded; shell fragments; siderite concretions.

Depth (ft.)	Description

3104.5-3107
Shale: black, fissile; few medium grained sandstone laminae.

3107-3119
Sandstone (UE_2): light grey, fine grained, fairly well sorted, clean; cross- and horizontal stratification, sharp cross-set boundaries, reactivation surfaces draped with shale; sand laminae and beds in regular alternation with shale, mud and/or siltstone laminae; black chert pebble stringers; abundant bioturbated horizons; bentonite, light grey, fine to medium grained biotite, 2" thick at 3119'.

3119-3121 (facies BIV)
Sandstone: dark grey, fine grained; cross-stratification remnants, sharp contacts, some scour and fill structures; homogenized by very strong bioturbation.

3121-3125 (facies BIII)
Sandstone: light grey, fine grained, clean, well sorted; inclined and horizontal stratification, sharp set boundaries, shale on foreset laminae; bioturbated horizons; shale laminae.

3125-3132 (facies BII)
Sandstone: light grey, fine grained, well sorted sandstone laminae; alternate fairly regularly with shale and mudstone laminae; moderately bioturbated horizons.

3132-3170 (facies BI)
Mudstone: dark grey; siltstone and very fine sandstone laminae and lenses; weak to strong bioturbation, *Zoophycus* sp., *Chondrites* sp., and *Terebellina* sp.; bentonites, light grey, medium to coarse biotite grains, 6" and 3" thick at 3153' and 3169'.

3170-3180 (facies BIV)
Pebbly Sandstone (L_3): dark, dirty, coarse to very coarse grained; black chert pebbles, up to 6 mm long diameter scattered throughout unit; abundant shale streaks; homogenized by strong bioturbation.

3180-3182 (facies BIII)
Sandstone: greenish grey, fine to medium grained, clean, well sorted; low angle, planar cross-lamination, glauconite drape foreset laminae; bioturbated horizons; calcareous cement.

Depth (ft.)	Description
3182-3210	(facies BI $\pm$ BII)

Sandstone: dark grey, very fine to fine grained, becoming muddy towards base; dirty; shaly; clean thin siltstone and very fine sandstone lenses between 3205' and 3210'; almost completely reworked by very strong bioturbation; bentonitic at base.

WESTCOAST SULPETRO HANNA

11-31-31-13W4M

K.B. 2780'

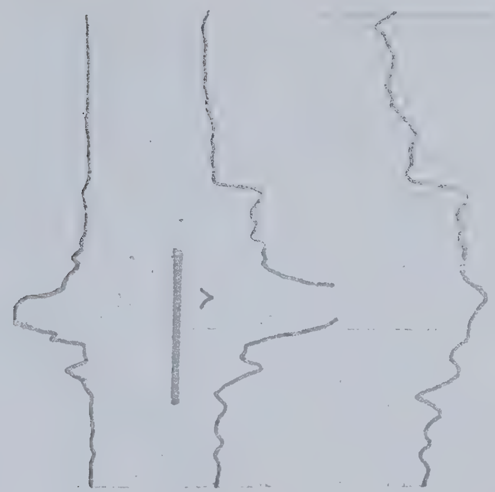

Core: 3"; fair recovery

Depth (ft.) Description

3275-3289 (facies BIV)
Sandstone (L_3): dark grey, muddy, very fine to fine grained, fine pebble horizons at 3276', and 3281'; shale laminae abundant, increase upward; bioturbation, strong, vertical burrows, increase downward.

3289-3305
Sandstone: dark grey and greenish in places; friable, fine to medium grained, black chert pebbles up to 1 cm long diameter dispersed throughout unit but more towards top; abundant shale streaks and laminae; homogenized by very strong bioturbation and therefore structureless; glauconite in places.

3305-3311 (facies BI)
Mudstone: dark, few sand lenses; moderate bioturbation; bentonite, light grey, fine grained, 2" thick at 3307'.

3311-3315
Sandstone: upper 6", light grey, very fine to fine grained, clean, well sorted; low angle, small scale, planar and simple cross- and horizontal stratification; remainder, muddy and shaly, moderately bioturbated.

3315-3325
Missing cores.

PHILLIPS HANDHILLS

10-3-32-17W4M

K.B. 2785'

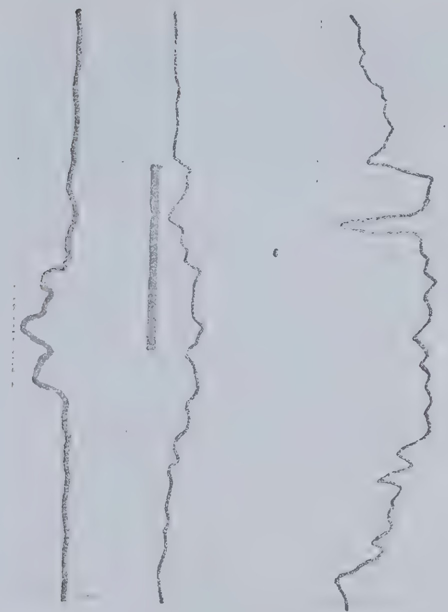

Core: 3"; good recovery

Depth (ft.)	Description

3515-3524
Siltstone: dark grey; shaly, muddy and sandy in places; homogenized by strong bioturbation.

3524-3548 (facies BI)
Mudstone: dark grey; fine to medium grained sandstone lenses, more near base and top; moderate bioturbation; bentonite, light grey, coarse biotite rich, 12" thick at 3530'; scoured basal contact.

3548-3553 (facies BIII)
Sandstone (L_3): light grey, fine to medium grained, clean, well sorted; horizontal and low angle, planar cross-stratification, sharp set contacts; scours; siderite concretions; bioturbation, weak, more at base.

3553-3563 (facies BII ± BI)
Sandstone: light grey, fine grained, clean, well sorted sandstone lenses alternate regularly with shale and/or mudstone; bioturbated horizons abundant.

Depth (ft.)	Description
3563-3564	(facies BIV)

Sandstone: dark grey, shaly, homogenized by bioturbation.

3564-3572	(facies BIII ± BII)

Sandstone: light grey, fine to medium grained, fair sorting; shalier toward base; bioturbated shaly horizons in regular alternation with non-bioturbated sandy horizons.

WESTCOAST PROD. STANMORE

11-7-32-12W4M

K.B. 2633'

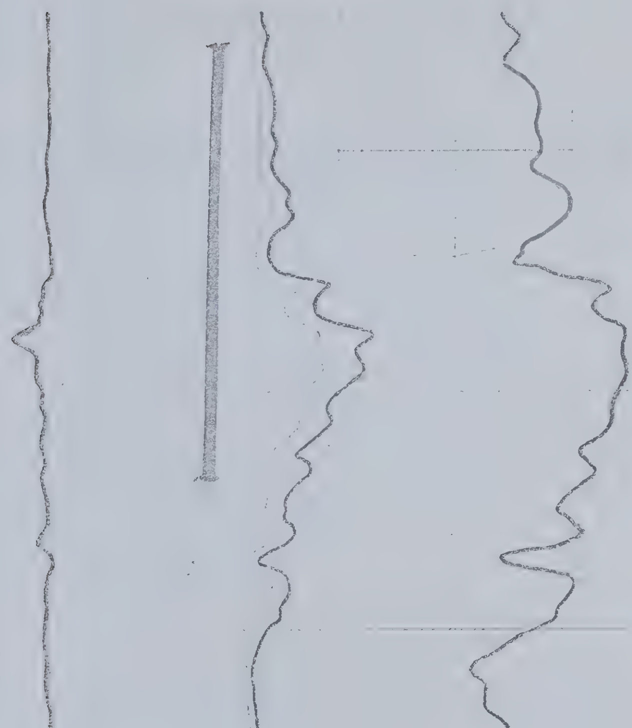

Core: 3"; good recovery

Depth (ft.)	Description
3176-3188	(facies BI) Mudstone: dark grey, fine to medium grained sandstone lenses; strongly bioturbated; bentonitic near top.
3188-3192	Sandstone (L_3): dark grey, medium to coarse grained; fine chert pebble horizons; abundant shale streaks and partings; strongly bioturbated.
3192-3200	Mudstone: dark grey, fine sandstone and siltstone lenses and laminae; strongly bioturbated.
3200-3208	Claystone: dark, massive; sandy toward base; weakly bioturbated.
3208-3218	Mudstone: dark grey; fine grained, well sorted, cross-stratified sandstone lens; moderate bioturbation; bentonitic at base.

10-20-30-12W4M

K.B. 2590'

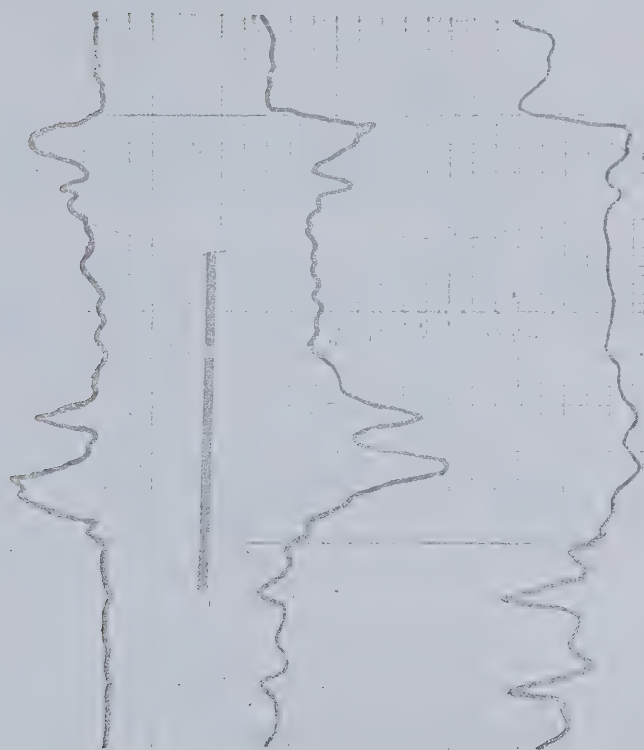

Core: 3"; good recovery

Depth (ft.)	Description

2987-2994 (facies BII)

Sandstone (UE_2): dark grey; sequence of alternating fine grained sandstone and shale laminae; moderately bioturbated horizons.

2994-3018 (facies BI)

Mudstone: dark grey, siltstone and very fine sandstone laminae and lenses, more toward base and top; strongly bioturbated and structureless; bentonite, dark grey, coarse biotite rich, 3" thick at 3007'.

3018-3021 (facies BIV)

Pebbly Sandstone (L_{4b}): dark grey, black chert pebbles up to 1 cm long dispersed in strongly bioturbated, medium to coarse grained sandstone with abundant shaly streaks.

Depth (ft.)	Description

3021-3025 (facies BIII)
Sandstone: light grey, fine to medium grained, clean, well sorted; horizontal and low angle cross-stratification; weakly bioturbated, increasing toward base.

3025-3031 (facies BI $\pm$ BII)
Mudstone: dark grey; some sandstone and siltstone lenses; fine chert pebbles dispersed in a silty shale lens at 3029'; moderately bioturbated.

3031-3034 (facies BIV)
Sandstone: dark grey, dirty, shaly, medium to coarse grained; strongly bioturbated, vertical burrows at 3033'.

3034-3045
Sandstone (L_{4b}): dark grey, dirty, shaly, friable in places; fine, darker and shalier at base, medium to coarse at top; homogenized by strong bioturbation; bentonite, dark grey, medium grained biotite; 3" thick at 3045'.

3045-3050
Sandstone: dark grey, fine to medium grained; abundant shale streaks and partings; strongly bioturbated; bentonite, light grey, fine grained, 2" thick at 3050'.

3050-3059
Shale: black; fissile, more massive near top; weak bioturbation towards top; bentonite, dark grey, medium biotite grains, greater than 6" thick at 3059'.

WESTCOAST SULPETRO SMORE

11-30-29-10W4M

K.B. 2508'

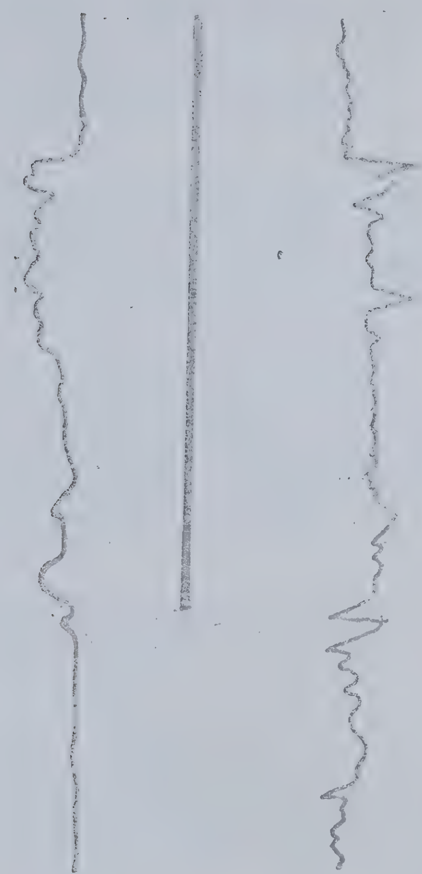

Core: 3"; fair recovery (partly slabbed)

Depth (ft.)	Description

2765-2799
Shale: black, fissile, sandy at base.

2799-2820
Sandstone (UE_2): light grey, fine to medium grained, clean, well sorted; sandstone beds 0.75 to 1.5' thick; stratification, horizontal, cross- and herringbone-like, sharp (erosive) cross-set boundaries; carbonaceous matter and shale on foreset laminae; reactivation surfaces; black chert pebble horizons at 2800', 2802', 2810', up to 1.5 cm long on top; regular interlaminae of dark grey shale, mudstone and siltstone; weakly and strongly bioturbated horizons, mottles, vertical burrows.

Depth (ft.) | Description

2820-2840
Calcareous Sandstone: light, fine grained, cross- and horizontally stratified, calcareous sandstone beds alternate with light grey, usually bioturbated, non-calcareous cross-stratified intervals; sharp contacts; shale laminae, some on foreset laminae, darker and shalier downwards.

2840-2870 (facies BI)
Mudstone: dark; abundant light grey siltstone to fine grained, cross-stratified, sandstone laminae and lenses; weakly bioturbated; bentonite, light grey, coarse biotite grains, 6" thick at 2866'.

2870-2876
Sandstone (L_{4b}): dark grey, dirty, muddy and shaly; medium to coarse grained; fine chert pebbles scattered near top; homogenized by strong bioturbation; calcareous; bentonite, light grey, fine grained, 3" thick at 2876'.

2876-2885 (facies BI)
Mudstone: dark grey, silt and fine sand laminae; weak to moderate bioturbation.

2885-2892
Sandstone (L_{4a}): dark grey, dirty, shaly and muddy; medium to coarse grained; fine black chert pebbles at top; strongly bioturbated, greater than 4" deep burrow (worm?) at top, structureless.

2892-2895 (facies BI)
Mudstone: dark grey; bentonitic; ripple laminated very fine grained sand lenses; moderately bioturbated; calcareous horizons.

TRIAD BPX COPG GARDEN

11-23-34-14W4M

K.B. 2712'

Cores: 2"; good recovery

Depth (ft.) Description

3220-3234
Shale: black, fissile; sandstone lens, a fine chert pebble stringer near base at 3227'.

3234-3236
Pebbly Sandstone: black and varicolored chert pebbles, well rounded; poorly sorted coarse grained sand matrix, 6" thick; sharply underlain by bioturbated mudstone with very fine sandstone lenses, 1.5' thick.

3236-3240
Mudstone: dark grey, siltstone and fine sandstone lenses; weak bioturbation, increases downward.

3240-3243
Sandstone: light grey, fine to medium grained, muddy, dirty, shaly; strongly bioturbated.

3243-3253 (facies BI)
Mudstone: dark grey, regular siltstone and fine sandstone lenses; weak to moderate bioturbation.

3253-3254
Pebbly Sandstone: black chert pebbles, fair sorting, dispersed in an indurated calcareous fairly well sorted coarse grained sandstone; sharp (erosive) contacts; upper 3" and lower 2" moderately bioturbated.

Depth (ft.)	Description

3254-3260

Sandstone: light grey, fine to medium grained; low angle, planar cross-stratification; shale laminae, more toward base; bioturbation, moderate, decreases upwards.

TRIAD B.P. SULLIVAN

7-2-35-14W4M

K.B. 2665'

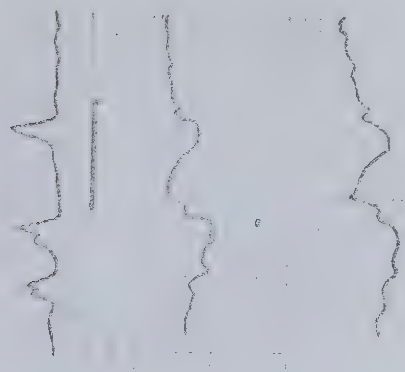

Core: 2"; good recovery

Depth (ft.) | Description

3220-3226
Shale: black, fissile; fine sandstone lenses at base.

3226-3232
Sandstone: light grey, friable, fine to medium grained; shale, streaks, partings, laminae; homogenized by strong bioturbation, vertical burrows on top.

3232-3255 (facies BI $\pm$ BII)
Mudstone: dark grey; siltstone and sandstone laminae and lenses, more towards top and base; bioturbation more towards top and base; bentonite, light grey, medium biotite grains, more than 6" thick at 3255'.

APPENDIX IIIf

Lower Sandstone Ridge Complex
(L_6 member)

B.V.X. LOC. PAN AM SCOLLARD
BOW VALLEY

11-2-34-20W4M

K.B. 2823'

Core: 3"; good recovery

Depth (ft.)	Description

3958-3976 (facies BI)

Mudstone: dark grey; siltstone and fine sandstone laminae and lenses at top and base; bentonite, dark grey, fine grained, less than 3" thick at 3975'; weak bioturbation.

3976-3976.4 (facies BV)

Pebble Conglomerate (L_6): black and varicolored chert pebbles, up to 8 mm maximum diameter, fairly well rounded, matrix support; matrix, fairly well sorted, coarse to very coarse sand; sharp (scour) basal contact; interlaminated with shale.

Depth (ft.)	Description

3976.4-3985
Sandstone: dark grey at base to light grey on top; fine to medium grained, fair sorting; abundant shale laminae, more towards the base; strongly bioturbated, more toward the base; basal 6" is dark mudstone with a sharp (erosive) lower contact.

3985-3987
Pebbly Sandstone: light grey, medium to coarse grained, clean, well sorted; medium angle, planar and simple cross-stratified; black chert pebbles, up to 1 cm long diameter, fairly well rounded, matrix supported; matrix, poorly sorted very coarse sand, thin, caps sequence and dispersed within the unit; interlaminated with shale and mudstone near base.

3987-3991
Pebbly Mudstone: black chert pebbles, up to 8 mm long diameter, scattered in dark grey bioturbated mudstone 12" from top; siltstone and sandstone laminae and lenses common in the remainder of the interval; greenish and glauconitic.

3991-3196
Sandstone: greenish grey, medium to coarse grained, fair sorting; low angle, planar cross-stratified, shale and glauconite drape foreset laminae; few shale laminae; moderate bioturbation at base; siderite concretions.

3196-4000 (facies BIV)
Sandstone: dark grey, very fine to fine grained; abundant shale streaks and partings; homogenized by bioturbation.

4000-4005 (facies BIII)
Sandstone: greenish grey, fine to medium grained, clean, well sorted; low angle, planar cross-stratification, glauconite and shale drape foreset laminae, sharp cross-set contacts; shaly towards base; siderite concretions; weakly bioturbated.

4005-4111 (facies BII)
Sandstone: dark grey, very fine to fine grained, well sorted sandstone lenses less than 4" thick interbedded with bioturbated shaly and/or muddy horizons or laminae; bioturbation increases downward.

Depth (ft.)	Description

4111-4115 (facies BI)

Mudstone: darker grey; blebs and wisps of sand; a few sandstone lenses; homogenized by strong bioturbation.

4115-4118

Sandstone: dark grey, fine grained, shale streaks and partings common, very strongly bioturbated and structureless.

C.D.R. ET AL FENN B.V.

2-30-35-19W4M

K.B. 2793'

Core: 3"; good recovery

Depth (ft.) Description

3835-3840 (facies BI)

Mudstone: dark grey, greenish in places; sandstone lenses, fine to medium grained, glauconitic; black chert pebbles, up to 1 cm longest diameter, scattered in core box around 3835'; moderate bioturbation near base.

3840-3845 (facies BIII)

Sandstone (L_6): greenish grey, coarse grained, fairly well sorted; low angle, planar cross-stratified, sharp set contacts, reactivation surfaces draped with mudstone film; shaly and darker downwards; moderate bioturbation at base.

3845-3847 (facies BII ± BI)

Sandstone: dark grey; interlamination of fine sand, mudstone and shale; moderate bioturbation.

Depth (ft.)	Description

3947-3851

Sandstone: dark grey, coarse grained, shaly; almost homogenized by strong bioturbation.

3851-3856

Sandstone: darker grey, fine to medium grained; a few horizontally laminated intervals; abundant shale streaks and partings; nearly homogenized by strong bioturbation.

APPENDIX IIIg

Lower Sandstone Ridge Complex
(L_7 member)

CAMAC CHEVRON HUXLEY

10-4-34-24W4M

K.B. 3045'

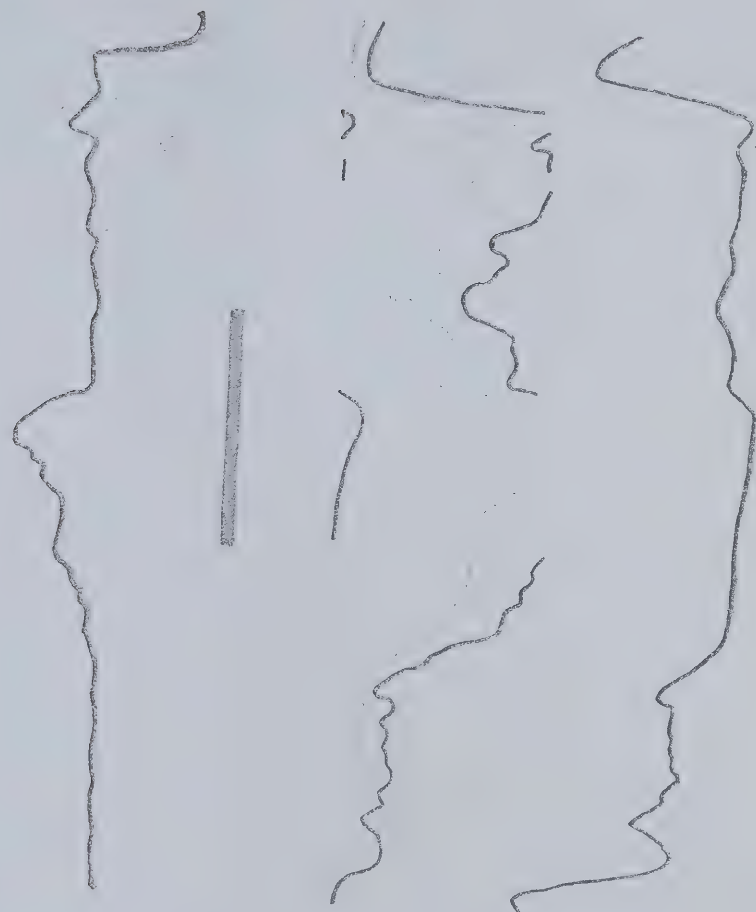

Core: 3"; fair recovery (slabbed)

Depth (ft.)	Description

4850-4868 (facies BI)

Mudstone: dark grey, abundant light grey, fine grained sandstone lenses, a few cross-stratified with sharp cross-set contacts; black chert pebbles (5 mm) dispersed in mudstone within 4851' to 4853'; bioturbation, weak.

4868-4880 (facies BIII)

Sandstone (L_7): light grey, fine to medium grained, clean, well sorted; low to medium angle, planar and simple cross-stratified, sharp set boundaries, shale drape on foreset laminae; shale laminae in places near base; a few bioturbated horizons, more at base; siderite concretions.

Depth (ft.)	Description
4880-4900	(facies BII)

Sandstone: dark to light grey, very fine to fine grained; clean, well sorted sandstone lenses, 1.25 cm to 5 cm thick, some horizontally and cross-stratified, alternate sharply with bioturbated shaly intervals of more or less same thickness; shale content and the degree of bioturbation decreases upward.

CAMAC MAVRK HUXLEY

6-20-34-24W4M

K.B. 3053'

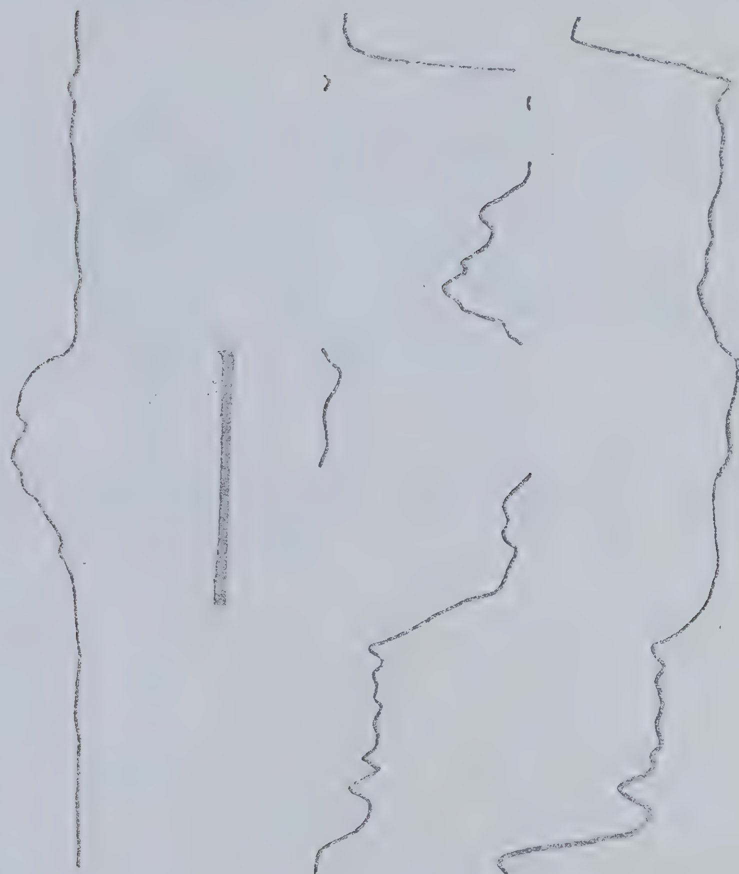

Core: 3"; good recovery (slabbed)

Depth (ft.) | Description

4892-4898 (facies BI)

Pebbly Mudstone (L_7): dark grey; lenses, siltstone, very fine to fine grained sandstone, pebbly sandstone; black chert pebbles scattered throughout interval; bioturbation, weak.

4898-4898.7 (facies BV)

Pebble Conglomerate: black and varicolored chert pebbles, shale clasts, fairly well rounded, up to 2 cm long axis; matrix, poorly sorted, coarse to very coarse grained sand; matrix support; sharp lower contact; protruding pebbles.

Depth (ft.)	Description

4898.7-4906 (facies BIII)

Sandstone: light grey, fine to medium grained, well sorted, clean; low angle, planar cross-stratification, shale drape foreset laminae; bioturbated horizons.

4906-4932 (facies BII)

Sandstone: dark grey, very fine to fine grained, clean, well sorted, structureless to cross-stratified sandstone laminae and beds (1-15 cm) thick; alternate regularly with bioturbated shaly horizons; sandstone bed thickness decreases downward and bioturbated horizons increase in thickness with depth; the unit becomes shalier and more bioturbated downwards; bentonite, light grey, fine grained, 1" thick at 4932'.

4932-4945 (facies BI)

Mudstone: dark grey, few fine sand lenses; almost homogenized by strong bioturbation, vertical burrows (*Rhizocorallium* sp.?); sandy on top.

DECALTA C.D.R. HUXLEY

6-36-34-25W4M

K.B. 3051'

Core: 3"; good recovery (slabbed)

Depth (ft.) Description

4950-4954 (facies BIII)

Sandstone (L_7): light grey, fine to medium grained, well sorted; low angle, planar and simple cross-stratification, shale drape foreset laminae; bioturbation, weak; shale content and bioturbation increase downward.

4954-4967 (facies BII)

Sandstone: light grey, fine grained, well sorted, clean, thin sandstone beds alternate regularly with dark shale laminae; bioturbation, moderate.

Depth (ft.)	Description

4967-4971 (facies BIII)

Sandstone: light grey, very fine to fine grained, fairly sorted and clean; low to medium angle, planar cross-stratification, shale drape foreset laminae; glauconitic; bioturbated horizons, vertical burrows at base; pyritic and sideritic.

CAN SEABOARD BANFF WIMBORNE

6-25-34-27W4M

K.B. 3066'

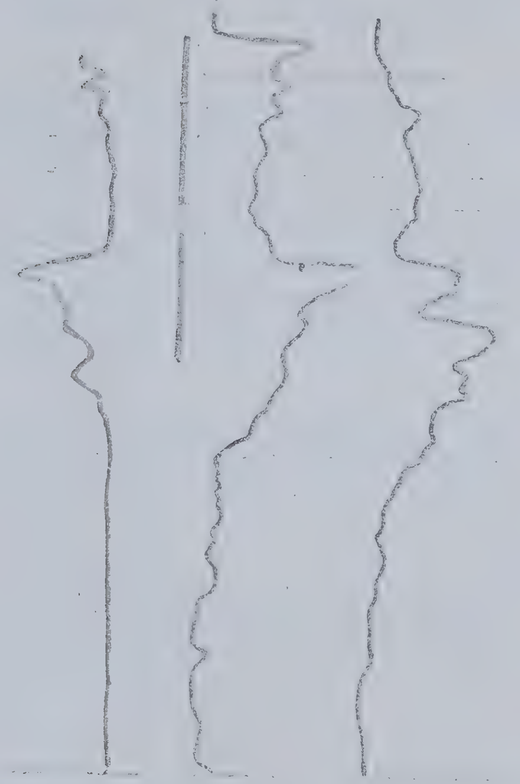

Core: 3"; good recovery

Depth (ft.) Description

5320-5323
Sandstone (UW_3): light grey, fine to medium grained, clean, well sorted; low angle, planar cross-stratified.

5323-5324
Mudstone: dark grey; sandstone lenses, some cross-stratified; bioturbated horizons.

5324-5326
Sandstone: light grey, very fine to medium grained, clean, well sorted; cross-stratified, sharp (scour) basal contact.

5326-5332
Mudstone: dark grey; abundant siltstone and sandstone lenses and laminae, some cross-stratified; bioturbated horizons.

Depth (ft.)	Description

5332-5336
Sandstone: light grey, very fine to medium grained, clean, well sorted; cross-stratified in places; bioturbated horizons, sharp (scour) basal contact.

5336-5340
Mudstone: dark grey; siltstone and sandstone lenses, abundant; bioturbated horizons.

5340-5347
Sandstone: dark grey, very fine to fine grained; muddy and shaly; low to medium angle, planar cross-stratified in places; sharp scour surfaces common; moderate bioturbation.

5347-5388
Mudstone: dark grey; siltstone and sandstone lenses, cross-stratified in places; weak bioturbation; interval 5371 to 5380' no cores cut.

5388-5390 (facies BV)
Pebble Conglomerate (L_7): black and varicolored chert pebbles, up to 1 cm long diameter, fairly well rounded; matrix, poorly sorted coarse sand; weakly cross-stratified; pebbles protrude into overlying mudstone.

5390-5398 (facies BIII)
Sandstone: light grey, medium grained, clean, well sorted; low to medium angle planar cross-stratification, shale drape foreset laminae, reactivation surfaces, sharp cross-set boundaries; weak bioturbation; siderite concretions.

5398-5407 (facies BII)
Sandstone: dark grey; fine grained sandstone lenses alternate regularly with bioturbated shaly and muddy horizons; more than 3" deep vertical burrows at 5403'; sharp contacts, some erosional.

5407-5413
Sandstone: dark grey, fine to medium grained; structureless due to very strong bioturbation.

5413-5420
Sandstone: darker grey, very fine to fine grained; muddy and shaly; some scour and fill structures; strongly bioturbated.

CEJA C.D.N. DUP. DARVEY

6-27-34-27W4M

K.B. 3178'

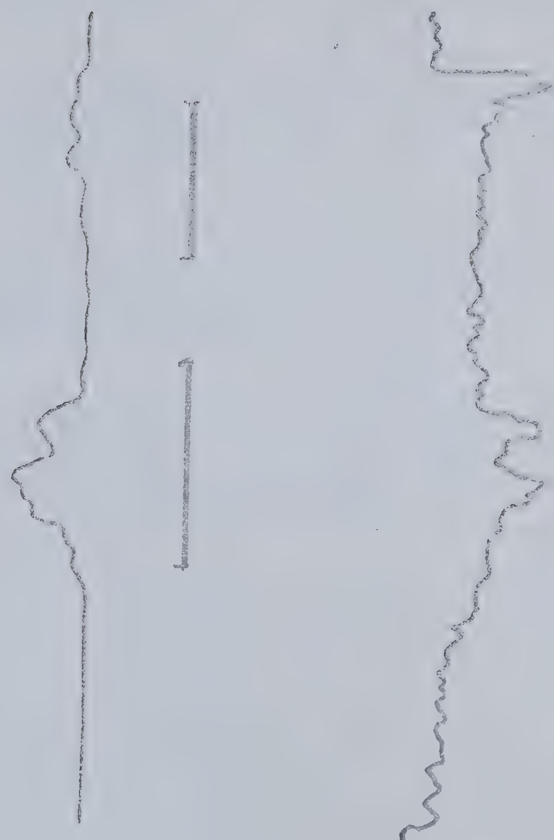

Core: 3"; good recovery

Depth (ft.)	Description

5510-5510.5
Pebble Conglomerate (UW_3): black and varicolored chert pebbles, up to 1.5 cm long diameter, fairly well rounded; matrix, poorly sorted coarse to very coarse sand; sharp (scour) lower contact.

5510.5-5511
Sandstone: light grey, medium to coarse grained, clean, well sorted, gradational base.

5511-5513
Mudstone: dark grey; fine sandstone lenses, abundant, more near top, some horizontal lamination; bioturbation, weak; siderite concretions; sharp (scour) lower contact.

Depth (ft.) | Description

5513-5517
Sandstone: light grey, fine to medium grained; horizontal and cross-stratification in places; scour surfaces; weakly bioturbated horizons.

5517-5519
Mudstone: dark grey; siltstone and fine sandstone laminae and lenses, some cross-stratified; bioturbation in places.

5519-5525
Sandstone: dark grey, fine grained; interlaminated with shale, siltstone and mudstone; scour surfaces, bioturbated horizons.

5525-5574 (facies BI)
Mudstone: dark grey; very fine to fine grained sandstone lenses, more in upper half; shaly; bioturbation, strong in lower half of interval; interval 5543 to 5565' is not cored.

5574-5581 (facies BIII)
Sandstone (L_7): greenish grey, fine to medium grained, clean, well sorted; low to medium angle, simple and planar cross-stratification, glauconite and shale drape foreset laminae, sharp set boundaries; reactivation surfaces, some draped by carbonaceous mud film; bioturbated horizons alternate sharply with clean sandstone intervals, vertical burrows up to 3" deep; pyritic and sideritic; unit capped by a thin nearly equidimensional black chert pebbles up to 1 cm long diameter.

5581-5587 (facies BII)
Sandstone: dark grey, very fine to fine grained; muddy and shaly interlaminae; moderately bioturbated horizons.

5587-5600 (facies BII $\pm$ BIII)
Sandstone: dark grey, fine to medium grained, dirty, muddy and shaly; nearly well homogenized by strong bioturbation; shale laminae and streaks common, scour surfaces, a few sharply based clean sandstone lenses; shale clasts at 5592'.

5600-5608 (facies BI)
Mudstone: darker grey, few siltstone and fine sandstone lenses, very strongly bioturbated, blebs, wisps and mottles of sand.

APPENDIX IIIh

Lower Joffre Sandstone Ridge Complex
(LJ_2 and LJ_3 members)

C.S. JOFFRE

13-33-38-26W4M

K.B. 3218'

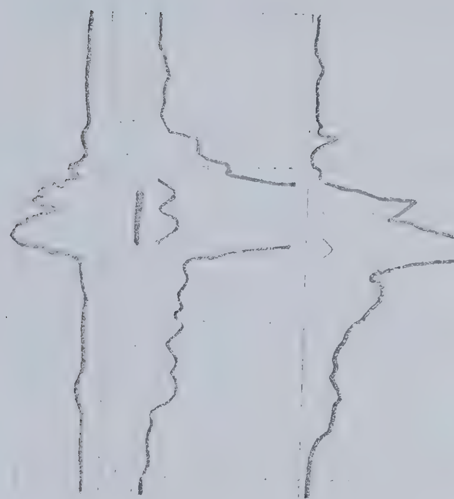

Core: 3"; good recovery

Depth (ft.) Description

5309-5314 (facies BIII)

Sandstone (LJ_2): greenish grey, coarse to very coarse grained, fairly well sorted; medium to high angle, planar and simple cross-stratification, sharp set boundaries, shale, glauconite, and carbonaceous mudstone, drape foreset laminae; weak bioturbation in places.

5314-5317 (facies BII ± BI)

Sandstone: dark grey, fine to medium grained sandstone lenses, less than 2" thick, alternate regularly with shale laminae; bioturbated horizons; underlain by a 3" thick sharply based, mudstone laminae.

5317-5319 (facies BIV)

Pebbly Sandstone (LJ_3): light grey, very coarse grained; black chert pebbles, (4mm-6mm) longest diameter, fairly well rounded, dispersed throughout interval, strongly bioturbated.

5319-5325 (facies BIII)

Sandstone: light grey, coarse to granule sand grains, well sorted; a few pebbles; cross-stratification, weak; shale streaks common near base; carbonaceous mudstone, 12" thick at 5320.5'; bioturbated horizons.

Depth (ft.)	Description

5325-5328 (facies BII)

Sandstone: dark grey; sand lenses, fine to medium grained, well sorted, clean, less than 2" thick, some cross stratified, and interlaminated with shale and mudstone; bioturbation, moderate to strong, finer sediments more affected; glauconite in places.

IMPERIAL BURBANK

13-15-39-27W4M

K.B. 2823'

Core: 3"; fair recovery (a few slabbed pieces)

Depth (ft.) Description

5100-5115.5
Claystone: black, massive; between 5113.5 and 5114.5', pebble conglomerate, cross-stratified coarse to very coarse grained sandstone, pebbly sandstone, pebble conglomerate, pebbly mudstone lenses, each less than 3" thick, are interbedded from top to base; these are in turn underlain by 12" thick dark mudstone; weak bioturbation.

5115.5-5116 (facies BV)
Pebble Conglomerate: black and varicolored chert pebbles, up to 8 mm longest diameter, fairly well rounded, matrix supported; matrix, poorly sorted, very coarse sand and mud.

5116-5119
Sandstone: light grey, coarse to very coarse grained; some shale laminae; strongly bioturbated, vertical burrows more than 4" deep; siderite concretions at top.

5119-5124 (facies BI)
Mudstone: light to dark grey; sandstone lenses, fine to medium grained, some horizontally or cross-stratified; few chert granule lenses, up to 3 mm longest diameter; bioturbation, moderate, vertical and horizontal burrows, sand mottles; bentonite, yellowish grey, fine grained, less than 2" thick at 5124'.

Depth (ft.)	Description

5124-5127 (facies BIV)

Sandstone (LJ3): light grey, medium to coarse grained, fairly well sorted; cross-stratified in places; interlaminae, less than 3" thick chert pebble conglomerate lenses, fissile black shale; bioturbation, moderate, at horizons.

5127-5135 (facies BV)

Pebble Conglomerate: black and varicolored chert pebbles, 4 mm - 15 mm longest diameter, fairly well rounded, matrix support; matrix, poorly sorted very coarse sand; weakly cross-stratified; few black fissile shale laminae; weakly bioturbated horizons.

5135-5138 (facies BII)

Pebbly Sandstone: black and varicolored chert pebbles, up to 6 mm longest diameter, fairly well rounded, 3 and 15" thick; interbeds of well sorted, clean very coarse sandstone, 6 and 15" thick, and shale; bioturbation, moderate, vertical burrows filled with very coarse sand.

5138-5150 (facies BI)

Mudstone: dark grey; sandstone and pebble horizons near top; moderate bioturbation.

CALSTAN JOFFRE

8-20-39-27W4M

K.B. 2905'

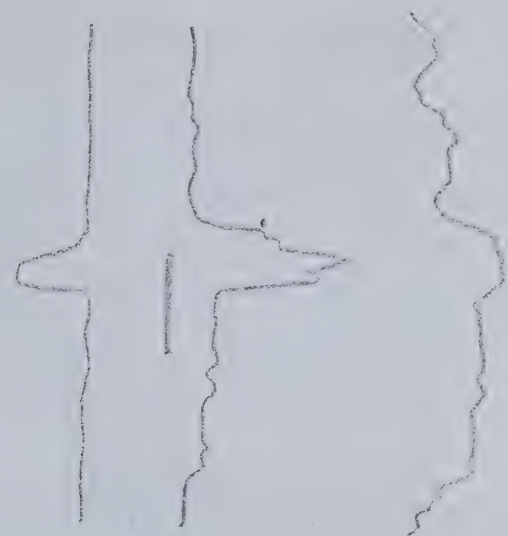

Core: 3"; good recovery

Depth (ft.)	Description
5267-5271	(facies BIV)

Sandstone (LJ_3): dark grey; abundant shaly and muddy horizons, often moderately bioturbated.

5271-5278 (facies BV)

Pebble Conglomerate: black and varicolored chert pebbles, 5 mm to 8 mm longest diameter, fairly well rounded, matrix support; matrix, poorly sorted, coarse to very coarse sand; faintly cross-stratified; few mudstone laminae.

5278-5281 (facies BII)

Sandstone: light grey; very coarse grained, becoming finer towards base; cross-stratified in places; fine chert pebble lenses, dark fissile shale laminae are common.

5281-5298 (facies BI)

Mudstone: dark grey; bioturbation, moderate, vertical burrows filled with coarse sand in places near top; shalier toward base.

APPENDIX IIIi

Lower Joarcam Sandstone Ridge Complex
(L_9 member)

CEJA P.C.P. LEO

6-31-36-16W4M

K.B. 2790'

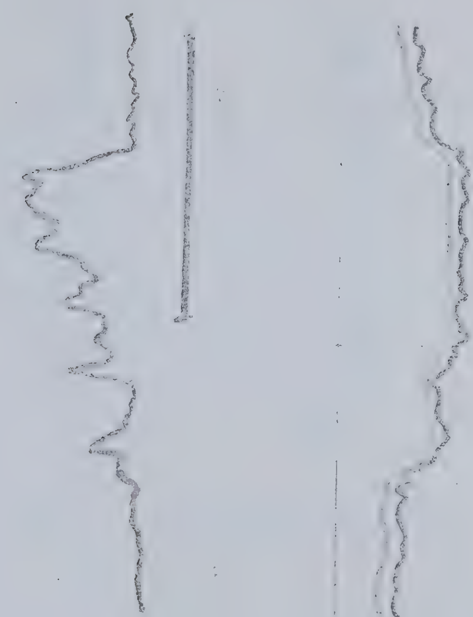

Core: 3"; good recovery

Depth (ft.) Description

3385-3405
Shale: dark, fissile, a few siltstone lenses toward base.

3405-3410 (facies BIV)
Mudstone: dark grey, a few siltstone and fine sandstone lenses; strongly bioturbated.

3410-3433 (facies BIII ± BII)
Sandstone: dark grey, fine to medium grained; low angle, planar and simple cross-stratification in places near top; very shaly; nearly homogenized by strong bioturbation.

3433-3439 (facies BI)
Mudstone: dark grey, blebs and wisps of sand, strongly bioturbated.

3439-3445
Sandstone: dark grey, very fine to fine grained; abundant shale streaks and partings; structureless due to strong bioturbation.

CEJA ET AL MAPLE

10-26-36-16W4M

K.B. 2811'

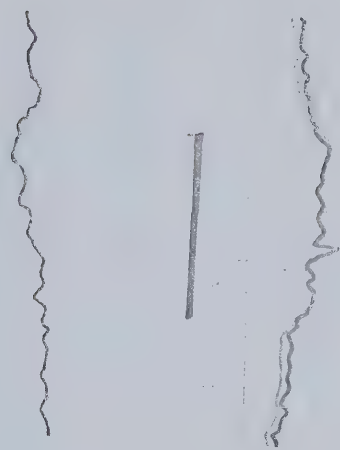

Core: 3"; good recovery

Depth (ft.)	Description

3310-3325 (facies BIII)
Sandstone: dark grey, muddy to fine grained; rare planar cross-stratified horizons; shale streaks and partings common; nearly structureless due to very strong bioturbation.

3325-3350 (facies BII)
Sandstone: dark grey, very fine to fine grained sandstone lenses, some horizontal or cross-stratified; alternate regularly with bioturbated shale or mudstone laminae; glauconitic in places; scoured surfaces.

3350-3359 (facies BI)
Mudstone: dark grey, few siltstone and fine sandstone lenses and laminae; moderate bioturbation; sharp (scoured) basal contact.

3359-3365 (facies BII)
Sandstone: dark grey, fine to medium grained, dirty, muddy and shaly; strongly bioturbated.

3365-3370 (facies BI)
Mudstone: dark grey, few siltstone laminae, moderately bioturbated.

CEJA WAIN MAPLE

7-35-36-15W4M

K.B. 2784'

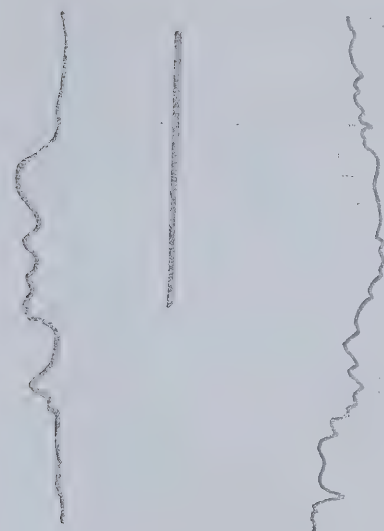

Core: 3"; good recovery

Depth (ft.) | Description

3268-3290
Shale: dark, fissile, a few siltstone and very fine sandstone lenses toward base.

3290-3295
Mudstone: dark grey; interlamination of very coarse sandstone, mudstone and fine pebbles 12" from top; bioturbation is moderate.

3295-3308
Sandstone: dark grey, fine to medium grained, dirty, muddy and shaly; homogenized by intense bioturbation.

3308-3328
Sandstone: dark grey, fine grained, dirty, muddy, and very shaly; moderate to strongly bioturbated horizons; glauconitic in places; mudstone and shale interbeds.

MOBIL C.P.O.G.

6-23-36-14W4M

K.B. 2692'

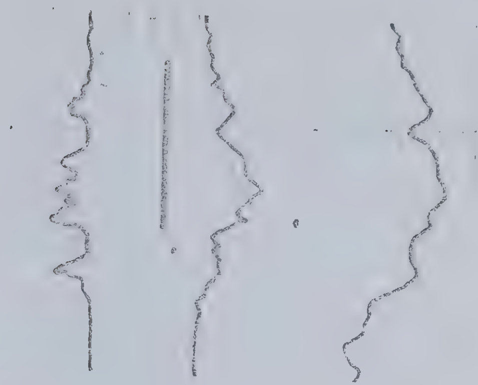

Core: 3"; poor recovery

Depth (ft.)	Description
3212-3218	Shale: black, a few silt and fine sand lenses toward base; sharp lower contact.
3218-3221	Mudstone: dark grey, sandy and moderately bioturbated; fine pebbly sandstone lens caps the unit; bentonite, dark grey, fine grained, thin at 3120'.
3221-3230	Sandstone: dark grey, fine to medium grained, dirty, muddy and shaly; completely reworked organically.
3230-3240	Mudstone: dark grey, few silt and sand lenses; reworked by strong bioturbation.
3240-3267	Muddy Sandstone: dark grey, some darker intervals due to higher shale content, fine to medium grained, dirty; structureless due to intense bioturbation; bentonitic at 3260'.

APPENDIX IIIj

Lower Joarcam Sandstone Ridge Complex
(LJC_2 member)

PAMOIL ET AL CHIGWELL

10-3-41-25W4M

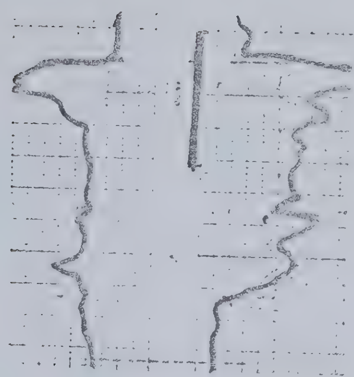

Core: 2"; good recovery

Depth (ft.)	Description

4580-4590

Shale: black, fissile or massive in places, pebble impressions at base.

4590-4590.3 (facies BV)

Pebble Conglomerate (LJC_2): black and varicolored chert pebbles, up to 1.5 cm longest diameter, fairly well rounded, matrix support; matrix, poorly sorted, coarse to very coarse sand; mud interlaminae; sharp upper contact.

4590.3-4600 (facies BIII)

Sandstone: light grey, medium grained, clean, well sorted; low to medium angle, simple and planar cross-stratification, cross-set thickness less than 6", sharp cross-set contacts, shale and glauconite drape foreset laminae; bioturbation, moderate, at shaly horizons, increases downwards; siderite concretions.

4600-4610 (facies BII)

Sandstone: dark grey, very fine to fine grained sandstone lenses less than 2.5 cm thick, in regular alternation with bioturbated shaly or muddy sandstone laminae and horizons; base, more bioturbated and shalier; sharp (scour) contacts; bentonitic at 4606'.

Depth (ft.)	Description

4610-4622 (facies BI)

Mudstone: darker grey; few silt and very fine sand lenses, often with sharp upper and lower contacts; bioturbation, moderate to strong.

APPENDIX IIIj

Lower Joarcam Sandstone Ridge Complex
(LJC_{12} member)

IMPERIAL DINANT

16-6V-48-20W4M

K.B. 2441'

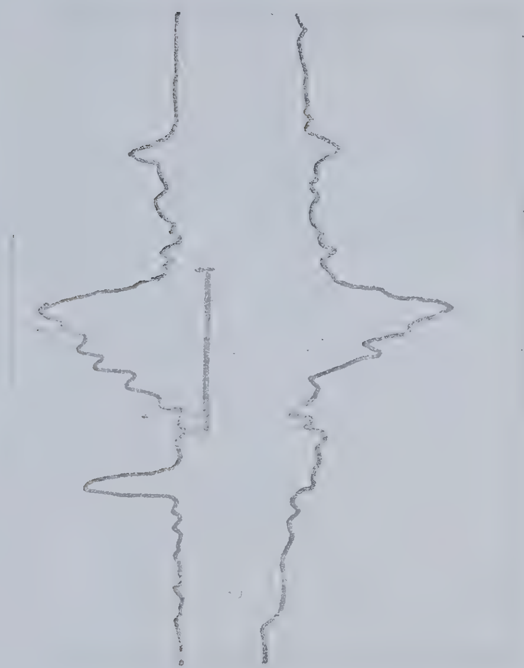

Core: 2"; good recovery (slabbed)

Depth (ft.) Description

3184-3190 (facies BIV)

Sandy Mudstone: dark grey; interbedding of fine to very coarse sand with black shale, carbonaceous mudstone, siltstone and mudstone; abundant sharp (scour) contacts; bioturbation, weak to moderate, horizons of finer sediments more susceptible, vertical burrows, mottles and pods of coarse sand.

3190-3197 (facies BIII)

Sandstone: dark grey, coarse to very coarse grained, fairly well sorted; weakly cross-stratified; glauconite drape foreset laminae; some shale laminae; bioturbation, weak, at horizons, vertical burrows up to 4" deep.

Depth (ft.)	Description

3197-3211 (facies BII)

Sandstone: dark grey, fine to very coarse grained, shaly and glauconitic; clean sandstone beds alternate with strongly bioturbated shaly lenses 2 to 4" thick; sharp contacts (scour); darker, shalier, and finer at base.

3211-3215 (facies BI)

Mudstone: dark grey; siltstone and very fine sandstone lenses, clean, plane laminated; bioturbation, moderate, mottles and pods of sand; bentonite, light grey, fine to medium biotite grains, 15" thick at 3212.5'.

SUPERIOR DINANT

10-8-48-20W4M

K.B. 2443'

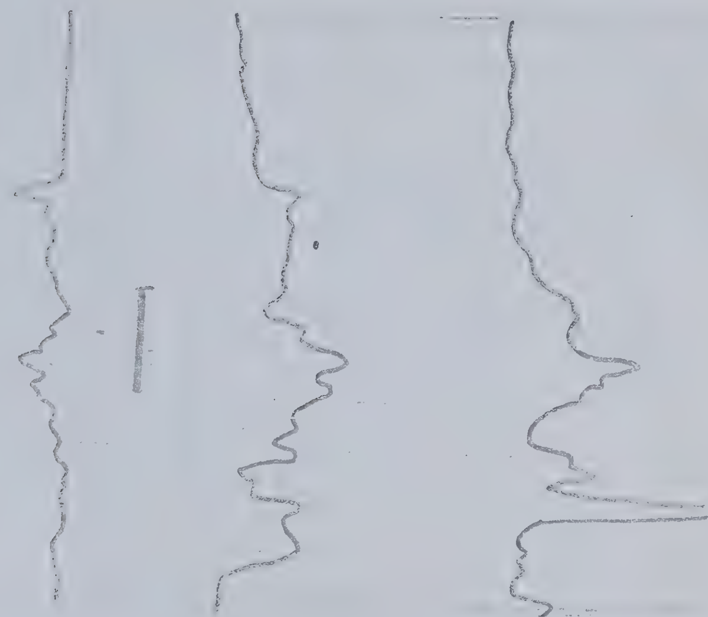

Core: 2"; poor recovery (slabbed)

Depth (ft.)	Description

3168-3177.2 (facies BIV)

Sandy Mudstone: dark grey; fine sand to granule size chert lenses less than 2" thick, often clean, well sorted, cross- and plane laminated; interbedded with bioturbated mudstone beds up to 4" thick; bentonite, light grey, fine to medium biotite grain, 2" thick at 3168.5'.

3177.2-3181.2

Missing cores.

3181.2-3184 (facies BII)

Sandstone: dark grey to greenish in places; coarse to very coarse sandstone lenses, up to 2.5" thick, fairly sorted, weakly cross-stratified; interlaminated with bioturbated mudstone and sandy mudstone beds less than 2 cm thick; common sharp (scour) contacts.

IMPERIAL ARMENA

1-13-48-21W4M

K.B. 2446.7'

Core: 2"; poor recovery (slabbed)

Depth (ft.)	Description
3200-3209	(facies BI) Mudstone: dark grey; abundant siltstone and very fine sandstone lenses, plane and cross-laminated in places; few dark, fissile shale laminae; moderately bioturbated.
3209-3213.6	(facies BIV) Sandstone: light grey, greenish in places, coarse to granule size sand, fairly sorted; some fine chert pebbly horizons; shale and mudstone laminae; bioturbated horizons. Interval appears made up of about 4 discrete coarsening upward units, each about 9-12" thick.
3213.6-3234.4	Missing cores.

Depth (ft.)	Description

3234.4-3240 (facies BII)

Sandstone: dark grey, fine to medium grained sand; abundant shale streaks, wisps, blebs and partings; homogenized by very strong bioturbation; two clean sand lenses with sharp (scour) contacts; bentonite, dark grey, fine to medium biotite grains, 11" thick at 3239.5'.

3240-3241 (facies BI)

Mudstone: dark grey, fine sand lens with sharp upper and lower contacts; nearly homogenized by very intense bioturbation.

IMPERIAL ARMENA

9-13V-48-21W4M

K.B. 2460'

Core: 2"; good recovery (slabbed)

Depth (ft.) Description

3205-3214 (facies BI)

Mudstone: dark grey; plane and cross-stratified siltstone and fine sandstone lenses up to 1.5 cm thick towards top, coarse to very coarse and pebbly sand lenses up to 5 cm thick and cross-stratified in places towards the base; abundant sharp contacts, some erosional; bioturbation, weak to moderate, at horizons; bentonitic at 3210'.

3214-3220 (facies BIV)

Sandstone: dark grey to greenish, coarse to granule size, fairly well sorted, cross-stratified in places; shale and mudstone wavy interlaminae, up to 5 cm thick where sandy; sharp contacts, some erosional; bioturbation, weak to moderate, at horizons.

Depth (ft.)	Description

3220-3238.5 (facies BIII)

Sandstone: greenish grey, medium to granule size grains, fairly well sorted; low angle, planar cross-stratified, sharp set boundaries, shale and glauconite drape foreset laminae; seems made up of several coarsening upward units 9 to 15" thick; bioturbation, weak to moderate, at shaly intervals or horizons.

3238.5-3243.5 (facies BII)

Sandstone: dark grey, fine to medium grained; abundant shale streaks, partings, wisps and blebs; nearly homogenized by very strong bioturbation; a few clean sandstone lenses with sharp contacts; darker, shalier, finer, and more bioturbated toward base.

3243.5-3247 (facies BI)

Mudstone: dark grey; strongly bioturbated (*Chondrites)*, abundant pods of sand gives a mottled appearance to unit; few clean sandstone lenses, some sharply based; bentonite, light grey, fine to medium biotite grain, about 12" thick at 3244'.

IMPERIAL DINANT

13-19V-48-20W4M

K.B. 2486'

Core: 2"; good recovery (slabbed)

Depth (ft.) Description

3218-3231 (facies BI)
Mudstone: dark grey; plane and cross-stratified siltstone and fine sandstone lenses near top, coarse to very coarse sand lenses up to 2.5 cm thick toward base; bioturbation, weak near top and moderate near base.

3231-3236 (facies BIII)
Sandstone: dark grey to greenish, very coarse grained, fairly sorted, low angle, planar cross-stratification in places; glauconitic; shale and mudstone laminae, more at top and base; moderate bioturbation near top and base; some sharp contacts (scour).

3236-3250 (facies BII)
Sandstone: dark grey, fine to coarse grained, very shaly and glauconitic; almost completely reworked by very intense bioturbation; a few siltstone and fine sandstone lenses less than 1.5 cm thick, shale laminae less than 2 mm thick; bentonite, light grey,

Depth (ft.) Description

medium biotite grains, more than 24" thick at 3247.5'.

3250-3253 (facies BI)

Mudstone: dark grey, homogenized by very strong bioturbation; bentonite, light grey, fine to medium biotite grain, 18" thick at 3251.5'.

APPENDIX IIIk

Upper Eastern Sandstone Ridge Complex
(UE_2 member)

U.S. SMELTING ACADIA

11-11-24-3W4M

K.B. 2415'

Core: 3"; good recovery (slabbed)

Depth (ft.) | Description

2445-2450
Shale: black, fissile or massive in places; thin chert granule stringer and fine sand lenses near base.

2450-2451 (facies BV)
Pebble Conglomerate: black and varicolored chert pebbles, up to 1 cm longest diameter, fairly well rounded, matrix support; matrix, poorly sorted, very coarse sand; shale and mudstone interlaminae, sharp lower contact; 10 cm thick; grades upward into 7.5 cm thick pebbly sandstone, up to 5 mm longest diameter, shale streaks; finally capped by 10 cm thick fine to medium grained, well sorted sandstone.

Depth (ft.)	Description
2451-2460	(facies BIII)

Sandstone: light grey, fine grained, clean, well sorted; friable, indurated and calcareous between 2451 and 2453.5'; medium scale, low angle simple cross-stratification; a few shaly horizons, some on foreset laminae; bioturbation, moderate near top, and at horizons.

UNION PERMO ACADIA VALLEY

7-11-25-3W4M

K.B. 2413'

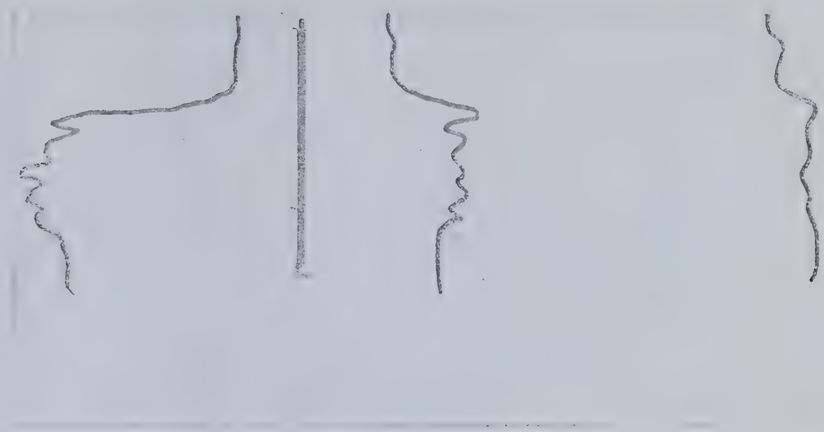

Core: 3"; good recovery (slabbed)

Depth (ft.) Description

2453-2470
Shale: black, fissile, sideritic, few siltstone stripes, sharp basal contact.

2470-2483 (facies BIV)
Sandstone: brownish grey, friable, fine grained, muddy, shale laminae in places; nearly homogenized by intense bioturbation, vertical and J-shaped burrows; a few low angle planar cross-stratified horizons, some with carbonaceous matter on foreset laminae; a 1.2 cm thick pebbly sandstone caps the unit.

2483-2503 (facies BIII)
Sandstone: light grey, yellowish brown in places, fine grained, clean, well sorted, slightly indurated; medium scale low angle, planar cross-stratified, sharp set boundaries, carbonaceous mudstone and shale on foreset laminae; shale laminae, more near base; bioturbation, vertical burrows, at horizons.

O.S.S. SMELTING ACADIA

10-2-25-2W4M

Core: 3"; good recovery (slabbed)

Depth (ft.)	Description

2438-2446
Shale: black, fissile; sandy and bioturbated near base.

2446-2447 (facies BV)
Pebble Conglomerate: black chert pebbles, up to 8 mm longest diameter, fairly well rounded, matrix supported; matrix, poorly sorted coarse to very coarse sand; interlaminated with dark shale, mudstone and pebbly sandstone; sharp lower contact.

2447-2453 (facies BIII)
Sandstone: light grey, fine grained, clean, well sorted; friable; calcareous and indurated between 2447 and 2449'; medium scale, low angle planar and simple cross-stratified, sharp set boundaries, shale drape foreset laminae; few shale and mudstone laminae, more near base; bioturbated horizons.

ANGLO ROYALITE KROY ACADIA

6-28-24-1W4M

K.B. 2397'

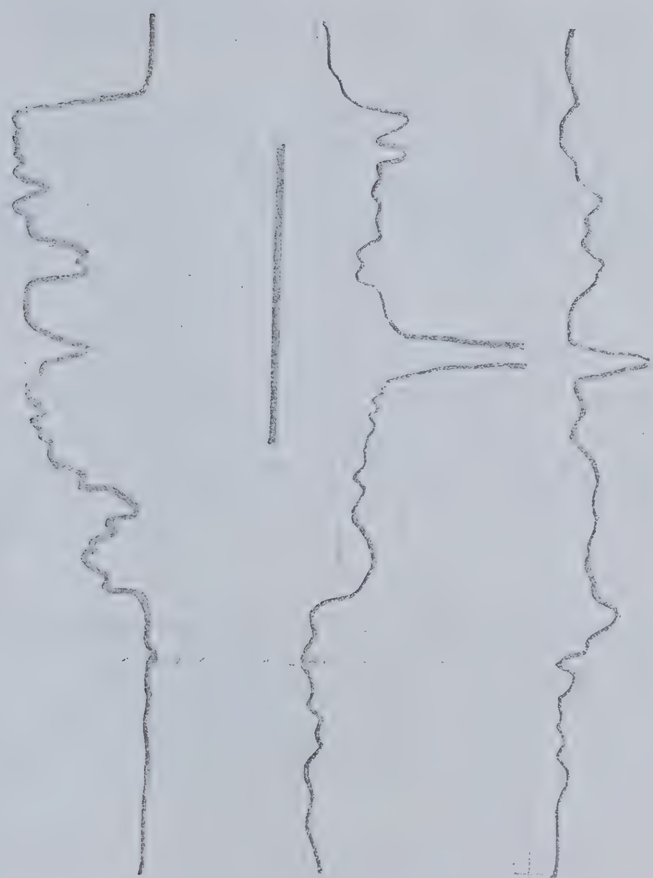

Core: 3"; good recovery (slabbed)

Depth (ft.) Description

2501-2510.3 (facies BIII)

Sandstone: light grey, very fine to fine grained, clean, well sorted; low angle, planar cross-stratification, small to medium scale, dark and red speckled (heulandite?) shale on foreset laminae, sharp cross-set boundaries; bioturbation, moderate, at two horizons, horizontal and vertical burrows.

2510.3-2510.6 (facies BII ± BI)

Shaly Sandstone: interlamination of very fine sand and shale; horizontal bioturbation predominant.

2510.6-2521.5 (facies BIII)

Sandstone: light grey, very fine to fine grained, friable, clean, well sorted; low angle, planar cross-stratification, medium scale, sharp cross-set boundaries, foreset laminae draped by shale or carbonaceous mudstone, some may be herringbone-type; clay clasts near base; weak bioturbation.

2521.5-2527.3 (facies BII ± BI)

Shaly Sandstone: two 26 to 28 cm thick, light grey, fine grained, clean, well sorted, and cross-stratified sandstone beds, alternate with bioturbated horizons of interlaminated very fine sandstone, mudstone and shale; wavy and lenticular bedding, scour surfaces.

2527.3-2545 (facies BIV)

Sandstone: light grey, very fine to fine grained, muddy; indurated calcareous band between 2538.9 and 2540.5'; strongly bioturbated, vertical burrows, *Zoophycus* sp.; few low angle, planar cross-stratified intervals; red speckled shale interlaminae common.

2545-2555 (facies BIII)

Sandstone: light grey, very fine to fine grained, clean, well sorted; low angle, planar cross-stratified, sharp cross-set boundaries, medium scale; very few shale laminae; bioturbation, moderate, at three horizons, *Zoophycus* sp., *Chondrites* sp., erosional contacts.

H.B. FARGO ACADIA VALLEY

10-11-26-2W4M

K.B. 2472'

Core: 3"; good recovery (slabbed)

Depth (ft.)	Descriptions

2500-2507

Shale: black, fissile; mudstone, siltstone, sandstone and granule sandstone lenses near base.

2507-2520 (facies BIII)

Sandstone: light grey, fine to medium grained, clean, well sorted; medium scale, low angle cross-stratified, sharp cross-set boundaries, shale and carbonaceous mud drape foreset laminae near base; calcareous and indurated between 2515.5 and 2518'; 4" thick interlaminated mudstone, pebbly sandstone, shale, and very coarse sand caps the unit; bioturbation at horizons.

P.P.C. AND O. ACADIA

11-21-26-3W4M

K.B. 2397'

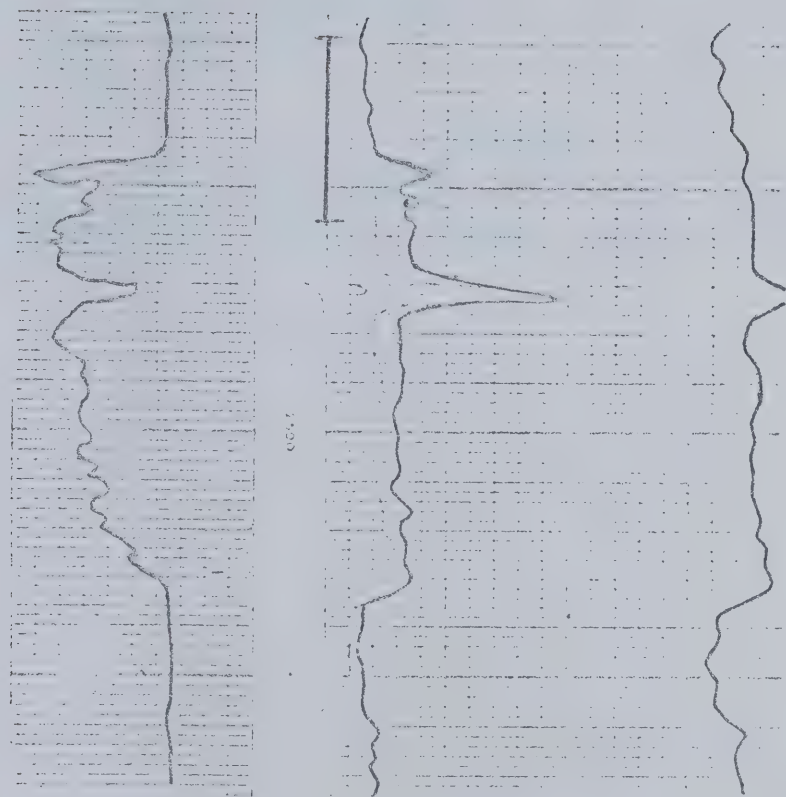

Core: 3"; fair recovery (slabbed)

Depth (ft.) | Description

2419-2445
Shale: black, fissile; a few siltstone laminae near base.

2445-2446.5 (facies BIV)
Sandstone: light grey, fine grained, friable, well sorted; structureless due to intense bioturbation, some horizontal and vertical burrows.

2446.5-2451.5 (facies BIII)
Sandstone: light grey, fine grained, clean, well sorted, friable; low angle, planar cross-stratified, sharp cross-set boundaries; shaly toward base; bioturbation, deep vertical burrows, at horizons.

Depth (ft.)	Description

2451.5-2456 (facies BII)

Sandstone: light grey, fine grained, well sorted, low angle, planar cross-stratified sandstone beds less than 2' thick, some with sharp cross-set boundaries, shale drape foreset laminae; in regular alternation with dark grey shaly sandstone intervals less than 6" thick; bioturbation, at horizons, more on the shaly intervals.

2456-2457 (facies BIII)

Sandstone: light grey, medium grained, clean, well sorted; medium angle cross-stratified, sharp cross-set boundaries, shale on foreset laminae, scoured surfaces.

MOBIL ALKALI CREEK

10-22-27-6W4M

K.B. 2454'

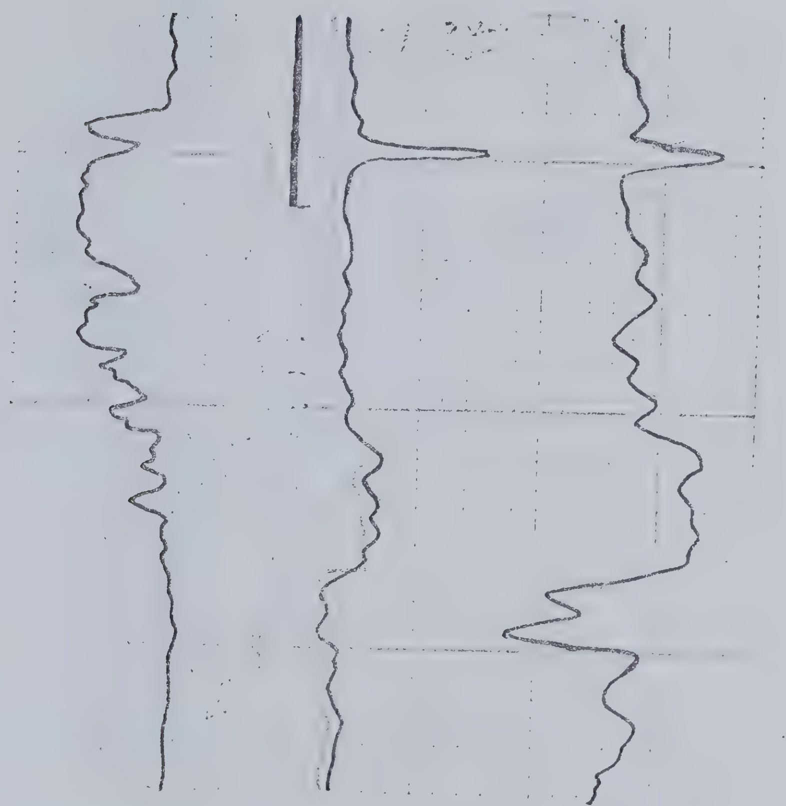

Core: 3"; good recovery (slabbed)

Depth (ft.)	Description

2480-2492

Shale: black, fissile; siltstone, sandstone and granule laminae, some cross-stratified between 2490 and 2492'.

2492-2510 (facies BIII)

Sandstone: light grey, fine grained, clean, well sorted, friable, low angle, cross-stratified; calcareous at 2495'. Unit is capped with pebbly sandstone, medium to coarse grained, about 4 mm longest diameter, 6" thick; indurated and calcareous, carbonaceous mudstone on foreset laminae, between 2547 to 2500'; muddy, shaly, more bioturbated horizons, and darker between 2500 and 2510'.

H.B. SIBBALD NO. I

7-20-27-2W4M

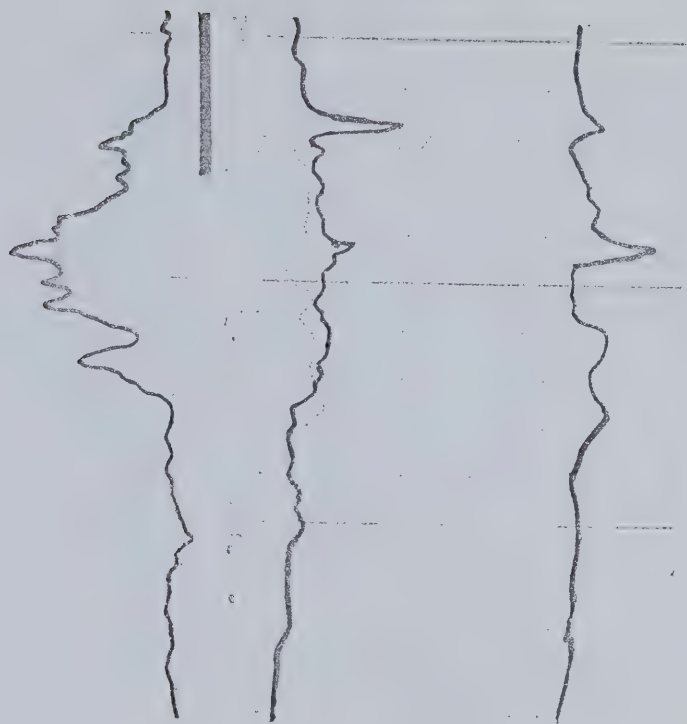

Core: 1"; poor recovery

Depth (ft.)	Description

2560-2564
Shale: black, fissile or massive in places; silty toward base.

2564-2565 (facies B1)
Pebble Conglomerate: black chert pebbles, up to 2 cm longest diameter, fairly well rounded, matrix supported; matrix, poorly sorted, very coarse sand; shaly interlaminae.

2565-2578
Sandstone: dark grey, medium grained, low angle, planar cross-stratified near top; abundant shale and mudstone interlaminae, more toward base, bioturbation moderate.

SAMEDAN CROWN OYEN

10-1-29-6W4M

K.B. 2554'

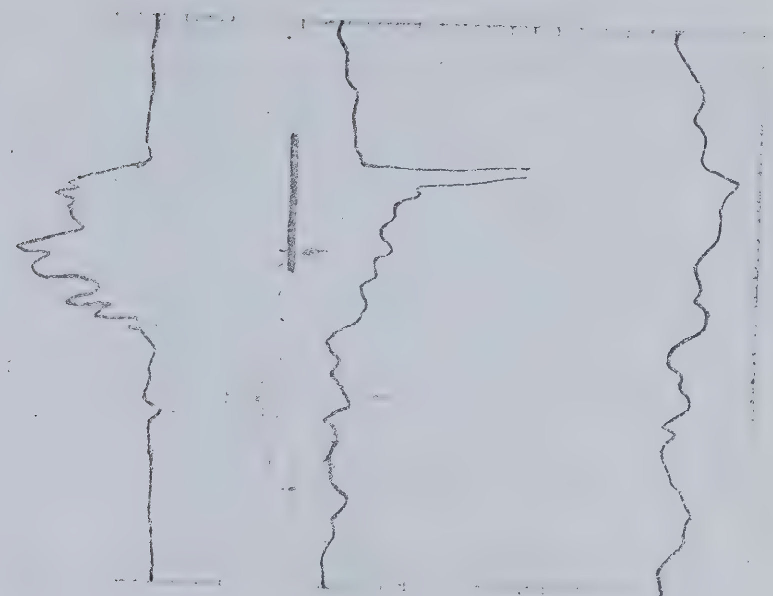

Core: 3"; fair recovery (slabbed)

Depth (ft.)	Description

2545-2554
Shale: black, fissile; cross-laminated fine sandstone lenses near base.

2554-2557
Sandstone: light grey, fine grained, muddy and friable; a few shale streaks and partings; bioturbation, weak to moderate, at horizons, *Zoophycus* sp.; a few chert pebbles scattered in coarse sand, more than 3" thick, caps the unit; calcareous between 2554.3 and 2556'.

2557-2568 (facies BII)
Shaly Sandstone: grey, fine grained, muddy and dirty sandstone beds; interbedded with fissile black shale up to 7.5 cm thick; bioturbation, intense, *Zoophycus* sp. and *Chondrites* sp.

2568-2570
Sandstone: light grey, medium grained, clean and well sorted; granule size black chert grains dispersed at top.

T.S.C.P. OYEN

6-29-29-4W4M

K.B. 2525'

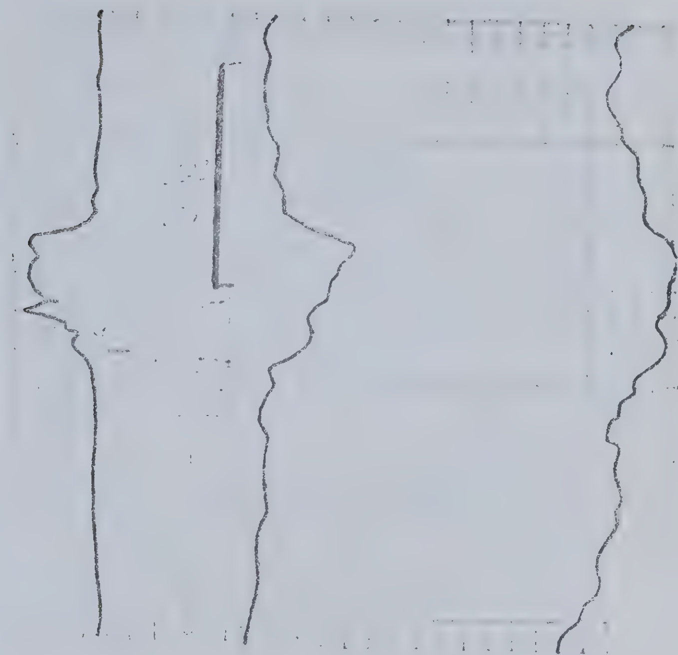

Core: 3"; fair recovery

<u>Depth (ft.)</u> <u>Description</u>

2485-2510
Shale: black and fissile.

2510-2515 (facies BI)
Mudstone: dark grey, siltstone lenses toward base, weak bioturbation.

2515-2520
No cores.

2520-2530
Sandstone: dark grey, fine to medium grained, dirty, muddy, shaly and friable; structureless due to very strong bioturbation.

MIDWEST GAS OYEN

6-23-29-4W4M

K.B. 2476'

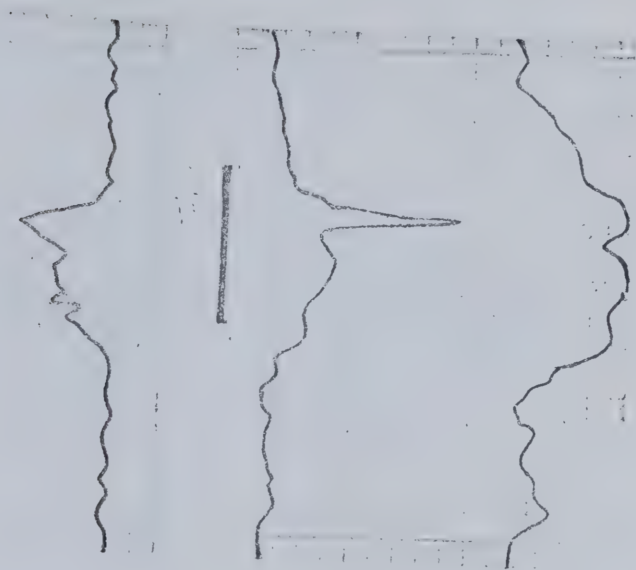

Core: 3"; good recovery

<u>Depth (ft.)</u> <u>Description</u>

2475-2479
Shale: black, fissile or massive in places, sideritic, sandy toward base.

2479-2480 (facies BV)
Pebble Conglomerate: black and varicolored chert pebbles, up to 1.5 cm longest diameter, fairly well rounded, matrix supported; matrix, mud; underlain by 7.5 cm thick bioturbated mudstone.

2480-2484 (facies BIII)
Sandstone: light grey, fine to medium grained, calcareous and indurated, weakly cross-stratified; shaly, more toward base.

2484-2492 (facies BIII ± BII)
Sandstone: dark grey, fine to medium grained, dirty, muddy, abundant regular shale laminae, low angle, planar cross-stratified in places; scour and fill structures; moderately bioturbated at horizons.

2492-2506 (facies BII)
Sandstone: darker grey, fine to medium grained, abundant shale laminae, streaks and partings; strongly bioturbated and structureless.

MOBIL OYEN

10-4-30-2W4M

K.B. 2481'

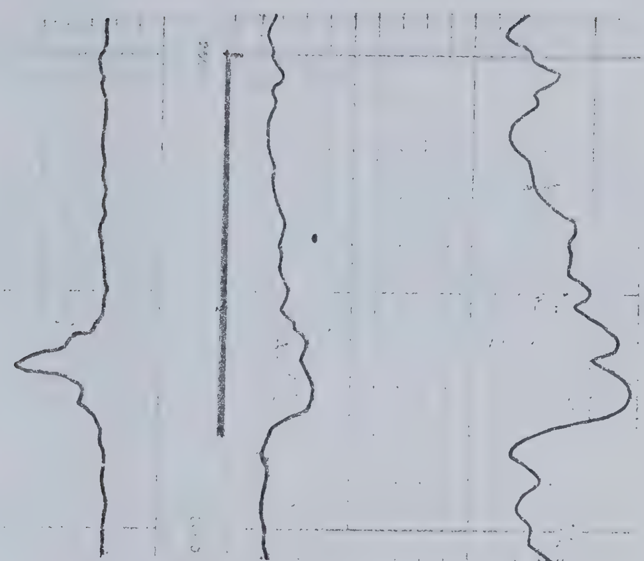

Core: 3"; fair recovery (slabbed)

Depth (ft.) | Description

2525-2556
Mudstone: dark grey, abundant shale and silt laminae, very fine sandstone lenses; weakly bioturbated; bentonitic at 2554'.

2556-2559 (facies BIV)
Pebbly Sandstone: dark grey, medium to coarse grained, dirty, muddy, poor sorting; black and varicolored chert pebbles, well rounded, up to 6 mm longest diameter, scattered throughout interval, but appears more concentrated at 2 horizons; strongly bioturbated.

2559-2567 (facies BIII)
Sandstone: dark grey, fine to medium grained, dirty and muddy; low to medium angle, horizontal, simple and planar cross-stratified, sharp cross-set boundaries, some draped by shale, shale on foreset laminae; sharp (erosive) contacts; common shale interlaminae; moderate to strong bioturbation, mostly at shaly horizons, vertical burrows common.

Depth (ft.)	Description

2567-2577 (facies BII)

Sandstone: darker grey, very fine to fine grained, dirty and muddy; shale, abundant as laminae, streaks and partings; bioturbation, very strong, vertical burrow up to 3" deep; sandstone beds alternate regularly with bioturbated shaly intervals usually less than 3 mm thick.

2577-2580 (facies BI)

Mudstone: dark, some greenish horizons; shale, silt-stone and sandstone interlaminae and lenses; herringbone cross-stratification, cross-set boundary erosive, some draped with bentonitic shale and glauconite; bioturbation, moderate to strong (*Terebellina* sp. or *Siphonites* sp.?).

TRECON SEDALIA

11-24-30-5W4M

K.B. 2322'

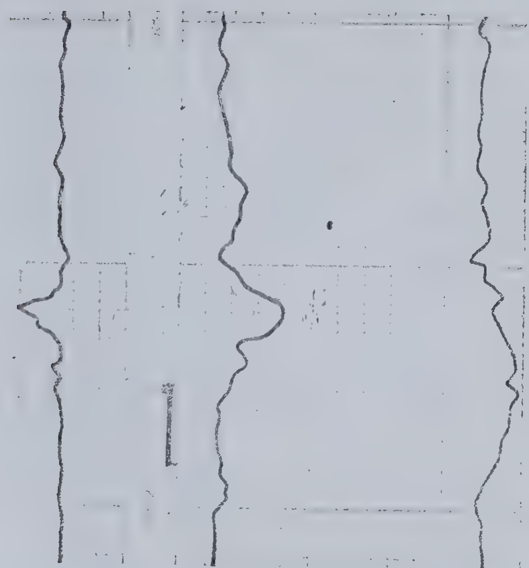

Core: 1"; good recovery

Depth (ft.)	Description
2318-2375	Lost cores.
2375-2385	Shale: black, fissile, muddy towards top; sharp basal contact.
2385-2391	Calcareous Shale: light grey, indurated, very calcareous.

CAN CHIEF PRUD. SEDALIA

13-35-30-6W4M

K.B. 2486'

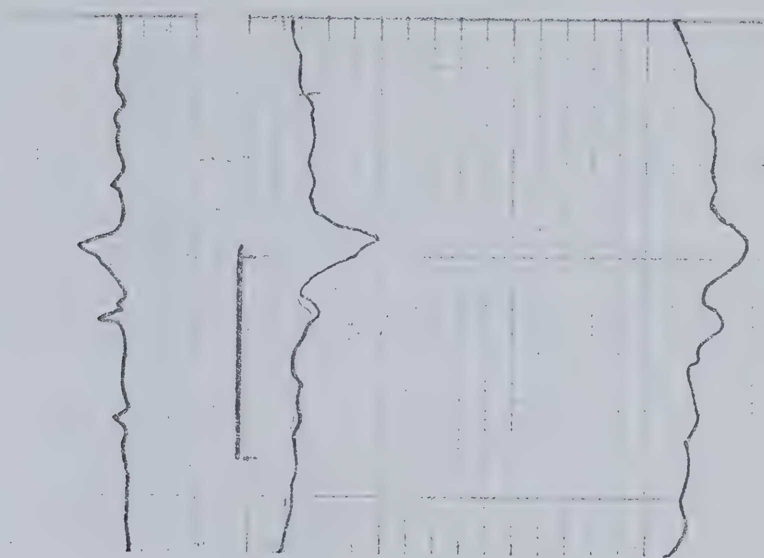

Core: 2"; poor recovery

Depth (ft.) | Description

2600-2605
Sandstone: dark grey, very fine to fine grained, muddy, shaly, and dirty; homogenized by bioturbation.

2605-2611
No cores cut.

2611-2612
Shale: black, fissile and bentonitic.

2612-2614
Sandstone: dark grey, very fine to fine grained, muddy, shaly, and dirty; homogenized by bioturbation.

2614-2621
No cores cut?

2621-2633
Shale: dark, fissile, silty near top, sandy toward base.

2633-2635
Sandstone: dark grey, fine grained; strongly bioturbated.

2635-2642
Shale: dark and fissile.

PAN AM B-I SEDALIA

10-35-30-4W4M

K.B. 2377'

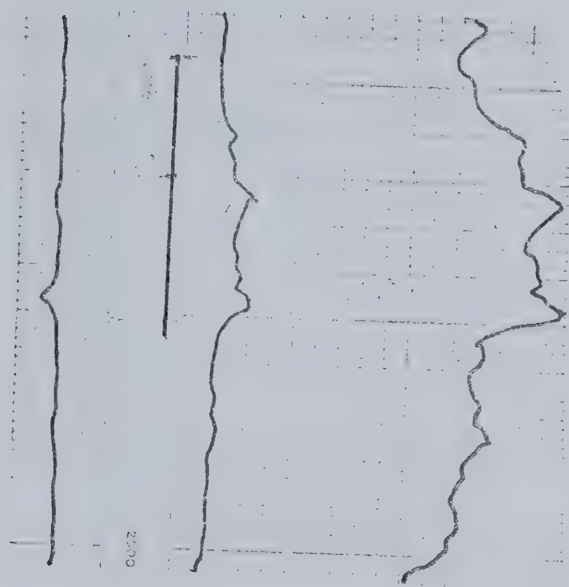

Core: 3"; fair recovery (slabbed)

Depth (ft.) | Description

2395-2410
Shale: black, fissile, siderite concretions.

2410-2422
Mudstone: dark grey, siltstone and fine sandstone laminae and lenses; horizons of weak bioturbation.

2422-2428.5
Sandy Mudstone: dark grey; interlaminae, siltstone, fine to coarse sandstone bed and pebble conglomerates $1\frac{1}{2}$" thick.

2428.5-2443
Mudstone: dark grey; siltstone and very fine sandstone laminae and lenses, herringbone cross-stratification with sharp (erosive) cross-set boundary; weak bioturbation.

2443-2445
Shale: dark, fissile and bentonitic.

Depth (ft.)	Description

2445-2448

Sandstone: light grey; black chert pebbles 4" thick and up to 6 mm longest diameter at base, fine grained sandstone on top; fairly sharp basal contact; low to medium angle, planar cross-stratification, shale laminae on foreset laminae (fining upward textural sequence).

2448-2451

Shale: black and fissile.

APPENDIX III1

Upper Central Sandstone
Ridge

(UC)

BANFF ET AL MATZIWIN

11-4-23-14W4M

K.B. 2295'

Core: 3"; good recovery

Depth (ft.)	Description

2558-2597
Shale: black, fissile, massive, sandy and bioturbated near base, bentonite beds, light to dark grey, fine grained, 15" and less than 1" thick, at 2582' and 2596'.

2597-2598 (facies BV)
Pebble Conglomerate: black and varicolored chert pebbles, up to 1.5 cm longest diameter, fairly well rounded, matrix supported; matrix, poorly sorted very coarse sand.

Depth (ft.)	Description
2598-2600	(facies BIII)

Pebbly Sandstone: light grey, coarse to very coarse grained, fairly well sorted; low angle, planar cross-stratified, sharp cross-set boundaries, chert pebbles dispersed throughout unit; dirty, some shale laminae.

MOBIL C.P.R. HUTTON

3-19-24-15W4M

K.B. 2476'

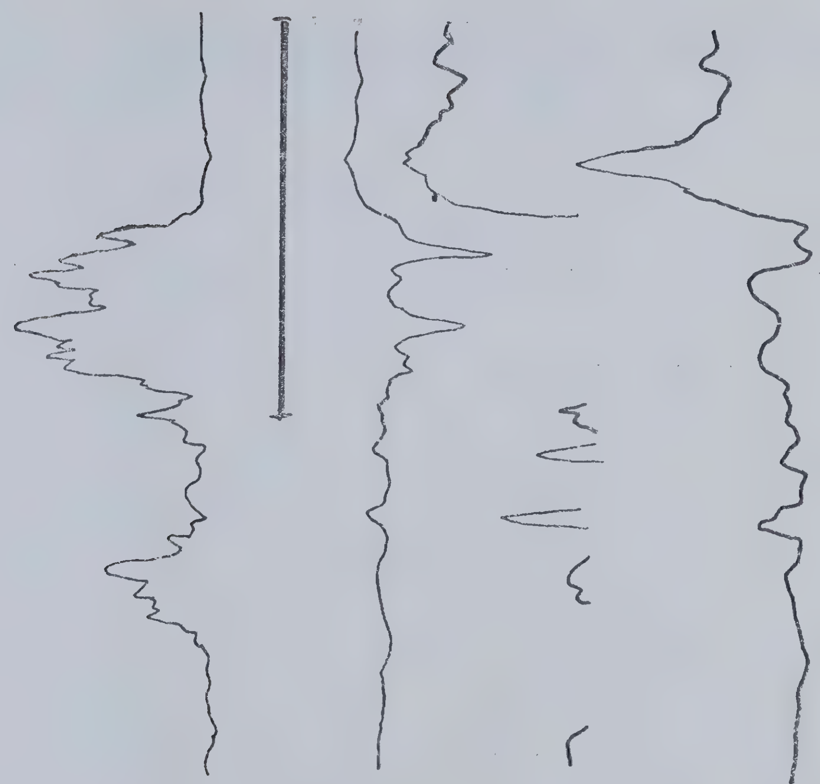

Core: 2"; poor recovery

Depth (ft.) Description

2898-2940
Shale: black, fissile; massive, sandy and bioturbated toward base; bentonite, dark grey, fine grained, 15" thick at 2926; some shale laminae.

2940-2945
No cores cut?

2945-2974 (facies BIII ± BII)
Sandstone: light grey, fine to medium grained, well sorted; low to medium angle, planar cross-stratified, medium scale, sharp cross-set boundaries, some draped by shale; shale laminae common; bioturbation, weak to moderate, at horizons. Unit is capped by a 1½" thick, black and varicolored chert pebbles,

Depth (ft.)	Description
	up to 8 mm longest diameter, fairly well rounded, matrix supported; matrix, poorly sorted, very coarse sand; sharply underlain by a 6" indurated calcareous sandstone band; siderite concretions.
2974-2982	(facies BII) Sandstone: dark grey, few horizontal laminated, fine sand lenses, abundant shale laminae; moderate bioturbation; bentonitic at base.

APPENDIX IIIm

Upper Western Sandstone Complex
(UW_3 member)

C.P.O.G. HUSSAR

10-2-25-20W4M

Core: 3"; good recovery

Depth (ft.)	Description

3870-3888
Shale: black, fissile; sandy toward base.

3888-3888.5
Pebbly Mudstone: 3" thick fine chert pebbles dispersed in a poorly sorted shaly medium grained sand matrix; underlain by a sharply based 3" thick shale.

Depth (ft.)	Description

3888.5-3911

Shaly Sandstone: light to dark grey; regular interbedding of sandstone and shale or mudstone; sandstone, very fine to fine grained, well sorted, often low angle planar cross-stratified, some with shale on foreset laminae, sharp corss-set boundaries, up to 2' thick; scour surfaces; shale content and degree of bioturbation increase downward.

C.P.O.G. CLARK HUSSAR

6-17-25-20W4M

Core: 3"; good recovery

Depth (ft.) | Description

3950-3958
Shale: black, fissile, sandy toward base.

3958-3959 (facies BV)
Pebble Conglomerate: black and varicolored chert pebbles, up to 1 cm longest diameter, fairly well rounded, matrix support; matrix, poorly sorted coarse sand; some shale interlaminae; underlain by a sharply based 1.5 cm thick mudstone.

Depth (ft.)	Description

3959-3964 (facies BIII)

Sandstone: dark grey, very fine to fine grained; cross-stratified; abundant shale laminae, some on foreset laminae; weak bioturbation.

3964-3968 (facies BII)

Shaly Sandstone: dark grey; very fine sand lenses interlaminated with shale and mudstone; weak to moderate bioturbated horizons.

3968-3977 (facies BII ± BI)

Muddy Sandstone: dark grey; sequence of interbedded sandstone, mudstone, shale and pebble conglomerates. Sandstone, fine to medium grained, some cross-stratified, up to 2' thick; shale and mudstone, less than 3 mm thick, usually sandy; pebble conglomerate, black and varicolored chert pebbles, fairly well rounded, matrix supported; matrix, mud; shale interlaminae; caps unit; bioturbation, weak to moderate, at horizons.

3977-3985 (facies BI)

Mudstone: dark grey; abundant fine sandstone lenses, some cross-stratified and horizontally laminated; moderate bioturbation.

3985-3987 (facies BIV)

Pebbly Sandstone: black and varicolored chert pebbles, up to 6 mm longest diameter, well rounded, scattered in a strongly bioturbated fine grained sandstone.

LALTA C.P.O.G. WAYNE

7-21-27-19W4M

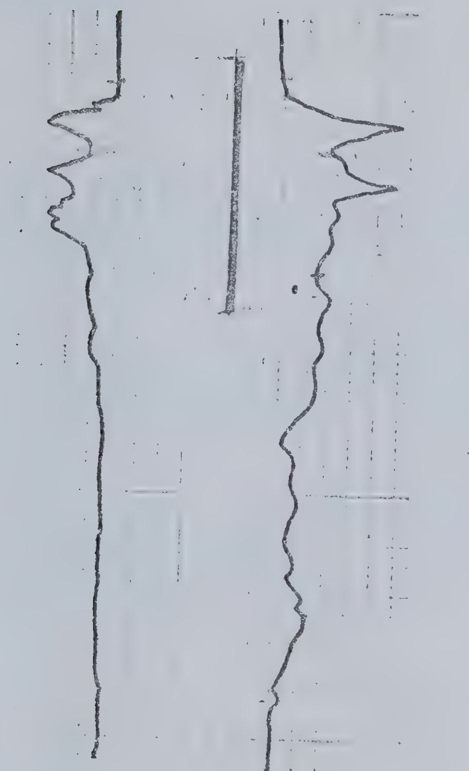

Core: 3"; fair recovery

Depth (ft.) — Description

3760-3769
Shale: black, massive or fissile in places.

3769-3771 (facies BV)
Pebbly Sandstone: black and varicolored chert pebbles, up to 8 mm longest diameter, fairly well rounded; dispersed in poorly sorted, very coarse grained, feldspathic sandstone.

3771-3773
Shale: black, fissile, sharp basal contact.

3773-3777 (facies BIII ± BII)
Sandstone: light grey, coarse to very coarse grained, feldspathic, weakly cross-stratified, friable; abundant shale laminae and streaks.

Depth (ft.)	Description

3777-3780 (facies BI)
Mudstone: dark grey, abundant siltstone and sandstone laminae; bioturbated in places.

3780-3785
No cores.

3785-3790 (facies BII)
Shaly Sandstone: dark grey; very fine to fine grained sandstone lenses, regularly interlaminated with shale and mudstone; moderate bioturbation in places.

3790-3800 (facies BII)
Sandstone: dark grey, very fine to fine grained, well sorted; cross-stratified in places; shale laminae common; moderate bioturbation at horizons.

3800-3812 (facies BI)
Mudstone: darker grey, greenish and glauconitic in places; abundant sandstone lenses, some ripple cross-laminated; scour surfaces; shale laminae toward base; moderate to strong bioturbation.

C.P.O.G. W. HUSSAR

6-18-27-20W4M

K.B. 2736'

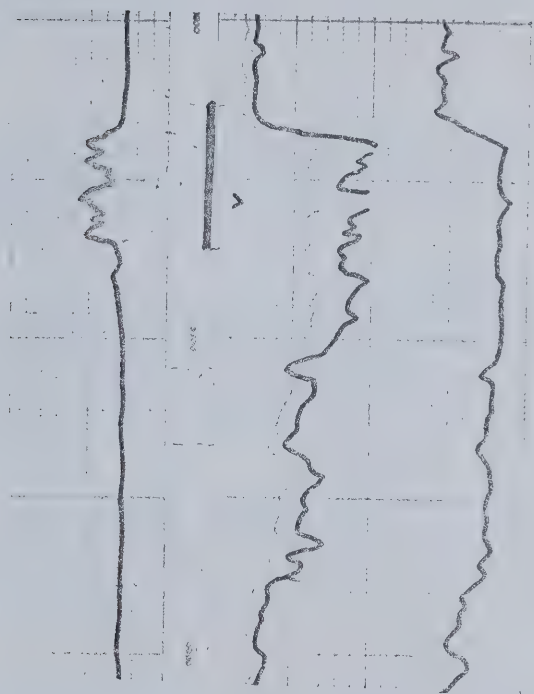

Core: 3"; good recovery

Depth (ft.)	Description

3825-3832
Shale: black, fissile or massive in places, sharp basal contact.

3832-3832.5 (facies BV)
Pebble Conglomerate: black chert pebbles, up to 1 cm longest diameter, well rounded, matrix supported; matrix, black mud.

3832.5-3839 (facies BIII ± BII)
Sandstone: dark grey, fine to medium grained, fairly sorted; plane and low angle, planar cross-stratification; sharp cross-set boundaires, shale on foreset laminae, some herringbone-like; shale laminae common; weak bioturbation.

3839-3841 (facies BI)
Mudstone: dark grey; abundant siltstone and fine sandstone laminae and lenses, some cross-stratified; moderate bioturbation.

Depth (ft.)	Description

3841-3847 (facies BII)

Sandstone: light grey, fine to medium grained, clean, fairly well sorted; low angle, planar cross-stratification, ripple cross-lamination; few shale laminae.

3847-3853 (facies BII ± BI)

Mudstone: dark grey; abundant very fine sand lenses, some cross-laminated; scour surfaces; moderate bioturbation.

3853-3855.5 (facies BV)

Pebble Conglomerate: black and varicolored chert pebbles, up to 3.5 cm longest diameter, fairly well rounded, grain supported; matrix, fairly sorted coarse to very coarse sand; shale interlaminae.

3855.5-3867 (facies BII)

Sandstone: dark grey; very fine to fine grained sandstone lenses, some planar cross-stratified; alternate regularly with shale or mudstone or siltstone laminae; bioturbation, moderate, at horizons.

3867-3872 (facies BI)

Mudstone: darker grey, fine sandstone lenses, scour surfaces, moderate bioturbation.

C.P.O.G. R. HUTTON

6-26-27-21W4M

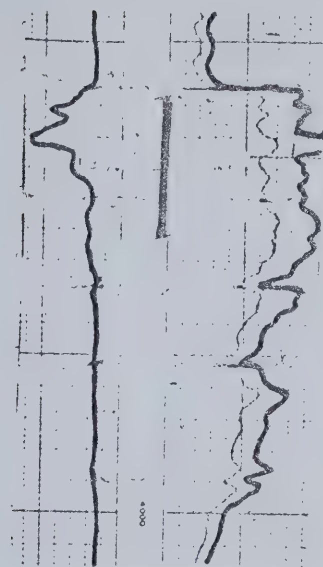

Core: 3"; good recovery

<u>Depth (ft.)</u> <u>Description</u>

3868-3873 (facies BIII)
Sandstone: light grey, fine to medium grained, fairly well sorted; low to medium angle planar cross-stratification; some shale laminae, more near base; weak bioturbation.

3873-3876 (facies BII)
Sandstone: light grey, very fine to fine grained sandstone lenses alternate with siltstone, mudstone and shale laminae; scour surfaces; weak bioturbation.

3876-3884 (facies BIII ± BII)
Sandstone: light grey, fine to medium grained, clean, fairly well sorted; low angle, planar cross-stratification; some shale laminae.

3884-3887 (facies BI)
Mudstone: dark grey; very fine sandstone lenses common; scour surfaces; moderate bioturbation.

3887-3894 (facies BII)
Sandstone: dark grey, fine to medium grained sandstone lenses; shale laminae, streaks and partings; highly reworked by bioturbation.

Depth (ft.)	Description
3894-3912	(facies BI)

Mudstone: dark grey, few very fine sandstone lenses; shalier, darker and more bioturbated toward base.

OAKRIDGE ET AL DRUMHELLER

7-1-29-19W4M

K.B. 2782'

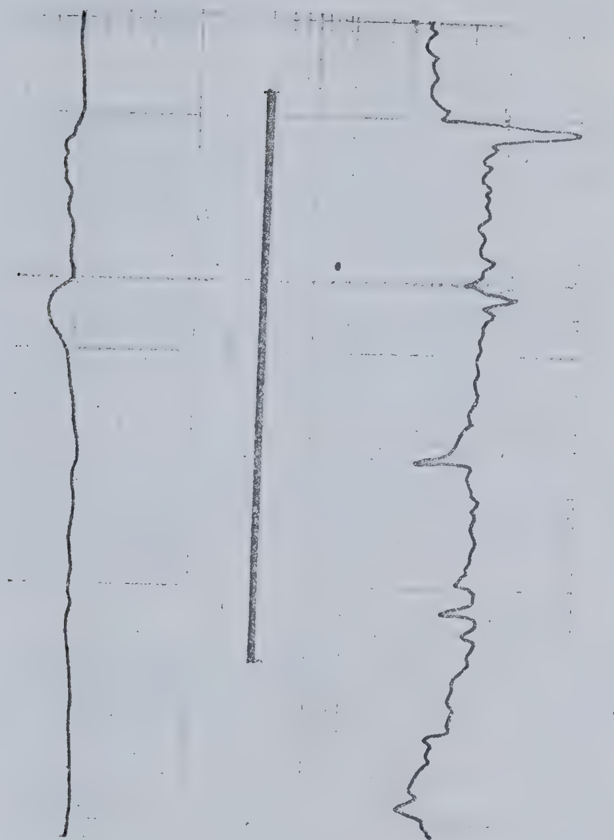

Core: 3"; good recovery

Depth (ft.)	Description

3645-3651
Shale: dark, fissile; base, sharp, may be erosional.

3651-3654 (facies BIII)
Sandstone: light grey, very fine grained, clean, well sorted; very muddy; low angle, planar cross-stratification in places.

3654-3675 (facies BII)
Sandstone: dark grey; regular alternation of very fine sandstone lenses with shale and mudstone laminae; bioturbation, weak to moderate, shaly horizons more affected; bentonite, light grey, medium biotite grains, 2" thick at 3659'.

Depth (ft.)	Description

3675-3687 (facies BI)
Mudstone: dark grey, abundant very fine sandstone lenses and shale laminae; strongly bioturbated; bentonite, light grey, fine grained, 1" thick at 3685'.

3687-3687.5 (facies BV)
Pebble Conglomerate: black and varicolored chert pebbles, up to 1.5 cm longest diameter, fairly well rounded, matrix supported; matrix, poorly sorted, very coarse sand; some mudstone interlaminae.

3687.5-3696 (facies BIII)
Sandstone: dark grey, fine to medium grained, well sorted; shale laminae, streaks, and partings; bioturbation, moderate to strong.

3696-3710 (facies BII)
Shaly Sandstone: dark grey; very fine to fine grained sandstone lenses alternate regularly with shale and mudstone laminae; moderate to strong bioturbation at shaly horizons.

3710-3765 (facies BI)
Mudstone: dark grey, weakly bioturbated, few sandstone lenses; bentonite, light to dark grey, fine to medium biotite grain, 3" thick at 3723' and 3755'.

Appendix IV (Table III)

Data Sheets for Quartz Grain Size Distribution

Location of cored well	Sample depth (ft.)	Quartz grain size (mm) distribution (counts)					Quartz mean size (mm) $\overline{X}$	Sorting coefficient (Arithmetic) σ	Matrix Frame-work	Facies	Facies Sequence
		0.031–0.0625	0.0625–0.125	0.125–0.25	0.25–0.5	0.5–1.0					
10-14-23 -1W5M	6386	14	118	68	--	--	0.14	0.1	--	Tidal Creek Channel	A(UW_1)
"	6390	--	--	50	145	5	0.33	0.09	--	"	BARRIER ISLAND
"	6435	--	--	107	88	5	0.26	0.07	--	Eolian	
"	6449	--	--	15	155	30	0.39	0.1	--	Middle Shore-face	
"	6456	--	3	170	27	--	0.21	0.05	--	"	
"	6467	--	10	110	75	5	0.26	0.08	--	Ebb-Tidal delta	
"	6468.5	--	2	95	103	--	0.26	0.06	--	"	
"	6470	70	118	12	--	--	0.08	0.03	--	"	

Table III (cont'd)

Location of cored well	Sample depth (ft.)	Quartz grain size (mm) distribution (counts) 0.031	0.0625	0.125	0.25	0.5	1.0	Quartz mean size (mm) $\overline{X}$	Sorting coefficient (Arithmetic) σ	Matrix Frame-work	Facies	Facies Sequence
6-26-34-7W4M (B_1)	2735	—	130	70	--	--		0.13	0.04	0.45	Hetero-lithic	B
10-18-33-9W4M (B_1)	2966	--	67	125	8	--		0.15	0.04	0.42	Cross-stra-tified	
2-28-33-9W4M (B_1)	2930	--	70	125	5	--		0.14	0.03	0.52	"	
"	2933	--	110	90	--	--		0.13	0.03	0.55	Hetero-lithic	
10-36-28-14W4M (L_3)	3112	--	35	160	5	--		0.15	0.03	0.23	Biotur-bated sand-stone	
	3122	--	10	130	60	--		0.22	0.09	0.55		
	3124	--	--	140	50	10		0.25	0.09	0.30	Cross-stra-tified sand-stone	

Table III (cont'd)

Location of cored well	Sample depth (ft.)	Quartz grain size (mm) distribution (counts)					Quartz mean size (mm) $\overline{X}$	Sorting coefficient (Arithmetic) σ	Matrix frame-work	Facies	Facies Sequence
		0.031 – 0.0625	0.0625 – 0.125	0.125 – 0.25	0.25 – 0.5	0.5 – 1.0					
10-36-28 -14W4M (L_3)	3134	--	--	165	35	--	0.21	0.05	0.15	Hetero-lithic	B
	3151	--	60	140	--	--	0.15	0.04	0.22	"	
7-22-29-14W4M (L_3)	3104	--	20	140	40	--	0.19	0.05	0.21	Biotur-bated Sand-stone	
6-23-30-14W4M (L_3)	3170	--	25	100	45	30	0.23	0.19	0.60	"	
	3180	--	--	85	105	10	0.27	0.07	0.22	Cross-stra-tified sand-stone	
6-20-34-24W4M (L_7)	4906	--	15	170	15	--	0.19	0.05	0.36	"	
	4912	--	10	165	25	--	0.19	0.05	0.15	"	
	4920	--	--	102	98	--	0.27	0.05	0.19	"	

Table III (cont'd)

Location of cored well	Sample depth (ft.)	Quartz grain size (mm) distribution (counts) 0.031–0.0625	0.0625–0.125	0.125–0.25	0.25–0.5	0.5–1.0	Quartz mean size (mm) $\overline{X}$	Sorting coefficient (Arithmetic) σ	Matrix Frame-work	Facies	Facies Sequence
6-20-34-24W4M (L_7)	4929	--	10	165	25	--	0.18	0.05	0.32	Hetero-lithic	B
	4945	--	155	45	--	--	0.10	0.36	0.75	Biotur-bated mud-stone	
6-36-34-25W4M (L_7)	4950	--	12	163	25	--	0.19	0.05	0.29	Cross-stra-tified sand-stone	
	4963	--	35	150	15	--	0.17	0.04	0.50		
	4965	--	5	100	90	5	0.26	0.06	0.33	Hetero-lithic	
	4971	--	20	170	10	--	0.19	0.04	0.38	"	
10-4-34-24W4M (L_7)	4866	--	--	140	60	--	0.24	0.05	0.33	Cross-stra-tified sand-stone	
	4878	--	24	176	--	--	0.16	0.04	0.38	Hetero-lithic	
	4890	--	5	170	25	--	0.19	0.04	0.34	"	

Table III (cont'd)

Location of cored well	Sample depth (ft.)	Quartz grain size (mm) distribution (counts) 0.031–0.0625	0.0625–0.125	0.125–0.25	0.25–0.5	0.5–1.0	Quartz mean size (mm) $\overline{X}$	Sorting coefficient (Arithmetic) σ	Matrix Frame-work	Facies	Facies Sequence
10-11-26-2W4M (UE_2)	2508	--	15	160	25	--	0.20	0.08	--	Cross-stratified sandstone	B
7-11-25-3W4M	2471	--	15	178	7	--	0.17	0.04	--		TIDAL CURRENT SANDRIDGE
6-28-24-1W4M	2501	--	55	136	4	5	0.17	0.1	--	"	
	2504.5	--	35	165	--	--	0.16	0.03	--	"	
	2509	--	65	130	5	--	0.15	0.04	--	"	
	2512	--	55	140	5	--	0.15	0.03	--	"	
	2540	--	145	55	--	--	0.11	0.02	--	"	
	2541.7	--	115	85	--	--	0.13	0.04	--	"	
	2555	--	155	45	--	--	0.11	0.02	--	"	

Appendix Va

Plate XVII

Continuous Core of Barrier Island Facies Sequence A;
A.N.D. #1 10-14-23-1W5M; (UW_1). C.I. 6370-6479 ft.

A-B Ebb-delta facies.

B-C Marginal or spillover channel facies.

C-D Middle shoreface facies.

D-E Transition (shoreface-offshore) facies.

E-F Upper shoreface - Beach facies.

F-G Eolian dune facies.

G-H Back barrier mudflat facies.

H-I Lagoonal facies (Washover (WO), Undermarsh clay (UC), Marsh (MS)).

I-J Mixed tidal flat facies.

J-K Tidal creek channel facies.

K-L Overbank facies.


TOP
TRAY NO.
CORE NO. I
FOOTAGE

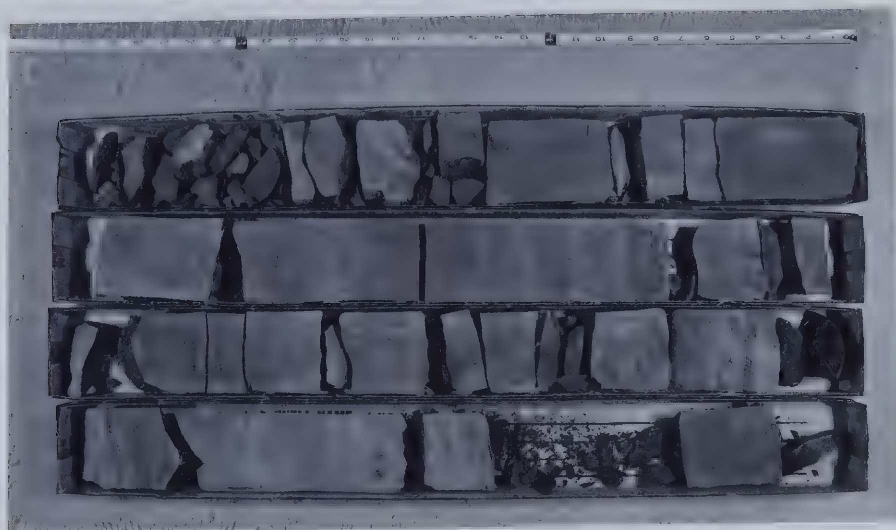


TOP
TOP

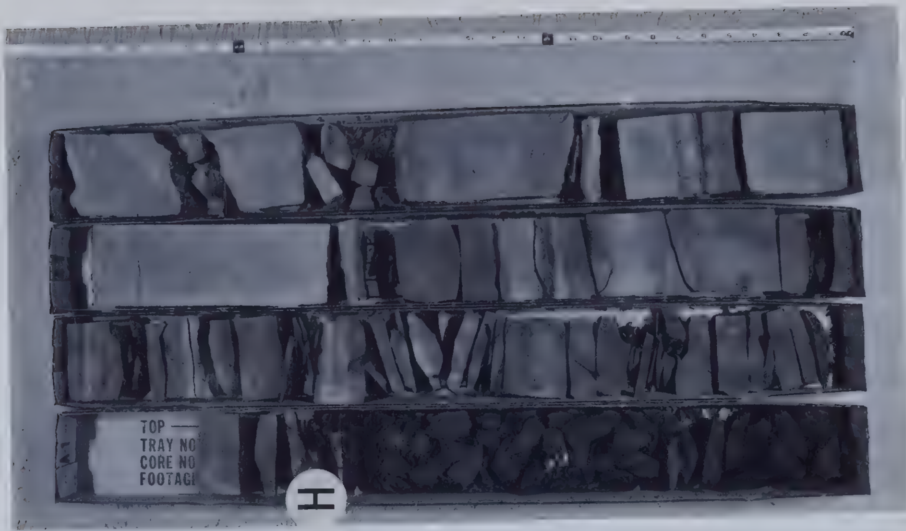
H


G
F


E
D


TOP
TRAY NO.
CORE NO.
TOP

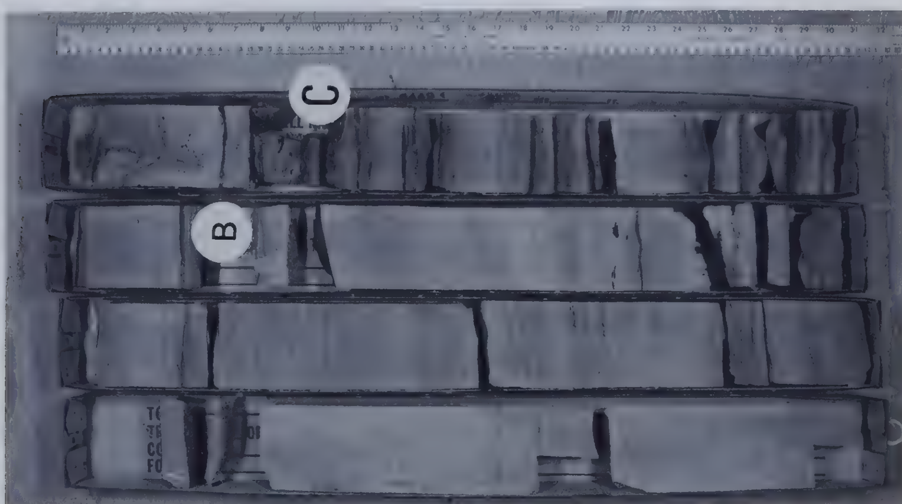
C
B

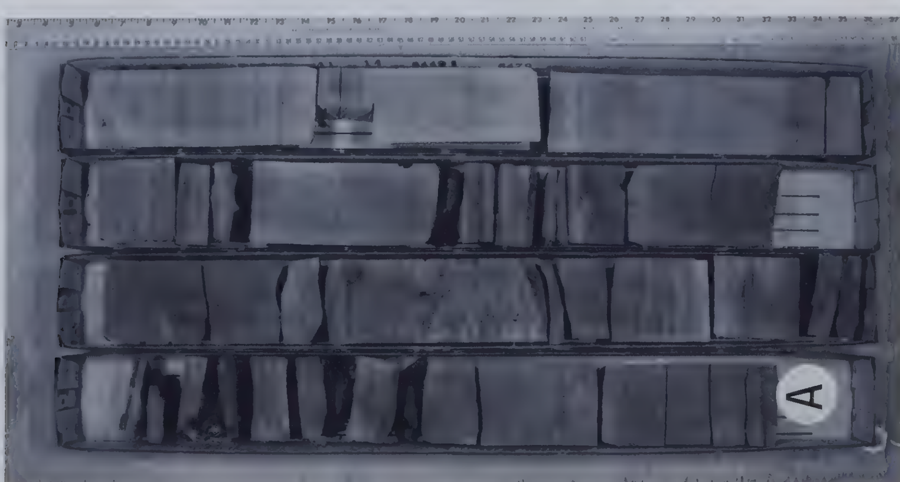
A

Appendix Vb

Plate XVIII

Continuous core of (tidal current?)
sand ridge facies;
Chevron Handhills 10-36-28-14 W4M; (L_3).
C.I. 3062 - 3164 ft.

R-S Heterolithic facies.

S-T Cross-bedded sandstone facies.

T-U Bioturbated sandstone facies.

U-V Bioturbated mudstone facies (Upper) with conglomerate facies (CF).


CF
V

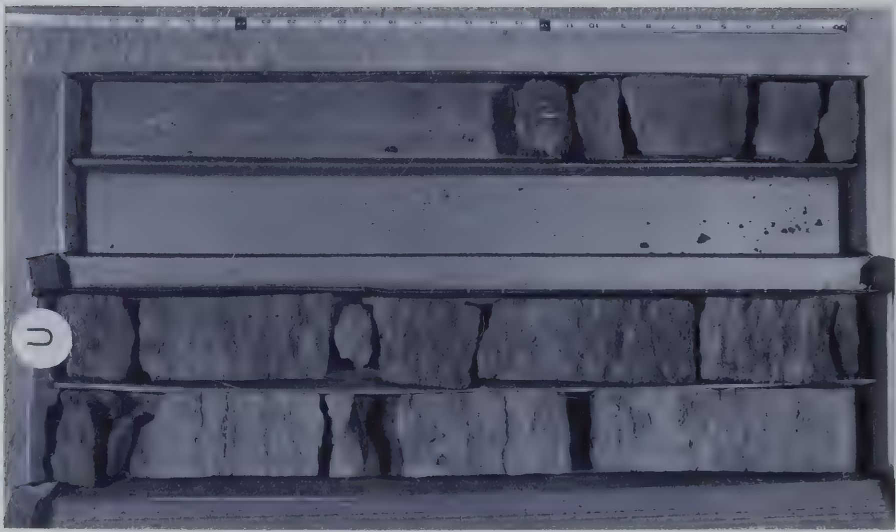
U

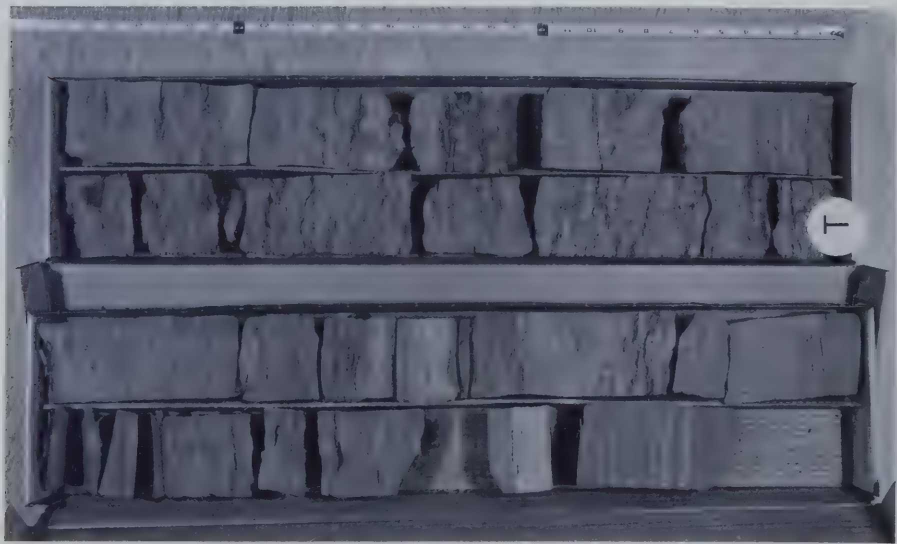
T


S


S


R

Appendix Vc

Plate XIX

Continuous core of (tidal current?)
sand ridge facies;
Camac Mavrk Huxley 6-20-34-24 W4M; (L7).
C.I. 4892 - 4945 Ft.

M-N Bioturbated mudstone facies (lower).

N-O Heterolithic facies.

O-P Cross-bedded sandstone facies with conglomerate facies (CF).

P-Q Bioturbated sandstone facies.

Q-R Mudstone facies (upper).

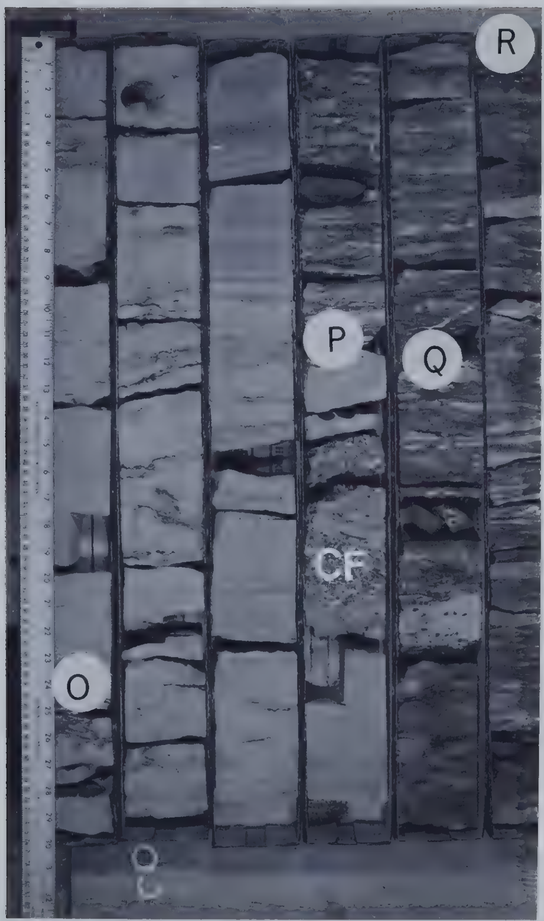
R
P
Q
CF
O

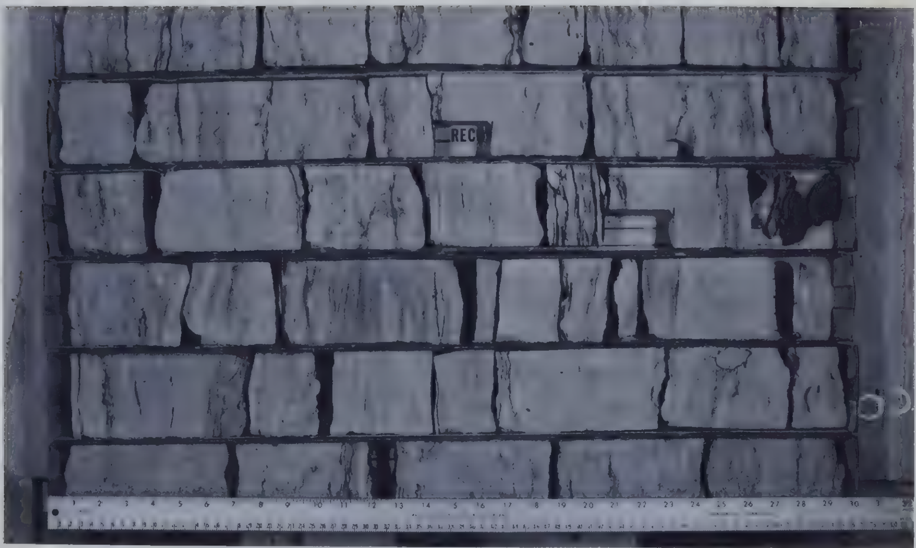


N
TOP → WELL
TRAY NO. OF LOCAT
CORE NO.
FOOTAGE


FOOTAGE
RECOVE FT.
M

Appendix Vd

Plate XX

Continuous Core of (tidal current?)
sand ridge facies;
Imperial Armena 9-13-48-21 W4M;(LJC_{12}).
C.I. 3205 - 3247.5 ft.

A-B, M-N, C-D, O-P, T-U	Bioturbated mudstone facies (lower). ± Heterolithic facies and C bentonite (C).
B-C, N-O, P-Q, R-S	Cross-bedded sandstone facies.
Q-R, S-T	Bioturbated sandstone facies.
D-E, T-U.	Mudstone facies (Upper).
C -	Bentonite C

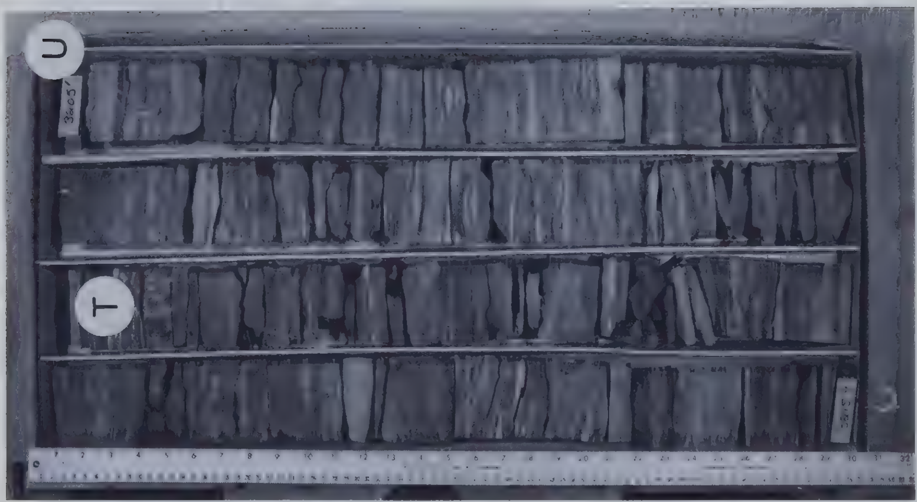
U
T


S
#5
#6
#7
#8
#9
#10
#11
#12


#13
#14
#15
#16
#17
#19
R
Q
P
3235.9'


#23
O
N
C


M
BOTTOM
CORE #1
3247.7'

Appendix Ve

Plate XXI

Continuous core of (tidal current?)
sand ridge facies;
Union Permo Acadia Valley 7-11-25-3W4M; (UE_2).
C.I. 2453 - 2503 ft.

O-P Heterolithic facies.

P-Q Cross-bedded sandstone facies.

Q-R Bioturbated sandstone facies.

R-S Lloydminster marine shale.


S
R


Q

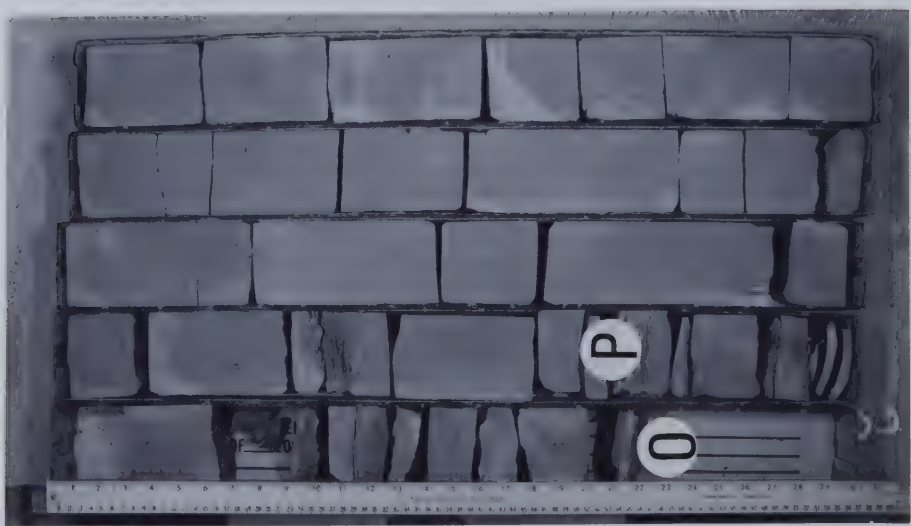
P
O

Appendix Vf

Plate XXII

Continuous core of (tidal current?)
sand ridge facies;
Anglo Royalite Kroy Acadia 6-28-24-1W4M; (UE_2).
C.I. 2501 - 2555 ft.

J-K, L-M, N-O	Bioturbated mudstone facies $\pm$ Heterolithic facies.
E-F, G-H, I-J, K-L, M-N, P-Q	Cross-bedded sandstone facies.
F-G, H-I, O-P	Bioturbated sandstone facies.

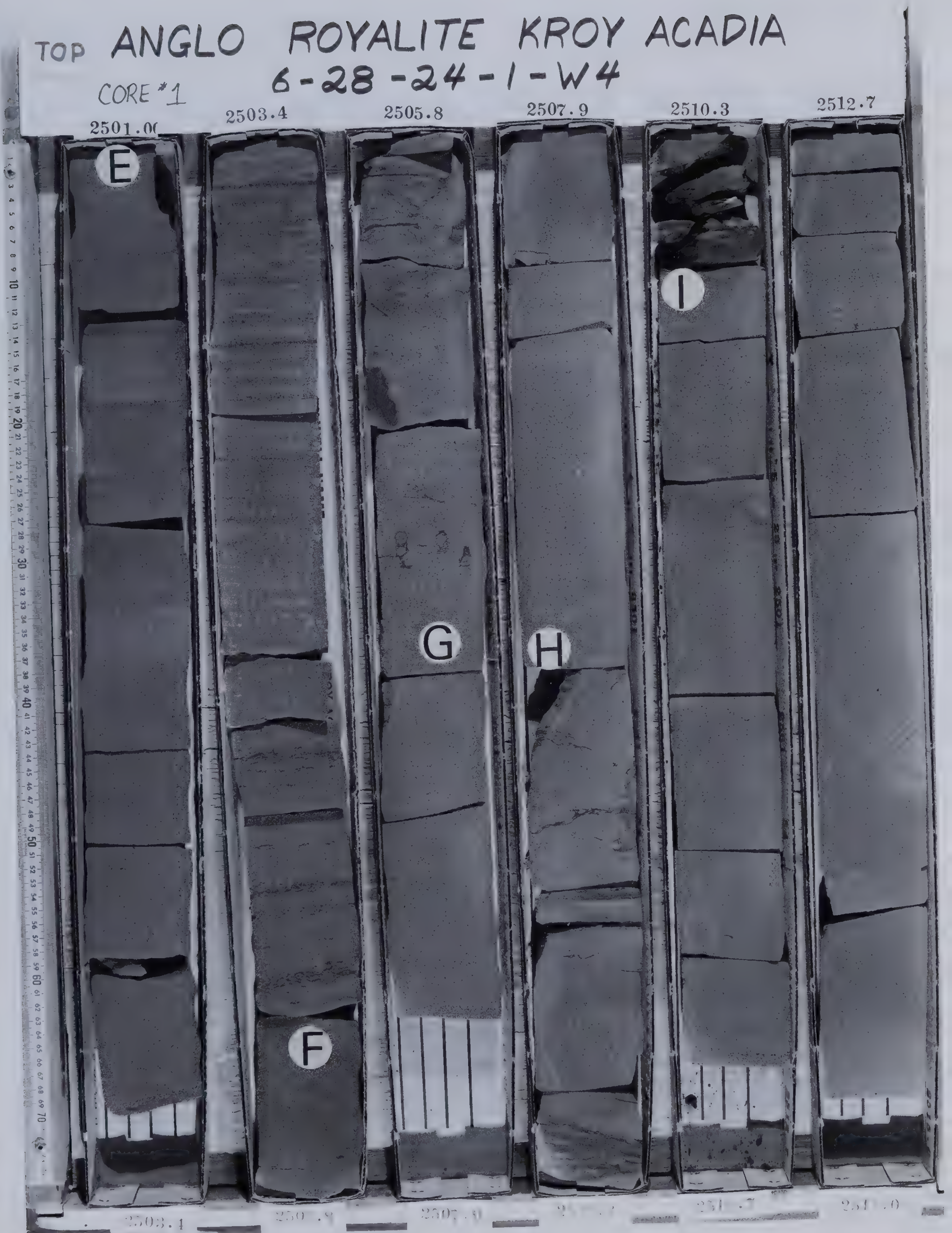
TOP ANGLO ROYALITE KROY ACADIA
6-28-24-1-W4
CORE #1
2501.00
2503.4
2505.8
2507.9
2510.3
2512.7
E
F
G
H
I

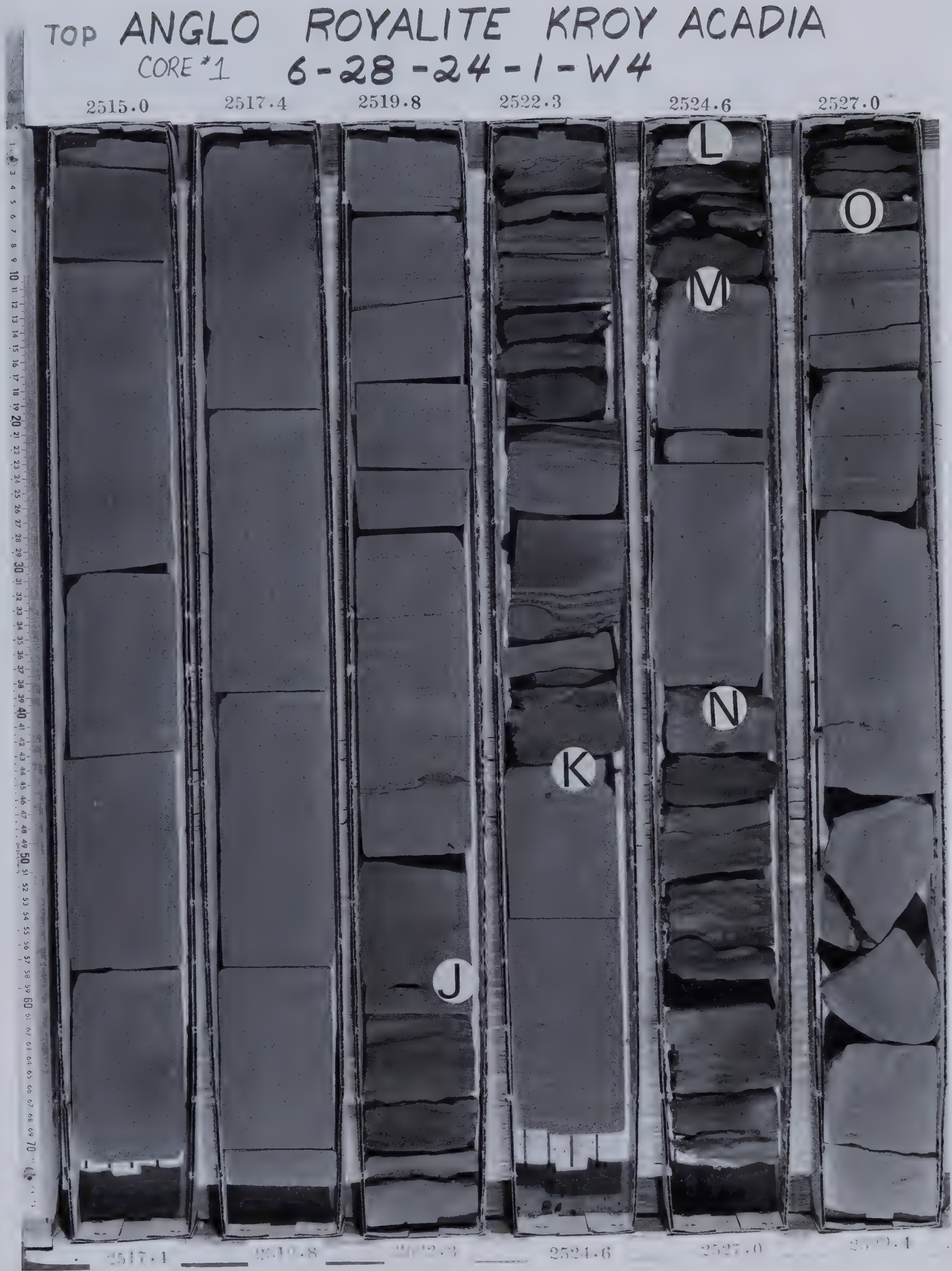
TOP ANGLO ROYALITE KROY ACADIA
CORE #1 6-28-24-1-W4
2515.0
2517.4
2519.8
2522.3
2524.6
2527.0
L
O
M
N
K
J
2517.4
2524.6
2527.0


TOP ANGLO ROYALITE KROY ACADIA
CORE #1 6-28-24-1-W4
2529.4
2531.9
2534.2
2536.4
2538.9
2541.2
2531.9
2538.9
2541.2

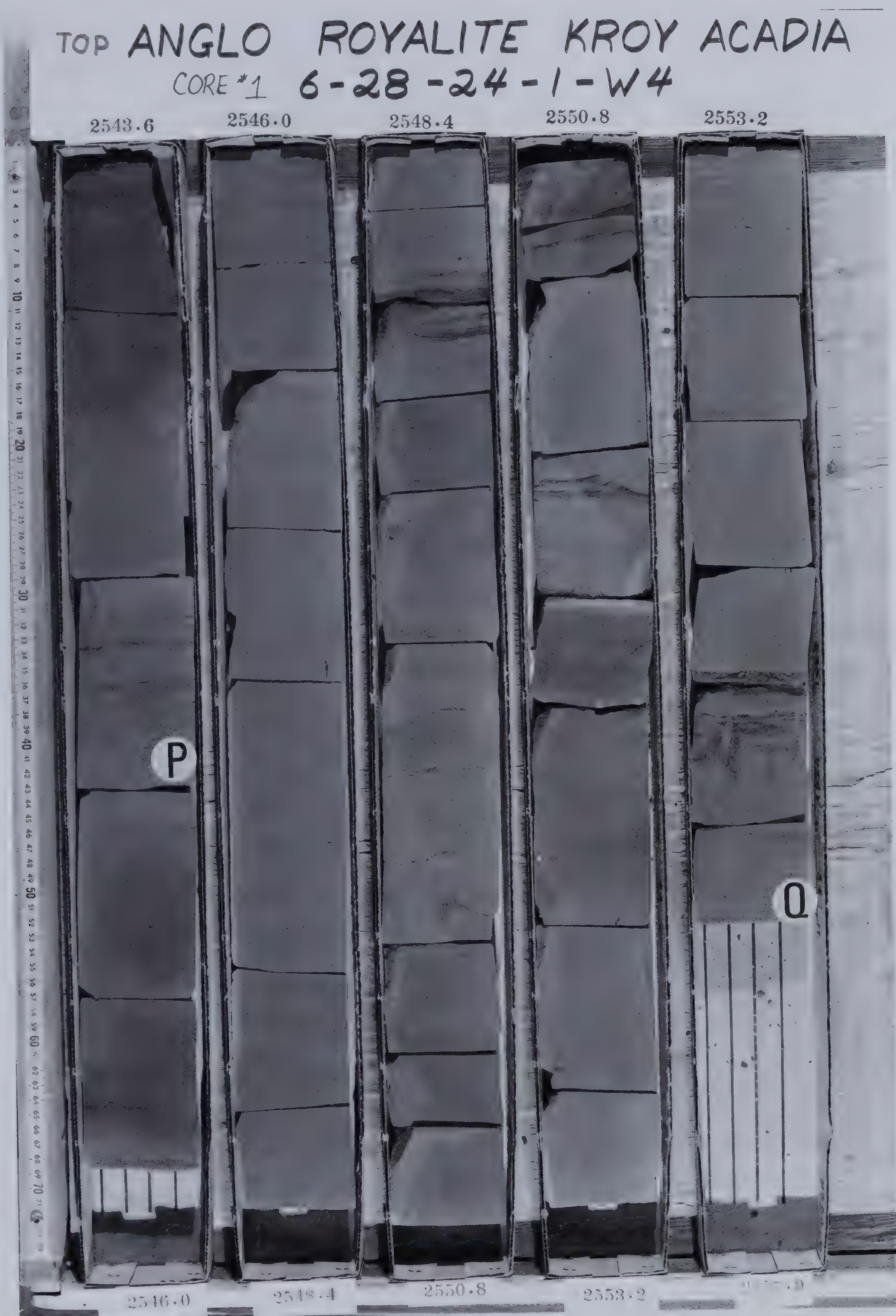
TOP ANGLO ROYALITE KROY ACADIA
CORE #1 6-28-24-1-W4
2543.6
2546.0
2548.4
2550.8
2553.2
P
Q
2546.0
2548.4
2550.8
2553.2

Appendix VI. Generalized legend for cross-sections, fence diagrams and vertical facies sequences of Viking sandbodies.

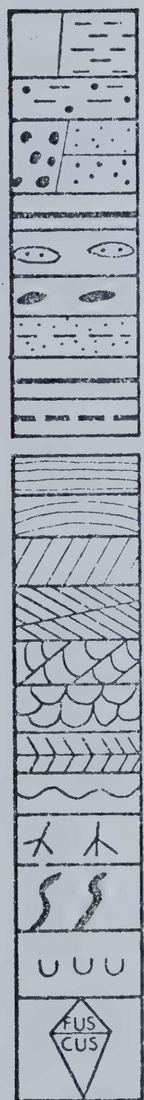

Lithology

shale
mudstone
sandstone
shale lamina
sand lenses
shale - mudstone clasts
interlamination of ss., mudst., and sh.
bentonite (E, D, C, A, A_0)
inferred position of bentonite

Sedimentary and biogenic structures

horizontal lamination
irregular lamination
simple foreset cross-stratification
planar foreset cross-stratification
ripple trough cross-lamination
trough cross-stratification
herringbone cross-stratification
scour surface
plant root
bioturbation
burrows
FUS (Fining Upward Sequence)
CUS (Coarsening Upward Sequence)

Other symbols

well identity (1), horizontal distance between wells in miles (| 2 |), Blairmore (BL), top of Mannville (TM), Joli Fou (JF), top of Viking (TV), Lloydminster (LYD), base of Fish Scales (BFS), datum (DAT/dat), reference line (Ref).